UNIVERSITA' DEGLI STUDI DI PALERMO
Facoltà di Ingegneria
Dipartimento di Ingegneria Civile, Ambientale, Aerospaziale e dei Materiali

DOTTORATO IN INGEGNERIA DELLE STRUTTURE

ULTRASONIC WAVES IN HETEROGENEOUS MATERIALS

MECHANICAL CHARACTERIZATION OF HETEROGENEOUS MATERIALS BY MEANS OF ULTRASONIC TESTS AND NUMERICAL MODELS: THE CONCRETE

Settore scientifico disciplinare
ICAR 08

Tesi di:
CAMMARATA MARCELLO

Coordinatore:
Prof. GIUSEPPE GIAMBANCO

Tutor:
Prof. GIUSEPPE GIAMBANCO

CICLO XXIII - ANNO ACCADEMICO 2012/2013

To my two girls:
Mom and Rosalia

ULTRASONIC WAVES
IN
HETEROGENEOUS MATERIALS

MECHANICAL CHARACTERIZATION OF HETEROGENEOUS MATERIALS BY MEANS OF ULTRASONIC TESTS AND NUMERICAL MODELS: THE CONCRETE

	DEDICATION	
	TABLE OF CONTENTS	I
	PREFACE	VII
	CHAPTER 1	
	INTRODUCTION	
1.1	Heterogeneous materials in civil engineering	1
1.1.1	*Masonry*	2
1.1.2	*Concrete*	3
1.1.3	*Bituminous*	4
1.1.4	*FRP*	9
1.2	Objectives	13
1.3	Outline of thesis	14
	CHAPTER 2	
	MECHANICAL TESTING OF HETEROGENEOUS MATERIALS	
2.1	Tests	19
2.2	Direct test methods	20
2.2.1	*The zwick /Roell & troni technik 4KN*	21
2.2.2	*Procedure for measure of elastic module*	24

2.3	Not destructive testing	26
2.3.1	*Penetrating liquid test*	27
2.3.2	*Radiografy*	30
2.3.3	*Eddy current testing*	35
2.3.4	*Visual testing*	37
2.3.5	*Magnetic particle*	38
2.3.6	*Acoustic emission testing*	41
2.3.7	*Thermal image infrared*	43
2.4	Virtual testing	45
2.5	The sonreb Method	46
2.6	The ultrasonic Method	47
2.6.1	*The control technique for contact*	48
	CHAPTER 3	
	THE CONCRETE	
3.1	Concrete: general aspects	59
3.2	Composition	60
3.2.1	*Aggregates*	60
3.2.2	*Cements*	70
3.2.3	*Portland cement*	72
3.2.4	*Composition of cements*	74
3.2.5	*Hydration of cements*	75
3.2.6	*Water and additives*	81
3.3	Mix design	83
3.3.1	*Software for mix design*	92
3.4	Casting and curing	95
3.5	Mechanical properties	98
3.5.1	*Fresh concrete*	99
3.5.2	*Hardened concrete*	103
	CHAPTER 4	
	NDT: ULTRASONIC WAVES AND SIGNAL PROCESSING THEORETICAL BACKGROUND AND VALIDATION MACHINE	
4.1	Theory of wave propagation in elastic media	107
4.1.1	*General aspects: longitudinal shear and flexural waves*	107
4.1.2	*Types of waves*	111
4.1.3	*Longitudinal waves*	111
4.1.4	*Transverse waves*	112
4.1.5	*Surface waves*	113
4.1.6	*Flexural waves*	114
4.1.7	*Snell law*	115

4.1.8	*Attenuation*	118
4.1.9	*Differential equation of propagation wave in elastic media*	119
4.1.10	*Mono dimensional case (ODE)*	119
4.1.11	*The Dirichlet problem*	123
4.1.12	*Tridimensional case (PDE)*	123
4.1.13	*Differential equation of propagation wave in micro structured media*	127
4.2	Signal processing	128
4.2.1	*The digital signal*	129
4.2.2	*Signal classification*	131
4.2.3	*Notable signals*	132
4.2.4	*Space time processing: the cross correlation*	135
4.2.5	*Frequency time processing: the Fourier transform*	140
4.2.6	*The Fourier transform for continuum signals*	143
4.2.7	*The Fourier transform for discrete signals*	145
4.2.8	*Discrete Fourier transform*	147
4.2.9	*Fast Fourier transform*	148
4.2.10	*Notable examples of FFT*	150
4.2.11	*The proposed algorithm*	156
4.3	Technologies	158
4.3.1	*The Pro-Pulser machine*	160
4.3.2	*The probes*	162
4.3.3	*The accessories: frame, concrete boxes, coaxial cable, gels*	167
4.3.4	*The software*	169
4.4	Machine validation	173
4.4.1	*UW propagation in alloy plate*	173
4.4.2	*UW propagation in steel cylinder*	179
4.4.3	*The baseline*	181
4.4.4	*Cylinder tests*	183
4.4.5	*Numerical models*	187
4.4.6	*Parametric study*	193

CHAPTER 5
EXPERIMENTAL TESTS AND NUMERICAL SIMULATIONS

5.1	Introduction	195
5.2	Fresh concrete	195
5.2.1	*Devices and environments*	198
5.2.2	*Time-space analysis*	204
5.2.3	*Results related whit elastic module measurements*	211

5.2.4	*Frequency space analysis*	214
5.3	Hardened concrete	220
5.3.1	*The NDT tests*	221
5.3.2	*Compression test*	222
5.3.3	*Data processing*	223
5.3.4	*Considerations*	225
5.3.5	*Clustering*	240
5.3.6	*The developed algorithm of clustering*	243
5.3.7	*Consideration on clustering method applied*	248
5.4	Modeling waves in heterogeneous materials	248
	CHAPTER 6	
	THE MULTI SCALE APPROACH	
6.1	Introduction	265
6.1.1	*The meso model*	266
6.1.2	*The macro model*	269
6.1.3	*The multiscale models*	270
6.2	The meshless method	270
6.2.1	*Approximation by MLS*	273
6.2.2	*Weight functions*	277
6.2.3	*The RVE proposed*	279
6.2.3.1	*Block*	282
6.2.3.2	*External block*	284
6.2.3.3	*Interfaces*	286
6.2.3.4	*System resolution*	288
6.3	Multiscale Analisys	290
	CHAPTER 7	
	CONCLUSIONS AND REMARKS	
7.1	Devices and instrumentations	301
7.2	Fresh concrete	302
7.3	Hardened concrete	304
7.4	Numerical simulations	305
7.5	Future aspects	306
A	**ANNEX A -RULES**	309
	REFERENCES	319
	ACKNOWLEDGEMENTS	333

PREFACE

This Ph.D thesis treats the propagation of ultrasonic waves in heterogeneous materials. It is widely known how waves propagate in homogeneous materials like metallic ones. But very few aspects are known about the propagation in the heterogeneous materials because of the complex behavior regarding these materials. The heterogeneity can be related with the intrinsic properties, elastic and chemical, of each phase of the material, or with the periodic or random arrangement of inclusions of constant or different shapes. Concrete is a common case.

In this work the first chapter gives a description of the main characteristics of heterogeneous materials.. In the second one, the methods of inspection on heterogeneous materials are presented, and in particular a view on NDT methods is discussed. The Ultrasonic Wave method is one of the more common NDT methods used to investigate the inner nature of materials. This method is well established in the medical field, but more studies are still needed for materials' science. With the aim to investigate on heterogeneous materials, concrete is considered. In chapter three the main characteristics of concrete are presented: the chapter discusses about the main constituents, namely aggregates, cements, water and additives. Fresh and hardened phases of concrete are also described. Chapter four presents the theoretical aspect related with the propagation of wave in homogeneous and heterogeneous continuum by presenting some aspects of micro-structured materials. In chapter four the signal processing is also presented, and an algorithm to process signals on heterogeneous materials is discussed. A prototype machine of ultrasonic test developed during the doctoral studies is presented, and in the last part of the fourth chapter FEM analysis and laboratory tests are discussed to validate the right working of the instrument.

Chapter five presents the results of laboratory tests conducted at DICAM department *fresh and hardened concrete, and the results of the investigation by mean of ultrasonic tests. Curve of velocity of UW in concrete during the curing time are determined and related with elastic modules. On hardened concrete, a database of 70 specimen is created. By using a cluster algorithm the Ultrasonic Test is able to predict the resistance of concrete with an acceptable level of confidence. A theoretical model is proposed and validated to explain the value of ultrasonic wave velocity propagating in heterogeneous media, and a model on resonant frequency is discussed.*

In chapter six a multi-scale finite element approach is developed to simulate the propagation of waves in heterogeneous materials. The model is based on the definition of an elementary cell (representative volume element or RVE) whose equilibrium equation are written based on a mesh-less approach. Follows a procedure that transforms the heterogeneous material in an anisotropic one. The comparison between numerical simulations conducted by applying heterogeneous models and the multi-scale mesh-less/FEM model shows a good agreement. Conclusions and future developments are given in chapter seven.

The author is grateful to the University of Palermo and prof. G. Giambanco for the great opportunity to develop in this work.

Palermo 04/2013

Fatti non foste a viver come bruti, ma per seguir virtute e canoscenza.
You were not made to live as brutes, but to follow virtue and knowledge.
A. DANTE

CHAPTER 1

INTRODUCTION

1.1 HETEROGENEOUS MATERIALS IN CIVIL ENGINEERING

Materials in Civil engineering are commonly computed as homogeneous, in order to simplify the modeling. However, the homogeneity is a macroscopic view of material in all its complexity. In order to understand local behaviors, an homogeneous model is not enough sufficient to evaluate mechanical behavior of the continuum of structures, but a richer model is need to know the local behavior. Observing materials at mesoscale, in fact, they are heterogeneous, constructions' materials are composed often of two or more constituents, different for nature and behaviors. The union of them constitutes a new one that has mechanical and chemical characteristics reflecting the average ones of the constituents. Usually heterogeneous materials are composed by a component conferring high mechanical properties at the final products, and a other one that confer continuity. A wide rule to obtain the average characteristics is defined as miscellaneous rule. Here the characteristics are defined proportionally per percentage of each components as below:

$$C = C_1 f_{1,\%} + C_2 f_{2,\%} \tag{1.1}$$

Where C is the average characteristic, C_i and $f_{i,\%}$ are respectively characteristic and percentage of each component. Materials of construction are employed in different

fields of civil engineering, as buildings, bridges, roads, as transportation field in aerospace and naval, and automotive engineering.

1.1.1 MANSONRY

Masonry is perhaps the oldest material used for constructions. It is constituted by natural stone elements, squared or shapeless, connected together by a binder paste of water and mortar. The mechanical characteristics of the masonry are linked with the characteristics of the stone and the mortar. A Ranking of the masonry, depend on the arrangement and shape of the stone elements. It is possible recognize brick squared masonry, if each stone element is smooth and prismatic shaped, the bricks are jointed each other by a regular strip of mortar, horizontal and vertical, the horizontal ones are called bed of mortar. Also an unshaped piece of stones can be mixed with a continuum of mortar, and glued together in a masonry called in sack.
In the case of shaped and unshaped mixed elements, it is possible that the external side of walls is made with regular bricks and a space between others is willed with mortar and unshaped stones. The characteristics of the masonry are related with the quality of the mortar and mechanical properties of the brick, that constitutes the masonry. kinds of mortar, can be classified by Eurocode 6, shall be identified on the basis of its characteristic compressive resistance MK where K is the cubic resistance value. The brick, can be based in clay, or rock. The mechanical properties of bricks are determined by direct tests on specimen. The final strength of the wall is obtained by direct test on three layer wall. However, Eurocode 6 suggests to adopt a resistance that to be attributed to the complex the value $f_k = k f_b^{0.65} f_m^{0.25}$ where k depend by arrangement of brick, f_b and f_m are the ultimate strength of brick and mortar. In elasto plastic constitutive models have been developed recently models that take into account the behavior of brick and mortar and

adherence between the two constituents, in particular in literature (Spada, Giambanco) are proposed two-phase constitutive models that take into account the degree of adhesion between mortar and brick.

(a) (b) ©

Figure 1.1: Masonry a) irregular, b) regular with stones, c)regular with brick

The constitutive behavior of masonry, can be obtained by an homogenization process. The Homogenization techniques permit to establish a constitutive relations in terms of averaged stresses and strains starting from the geometry and constitutive relations of the individual components. To consider the complexity of masonry, more information can be reached studying regular masonry structures, first of all is need to individuate the periodic repetition of the microstructure occurs due to a constant arrangement of the elements.

1.1.2 CONCRETE

Already known from the ancient Romans, the concrete is the building material most economic on the market. It is obtained from the mixture of water sand gravel and

binder. The binder classically adopted is the cement. However there are innovations related to particular types of aggregate special cements. The concrete belongs to the heterogeneous materials, because formed by the union of elements of different nature, and it consists, in mesoscopic scale, by a continuous matrix of cement paste with a presence of aggregates as inclusions. The aggregates are able to be transmit the mechanical actions thanks at the cement paste that binds them together. A more complete description of the material will be presented in Chapter 3.

1.1.3 BITUMINOUS

The bituminous conglomerate and a multiphase is a material consisting of a mixture of aggregates of various granulometry linked by bitumen, containing a certain quantity of air voids.

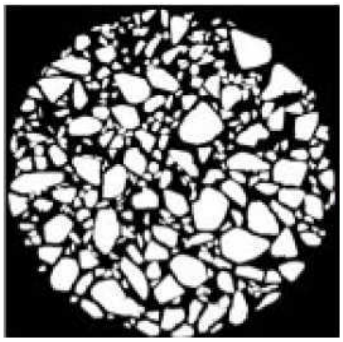

figure 1.2: Section of bituminous conglomerate

The bituminous conglomerate is therefore a heterogeneous material, whose mechanical behavior is strongly influenced by properties of the phases constitute, in particular on the characteristics of the aggregate (shape, texture superficial, skeletal structure, form, etc..), from the properties of the bitumen (complex

modulus, cohesion, etc..) and their mutual interactions (adhesion, absorption, physical-chemical interactions). The aggregate material that has multiple forms, surface textures and guidelines, in a typical mixture the size of the aggregate varies from a minimum of 0.075 mm to a maximum of 37.5 mm. Bitumen is also a material with complex properties that depend on the temperature and frequency load. It is very complex to predict performances of materials, such as stiffness, viscosity and ultimate strength. Employing some simplification and anyway possible to construct mathematical models that allow an adequate approximation physical properties of the conglomerate. Over the years, many researchers have developed microscopic models that provide fundamental properties of mixtures based on those of the constituent phases. Relevant properties of the material under examination, are modulus, creep resistance, tensile strength and properties at break. It is also relevant to predict the deformation response and performance of the road paving as a whole.

Buttlar and You (2001) had classified the different micromechanical models in several categories: models which did not provide the interaction between the particles and models that on the contrary, provided, empirical models, finite element models and discrete. The mechanical behavior of the concrete is determined by mutual interaction between the various heterogeneous phases that compose it. However, even in calculation methods more evolved, this material and schematized by a layer with homogeneous equivalent characteristics, the recent approach of micromechanics offers the possibility to accurately predict the behavior breakage of the bituminous conglomerate and to relate with some parameters such as the properties of the bitumen, the particle size of the aggregate and the degree of compaction (Dai et al., 2005). Figure 1.3 shows a brief synthesis of the models developed in literature and their authors.

Model Category		**Model developers**	**Applications at asphals**
Non-interacting particles Geometry non specified		Einstein Hashin	Schapery and Lytton Buttlar and Roque
Non-interacting particles Geometry specified		Hashin and shtnikman Christensen and Lo	Buttlar and Roque Shashdhar and shenoy
Particle interaction allowed	Simplified geometry specification		Chang and Meegora Rothenburg
	Complex geometry specification	FEM and MDEM methods	Kose

figure 1.3: Constitutive law for bituminous conglomerate

These models possess the benefit of reducing or even eliminating costly test characterization of the mix for the design of road pavements. The first two categories, which is not allowed the interaction between the particles, provide poor results in the modeling of the concrete, due to excessive simplification of the model in simulating contacts between the elements and the transmission of efforts through the skeleton (Buttlar and Roque, 1996-1997). However, these models have nonetheless expendable results in the study of special mixtures and of mastics, with whose name is meant a compound of aggregates, sand and fine particles dipped in a bitumen matrix (Buttlar et al., 1999; Shashidhar and Shenoy, 2000). The models that do not include the interaction between the particles are simple and does not

have the accuracy needed to be applied to conglomerates bitumen, which is very important in the interaction that occurs between the aggregates.

In order to develop a micromechanical model to simulate correctly material in question, must be conducted on the phases appropriate simplifications up the asphalt. The aggregate is usually much more compact than the bitumen and the reason is treated as a set of rigid particles of elliptical shape and variable size; unlike the bitumen and a material with elastic properties, plastics and has a behavior that is time dependent. It is assumed that the micromechanical system of transferring of load is related with adjacent aggregates and takes place through an effective area of binder, as shown in Figure 1.4. The force exchanged beetween particles in contact can then be decomposed into components normal Fn and tangential Ft when M.

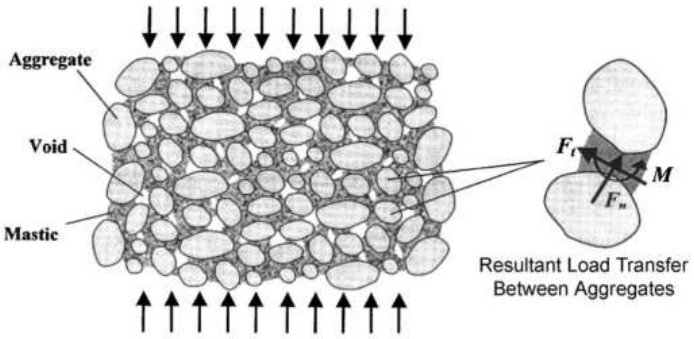

figure 1.4: mechanical model for bituminous conglomerate

If a axial tensile tests is conducted, the stress-strain diagram is as the one reported in figure 1.5 which ascending branch and characteristic of a type behavior softening, while the branch descending and characteristic of a failure criterion.

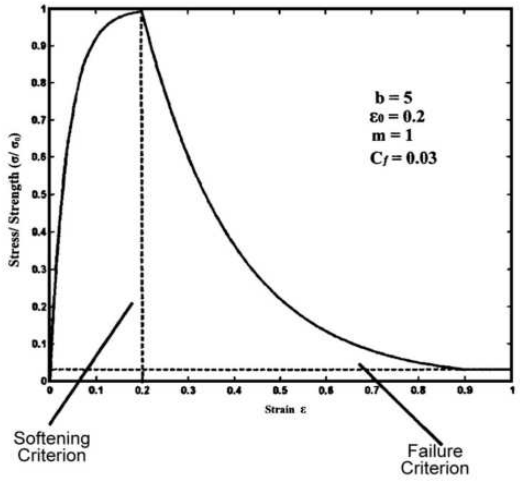

figure 1.5: constitutive law for bituminous conglomerate

During the compression tests it was observed that the space between pairs of particles occupied by bitumen decreases with increasing load.

Several studies proven that the modulus of the conglomerate and strongly influenced by the interaction that exists between the particles for this reason some models assume that the spaces aggregate and bitumen are modeled as a set of discrete bodies and distinct that interact with each other in mutual points of contact, which are responsible for the transmission of forces in the material.

Some studies (You and Dai, 2007)lead to predict the properties of the mixture of asphalt starting form the aggregate properties (Young's modulus, Poisson ratio, stiffness normal and tangential friction angle) and those of the bitumen (viscosity, elastic modulus, bitumen content). The particles are defined with a constitutive law of the elastic type, while for the binder, treated as an incompressible Newtonian fluid, and a viscoelastic link arranged with a pair of elements in series spring-damper (Voigt model) along the directions normal and tangential is hypothesized (Figure 1.6).

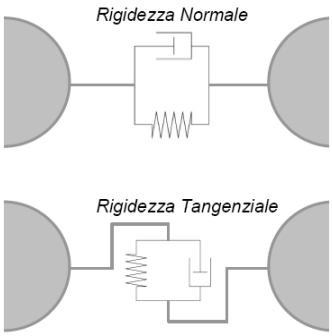

figure 1.6: mechanical model for bituminous conglomerate

1.1.4 FRP

The acronym FRP means fiber reinforced polymer. it is a material consisting of two or more insoluble components: a polymeric matrix and a an arrangement of fibers, these materials are also called innovative composite material to make a difference from classical composite materials as rebar reinforced concrete or mixed steel-concrete elements. Usually composites are bi-components: the component more resistant is present in the form of discontinuous phase, fibrous or particulate and is called reinforcement; the less resistant component is present as a continuous phase and it is known as matrix. The physical and mechanical properties of composite materials are related to:

1. the mechanical characteristics of the individual components;
2. the concentration of each component in the composite;
3. the shape, the size, distribution and orientation of the reinforcement.

The final properties of the composite can be achieved, in a first approximation using the "rule of mixtures". If Pf and Pm are the properties related with reinforcement and matrix, and X_m and X_f are the relative volume percentages of the

two components, then the corresponding properties of the composite Pc can be obtained as:

$$P_c = \frac{P_f X_f + P_m X_m}{X_f + X_m} \tag{1.2}$$

Obviously, the knowledge of the real physical and mechanical characteristics must pass through experimental investigations on the product.

The composite materials, in general, show considerable mechanical properties in the directions where are arranged the fibers, but much more reduced performance in the other directions.

Classification of composite materials pass through different aspects. A useful classification is related with the mechanism of resistance, which depends on the shape and orientation of the reinforcement. We distinguish between the fiber-reinforced composites, reinforced with particles or with the flakes. Particles and flakes have a random orientation. The fiber-reinforced composites can be constituted by a single layer or multiple layer, the fiber can be continuous (long) or discontinuous (short). The fiber reinforcement can be unidirectional or multidirectional random. It will consider fibrous composites because they are most used in the design and production of structural elements. Their success is due to the high strength / weight ratio (specific strength) and stiffness / weight (specific stiffness). Furthermore it is possible, varying the concentration and the orientation of the fibers, to obtain materials having the optimum characteristics for given direction.

The layer of a composite material is a bi-directional plate with thickness greater than 0.1mm, consisting of the reinforcement present in continuous fiber immersed in a matrix. The fibers can be arranged as unidirectionally or in shape of fabrics (woven mat). In these fabrics, fibers can be arranged at 90 °, or other angles, or randomly. The combination of more layers rise specific property of laminate. The

laminate can have all the layer with unidirectional fibers parallel (single ply) or more commonly each ply with different orientation (angle ply).

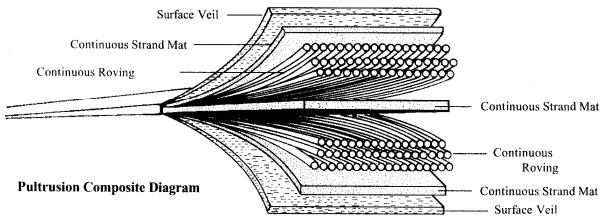

figure 1.7: Laminate scheme

It is observed experimentally that the resistance of a material increases significantly if it is produced in thin fibers. The explanation for this remarkable phenomenon, is due to the decrease in the number and size of defects (blowholes, inclusions, cracks) present in the fiber. The specific resistance of the fibers used in composites is, in fact, on average, about 10 times higher than that of traditional materials.

The fibers used in the production of composites are glass fibers , carbon fibers, aramid (Kevlar) and boron. The glass fibers are the most common, and are constituted by silic -aluminates, have high strength (σ = 2500-4800 MPa), good stiffness (E = 72-90 GPa) high resistance to corrosion and electric current, low cost . the carbon fibers, are obtained from poly-acryl nitrate, by heating up to 2500 ° C. We can distinguish two types: high-strength (high strength) σ = 7000 MPa and, alternately, high rigidity (high modulus) E = 960 GPa. The latter are obtained from the first by further increasing the temperature during production. The aramid fibers have high impact performance, and are commonly known under the name Kevlar. The fibers of boron are obtained from the condensation of vapors of boron

on a tungsten filament, and high costs have diameters larger that also confer a resistance to compression.

The matrix is the continuous phase of the composite material, it performs the following main functions:

hold the fibers together; to transfer the external load to the fibers and protect the fibers from damage due to mechanical action from environmental factors (UV, moisture, corrosion). In relationship with the materials of matrix, the composites can be divided into polymer metal or ceramic matrix composites.

The resins constituting the polymer matrices may be thermoplastic or thermosetting, depending on whether they are subjected to soften or not in the presence of reactors harden. Normally the thermosetting polymer are preferred, since they allow to achieve high volumetric ratios of fiber in the matrix (70-80%).

These have a chemical structure similar to the fiber, and then impregnate it better (high wet ability).The main thermohardered setting resins are the polyester that have poor mechanical properties (low resistance, high shrinkage, fragility), but also it is the cheapest and the most widely used for this, is then followed vinyl and epoxy characterized by good resistance, good adhesion fiber- matrix. The phenol and polyamide are suitable if you also require a fire resistance and low smoke emission combustion. Are added to the resin addition of additives which are intended to improve certain benefits, such as diluents to lower the viscosity during the implementation, flame retardants that increase its resistance to fire, pigments and dyes, fillers that lower the specific weight , rubbery additives which improve the impact resistance, catalysts that control the polymerization process.

1.2 OBJECTIVES

Non destructive testing lead to understand develop behavior of structures using approach able to preserve the integrity of materials.

Architectonic Hermitage of countries need to be preserved from time effects. Some ancient building are subjected at worsening, caused of seismic action, meteorological actions as wind, acid rain, snows, umidity.

Also, in some building of the beginning of century, normative approach of material was still not enough developed, and any qualification of materials was made.

In new building, activity of refurbish, renewal, pass through materials qualification. However, to qualify materials of built structure, the classic approach need to extract some specimen of materials and test them in laboratory. The removal of materials can be limited at some representative points of the structure, and cannot create static prejudice of structure. So, to develop destructive test need to transport specimens from situ to laboratory. A valid alternative at destructive test is the not destructive testing. Many are the vantages to use this class of tests.

Non Destructive testing and health structural monitoring (here in after NDT&HSM) are new field of science that lead to develop behavior of structures by investigate structures in situ, with no damage of It.

First of all, structures tested using NDT will be not destroyed, but only investigate in the real state where they are. NDT testing permit to investigate the structures in many points, with relative low cost of test, because NDT approach need less manpower, and the cost of advanced technology for conduct NDT can be amortized in some more test.

In Italy is present a large heritage of architectonic opera, and historical building, the national art patrimony correspond at the important percentage of the word art, seismic risk and time worsening are the main enemies of these building. In order to preserve them a campaign of Investigation is need, to qualify the materials of some

constructed building. To know mechanical characteristic of materials is important for establish with behavior could have the structure below seismic action however to implement systems of conservation of materials to prevent time actions.
Another aspect that in the last years raise up, it the quality of materials. More often authority and institution ask to construction company to use qualified materials, and also Italian rule, fix class of construction materials not by constituents but by quality in term of resistance (DM 14/01/2008).
Materials of construction, as concrete or masonry need time before to raise the final mechanical characteristics', at this time, it is possible to make destructive test on specimen collected during the construction time, to qualify materials. It is wise view, that if materials are not as in the project, Trouble could comes between construction company authority and customer or institution.
NDT and SHM method can be an aid tool to investigate state of materials during the process of maturation, and they permit to have a projection of quality of materials just with easy and cheap test on the just made materials.
It is understandable how NDT method can strong help designer of building to qualify mechanic properties of material with no heavy cost and damaging on the building, how they can aid company to know if their material have enough resistance, or it is need to adjust the recepies of the material.

1.3 OUTLINE OF THESIS

New sensibility of rules at the quality of materials is in recent past years is introduced. Seismic refurbish old building in object of owning national heritage of building, left for some years at the wellness of time. Relevant approach to understand real behavior of material is need. Classical approach give often average behavior of structures, but in particular cases, a local investigation is need to

understand how stress and strains works. The advance of science goal to describe materials though properties of all these constituent.

NDT method can reduce costs, time and level of damage for investigate the behavior of materials. NDT method in some cases are more appropriate of classical methods to determine quality and physical quantities of materials than classic methods. Also with NDT method the structural investigation can be conducted not just in some representative points of the structure, but is a strong quantity of tested points. With same level of test cost, an deepen investigation can be conducted, and better knowledge of characteristics of structure can be obtained.

In some cased NDT in the only approach to investigate structures, as in some building below the control of superintendence to conduct destructive testing can be pretty hard, because the destroying of part of structures. In these case only NDT can help designer for determine state of materials.

This project lead to investigate materials by mean of Ultrasonic tests, The choosing of ultrasonic test approach is related at the possibility of the method to be of easy application in investigation field, can approach different kind of materials switching field of frequencies, form stone, to wood, to metals.

Ultrasonic test is, in NDT, one of the more advanced field. One of the Strong aspect is related with the capacity of ultrasonic tools to be easily transported in workplaces, Test are simples, and doesn't need cumbersome other tools.

In commercial field are ready for use some devices for ultrasonic investigation, and some methods are implemented to qualify materials or to detect fractures leaks. More of there are applied in Welding field, and they lead to check If the welding part is continuum or there are some interruptions. In materials field, the UT are used to qualify material by the mean of time of fly, because it is related with mechanical elastic module of material. Even time of fly is detected for develop the deep of some void inside material by using a impulse-echo methods. All these methods investigate not the signal sent and the signal detect but the time that

signal need to travel to receiver from receiver, independently of signal shape of frequency contents.

A processing of signal can be conducted on the signals sent and detected to determine some other properties of material that these can be related with parameter of signals.

The purpose of these work is to describe the propagation of ultrasonic wave in heterogeneous media, by using the mathematical approach. Numerical simulation are conducted to verify the according with mathematical solutions. Ultrasonic tests on heterogeneous materials are conducted for observe the physical phenomena of ultrasonic propagation of wave in heterogeneous media. Mathematical model is scaled for follow the experimental phenomena simulated.

Concrete is, in Italy as in other parts of world, one of the most common and used materials, It is, as know, an homogeneous material. Quality of it are related with its constituents, and with the ratio between these. Ratios water/cement, aggregate/cement, sand/aggregates can be chosen according with the properties that are required. quality of cement, dimensions distribution of aggregates, quality of rock where aggregate came, and some additives can be added at the final product.

It is clear how an investigation on concrete as heterogeneous material is need, in order to obtain such of mechanical properties to suggest at designers level of performance of concrete material for repair and remaking interventions on building.

In some of these operas, the status of material is so changeable that a single test in a part of the structure is absolutely not representative of the all parts of it. It is need a strong testing campaign. And for do that, applying destructive method can be dramatic for the structure. In this way NDT is the only approach to quality materials, and the variation of it in all same structures

The project lead to characterize concrete in mechanical properties, by mean of ultrasonic wave. Concrete is approached as heterogeneous material, a scientific approach on mix design is given to control level of heterogeneity present in materials, The concrete is observed during all the curing time and after the 28days. Study are conduced so in fresh and hard concrete.

The investigation are conducted focusing on ultrasonic wave signals, In the work are investigate different wave shape as sinusoidal, saw square, hammer hit shapes, to qualify how ultrasonic shape can be give information on material, or to know with shape is more sensible to travel to materials. Different frequencies are tried, from 50KHz to 1MHz. Also the coupling between probes and material is investigated, tests are conducted, to use soaps, water, grease, viscous polymers, silicones'.

A signal processing analysis was conducted. Signals are processed in time space as in frequencies space, convolution integral of Fourier and wavelet are detected. Adaptive windowing and full analysis are used.

Ultrasonic test associated with a adequate signal processing can drive test to determine properties of heterogeneous materials as elastic module, resistance, degree of heterogeneity. These quantities allow designer to have best knowledge about mechanical aspects of constituents of material applied at the structures.

Misura ciò che è misurabile, e rendi misurabile ciò che non lo è.
Measure what is measurable, and make measurable what is not.
G. Galilei

CHAPTER 2

MECHANICAL TESTING OF HETEROGENEOUS MATERIALS

2.1 TESTS

Tests are procedures need to determine and qualify properties of materials. Tests can be divided according to the investigated materials, to the place where the tests are conducted: in situ or in labs, or by the grade of damage of tested materials in destructive and not destructive, for the mechanical or chemical characteristics, that test is led to determine the mechanical properties of materials and structures. The investigation can be conducted on a whole structure or on some samples of materials. In this section, tests on structures (i.e. dynamic analysis, velocity shear soil waves) are not treated.

Testing approach are divided in situ approach if the test is conducted in the place where opera is located and laboratory approach, through which a specimen of material is detected and test is conducted in the laboratory.

Tests can be conducted to determine compressive, tensile, flexural, shear resistance of materials, or to determine elastic and plastic tangent and secant shear, compressive or tensile module, or Poisson ratio. These quantities are the engineering quantities classically investigated.

The destructive tests determine directly these quantities by destroying the specimen, instead, in not destructive test, these physical characteristics are determined by using a correlation with some other quantities.
In each country, the committees have defined a standard method for conducting tests in order to compare results from different tests. Here are some of the main national and international committees enabled at this standardization:

ASTM American Society of testing and materials
BSI British Standards Institution
ISO International Organization of Standardization (European)
ASI Australian Standard International
DIN German Standard Institution (Deutsches Institut fur Normurng)
DGZfP German Society for non-destructive Testing
ACI American concrete Institute
NDIS Japanese Society for non-destructive Inspection
JCI Japan Concrete institution

2.2 DIRECT TEST METHODS

Destructive test is a kind of test where part of structure or material is destroyed in order to search the unknown characteristic.
The destructive classic test is the compressive or tensile test. Here, a specimen of material is extracted from the side where the structure is located and brought in a testing laboratory, where, using dedicated machines (as presses), the test is conduced. At the end of test, the mechanical qualification of material is knew, resistance and elastic and/or plastic module is determined, and as consequence, the specimen is destroyed, where the specimen is subtracted, tensional state of structure is locally modified. In relation with the kind of structures and materials, different destructive tests can be conducted, by different invasive levels. Looking at

some national approaches of destructive test, a classification of them could be done, the more common methods applied are charioting, press test, blending test, tensile test, 3 point blending test, dishes actuator, Brazilians test.
This thesis investigates the non-destructive testing method, here in after NDT, and for these, details about destructive approach are sent at specific bibliography.

2.2.1 THE ZWICK/ROELL & TONI TECHNIK 4MN

One of the more common test method is related with the use of a universal press machine, it permit the measure of the elastic moduli and the resistance of materials, in this paragraph it is presented the instrumentation used as destructive test adopted in this thesis.
The destructive tests were performed by means of a press *Zwick/Roell & Toni Technik*, capable of developing a load of 4 MN, controlled by hydraulic devices, operating under force or displacement control. The machine is controlled by an electronic unit *Tonitroll* interfaced with the user via a PC equipped with software V7.11 *testXpert* provided by the manufacturer. In figure 2.1 the universal machine is reported.

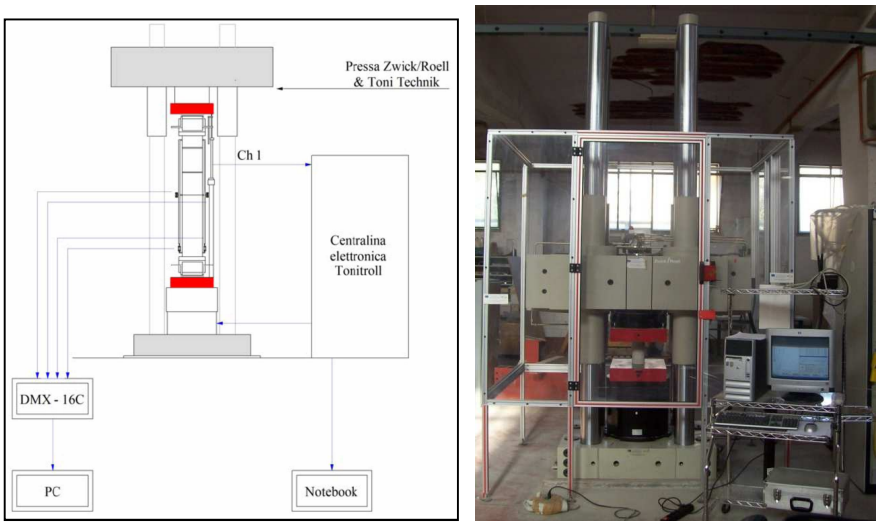

Figure 2.1. Scheme and picture of universal machine

For the measurement of displacement, 2 strain gauge of the type DD1 producted from HBM are used, they are reported in figure 2.2, this device are able to measure max diplacment of 2.5mm, with a sensitivity tolerance of 0.1%, the conversion factor is 2.5mV/V, the terminal part, in contact with specimen can be with dish or knife terminals.

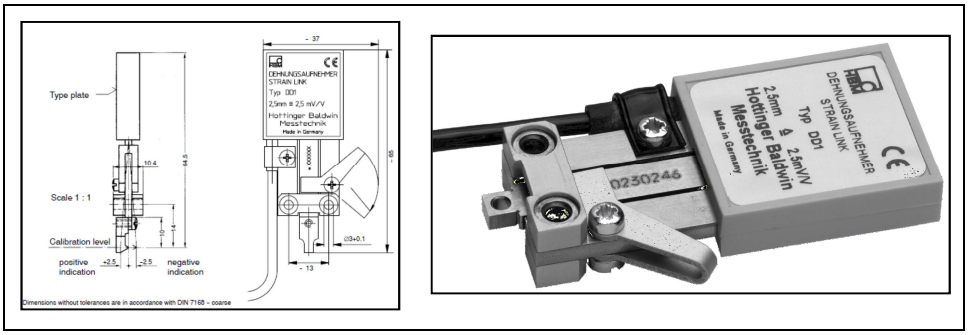

Figure 2.2. Scheme and picture of strain gauge DD1.

In order to measure the deformation ε is need to know the ΔL of the specimen. So strain gauges are hold on a frame, and positioned in two opposite lines of the specimen. On each side a graduated beam hold the DD1, and is possible to set the reference base of deformation measurement L_o. At each side, one couple of knifes is fixed (i.e. the upper ones), and the other ones(i.e. the lower one) are mobile. In this way two ΔL are measured, and ad average of ε can be conducted. As know the deformation is:

$$\varepsilon = \frac{\Delta L}{L_o} \tag{2.1}$$

The frame is adjustable in order to be adapted at cylindrical or cubic specimen, with different measures.

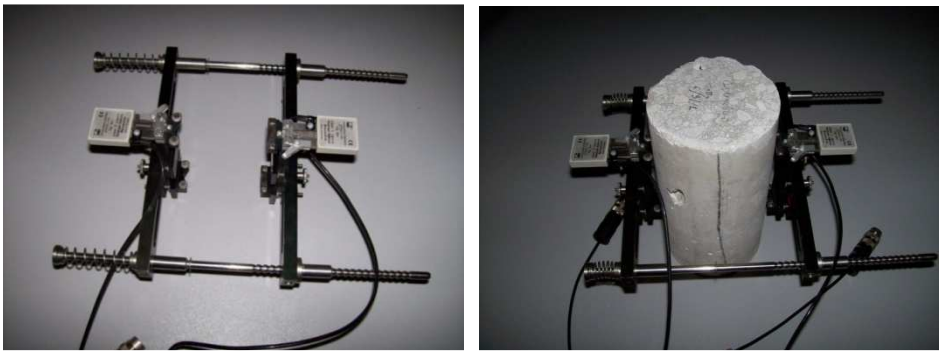

(a) (b)

Figure 2.3. (a)frame for Strain gauges (b)specimen with strain gauges

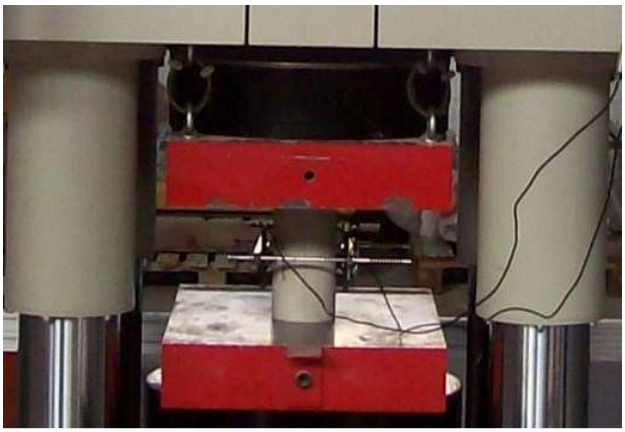

Figure 2.4. A specimen of concrete with strain gauges frame below the universal press

2.2.2 PROCEDURE FOR MEASURE OF ELASTIC MODULI

The procedure for the measure of elastic module of concrete is determined of UNI-6556. The test lead to measure Elastic secant module.

Specimen need to have a circular or square section, a ratio b/H need to be hold between 2.5 and 4, the test can be conducted on 3 specimen, with same curing history. Reference base of measure can be less of 1/3 of height, and non less than 2 times of maximum aggregate, dimension of transversal cross section of specimen can be measured with 1mm of precision.

Before starting the test is need to Know the break load of the specimen. The elastic module measurement must be conducted between levels of load between $1/3\sigma_{break}$ and $1/10\sigma_{max}=1/30\sigma_{break}$. (i.e. in the σ_{break}=30MPa, it means 1-10MPa interval), in order to be sure the elastic steam is considered. This elastic range must be divided in 3 equal intervals, and for each intervals [σ_{min} σ_{max}], in each step the gradient of load $\Delta\sigma$ need to be equal to 24.5±4.9N/(cm^{2}s) (the half speed used for determining resistance, to eliminate inertial effects)

For each of the 3 intervals .the test consists, , in the increase of the stress from to σ_{max}, to then be kept constant it for about 90 seconds, in the first 60 seconds going on the stabilization of the displacement at the strain gauges and at the load cell, and in the next 30 seconds displacements and stress σ_{upper} are measured. The specimen is then downloaded to the lower stress level, others 60second are of wait for the stabilization of measures, and in the next 30 seconds the new measure are read σ_{lower}.

The elastic secant moduli is obtained by:

$$E_{\sec ant} = \frac{\sigma_{upper} - \sigma_{lower}}{\varepsilon_{upper} - \varepsilon_{lower}} \tag{2.2}$$

The final elastic module is the average of the three values.

The chat reported in figure 2.5 is the σ–ε diagram divided in 3 parts for the elastic module measure.

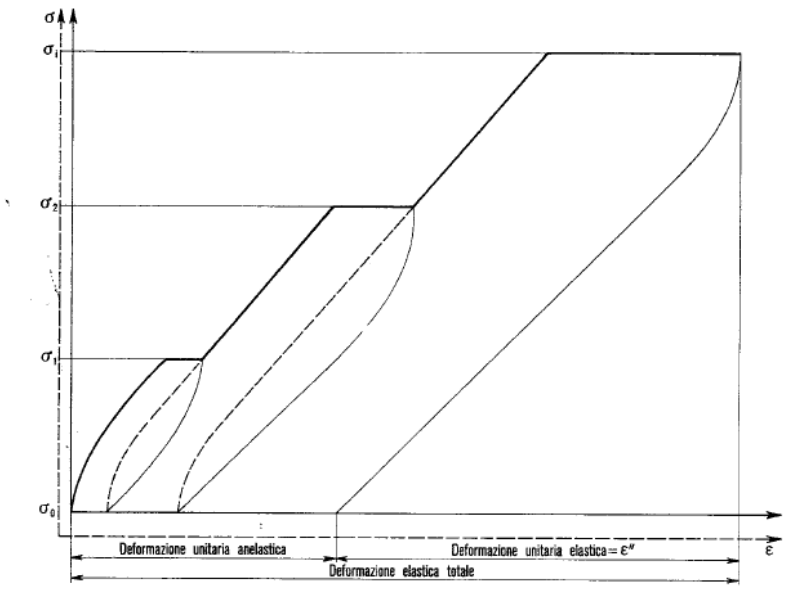

Figure 2.5 σ–ε diagram of UNI 6556

Afther the measure of elastic moduli, the specimen is loaded until it going at the breaking load.

2.3 NOT DESTRUCTIVE TESTING

NDT evaluation is an approach of testing conducted by mean of tools that not change natural qualities of materials, and doesn't need the destroying or subtraction of specimen from the examined structure. They can be applied for characterizing mechanical properties of materials or for searching internal or surfaced defects. tests are intended to character materials and the purpose is to determine mechanical constants as elastic or plastic module, Poisson ratio, resistances. Defects can be settled at different deep of specimen or structure. NDT method can examine elements with a qualitative approach to individuate the presence of defects, and then qualify dimensions and deepness of defects. Searching defects by ultrasonic-NDT methods, for example, is a good consolidated procedure in wielding field.

Some International and National committees are been applied to determine classification and methods to conduct NDT testing. Here is a brief review of the more common methods for heterogeneous materials.

- *PT - Penetrating Liquid Test*
- *RT - Radiographic Testing*
- *ECT - Eddy-current testing*
- *VT - Visual inspection*
- *MT - Magnetic Particle Testing*
- *AE - Acoustic Emission*
- *TIR - Infrared thermography*
- *UT – Ultrasonic Testing*

Specifically for concrete, as for heterogeneous materials, it is possible to individuate a subgroup of NDT, that use the principles of previous methods as:

- *Half-cell electrical potential method*
- *Schmidt rebound hammer test*
- *Carbonation depth measurement test*
- *Permeability test*
- *Penetration resistance or Windsor probe test*
- *Resistivity measurement*
- *Ground penetrating radar*
- *Radioisotope gauges*

The choose of the right method depends by the nature of materials, and objective of test. Some of these method are applied only to metallic materials, as eddy current, or magnetic method, because they take advantage of the ferromagnetic properties, some of these lead to develop defect, some other to qualify chemical properties of materials and from these to deduce historical properties.

NDT methods can be classified in relation to the investigate part depending if it is a volume or a surface. In a RT UT AE TIR the whole considered volume can be analyzed, PT or VT however can produce information only on the surface or in sub-surface part as ECT or MT.

2.3.1 PENETRATING LIQUID TEST (PT)

Scope of Penetrating liquid test is to verify the presence of leak of fractures inside the continuum of material, as well the measure of opened porosity of material.

This technique was born for metallic materials but can be used also for heterogeneous, a requirement is the non porosity of material, and the not reactive behavior of with liquids.

The test requires that the liquid substance is placed on the piece to be tested. This substance is absorbed by the surface defects and sub-surface by capillarity and gravity. Subsequently, the capillary rise is highlighted by a second substance called detector. Some visual indications (spots) are formed for the location of the defect. The time required for liquid to penetrate depends on the viscosity, which means that more viscous products generally require penetration times longer. In Figure 2.6 is shown, schematically, a fault and the disposal of the liquid with respect to it. The capillary force driving the liquid inside the crack (of radius r) due to surface tension γLV agent with contact angle θ.

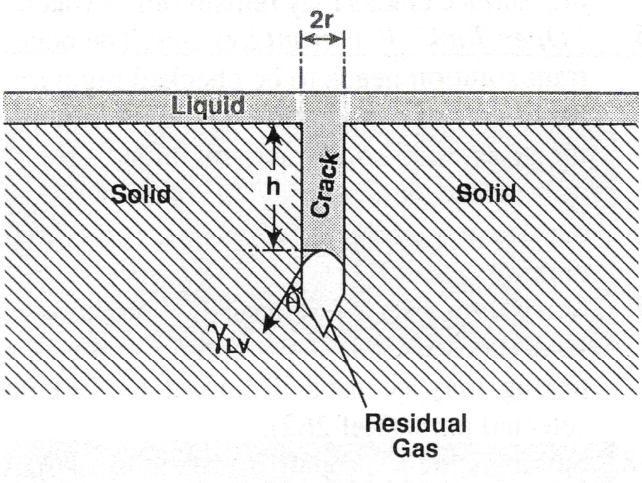

Figure 2.6 Penetrate liquid scheme

More specifically, the phases of the procedure are:

- Preparation of the surface. In this phase are removed by mechanical or chemical parts, as contaminants, deposits, oil, paint, water, residues that could potentially prevent or limit access of the penetration in the defects.

- Application of penetrating liquid. The penetrating liquid is applied by dipping, brushing or spraying. It is need that liquid create an uniform layer for cover the entire surface to be examined. In general, the variables to take into consideration concern the sensitivity required, the type of material to be tested, the number of components to be tested, the extension of the surface to be checked. For example, the sensitivity required, understood as the ability to detect very small defects, determines the choice of using a fluorescent penetrating liquid or a visible one. Generally, fluorescent penetrating liquid admits the possibility of detecting smaller defects because the eye is particularly sensitive to such claims. A visible piercing liquid is more appropriate if the test lead at identifying visible defects in the analysis of large or very rough surfaces. In these cases a high sensitivity would give rise to numerous indications irrelevant.
- Waiting. The penetrating liquid must be left to act on the surface for a time sufficient to allow the maximum possible absorption by capillary action on the part of plate with the defect. The waiting time is usually a specific characteristic of the product used and it depends by the viscosity; generally it takes between 5 and 60 minutes.
- Removal the excess penetrating liquid. The excess penetrating can be removed from the surface by using a rapid evaporation solvents, or a sponge.
- Application of the detector. A thin layer of the detector is subsequently applied on the specimen in order to draw the penetrating trapped in the defects on the surface, until it will become visible. According to the principle of operation it is possible to distinguish: fluorescence detectors, the fine particles of the substances development reflect and refract light incident ultraviolet, and increase the effectiveness of the effect of

fluorescence; white detectors if the liquid create an effective level of contrast with the red color of the penetrating liquid.

- Examination of information. In this phase a visual inspection is conducted employing an appropriate type of lights. The examination must be made after a certain time, after applying the contrast liquid; detection time is between 7 and 30 minutes. Relevant, non-indicative and false signals are observed. the indicative signals includes lines (jagged cracks), broken lines, small round holes (related to the presence of gas porosity induced by high grain size). The main advantages of this test method are summarized below.

The method is highly sensitive to the presence of small surface discontinuities; It can be tested on metallic and non metallic, magnetic and non magnetic, conductive and non conductive specimens; large areas and volumes can be inspected quickly and cheaply; complex geometries are commonly tested; the availability of liquid penetrating spray format allows you to perform the test anywhere; consumables (penetrating and revealing) can be acquired with relevant low cost.

There are also drawbacks that limit its applicability, the most common are mentioned. The ability to view only or surface defects or the ones that lead to the surface; the method is applicable only in non-porous materials; It is needed a particular care for preparing the specimens; the need for early treatment and a storage of chemicals used; if defects are too small, they can be not penetrable by the liquid; the interpretation of results is often subjective.

2.3.2 RADIOGRAPHY (RT)

The x-ray is the technique that allows to obtain images of the interior of a solid by means of impression of a photosensitive member (film, screen, etc.), by ionizing radiation such as X-rays or γ rays. The mechanism of formation of the image is

related to the different absorption of radiation in the medium in function of the thickness variation, of different chemical constituents, for non-uniformity in the density, the presence of defects. The information obtained from a single control is two-dimensional X-ray. Must therefore be integrated with other X-rays or with other methods volumetric that any discontinuity can be fully characterized.

The radiation energy is emitted by a radioactive source which propagates in the space. The propagation of radiation is electromagnetic wave phenomena, treated as continuous or discrete packets of energy (photons). In particular, we say the ionizing radiation carries sufficient energy to produce ions in matter. The unit of measurement that is used to quantify the energy of the radiation is electronvolts (eV). Among the ionizing radiation include:

- α. It is a particle emitted from the nucleus of an atom that contains two neutrons and two protons that a nucleus of an atom of He without electrons;
- β. High-speed particle, identical to the electrons, emitted from the nucleus of an atom;
- γ. Electromagnetic waves (or photons) emitted from the nucleus of an atom;
- X-Rays Electromagnetic waves (or photons) due to changes in the energy of the electrons.

The X-ray and γ- ray may penetrate into the field propagating in a straight line to the speed of light. They are differentially absorbed and produce photochemical effects on photographic emulsions. X-rays are produced whenever a substance is bombarded by electrons at high speed. Are normally generated by tubes of Coolidge supplied with direct current. The γ-rays are formed by the disintegration of a radioactive isotope. Radiological sources most used are cobalt (Co-60), iridium (Ir-92), cesium (Cs-173). The radiation originating from the cobalt can penetrate a steel plate of a thickness of more than 20 cm. Compared to the X-ray source has a

smaller size. Moreover, their penetrating power is high compared to a relatively lower price compared to some X-ray equipment. Another advantage is that it requires no power source. However, the images that are obtained are equipped with little contrast and the method has significant safety problems.

Figure 2.7 illustrates the radiographic procedure. The source originates has a divergent beam of radiation that passes through the specimen. On the inside, this beam is absorbed differently according to the physic-chemical characteristics. Finally, it impresses a sensitive film, a fluorescent screen, a photon converter (scintillator). The image that is obtained (gray scale) must then be interpreted to assess the presence of gaps and their characteristics that produce different levels of image density.

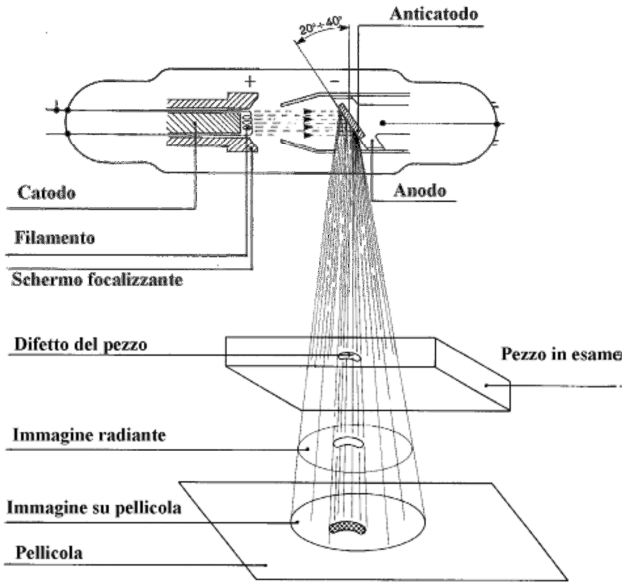

Figure 2.7 Representation of the radiographic procedure

It is possible to observe how defects appear represented in different ways (cracks oriented perpendicularly to each other) in the images in dependence of the

orientation of defects. Because the discontinuity oriented parallel to the direction of propagation of the beam appears more clearly distinguishable from the same one oriented perpendicularly to it. A schematic image is given in figure 2.8

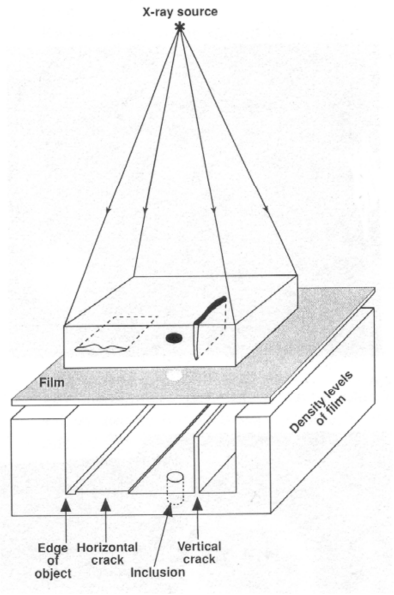

Figure 2.8 Display of defects

X-rays produce an image variously contrasted in relation with the attenuation that occurs as a result of phenomena of scattering and absorption. Scattering (dispersion) is the phenomenon where a part of the rays, after passing through the absorbent body, they follow different directions respect the incident ray angles. This radiation is also called diffuse radiation. The absorption is the attenuation of the intensity of a ray when passing through a material. This attenuation is proportional to the intensity of the ray and the thickness of the material. The constant of proportionality is called the linear absorption coefficient and expresses the fraction of energy absorbed per centimeter of material traversed. During exposure to the rays, a fraction of radiation that pass through the test piece and has

not been absorbed by the radiation and scattering will go to impress a film. Depending on the thickness of the material, of the defects present, or the presence of any inclusions of materials in different absorption coefficient, the radiation undergo a different level of attenuation. The ray finally goes to affect the film, impress in different ways with different densities of blackening. The rays can be detected using a variety of media such as photographic film, ionization chambers, scintillators, geiger counters, etc.. In industrial practice, the radiographic film is by far the most used.

The characteristic parameters of a radiographic image are: the contrast, the definition and sensitivity. The contrast can be defined as the difference in density that is recorded in the film, from the existence of a variation in thickness or density of the radio graphed piece. This parameter is particularly critical for the purposes of the goodness of the radiographic control, in fact a defect can be detected in the image radiographic precisely because of the contrast between the density of its image and the density of the surrounding material. More significant is this difference more easier becomes to trace the defect within the piece.

The radiographic definition is a measure of how the transition between adjacent regions of different density radiography. Obtain a high definition means to be able to distinguish clearly in the edges of the piece the contours of any discontinuities, whereas, when the definition is poor, the image appears veiled and t is difficult to read it. The sensitivity radiographic conventionally expresses the minimum difference in thickness of the test material that may be detected on the final image, as assessed in the direction of the primary ray. This parameter has a direct feedback on the clarity with the radiography is able to highlight the discontinuities in the piece X-rayed. The practical evaluation of radiographic sensitivity is effected through the use of so-called "deepness meters" or "Image Quality Indicators" (IQI). The most widespread type is that of IQI wire, which are constituted by a series of seven wires of different diameter pressed on a plastic support. The radiographic

sensitivity (percentage) is calculated as the ratio between the diameter of the thinner wire visible on the radiograph and the thickness of the work piece X-rayed. In recent years, moreover, have been developed computational methods aimed at the image analysis, which allow through a digital scanning of images, to obtain an assessment of the state of damage of the specimen to be inspected.

2.3.3 EDDY CURRENT TESTING (ECT)

The eddy current inspection (ECT) is a non-destructive test that uses the principles of electromagnetism. With this method may in fact be detected surface defects such as cracks and corrosion fatigue, or sub-surface, as inclusions and voids. This method often used for metallic materials is used also in reinforcement concrete, the method is used to evaluate level of corrosion of steel or the diameters of internal rebars. One of the more common applications of the eddy current , is the pacometer method.

In this test a coil (probe) is subjected to an alternating current, with a variable frequency between 50 Hz and 5 MHz. For the phenomenon of electromagnetic induction generates a magnetic field. This magnetic field is not constant in time but increases when the alternating current reaches the maximum, and decreases when the current is zero. If another conductor is brought into proximity of this magnetic field, a current will circulate in it, according to the Second Law of Faraday. The currents induced in the conductive material allow you to test it, move in closed circuits, normally circular, called eddies (vortices). They generate a secondary magnetic field which causes a change in the impedance of the coil. The impedance Z of a circuit for alternating current in which there are resistors and inductors is a vector quantity of which the resistance R and inductance L are respectively the real part and imaginary part: Z=R+iL. For these circuits continues to be valid the Ohm's law in form i=Volts/Z. The change of impedance Z is measured and placed in

relation to the characteristics of the defect. The impedance increases due to the distortions of the induced currents in the regions of the sample where there are discontinuities such as cracks or changes in characteristics of the material. By viewing impedance changes when you slide the probe along the sample is obtained with the defect known as "eddy current signal." The peak-to-peak amplitude of this signal provides information on the severity of the damage. The phase angle of the signal with respect to alternating current depends instead on the position or the depth of the defect. The variations in the phase and intensity of the induced currents can be monitored using a second coil "research".

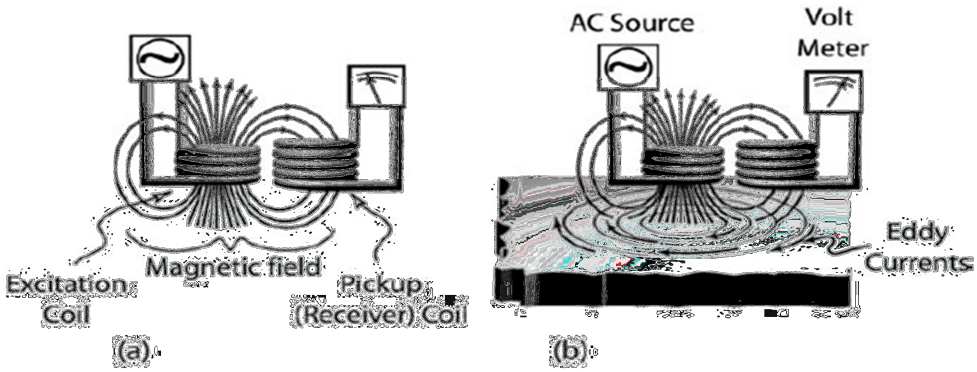

Figure 2.9 eddy current scheme

The main parameters that have influence on the induced currents are the electrical conductivity of the material. The flow of induced currents on the surface of the sample increases with the conductivity. The magnetic permeability, which indicates the trend that has a material to be magnetized. Characteristics in non-ferrous and high in ferrous ones, its value can vary significantly even within the same material because of particular local states; the frequency of the alternating current, which has a great influence on the depth of penetration of the induced currents in the material. This depth decreases with increasing frequency, as well as the

conductivity and permeability. With this method, different types of inspections and measurements can be performed. In fact it can be used to: search for defects; measurements of internal metallic thickness of the sample; thickness measurements of layers of different materials; measurements of conductivity for the identification of a level of corrosion. The advantages of this technique are: sensitivity to small defects; the determination of surface defects and sub-surface; the immediate response; the easily portable instrument; the surfaces to be tested do not require special preparation; do not require contact with the sample; it is used to test materials of various shapes and sizes; the process is easily automated. Some limitations of the method are: the applicability only to conducting materials; the surface must be accessible to the probe; finishing and roughness of the surface may interfere with the results; the maximum thickness is inspected is pretty limited in relation of the impedance of concrete; defects oriented parallel or tangent to the induced currents, which are therefore not significantly disrupted, and cannot be identified.

2.3.4 VISUAL TESTING (VT)

Visual inspection is the simplest and oldest form of evidence that may provide information on the degradation of structures. It is based on the use of light as a means of detection of surface discontinuities on any type of material. This survey methodology is very susceptible to the experience and skill of the operator. Can be conducted to the naked eye or with the aid of optical instruments, among which the most important are the microscopes, endoscopes, the micro-cameras. The introduction of optical fiber technology always introduces new possibilities of investigation. It is reasonable to assume that both liquids penetrating the magnetic particles are aids to visual inspection.

The discontinuities detectable with this type of control are cracks, corrosion, contamination and defects of junction; in each of these cases the operator need to have the task of interpreting the images observed with the naked eye, documenting where it is necessary.

Direct inspection, which requires accessibility by the operator at the surface inspected, is added to the use of precision instruments, optical suitable for inspecting hollow bodies of non-accessible form also complex. The endoscope is basically constituted by an outer sheath rigid or flexible, variable length, to the front end of which is incorporated an optical device (lens and camera) able to reproduce the image of an object placed in front of the instrument. The illumination of the area under examination is carried out by a small low-power lamp positioned close to the lens, an integral part of the endoscope; the image is transmitted to the eyepiece, located at the rear end, via an appropriate system of prisms and lens positioned within the sheath or in the monitor if the devices are electronics.

2.3.5 MAGNETIC PARTICLE (MT)

This method is related with ferromagnetic materials, frp with metal based matrix, of ceramic based matrix with metal reinforced dispersion are often investigated with these methods.

The non-destructive testing by means of the magnetic particles is a method for locating surface defects and sub-surface in ferromagnetic materials. The verification MT provides for the magnetization of the material that is meant to be evaluated. The magnetic particle, in order to detect discontinuities in the components under examination, takes advantage of the magnetic fields and of small magnetic particles as metal filings. The unique and critical requirement for the application of the technique in question is that the object under observation is

made of ferromagnetic material such as iron, nickel, cobalt or some of their alloys; if this condition is not met would not be possible to magnetize the material to a level that will make the results of the verification reliable.

Using the control magneto-scopic it is observed that when the object to be tested is magnetized the discontinuities that are located in one direction, generally transverse to the magnetic field, determine a deviation of the flow lines of the magnetic field itself. If the defect rises to the surface part of the flux lines of the magnetic field are dispersed over the surface itself. To highlight the irregularities is sufficient to spray, on surfaces considered, adequate suspensions of ferromagnetic powders, colored or fluorescent. The particles are concentrated aligning along the flow lines of the magnetic field, forming a "profile" of the discontinuity which generally indicates the location, size, shape and extension.

The examinations magneto-scopic exploit the ferromagnetism of the materials to highlight the anomalies of the flux lines of the magnetic field near the surface irregularities. In general the flow lines, which represent the intensity of the local magnetic field, through a material such as steel (generally ferromagnetic metal at room temperature) in a uniform manner but, in the vicinity of a discontinuity thicken or disperse, deviating locally and creating an abnormality of the magnetic field at the edges of the defect.

A process very important to reliably detect defects is the correct magnetization of the sample. By means of an electromagnet can be created in the test sample a magnetic field. Such an instrument can in fact be used to close the magnetic circuit between two pole pieces, generally adaptable to its geometry (yoke), and then create an internal magnetic field, or it is possible to generate this field directly in the sample by the passage of electric current (stanchions). The magnetization is important because in order to reveal defects in the best way, they must be oriented in a direction perpendicular to the flow lines of the magnetic field. Are distinguished essentially two basic types of magnetization or the longitudinal and

the circular one, which may be used individually, alternately or suitably combined with each other.

In order to obtain an indication of the defects in the materials under control MT, the magnetic field that affects the analyzed sample, must meet the discontinuity at an angle sufficiently large to cause the localized distortion of the force lines of the magnetic field: the best results are obtained when this angle is 90 °, thus the size, shape and direction of the discontinuity are very important. Observing the figure 2.10, in which a sample is magnetized in a circular manner, it is noted that in these conditions an irregularity, such as that indicated by the letter A, can not be detected because it is regular in shape and lying in a direction parallel to that of the field magnetic. While in the case indicated by the letter B if the discontinuity, while lying parallel to the magnetic field, has an irregular shape there is a good probability that it will be highlighted even if the indication will be weak. However, when they have defects which the predominant direction is 45 ° with respect to the magnetic field, as in the case of C, D and E, the conditions are more favorable but depend on the shape and size of the discontinuity.

This inspection techniques is less bound to subjective errors of the operator and in addition does not necessarily require the perfect cleaning of the surfaces prior. So, if properly used the magnetic particle, is more rapid, less labor intensive and more effective than the method PT, but it is not very suitable for examining the integrity of the surface of materials with surfaces too rough, wrinkled, threaded or too complex geometry. The minimum size of a defect can be detected with magnetic particle and mainly depends on its distance from the surface.

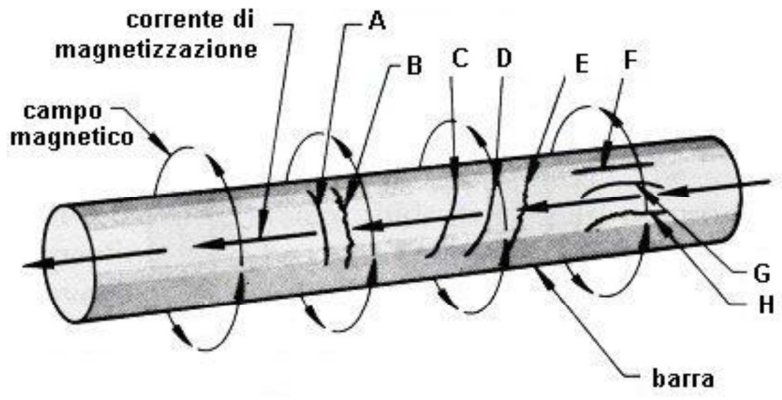

Figure 2.10 Sample subjected to magnetic particle

Among the disadvantages of the method exists the transportability of the test instrumentation; in fact, the technologies for the magnetization, in general, are bulky and require the use of a significant source of electrical power to activate the magnet.

2.3.6 ACOUSTIC EMISSION TESTING (AE)

The acoustic emission Test (AE) is a passive method of investigation, and requires, for its application, that the specimen is capable of producing noise, as urged by mechanical action. The methodology in question is used mainly during the course of traditional mechanical tests. The defects active, while they are forming or are increased, generate elastic waves which can be picked up by receivers. The acoustic emission technique is so effective in locating shows fractures of active structures and artifacts in real time. A prerequisite for an effective monitoring system is to have a permanent acquisition with a high rating. Many of the characteristic parameters of signals as the amplitude, time of flight, and the energy content are

analyzed in real time and obviously related with the possible presence of a fracture. The simple location of the defect, is made through a procedure quite direct providing for the acquisition of the flight time by more control points. Moreover, it has now appropriate techniques to identify the type of defect. Instead using AE is possible to localize the defect during its formation, as a triangulation by the appliance of minimum 3 sensors, and is possible to reconstruct evolution of cracks inside a materials, during a load history.

The success of this non-destructive technique is mainly due to the possibility of real-time analysis.

As shown in figure 2.11, a specimen is loaded, and brought at the formation of leaks; during the formation of leaks it produce a noise, sensors are glued with the specimen, and connected with a PC, the noise starts from crack and travels through the material to the sensors, the AE instrument, knowing property of material, is able to process the signal and localize the defects.

However, what constitutes a limit to its use is that the test is not able to detect defects existing because, as already discussed, it is precisely the occurrence of the defect which produces an emission noise.

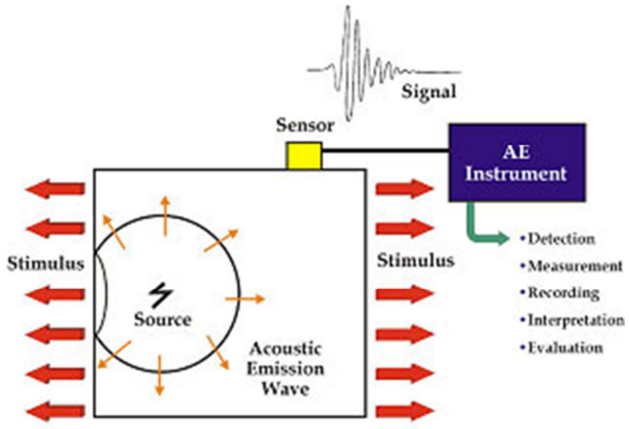

Figure 2.11 Procedure for Acoustic Emission

Other advantages are the ease of testing, the good portability of the instruments. Among the negative aspects, it will highlight the high cost of the equipment for detection of acoustic emissions and the need for an external stress that induces the noise emission of the specimen.

2.3.7 THERMAL IMAGE INFRARED (TIR)

Infrared thermal image is based on the principle that the anomalies of the surface of a material can be found in differences of surface temperature due to the different distribution of heat flows through the areas affected by defects. thermal image is capable of picking up the emission of thermal radiation emitted from the surface of the material and produces a visible image. The image translates the thermal signal, which is influenced by the presence and extent of an internal fault. Most applications involve the use of a thermal camera. Sources are used as active or passive flash lamps or solar radiation. A very common configuration is the thermal image pulses in which induces a flow of heat in transit, monitoring the change in thermal surface over time.

Advantages of the using of this technique in the monitoring of the structures consist in the rapidity with the test run and the ability to inspect large areas, as well as the ability to estimate the extent of the defect. Some drawbacks, however, are due to the influence on the proof of the nature of the surface, and by necessity, sometimes it needs to heat uniformly the surface before being able to observe the thermal emission. In the case of analysis of buildings, for example, the presence of heating will greatly influence the outcome of the tests. The equipments, in general, are easily transportable. The mapping of the thermal gradients measured, is always associated with an image analysis system that can process these gradients for the characterization of material properties or for the identification of the defect.

Through experimentation TIR is possible to qualify the material, known as the power of the thermal source, and the temperature detected on its surfaces can correlate the heat transmitted with the mechanical characteristics of the specimen. In figure 2.12 a thermocamera is shown.

Figure 2.12 Thermo-camera

The TIR is often used in electrical field, the joule effect is the heating of cables for effect of electrical dispersion, so, in these way, to analyze electrical connection is possible to establish quality of connections; another application is related with thermal bridge in walls, the presence of cold areas is symptomatic of a leak in wall connections; Sometimes TIR is used to measure the uniformity of a surface, as, if in a wall of brick and masonry, it can be relevant to investigate the localization of joints and bricks with no removing of plater, for this purpose, you can shoot a camera pictures in the wall, the main problem is the necessity to have an uniform grade of temperature in the other side of wall, this is classically obtained by testing the structure during a sun day, otherwise it is need to heat the surface.
Another important application is related with the overeating of materials during the plastic phase in a destructive test, the increment of heat in the point where fracture is located can be measured and related with the losing of energy of specimen. Many others applications can be conducted, easily and quickly just using the TIR method.

2.4 VIRTUAL TESTING

Virtual testing in composite materials a technique based on mathematical model applied to well-characterized atomic and molecular arrangements. The simulation of the spatial distribution of component of heterogeneous material lead to develop properties of its. The virtual testing of cement and concrete is a computational test based that starting from ideal model, knowing chemical composition of the material, the correct proportioning and arrangement of atoms, look to find properties of materials. This idealized model, however, is still long away to be reached with modern-day computers.

Science-based virtual models need high quality of data as input to reach a careful characterization of the materials. In these models there are some fundamental parameters determinate from empirical testing. Measuring the fineness of aggregates can give a characterization of a cement powder but this should be not enough to provide to an useful data for a model without an hypothetic distribution of grains. A careful measurement of the cement particle size distribution (PSD) by using laser diffraction can help the computer to model the continuous. Other technique are need to be applied to built a models close with the real material. In figure 2.13 a cube of concrete is reported, usually, in the Virtual Testing different colorations are used to recognize grain distributions.

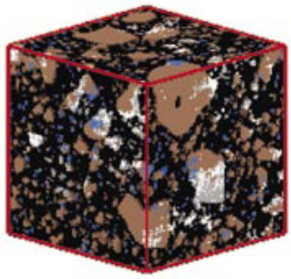

Figure 2.13 A typical virtual testing image

2.5 THE SONREB METHOD

One of the more common NDT method used in heterogeneous materials as Concrete is the *Sonreb method*. It is a combined method that use ultrasonic emission and the *Schmidt Hammer.* In This method, classically a correlation curve is determined on a set of concrete specimens extracted from the structure where the test have to be conducted, after to characterize the correlation between resistance, velocity of wave and rebound index. The resistance on specimens is determined by destructive test on them.

Afther to have the formulation, it is possible to investigate resistance of structure constituted form the considered material for the developed correlation.

However, some researcher have tried to develop a standard relationship that can be available for all concrete structures. These methods come from a characterization of correlation curves by using huge database of specimen.

Tuscany region in a local rule suggest 3possible correlations that can be used. Here we report these three law as representative of these approach.

1- Gasparirik "*Prove non distruttive in edilizia*" AIPND 1992- Brescia

$R = 0.0286 S^{1.246} V^{1.85}$ with R=[MPa], V=[km/sec]

2- Di Leo A, Pascale G. "*Prove non distruttive sulle costruzioni in cemento armato*" Conferenze SIAE 21.10.1994 Bologna

$R = 1.2 \cdot 10^{-9} S^{1.058} V^{2.446}$ with R=[MPa], V=[m/sec]

3- Giachetti R. Laquantini L. "*Controlli non distruttivi su impalcati da ponte in calcestruzzo armato*" Univ. Di Ancona, nota tecnica 04,18980

$R = 7.695 \cdot 10^{-10} S^{1.4} V^{2.6}$ with R=[Kg/cm^2], V=[m/sec]

Some others relationships it is possible to find in literature, but, ase these ones, some of them upper estimate the resistance of concrete, and don't have efficient affordability to accept resistance of material.

2.6 THE ULTRASONIC METHOD

The Non-destructive testing with ultrasound is related with the phenomena of elastic wave propagation in solids, liquids or gases. European committee regulate the test standard by the UNI EN 12504-4 2005. The waves are transmitted thought a material specimen, during the travel inside the materials they are attenuated, reflected, absorbed or diverted depending of the discontinuities and heterogeneous level.

The phenomena are based on the effects of vibrational propagation of pulses applied to a solid medium. They are based on two principles:

• the speed that the waves are propagated in the medium is function of the elastic properties (Young's modulus and Poisson's ratio) of the medium and its density;

• the lack of homogeneity due to slots, degraded areas, cavities, affect the speed and the propagation of the waves.

The ultrasonic investigations, therefore, allow the determination of the mechanical characteristics of the materials, through the analysis of the propagation of elastic waves. This technique allows us to assess the degree of homogeneity of the material and the presence of fractures, cavities, delamination.

The UT method is certainly the most widespread than other non-destructive methods used for the detection of mechanical properties and internal defects of materials. This common use is due to: the ease of conduct an examination, the speed of execution, the high level of sensitivity. The main advantages provided by the control Ultrasonic compared to other methods of non-destructive testing are:

- greater penetration in the middle, a feature that allows you to detect discontinuities that are located within the material;
- high sensitivity that allows the detection of very small discontinuity;
- Improved accuracy in determining the location of internal defects in the assessment of their shape and orientation;

- accessibility from only one side of the structure;
- volumetric control of the piece from the upper surface to the lower one;
- portability.

Among the limitations of the method are known:

- the difficulty in the control of pieces of complex geometry;
- the difficulty in controlling the high acoustic attenuation materials (wood, concrete and ferrous and non-ferrous coarse grain) or high temperature;
- the sensitivity of the test conditional on the state workpiece surface;
- the relative difficulty in the interpretation of the signals, which requires a prolonged experience and a specific training of the personnel.

2.6.1 THE CONTROL TECHNIQUE FOR CONTACT

The technique for contact is divided into two basic methodologies:

- *technique for reflection (pulse-echo);*
- *technique for transparency.*

The *technique of reflection* allows you to receive and evaluate the reflected waves from the discontinuities or areas bordering the component. This method requires a single transducer that functions as transmitter and receiver; for these reasons, this is the most commonly used. With this technique, if there are no discontinuities in the specimen observed only the echo of the bottom given by the reflection of the final surface. Instead, if along its path the wave encounter a defect, an intermediate echo is creates that wave will received temporally before of the echo due at the reflection of the ultrasonic wave with the opposite surface , and the defect is so detected.

The resulting echo amplitude depends of the energy that the transducer receives, due to reflection from any surface. In the case of the presence of defects in the

material, the energy that the wave is reflected towards the transducer is a function of their size, angle and distance from the source. Being constant the energy emitted by the transmitter, if part of it is reflected by the defect then the bottom surface will receive less energy to reflect, then the echo of the bottom will be smaller than the echo in the case without discontinuity; also the power of the peak echo is the energy reflected by the defect that arrives at the receiver a tipical chart is shown in figure 2.14.

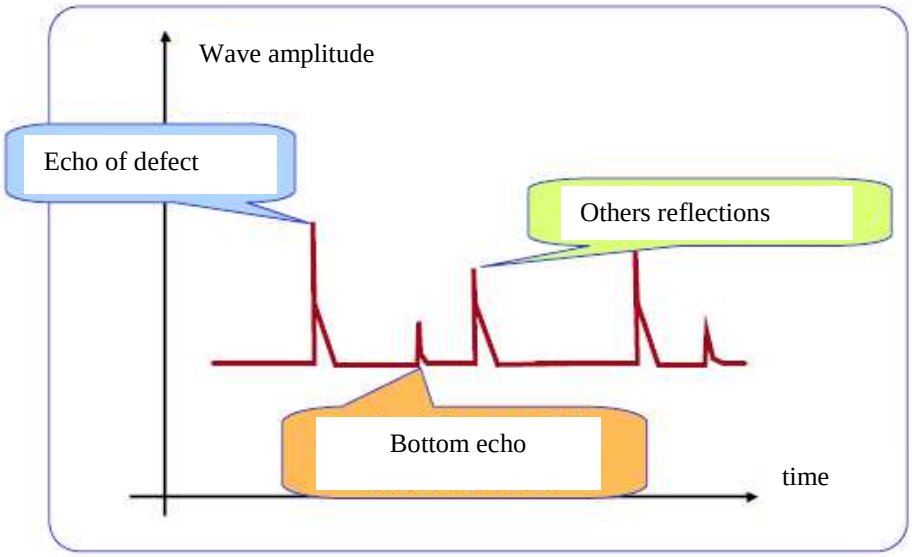

Figure 2.14 Example of the graph of a wave in the oscilloscope

It can be assumed that ultrasonic wave propagates a constant speed in the specimen, after proper calibration, the arrival time of echo can be related with the distance of the discontinuity from the source of the wave.

In the *transparency procedure* the signal is transmitted through the material form one side to the other. The sensors can be less sensitive respect the echo approach, and it requires the use of two transducers that operate one as a transmitter and

the other as a receiver of the signal. This technique permit to examine, with no difficulties, specimen of small thickness.

This technique can be carried out in more methods in relation to the need and the possibility of examination of the piece:

- *direct method (or transparency);*
- *semi-direct method (or reflection);*
- *indirect method (or surface propagation).*

In all three methods, the excitation of the transmitted transducer can be carried out in a continuous or pulsed.

In the technique for transparency, shown in figure 2.15, with the direct method are used two transducers, positioned opposite one another on the two opposite surfaces of the examined workpiece. one of the two transducers acts as the emitter, the other as a receiver. If the ultrasound wave generated by the first transducer encounters a discontinuity on its path is partially reflected the signal received by the second transducer will be reduced in amplitude compared to the case of absence of discontinuities. The reduction of the signal, detected by the receiving probe, is an indication of discontinuities; from the value of this reduction is possible to trace the equivalent diameter of the discontinuity. In the technique to transparency with the transmission method is not possible to found the depth or the shape of defect.

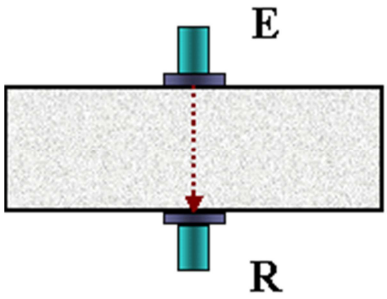

Figure 2.15 Technique for transparency with the direct method

Presented in fig 2.16, the semi-direct method is very similar to the previous one with the difference that the two probes are positioned on the same surface of the piece, however, is less accurate because only a part of the energy emitted by the probe issuer is directed to that recipient. It will be necessary to measure with the utmost accuracy the distance from center to center of the faces of the transducers.

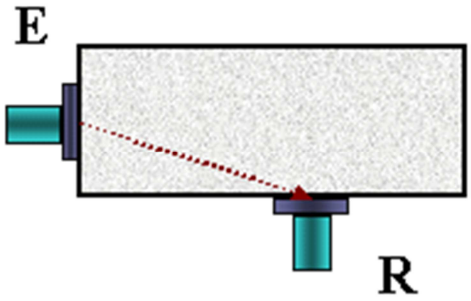

Figure 2.16 Technique for transparency with the semi-direct method

The indirect method is defined if the probes are applied in two aligned points of the same surface, on the object to be investigated, in the configuration shown in figure 2.17. This type of survey is less precise than the previous one in that only a fraction of the energy emitted by the probe issuer is directed to that recipient. The speed of the pulse is usually influenced by the surface layer of the material, which usually has different characteristics from the deep states. For this reason it is necessary to perform a series of measurements with the probe located at various distances. The probe transmitter must be kept stationary in a certain position, while doing vary the position of the receiver which must be placed at distances equal successive along a predetermined line. The transmission times measured allow determining an average speed of the pulse. The technique allow to measure shear moduli, and investigate presence of undersurface defects, particular class of

waves as *Rayleigh*, or *Lamb* wave are surficial waves, and only with this technique is possible to apply methods related with them theory.

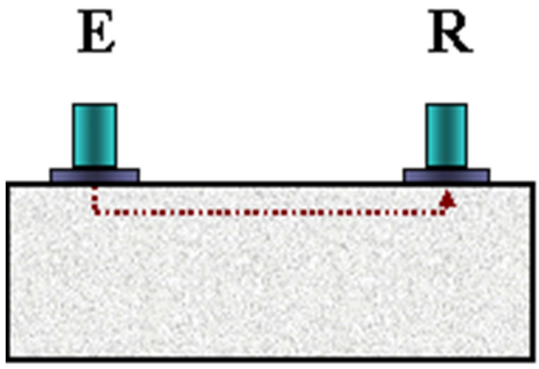

Figure 2.17 Technique for transparency with the indirect method

Numero pondere et mensura Deus omnia condidit.
God created everything by number, weight and measure.
I. Newton

CHAPTER 3

THE CONCRETE

3.1 CONCRETE: GENERAL ASPECTS

In construction field, concrete is a traditional material used for the structures. First use of concrete came from ancient roman empire. "*Opus Incertum*" was the Latin name of a mixture of sand, straw, water, clay, and binder. Commonly, the most used binder was the Pozzolanic sand. Pozzolanic sand is particular sand that is able to create strong connection between constitutive elements of concrete.

During the centuries, the composition of concrete was improved. At the beginning of the XXth century, the concrete becomes the more common material of construction. Mainly it is dues at the new architectural concept: the rationalism. At this concept, the livable space becomes available. The thick masonry constructions are left to give space to the new materials. The concrete permits do define a project of material, after to be established the level of maximum stress, workability, and durability. The concrete design born in order to find how the mix of the constituent materials can be choose in order to obtain the material with the required performance.

To avoid this result, many experimental tests are conducted, during the past years, and some rules are developed to define how constituents need to be combined. In this part, the basic constituents of concrete are presented, and a normative mix design procedures are discussed.

3.2 COMPOSITION

The materials engineering, today, permit to define the right combination of the constituents to follow the design requirements. Basic constituents of concrete are aggregates, cements, water and additives; if the objective is to create a well-designed material, attention have to given at the characteristics of constituents. This work doesn't have the claim to treat thoroughly properties of concrete constituents, it leads to give a brief review on how the constituents are related with mechanical property, and how them properties influence the wave propagation in heterogeneous media.

3.2.1 AGGREGATES

The term aggregates, usually, is intended natural crushed stone materials. Aggregates are so enough common in the environment as cheap, that they take the maximum part of the concrete. Aggregates are selected by their characteristics, a classic characterization is based on physical aspects: dimensions, shape, edge shape, porosity, divided in open and closed one; chemical composition, geological history, impurity grade, clearness, levels or reactivity with some substances (as plaster, oxygen, sulfates), mechanical characteristics: weight, density, resistance, water content, homogeneity, isotropy, elasticity module, fracture energy, natural tilt angle. Some of these main aspects are below presented.

A First classification of aggregates can be conducted by dimensions. If an element of aggregates is considered, it is possible to define a sphere that circumscribe it. The maximum diameter of the sphere is a parameter to define the aggregate diameter.

To find how many aggregates elements has diameter with than a certain value, a sieve with constant texture can be used. Starting from specimen a variegate aggregates, it can be sieved. All the material part that pass down the considered sieve have diameter less on the sieve diameter, as shown in figure 3.1.

Figure 3.1-Columns of sieves

The collect of all aggregates with the same diameter interval $D_1<\phi<D_2$, is obtainable by using two sieves. The materials collected between the two sieve is called volumetric fraction.

Usually, if it is considered a specimen of an aggregates, there are different aggregates with a variety of diameters. A procedure consents to classify how many aggregates for each diameter in percent are presented. The procedure is named *seiving*, and permit to obtain a curve in a half-logarithmic chart percent versus diameter called grain-metric fuse. The standard diameter of sieves are reported in table 3.1

Sieve n°	Diameter ϕ[mm]	Sieve n°	Diameter ϕ[mm]	Sieve n°	Diameter ϕ[mm]
	76,100		2,800	60	0,250
	50,800	8	2,360	80	0,180
	37,500	10	2,000	100	0,150
	25,400	14	1,410	120	0,125
	19,000	16	1,180	140	0,106
	12,500	20	0,850	200	0,075
4	9,500	30	0,600	270	0,053
	6,300	40	0,475	400	0,037
	5,000	45	0,355		

Table 3.1-Standard diameter of sieve EU and ASTM

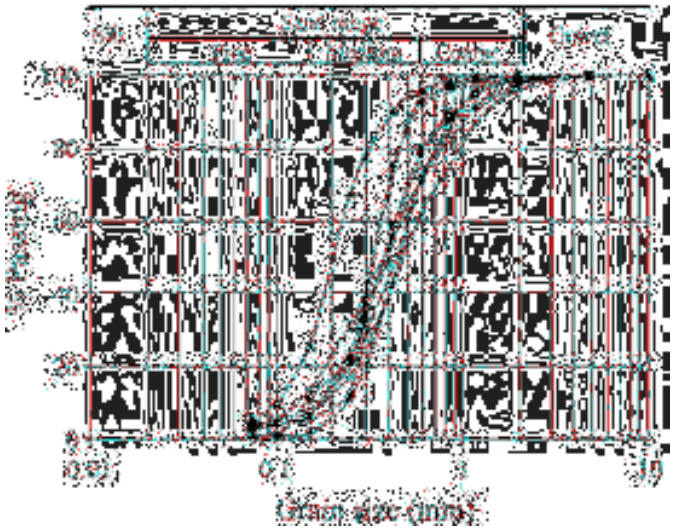

Figure 3.2-Grain-metric fuse

For each sieve it is called passant percentage the percentage of aggregates that has diameters less of sieve. In a chart, as reported in figure 3.2, Passant for each diameter.

A common classification of aggregates divided them in 2 main classes, if diameter is less than a certain value it is a sand, however it is a gravel, gravels usually are divided in 2 other class, small and big gravels. European committee fixed limit of sand at 2.00mm, American association ASTM use to classify a aggregates in fine (sand) if diameter is less of 4.75mm (sieve N 4) or coarse in other cases.

Related to this definition of fineness modulus FM is a measurement the fineness of sand. It is a factor obtained by adding the percentages of material, in the sample, that pass at each of the following sieves N 4, 8, 16, 30, 50, 100 (cumulative percentages retained), and dividing by 100. The formulation is below reported, and its variation is between 2 and 4.

$$FM = (\text{Cumulative percent retained})/100 \quad (3.1)$$

According with ASTM C 33 *Standard Specification for Concrete Aggregat*es, the fine aggregates (different of sand definition) need to have grading with diameter able to pass for all grain at the sieve of 3/8' (9.52mm) and with minimum diameter bigger than 150-μm (all material not pass at the Sieve N 100).

Shape of aggregates is important to understand how each grain is able to fill the empties. The aggregate can be with spherical or plate shape. If some plate shape element are present in the aggregates, the concrete can be made of less quality, related with the orientation of each of them in one direction, during the casting. Also important is the edge shape. That can be rounded or picked, the rounded shape means that it can come from rivers, and the erosion of water destroyed the picked, instead picked shape means gravel came from caves. The hit gravels are fine because the connection between them is better than the rounded one, and less empties are leaved inside.

Porosity is a properties about the voids present inside each element, the porosity is measured as percentage of the volume of the element. Porosity can be open and/or interconnected, or closed. Porosity is related with the weight of the concrete; it is

defined as porosity=V_{void}/V_{total}; if the porosity is closed water and cement mold never will be inside, and the final weight will be less heavy, and so less resistant the final product. It porosity is interconnected or opened, that should be a better quality. In some cases, to have a light concrete (900-1600 Kg/m^3) a eruptive stone as pumice or expanded clay is used, to take advantage of close porosity. Natural pumice-stone of artificial clay, are aggregates with close porosity, and are often used for light concrete.

Gravels come usually from caves that are in the hinterland where the opera is realized. The geological origin of the cave determine characteristics of gravels. The stone can have igneous, sedimentary of metamorphic origin. The igneous stones come from the solidification of magma and are fragile and rich of impurity, the sedimentary ones are formed by glued of dusts during the centuries and metamorphic ones came from the precedents categories but natural processes have compacted, compressed blind the stone in a better compact final state. Metamorphic gravels are the most used for compose concrete, because are enough compact, and with zero or almost-zero porosity.

The more common substances how aggregates are composed are silicates and carbonates, ($X\text{-}SO_3$ $X\text{-}SO_4$, $X\text{-}CO_4$) where X are captions as Ca, Na, Mg, Fe,…. and some other positive polar elements. Silicates presents an yellow color and carbonates look as white, however, presence of impurity can change it. More of them have also other colorations, red ones mean presence of some iron impurity as green is related with copper, dark yellow mean presence of sulfates. These component usually are stable in water, and with strong chemical resistance if they are attached by acid or basis. This propriety is important because this is a measure of the durability of the opera. If aggregates are easy –acid attachable, acid rain can damage durability of the structure. If in the place where the opera is located is present plaster of sulfate (volcanoes places) or sodium chlorate (sea water or close to sea places), gravel can be attached and the concrete could be deteriorated in few

years, if adequate solution are not adopted. The more common solutions provide the use of cements that are alkaline- resistant, and the cast of a low porosity concrete.

The specimens of gravels, as each material, can be tested and qualified in laboratory to determine mechanical and chemical characteristics. In order to measure resistance and module it is need to extract a specimen with standard dimensions to be tested in a press. Homogeneity and isotropy are dependent of the nature of the cave, in the cave are present some quantity of impurity substances. Depending on the level of impurity, the homogeneity of the specimen can be not adequate for characterization, especially if the inclusions are located inside the specimen, because there can be a preferential plane of cracks. Isotropy of gravels depend of the stratification of the cave.

If in the gravels are present clay inclusions, is need to observe that clays are made by bi-dimensional sheets of molecules and in parallel to this planes the distortion is possible. A mechanical test permits to determine the elastic modules E and G and the breaking load, and so the ultimate tension of resistance. Stone is a fragile material and data are often more dispersive, the break is usually improvise and with very low deformation. Stone have Elastic module over between 1 and 100 GPa. the tilt of elastic ramp is high and any plastic state is present. In the concrete, the gravels are disposed in random distribution and the anisotropy not play an important rule.

About density, there are two meaning: apparent, and effective, depending if the void are considered or not. Density is determined by ratio of weight and volume. The weight is determined in dry condition, specimen is stewed ad 110 degree in a oven, for 30 minute, to reduce humidity to zero. It is possible do classify the real volume of material if the porosity is open and interconnected or apparent volume if the porosity is closed. If you look at the apparent density, the specimen volume need to be the apparent one, it is measured using a water tank, the connected

porosity is saturated of water using a pressure porosity machine. The difference of initial and final water level is a volume measured. If you need to found the effective density is need to cracked the specimen in dust, and as before, using a water tank the effective volume is determined.

For bulk material it is also defined the bulk density as ratio of weight and bulk volume, that it is the volume that gravels have when are in bulk shape.

In literature, some relationship permit to pass from one density to the other by know the porosity and/or the percentage of void in buck state.

For bulk material the bulk angle is defined, it is the natural slope angle that aggregated are disposed if they are left in a plane. It is a measure of the interconnection level of gravels related with the friction resistance. if the same gravels are wet, water become a lubricant and the natural slope angle will be lower.

The fracture of gravel is related with the shape and dimension of the voids. Based on fracture theory, if a material is subjected an certain level of tension, close with the void the stress become high, because the imperfection. Related with the curvature ray of the void, the tension going to increase, the level of resistance raise until the limit resistance is reached, now the crack being the propagation, and it will be stopped at the next void, the area between the two void is now not more connected by material and the average tension at that section material increase. If all alienated void will become connected, the fracture become to propagates in an internal surface of the specimen, until disconnect all faces of the section of material. At this point the break is done.

A fundamental aspect for cast a good quality concrete is the grain metric distribution of the aggregates, in fact a suitable percentages of large, medium and fine forming the best mixture of the aggregates, the assortment of aggregate diameter is need to have different specific surfaces where connection with cement dough can be created.

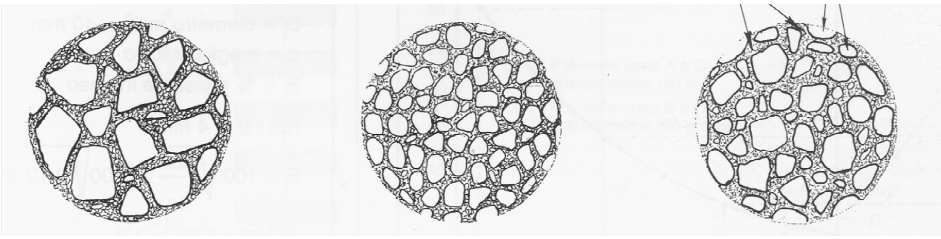

Figure 3.3-Influence the size of the aggregates in the compactness of the concrete

The aggregates, constitute the skeleton of the concrete and thus represent an essential components, and the deformability of the durability of the finished product. These are elements that do not participate in chemical processes of setting and hardening and are added to the mixture was dissolved with sizes and dimensions.

Not all natural crushed aggregates are necessarily suitable for the production of concrete; they may contain substances that may compromise the durability of concrete. The more common dangerous substances are chloride, sulfate, alkali-silica reagents (plaster), the clayey silt and organic parts. It must also be frost proof resistant.

The sand should be preferably silica, a coarse grain pattern, with elements of assorted diameter and with the absence of silts or clays, because they can be interposed between the cement dough and aggregates thereby reducing the resistance of the transition zone. the transition zone is a film of cement dough that is interposed between the aggregates. The micro cracks in the transition zone are in fact one of the main factors for the permeability of the concrete.

In literature some studies on aggregate distribution shown how to choose diameters ad percentage of aggregates to obtain the minimum void between the stones. In 1907 Fuller and Thomson, proposed a law, to described analytically the passant for each percentage.

$$p = \left(\frac{d}{D_{max}}\right)^n \tag{3.2}$$

Where n vary between 0.2 and 0.5, in relationship of the tilt of distribution, D_{max} is the maximum diameter of aggregates, in figure 3.4 two fullers distributions are shown.

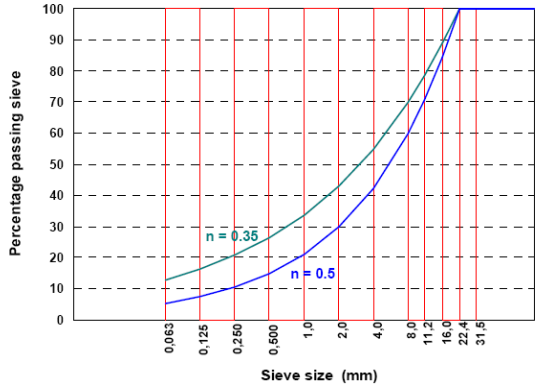

Figure 3.4-Fullers curves

With this choosing of aggregate distribution a concrete maximum density is obtained, but the workability will be low. Bolomey proposed a modification to this formula with the introduction of an A parameter dependent on the workability request and the type of aggregate available. The Bolomey law is expressed by the following formula:

$$P = A + (100 - A)\sqrt{\frac{d}{D_{max}}}\ ; \tag{3.3}$$

where P is still passing through a sieve opening d, D_{max} is the max size of aggregate considered and A is the parameter function of aggregate and workability.

The parameter A increases with the workability and also passing from natural aggregates, more rounded, to crushed aggregates, more irregular; A causes that

also increases the amount of fines present in the aggregate. The parameter A assumes the value given in table 3.2.

Aggregates	Consistently		
	humid	plastic	fluid
Natural	8	10	12
Crashed	10	12	14

Table 3.2-Parameter values of A

It is preferred to use the Bolomey's curve for concretes, especially if they have to be pumped. Since the equations (3.2) and (3.3) represent the ideal particle size distributions of the aggregate system more concrete, they may also be referred to aggregate only if you know the percentage of cement (C) referred to the weight of all solids (more concrete aggregates). It can then proceeds to the determination of the optimal curves of Fuller and Bolomey with the following formulas [19]:

$$P = \frac{100\sqrt{\frac{d}{D_{Max}} - C}}{100 - C}100 \qquad Füller\ optimal \tag{3.4}$$

$$P = \frac{A + (100 - A)\sqrt{\frac{d}{D_{Max}} - C}}{100 - C}100 \qquad Bolomey\ optimal \tag{3.5}$$

where C and the percentage of cement expressed by weight of all solids (aggregate more concrete) and P and the percentage of passing through a sieve with mesh opening d.

Determined the optimal curve, we will try the combination of aggregates that best approximates the curve calculated. However it is very difficult to have the aggregates making it possible to follow the curve calculated, for this we proceed by

composition of different aggregates size so as to get as close as possible to the optimum.

3.2.2 CEMENTS

The European standard UNI EN 197/1 defines the cement as a hydraulic binder, that is, an inorganic material that finely ground, mixed with water, form a dough which coagulates and hardens as a result of reactions and processes of hydration and, once hardened, retains its strength and stability even under water.
From the chemical point of view it is in general a mixture of calcium silicates, oxides of aluminum and iron, obtained by cooking at high temperature (1400-1600 ° C) of limestone and clay. The product cooked and cracked takes the name of clinker. The clinker mixed with water is characterized by a quick-reaction of hardening. In order to delay their property it is added a certain quantity of mineral sulphates (gypsum or anhydrite) of about 5% on the cement. The mixing between clinker and gypsum is called Portland cement.
In addition to Portland cement there are numerous other types of cement, mostly obtained by adding to the clinker of portland other substances of a mineral nature, such as volcanic pozzolan natural, artificial pozzolan, the blast furnace slag, fly ash, the smoke of silicon,
The legislation calls the concrete under the symbol CEM, and The 5 main types of cement used mostly in construction are as follows [S4]:

- Portland cement clinker with a percentage equal to 95%.
- Portland cement composite with a percentage of clinker of at least 65%.
- Blast-furnace cement, with a percentage of blast furnace slag 36-95%.

- Pozzolanic cement with pozzolanic material from 11 to 55%.
- Composite cement, obtained by simultaneous addition of Portland cement clinker (20 to 64%), of blast furnace slag (from 18 to 50%) and pozzolanic material (from 18% to 50%).

Below in table 3.3 are reported the types of cement according to UNI EN 197/1 with the respective names.

Tipi di cemento	Denominazione	Sigla	Clinker K	Loppa d'altoforno granulata S	Micro-silice D	Pozzolana Naturale P	Pozzolana Industriale Q	Cenere Volante Silicica V	Cenere Volante Calcica W	Scisto Calcinato T	Calcare Calcare L	Costituenti secondari
I	Cem. Portland	I	95-100	-	-	-	-	-	-	-	-	0-5
II	Cem. Portland alla loppa	II/A-S	80-94	6-20	-	-	-	-	-	-	-	0-5
		II/B-S	65-79	21-35	-	-	-	-	-	-	-	0-5
	Cem. Portland alla microsilice	II/A-D	90-94	-	6-10	-	-	-	-	-	-	0-5
	Cemento Portland alla pozzolana	II/A-P	80-94	-	-	6-20	-	-	-	-	-	0-5
		II/B-P	65-79	-	-	21-35	-	-	-	-	-	0-5
		II/A-Q	80-94	-	-	-	6-20	-	-	-	-	0-5
		II/B-Q	65-79	-	-	-	21-35	-	-	-	-	0-5
	Cemento Portland alle ceneri volanti	II/A-V	80-94	-	-	-	-	6-20	-	-	-	0-5
		II/B-V	65-79	-	-	-	-	21-35	-	-	-	0-5
		II/A-W	80-94	-	-	-	-	-	6-20	-	-	0-5
		II/B-W	65-79	-	-	-	-	-	21-35	-	-	0-5
	Cem. Port. allo scisto calcinato	II/A-T	80-94	-	-	-	-	-	-	6-20	-	0-5
		II/B-T	65-79	-	-	-	-	-	-	21-35	-	0-5
	Cem. Portland al calcare	II/A-L	80-94	-	-	-	-	-	-	-	6-20	0-5
		II/B-L	65-79	-	-	-	-	-	-	-	21-35	0-5
	Cem. Portland composito	II/A-M	80-94	← 6-20 →								
		II/B-M	65-79	← 21-35 →								
III	Cemento d'altoforno	III/A	35-64	36-65	-	-	-	-	-	-	-	0-5
		III/B	20-34	66-80	-	-	-	-	-	-	-	0-5
		III/C	5-19	81-95	-	-	-	-	-	-	-	0-5
IV	Cemento pozzolanico	IV/A	65-89	-	← 11-35 →				-	-	-	0-5
		IV/B	45-64	-	← 36-55 →				-	-	-	0-5
V	Cemento composito	V/A	40-64	18-30	-	← 18-30 →			-	-	-	0-5
		V/B	20-39	31-50	-	← 31-50 →			-	-	-	0-5

Table 3.3-Types of cements according to the UNI EN 197/1

European legislation classifies cements according to the class of normalized resistance (at 28 days), expressed in MPa with regard to resistance to initial

compression. Then each type of cement is divided into six different classes of resistance normalized, and each class is divided into two subclasses of early strength, relative to 2 days and the other to 7 days. table 3.4 shows the classes of resistance of cement.

The characteristics of the cement determinants for the mechanical strength properties of the hardened concrete are: the content of silicates, the ratio by mass between tricalcium silicate and dicalcium silicate, and the fineness of grinding.

Classi di resistenza dei cementi secondo UNI EN 197-1				
Classe di resistenza	Resistenza a compressione N/mm^2			
	Resistenza iniziale		Resistenza normalizzata	
	2 giorni	7 giorni	28 giorni	
32,5	-	≥ 16,0	≥ 32,5	≤ 52,5
32,5 R	≥ 10,0	-		
45,5	≥ 10,0	-	≥ 42,5	≤ 62,5
42,5 R	≥ 20,0	-		
52,5	≥ 20,0	-	≥ 52,5	-
52,5 R	≥ 30,0	-		

Table 3.4-Strength classes of cements according to the UNI EN 197/1

Cement is a hydraulic binder, that is capable of hardening, as well as on exposure to air, even in water. This property is due to the presence in it of compounds such as silicates, aluminates and ferrites of calcium, whose crystalline hydrated forms and are insoluble in water and have cementing properties.

3.2.3 THE PORTLAND CEMENT

The manufacture of Portland cement comprises substantially the following steps: mixing and grinding of raw materials, baking, cooling, further regrinding the product of cooking (which takes the name of clinker) and addition of gypsum or anhydrite.

The raw materials are mainly limestone, calcareous marl and clay, pyrite ash, silica sand. Such material must provide four basic components: CaO, Al_2O_3, SiO_2, Fe_2O_3 that in concrete technology, we denote by C, A, S, F.

On an oven, the temperature goes gradually increasing until to reach the 1450 ° C, the stones are hold in contact with hot combustion gases. During this warming the constituents of limestone and clay become a compounds with hydraulic properties. The reactions in act are the dehydration, the dissociation of calcium carbonate, the dried clay decomposition, the formation of aluminates (C_4AF, C_3A) and silicate (C_2S, C_3S). These reactions occur at different temperatures; it is observed the elimination of the water content of the clay at about 100 ° C, and the decomposition of constituents is started at 500 ° C approximately; follow the dissociation of calcium carbonate and its reaction with the silica take part. now the silica is liberated from the clays and the oxides are liberated from the carbonate at 800-900 ° C. At higher temperatures, 1000-1200 ° C, aluminates are formed by reaction of alumina with lime, the reaction between lime and silica form the di-calcium silicate C_2S; at temperatures of 1200-1300 ° C the free lime still present form the tri-calcium silicate C_3S.

The clinker should not contain free lime because if it was present, it would be certainly overcooked, or in such conditions slowly hydrates. This hydration cause an expansion in the hardened material that will have deleterious effects. The rest of clinker present in the furnace undergoes in a rapid cooling.

After the cooling process, the clinker is maintained in stable temperature in a environment, in order to limit the crystallization of the components of the molten phase. From the technological point of view the clinker is cooled rapidly in order to be more brittle and easier milling.

3.2.4 COMPOSITION OF CEMENTS

The cement mixed with water initially assumes a dough consistency. This dough mass undergoes after a certain time to an abrupt change of fluidity and it is consolidated (setting), then becoming a hard and monolithic mass (hardening). This occurs for the complex system of chemical reactions between constituents of the cement and the water that takes the name of hydration.

The term *setting* conventionally defines the initial period, when the mass, while achieving a high degree of consistency still retains a certain plasticity and penetrability. The limits of the temporal phase outlet are determined conventionally by the resistance offered by a specimen consisting of a cube of cement mixed with water, with thickness of 4 cm, the penetration of a needle of iron smooth cylindrical diameter of 1.13 mm (section $1mm^2$) and weight of 300g. The setting begins when the needle stops at 3 cm from the bottom and ends when the needle penetrates the pasta for less than half millimeter [EN 196-3]. According to the rules again, that statement should not start until an hour after the dough and finish earlier than four hours. The reason for these limits imposed by the standards is to ensure a sufficient workability of the mixes for the time necessary for their transportation and installation. However, it should not extend to the state of plasticity of the product to not disturb the phenomena that occur in the subsequent hardening phase.

The hardening begins at the end of the period of setting and takes a long time, even years. However, conventionally, after 28 days from the implementation of the material, it is considered that the material has reached 90% of the resistance. Between the two processes does not exist solution of continuity, the consistency of the material increases progressively from that of a typical mud to a dry ground until to become a compact material.

3.2.5 HYDRATION REACTIONS

The clinker is composed of two calcium silicates and two calcium aluminates in a 4:1 ratio [11]. In principle the two calcium aluminates contribute to the phenomenon of the setting, while the two silicates are decisive for the hardening.
The C_3A and C_4AF are required to lower the firing temperature of the clinker and make reasonably low the cost of cement production. They play a crucial role in the early hours of the reaction between water and cement. The reactions of aluminates in water give rise to a family of products indicated by the abbreviation CAH called also ettringite figure 3.5 (calcium-aluminate-hydrated):

$$C_4AF + H_20 \text{ --> } CAH \qquad (3.6)$$

$$C_3A + H_20 \text{ --> } CAH$$

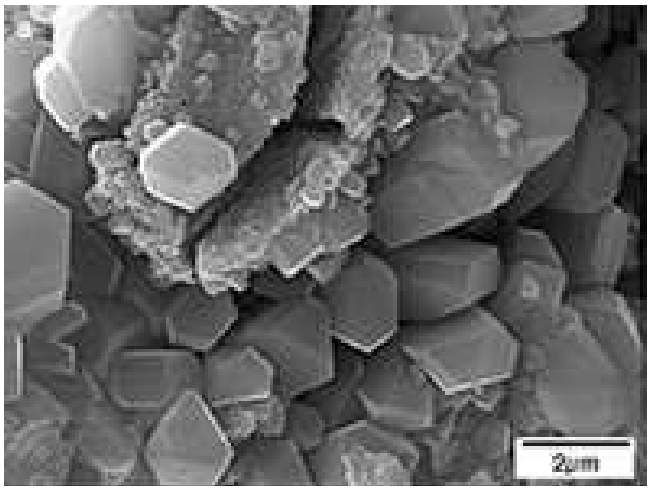

Figure 3.5 CAH in a microscope image

These reactions occur suddenly without, however, contribute significantly to the development of mechanical strength, except for a small but rapid increase during the first hours. In essence, the rapid reaction of the aluminate with water is

accompanied by an immediate loss of plasticity (fast setting). This depends on the morphology of the crystals CAH mainly composed of hexagonal plates or cubic crystals. This structure is highly conducive to the development of mechanical strength, unlike what happens instead in fibrous products CSH.

In a calcium aluminates cement, the CSH are not in water, but in a solution of calcium hydrate (which as will be seen is the result of hydration of silicates). For this reason does not happened the hydrolysis of C_3A and C_4AF, but the compounds react with the lime, forming aluminates more basic C_4A $12H_20$ and C4F-12 ÷ 14 H_2O. In fact the latter is the product of 'hydration of the only CF, one of the two compounds in which cleaves the C_4AF in water.

The hydration of the two main silicates C_3S and C_2S gives rise to a family of structurally similar called calcium silicate hydrates. Their composition is, however, different as regards the relationship silica/calcium and the content of chemically bound water. These products are referred to as CSH gel or cement. When the hydration is complete, corresponds approximately to the formula $C_3S_2H_3$ which usually is used in stoichiometric calculations. If you put the C_3S finely ground in water can be seen after a few hours, the appearance, around silicate grains originating in anhydrous crystals of calcium hydrate. It has also the formation of calcium silicate hydrate type colloidal, ie in the form of particles of submicroscopic dimensions. Depending on the concentration of CaO of the contact solution, the product can be C_2S-H_20 or CS-H_20. In case the solution contains less lime, the composition of the silicate hydrate would range between C_3S_2-H_20 and CS-H_20 shown in figure 3.6 . The hydration of C_3S and C_2S gives the same products but the proportions are different, as you can see from their reactions:

$$2\ C3S+6H = C3S2H3+3Ca(OH)2 \quad (3.7a)$$

$$2\ C2S+4H = C3S2H3+Ca(OH)2 \quad (3.7b)$$

Starting from constant mass of hydrated clinker, the mass of CSH produced from hydration of C_2S is greater than that produced hydration of C_3S (82% vs. 61%) and therefore the amount of calcium hydroxide is lower (18% versus 39%).

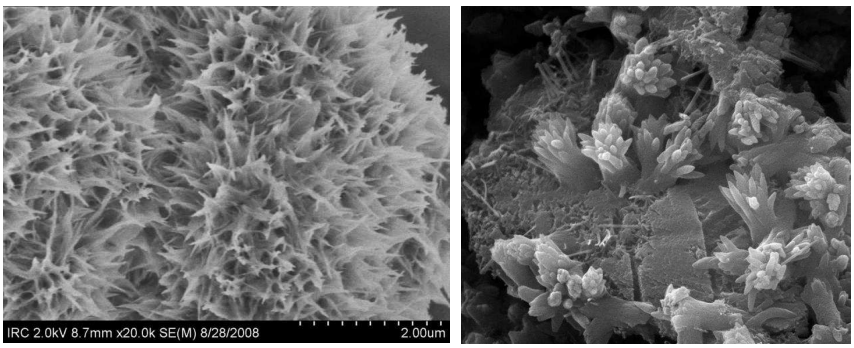

Figure 3.6-CSH needles , different zoom levels at microscope

There is also a difference in water consumption in the two cases: it is slightly higher in the case of hydration of C_3S (24% compared to 21% of C_2S). For these reasons, a different content of C_3S and C_2S in the cement paste influences the behavior, especially that relating to durability. The rate of hydration of the two silicates are different: the reaction of C_3S is much faster, for which gives rise to a more rapid development of mechanical strength.

The CSH hydration produces hexagonal crystals of calcium hydroxide $Ca(OH)_2$ that are much larger crystallites than the ones of CSH. These crystals are easily prone to fracture due to the weak bond between the layers that constitute them.

The CSH, constitutes about 80% of the volume and about 50% by weight of the final hardened, and is responsible for the final mechanical resistance. Its structure is ill-defined and of very small size, consisting of small solid particles of extremely thin lamellar shape and thickness of the order of nanometer that stretch for tens or hundreds of nanometers in the other two directions. Between the thin needles of CSH, cavities remain of the same order of magnitude that they give rise to the

pores of the gel denominated capillary pores which adversely affect much on the mechanical strength as the durability of the material. The high porosity increase the permeability and therefore the penetration of the cement system by aggressive agents. To reduce the capillary porosity, and thus increase both the mechanical strength and durability, you can reduce, to equal cement, the quantity of water, or increase the cement, with the same water. In both cases, it reduces the water/cement ratio and therefore prepares a more densities interweaving of the fibers for the shortest distance between the cement grains.

If the cement clinker is not added any regulator, at the time of its mixture with water, it will have a rapid passage in tri-calcium aluminate solution with subsequent crystallization of the compound hydrate. This occurs because it is not yet available lime of hydrolysis, since the C_3S tends to hydrolyze with a certain slowness. The mass of gels become hardened in a less than one hour, this will make it impossible to transport and dispose of the fresh concrete in a reasonably time.

To obviate this drawback is used to addict of gypsum ($CaSO_4$-$2H_20$) or calcium sulfate ($CaSO_4$) which have the specific function to slow the rate of hydration of the aluminates. They, in fact, rapidly dissolving in water just react with aluminates forming the sulfate aluminate called *ettringite* of formula C_3A $3CaSO_4$-$32H_2O$. The *ettringite* is formed during the first hours of hydration of the cement in the aluminates is called primary, secondary to distinguish it from that which may be formed later and can damage the concrete because it is expansive. The formation of *ettringite* primary delays the hydration of aluminates as it is deposited on the surface of C_3A and C_4AF in the form of crystals temporarily preventing the contact with water. In the absence of gypsum, as repeatedly stated, is formed immediately CAH in the form of laminar products which, by acting as bridges between the particles of clinker, cause a rapid loss of plasticity. The amount of gypsum to be used first of all must delay sufficiently the setting. This amount should also contribute to the development, especially initial mechanical strength. At this initial

development of mechanical strength will contribute the ettringite, much more of the CAH, thanks to its fibrous morphology. Therefore the resistance of the Portland cement is greater than that of the corresponding clinker. The addition of gypsum, however, must remain below the limits fixed by the standard (7-8% of chalk) to prevent the expansion of ettringite disruptive if this one will be hydrated after the setting time.

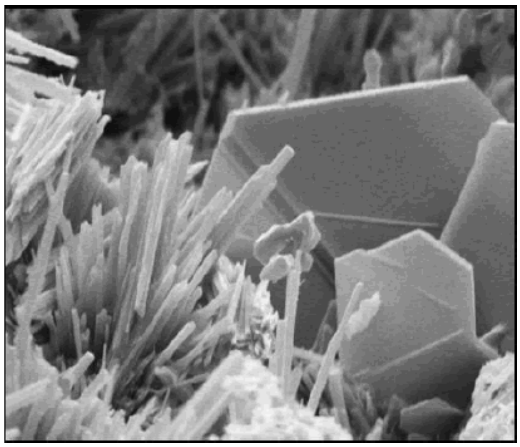

Figure 3.7-Plate of CAH and ettringite needles

Based on the above reactions can also calculate the theoretical amount of water fixed by a cement-curing completely occurred. It is found that it is approximately equal to 25% of the weight of the cement; however, this value varies with the composition of the clinker, because the different compounds do not lay down all the same amount of water. During this process happed a decrease in the volume of water, equal to about 25% of the volume that is chemically combined with clinker; the volume that is occupied by the cement and water is greater than the volume occupied by the hydrated cement.

During the hardening of a cement paste, a series of pores are created that will greatly influence the mechanical properties of the manufactured articles. In figure

3.8 is presented the distribution of water in relation at the dough porosity. This water goes to occupy the interstices between the granules. A fraction of water, about 15% of the cement weight, remains incorporated in gels originated from silicates and aluminates. This water, which permeates the gels, is still eliminable in a dry or for heating, but is not able to react with any components not hydrated, which considers not totally free, but constrained by binding forces of weak entity .

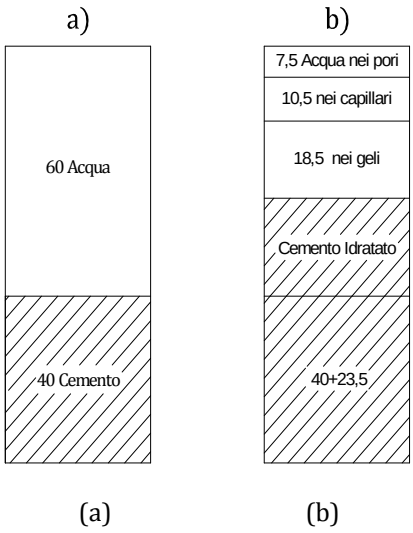

Figure 3.8-Schemes phase concentrated volumes of the constituents of a cement paste before (a) and after (b) hydration

However the only chemical reactions are not able to explain why a paste of Portland cement is gradually transformed from the initial plastic mass to a rigid material and hard as a stone. One theory considers that the components anhydrous, dissolving water in the mix could then precipitate in the form hydrates, crystalline, since the hydrated form of a salt is less soluble than the anhydrous. In the figure 3.9 it is shown the distribution of porosity in cement dough.

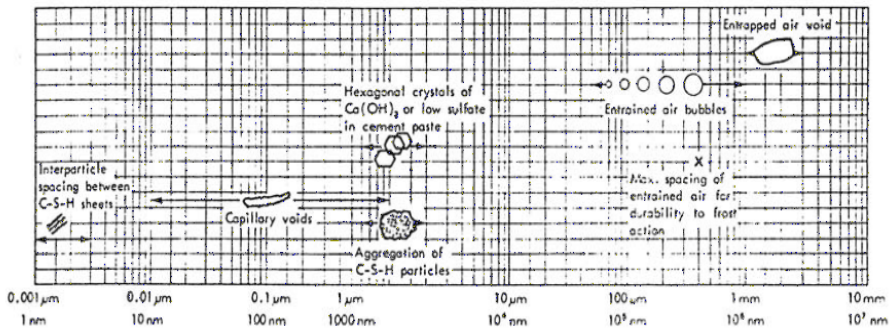

Figure 3.9-dimentional range of solid and pores in cement dough

3.2.6 WATER AND ADDITIVES

Water is an important element in the production of concrete, without it can not have the phenomenon of hydration which transforms the mixture into a solid mixture. However, the water must also perform the function of lubricant in the dough, making it sufficiently fluid to be workable. For this reason, the water used in the dough must be in an amount greater than that strictly necessary for the hydration of the cement. However, one should keep in mind that as the water can significantly worsen the mechanical properties of concrete. The mechanical strength and durability of concrete is not excessive penalized of water in absolute, but from an excessive ratio of the quantity of water (a) and that of the cement (c). The ratio water/cement (w/c) per cubic meter of material which is of fundamental importance in the process of production of the concrete. A high value of the ratio a/c generates a concrete extremely porous and thus not very resistant; on the contrary, a ratio a/c produces a low-resistant material and compact but little workable. The theoretical optimal ration of water is amounts to 0,28 to 0,30, which consist only in the necessary water hydration of the binder. This value, however,

does not allow complete hydration of the grains of cement, therefore generally one operates with higher values ranging between 0.45 and 0.65.

The water for the dough should be clear, pure, does not contain harmful salts in percentages and not be aggressive. The presence of impurities, in fact, interferes with the setting, causing a reduction in strength of the conglomerate. Virtually all normal natural waters may be used for the concretes. Excludes water and industrial discharges, or that contain sugar, oils and fats, and if hot water is used for the dough, the temperature should not exceed 60 ° C.

The additives are added chemicals, usually in small amounts, to the other ingredients of the concrete in order to improve one or more performance. The use of additives should be made with caution and are not always necessary, it can also be obtained poor results or negative.

Depending on the function involved in improving additives can be classified into various types, the most important are the following:

- plasticizers and super-plasticizers, which serve to reduce the water content in the dough without affecting the consistency,
- retardants or accelerators of the setting or hardening,
- retainers of water, enough to contain micro bubbles of air homogeneously distributed or reduce the loss of water,
- corrosion inhibitors, which prevent the corrosion of reinforcing steel caused by chloride
- water-resistant agents, which reduce the capillary absorption of hardened concrete,
- anti-withdrawal, which serve to reduce shrinkage.

3.3 MIX DESIGN

Mix-design is the "calculation of the composition of the concrete starting from the required performance (workability, mechanical resistance, durability, etc..) and the characteristics of available raw materials (cement, aggregates, additives) ".
The mix design is based on some experimental correlations between the composition of the concrete and its benefits. The five basic relationships are:

- the workability of the fresh concrete depend of the quantity of water, in kg/m^3, and of the type of aggregate (crushed or roundish), its size (maximum diameter), and of the presence of additives (water reducers and air-entraining);
- the ratio between the quantity of water and the cement a/c that should be adopted depends on the mechanical strength of the hardened mix (R_{ck}), as well as the type and class of cement; and the durability of conglomerate hardened in relation to the degree of environmental aggression (exposure class) where the structure is exposed.
- The volume of inert V_i is obtained by difference through volume of concrete V_{cls}, and volumes of the other ingredients V_a, V_c and $V_{a'}$,respectively the volumes in liters of water, cement and air. the first two are calculated from the masses through the corresponding densities (1 kg/L for the water and 3.1 kg / L for the cement); the third volume ($V_{a'}$) is obtained experimentally by table based on the maximum diameter of aggregate (D_{MAX} and the exposure class;
- The volume of aggregate V_i total is divided into that of individual aggregates (for example sand and gravel) according to the grain

metric curves of the latter with respect to the chosen reference curve (Fuller, Bolomey, etc. ...), as it is required for the combination optimum of aggregate. The volumes of sand (V_S) and gravel (V_g) obtained are converted into the corresponding masses (s e g) using the corresponding densities and m_s m_g.

The *workability* is the characteristic that indicates the capacity of the concrete to be moved and compacted, eliminating the gaps, when the material is introduced inside a formwork. The ability at the mobility is important to facilitate the carriage, the setting and the winding of reinforcing rods inside the formwork; instead the ability to compact it is important to facilitate the expulsion of air trapped in the fresh concrete, thus as the ensure of the maximum possible density of the hardened material.

There are numerous methods for measuring the workability, but the most widely used because of its simplicity is the slump test or test of lowering the Abrams cone. The Abrams cone is a truncated cone-shaped receptacle, open from both ends and 300 mm high, which is supported on the metal base and then filled with concrete, which is compacted in standard mode. Lifting the cone the concrete, because of the force of gravity, tends to expand on the support base until it reaches equilibrium. The lowering of the concrete is a measure of machinability, which allows defining the 4 consistency classes. Another method for measuring the workability is the so-called VEBE, which is used to dry concrete. In this method always uses the Abrams cone in which the concrete is poured; in this case, however, the cone is then covered with a transparent disc and subjected to vibration of a vibrating table standard. This vibration is stopped when the operator observes that the transparent disk is all in contact with the concrete, the time taken depends on the difficulty of compacting the concrete and it is the longer the more difficult it is compacting.

The workability of a concrete is influenced, of the mix design, by several factors which are: the water content, the characteristics of particle aggregates, the characteristics of the cement and additives. Other factors which determine the temperatures are, in fact, to grow it the workability decreases, and the time, 'cause the workability from the time of the dough decreases gradually over time and is reset when the concrete begins to set.

Figure 3.10-Samples of different consistency classes and Abrams cone

The measurement is made filling of concrete the cone and gradually settle down with a bar. After two minutes from filling, the cone is takes off and a measure of the lowering of the dust is measured. It is called a slump. Its measure defines five classes of lowering corresponding to five different ranges of workability. There are several correlations between slump and quantity of water, depending on the maximum diameter, such as the rule of Lyse. It can be expressed in two utterances equivalent.

The UNI EN 206 – 2006 e UNI 11104:2004 established the classes reported in table 3.5:

Consistency	**Name**	**Slump [mm]**
S1	Humid	10-40
S2	Plastic	50-90
S3	Half fluid	100-150
S4	Fluid	160-200
S5	Super Fluid	>210

Table 3.5-Classes of consistency for concrete

Setting the workability, the slump required is done, the amount of water that is needed to achieve this workability is as less as bigger is the aggregate. Increasing the maximum diameter (D_{MAX}), it reduces the specific surface area of aggregate and then the water necessary to wet the surface. Also hold constant D_{MAX}, the amount of water that should be used for manufacturing a concrete with a given slump, is greater if you use an aggregate crushed by the irregular contour, rather than an natural ones with the contour roundish. At constant size, an aggregate with irregular contour presents a greater friction against the cement matrix and therefore requires a greater quantity of water to achieve the same workability. To follow this principle, the needed water must be increased of 10 kg/m^3 in the case of crushed aggregates from irregular contour, and decreased to 10 kg/m^3 in the case of natural aggregates by the contour.

The rule of Lyse (1932) is adopted to set the quantity of water need for a m^3 of concrete in relation to slump and D_{max} in the follow chart and table are reported the adopted value of water for workability class and D_{max}.

D_{max}	Crushed [l/m³]					Natural [l/m³]				
	S1	S2	S3	S4	S5	S1	S2	S3	S4	S5
8	200	215	235	255	260	180	195	215	235	240
16	185	200	220	230	235	165	180	200	210	215
32	160	175	195	210	215	140	155	175	190	195

Table 3.6-Law of Lyse in tabular form

The follow chart show a synthesis of the lyse rule:

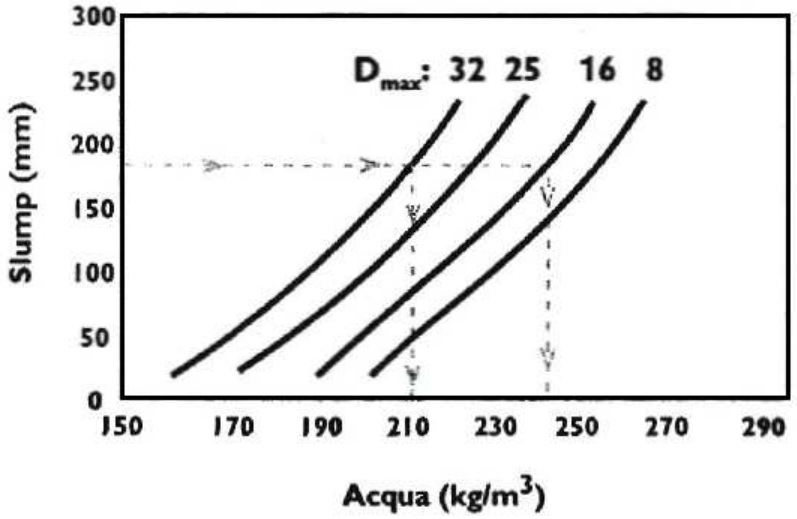

Figure 3.11 Graphical representation of the Rule of Lyse

If, however, some additives are used, it can reduce the quantity of water required, obviously depending on the type and dosage of additive.

Once you have the total volume of the mixture of aggregates, you must obtain an optimum particle size range of aggregates, from which we have:

- the minimum volume of the voids between the aggregates, that is, the maximum density, in a manner that minimizes the amount of cement paste required;
- the maximum workability;
- the minimum segregation of the mix, that is the separation of the different components of the concrete mix (water, cement and aggregates, etc..) constituting the mixture.

It is necessary, however, a compromise between these conditions because they can not be matched simultaneously.

Dmax	water L/m³ of cement							
	9.5	12.5	19	25	37.5	50	75	180
slump, [mm]	not air-entrained concrete							
25-50	207	199	190	179	166	154	130	113
75-100	228	216	205	193	181	169	145	124
150-175	243	228	216	202	190	178	160	-
Approssimate ammount of intrapped air in %	*3*	*2.5*	*2*	*1.5*	*1*	*0.5*	*0.3*	*0.2*
	air-entrained concrete							
25-50	181	175	168	160	150	142	122	107
75-100	202	193	184	175	165	157	133	119
150-175	216	205	197	184	174	166	154	-
	Reccomennded average total air content percent for level of exposure							
Mild exposure	*4.5*	*4.0*	*3.5*	*3.0*	*2.5*	*2.0*	*1.5*	*1.0*
Moderate exposure	*6.0*	*5.5*	*5.0*	*4.5*	*4.5*	*4.0*	*3.5*	*3.0*
Extreme exposure	*7.5*	*7.0*	*6.0*	*6.0*	*5.5*	*5.0*	*4.5*	*4.0*

Table 3.7-Influence of correlation slump and D_{max} on mixing water

For the choice of the amount of water required, reference is made to the international standard ACI 211.1-91, in which is inserted the table A1.5.3.3 (Table

3.7) which relates the amount of water with the workability (slump) and the maximum diameter of the aggregates, both in the case or presence of absence of entrapped air in the concrete.

To follow the law of Abrams the mechanical strength at a given curing and at a given temperature increases with decreasing the water/cement ratio, according to the following equation:

$$R = \frac{K_1}{K_2^{a/c}} \tag{3.8}$$

where R is the mechanical resistance to compression, K1 and K2 are two constants which depend on the type of cement, by time and temperature of curing.

This relation is valid if the concrete is well compacted to maximum; then if this condition is not verified the compressive strength R decreases proportionally to the degree of compaction.

The correlation between the ratio a/c and the mechanical strength is represented in table A1.5.3.4(a) reported here in table 3.8, which is located in the international standard, which refers to a concrete designed without entrapped air.

(28 day-R_{ck}) [Mpa]	ratio w/c	
	without entrapped air	with entrapped air
40	0.42	-
35	0.47	0.39
30	0.54	0.45
25	0.61	0.52
20	0.69	0.60
15	0.79	0.70

Table 3.8-Relationship between the w/c ratio compressive strength R_{ck}

So by setting the values of the slump, the maximum diameter D_{max} of the aggregate and the mechanical strength R_{ck} is possible to determine the amount of water required (a) and the ratio a/c through the table 3.7 and 3.8 for the two correlations described previously by the ratio between a and a/c we get the quantity of cement (c) in Kg necessary.

In order to estimate the amount in kg of coarse aggregate (P_{course}) through the table A1.5.3.6 (Table 3.9) included in international law, this table relates the volume of coarse aggregate with a maximum diameter of the aggregate and the MF. To obtain the weight in kg of coarse aggregate must multiply the volume of coarse (in m^3) for the density of the aggregate expressed in Kg/m^3.

D_{max}	Volume of dry coarse aggregate in m^3			
MF	2.40	2.60	2.80	3.00
9.5	0.50	0.48	0.46	0.44
12.5	0.59	0.57	0.55	0.53
19	0.66	0.64	0.62	0.60
25	0.71	0.69	0.67	0.65
37.5	0.75	0.73	0.71	0.69
50	0.78	0.76	0.74	0.72
75	0.82	0.80	0.78	0.76
150	0.87	0.85	0.83	0.81

Table 3.9-Volume of dry aggregate related with MF and D_{max}

To obtain a concrete with a maximum density and a minimum of voids, the coarse aggregate will be divided into various classes with different diameters d and standardized, corresponding to the openings of the sieves. The legislation ACI 211.1-91 shows an equation derived from Fuller and Thompson theory, which combines the different diameters of the coarse aggregates and generates a curve

that is close as possible to the optimal one. The equation proposes in the legislation is the follows:

$$P = \frac{d^x - 0.1875^x}{{D_{max}}^x - 0.1875^x} \quad (3.9)$$

where P is the percentage of passant by weight in sieve of diameter d, where d is the diameter of the sieve and x is a constant equal to 0.5 and 0.8 for rounded aggregates crushed aggregates with irregular contour.

After having determined the amount of water, cement and coarse aggregate, it passes to the determination of the amount in kg of aggregate up (P_{fine}), which is determined with the following relationship:

$$P_{fine} = P_{concrete} - (P_{course} + a + c) \quad (3.10)$$

where $P_{concrete}$ is the weight in Kg of concrete required. The weight of concrete is determined through the A1.5.3.7.1 table (Table 3.10) present in the ACI, that correlates D_{max}, and concrete with/without the presence of entrapped air.

D_{max}	**Weight of Kg/m^3 of concrete**	
	without entrapped air	**with entrapped air**
9.5	2280	2200
12.5	2310	2230
19	2345	2275
25	2380	2290
37.5	2410	2350
50	2445	2345
75	2490	2405
150	2530	2435

Table 3.10-Volume of dry aggregate function in the of finesse and D_{max}

3.3.1 SOFTWARE FOR MIX DESIGN

In this thesis, the mix design procedure is been implement in a software able to define a mix design starting from parameters of design.
In the software Dmax, slump, MF σ and ρ_{coarse} are fixed; In the follow diadram the algoritm is shown:

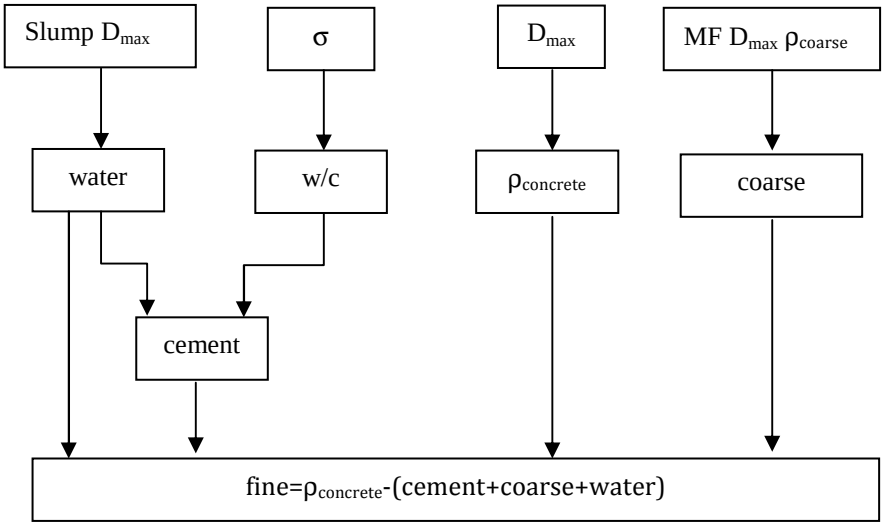

Figure 3.12 Flow diagram for mix design according with ACI

Starting from workability and Dmax the water need for a m3 of concrete is determined using a multiple quadratic regression developed using data from table 3.7,

$$Water\ [liter]=202.7+0.41118x-1.689y-0.0009834x^2+0.0001342xy+0.006355y^2 \quad (3.11)$$

$$R_{fit}=0.996$$

Using data in table 3.8, in the case without entrapped air, it is been possible to implement a data interpolation in order to reach relationship resistance/w/c ratio.

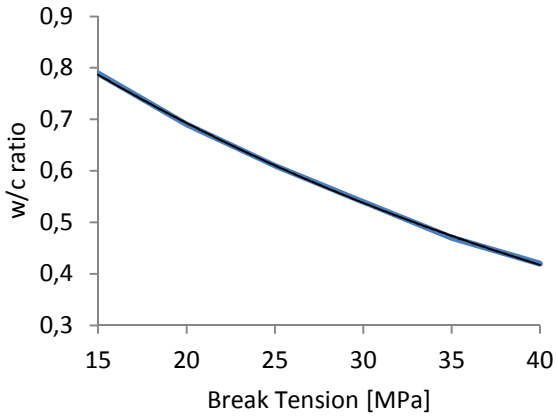

$$ratio = 1{,}1502*10^{0{,}025\sigma} \qquad R^2 = 0{,}9994 \qquad (3.12)$$

Now, the cement contend is easy obtained by the follow relation:

$$Cement=(w/c)/water \qquad (3.13)$$

Using the table 3.10, the weight of a m^3 of concrete is determined in relation at the D_{max}:

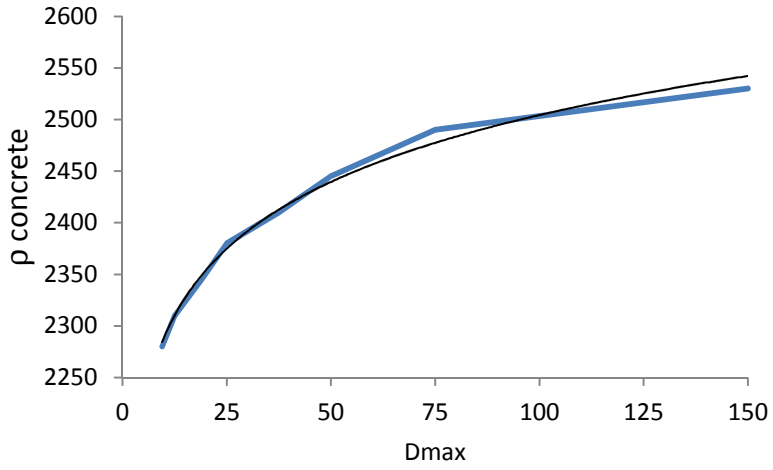

$$\rho_{concrete} = 93{,}448\ln(D_{max}) + 2074 \qquad R^2 = 0{,}9923 \qquad (3.14)$$

Another nonlinear multiple regression was been conducted on data from table 3.9, to determine relations between D_{max} MF and volume of coarse.

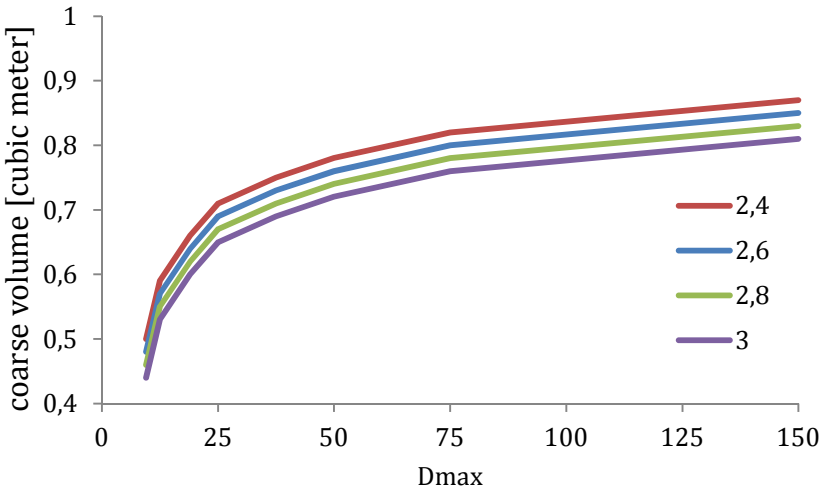

$$V_{coarse}=0.1282*\log(51.29D_{max})-0.1MF; \qquad (3.15)$$

After to obtain the coarse volume times by coarse density, the mass of it is determined.

The fine fraction is determined as difference from mass of concrete less mass of water, coarse and cement.

The coarse mass is now distributed in different diameters using the relation 3.8.

All these calculus are implemented in a graphical interface to obtain in a click the need quantity.

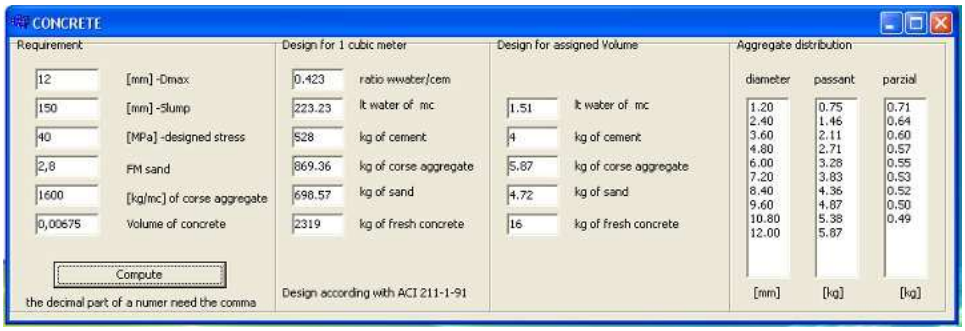

Figure 3.13 Software proposed for mix design

3.4 CASTING AND CURING

Concrete is an artificial stone material that is obtained with the mixing of stone aggregate with different sizes joined together by a hydraulic binder (concrete) which is activated by means of chemical reactions with water.

the execution of concrete dough to get the fresh concrete, is an operation that will determine the homogeneity of the concrete.

Usually the concrete mixing plants that are located in the centers of production and then it is transported to the worksite by truck mixer, alternatively it can be produced directly in the pipeline by means of concrete mixers oscillating. The transport does not affect the final quality of the concrete, but it can lose workability, due to the methods and transport time and the ambient conditions.

The loss of workability depends on the amount of water present, the type of cement and by the presence of additives, on environmental conditions, temperature and humidity and it can be subjected of the evaporation of the water.
After mixing the concrete, is settled in formwork in wood, plastic or metallic materials these formworks have dimensions in accordance with the structural project of the building.
Once cast the concrete into formwork, it must be suitably vibrated, to avoid the formation of cavities within the article and micro-defects, because porosity make the cement matrix more permeable to the aggressive external agents this reduce the durability of concrete and create dangerous discontinuities of the material.
The simplest system for the casting of the concrete is a crane arm, with a bucket that can download the concrete directly into the established point; when necessary to carry and pour the concrete is used a pumping system. In these cases, care must be taken that the components do not separate, because the larger aggregates tend to move downwards, while the sand and the water back to the surface. To avoid this phenomenon the concrete must be not subjected to excessive shock and vibration, is not dropped from great heights or slid into too long slides.
The passage from the fluid state to the solid state of the concrete occurs through the phenomenon of setting and hardening, and it is indicated with the term concrete curing or seasoning and take time until the material reach the mechanical performance required.
The setting is a process where the concrete loses its plasticity and workability and, in a few hours, become stiff. Instead hardening is a process, which begins immediately after the setting, it assumes the rigidity typical of a natural stone and develops an appreciable mechanical resistance. In contrast to the setting, curing continues indefinitely over time even if after a few weeks the mixes based on cement mechanical resistance have already reach the designed resistance. These phenomena depend on the hydration of cement, the water reacts with the cement,

transforming the grains of cement in crystals, by interacting between them, also after than the concrete is hardened.

The maturation of the concrete, and then the reaction of hydration of the cement mass, determines the characteristics of strength and durability required of the manufactured structure. When the concrete is cured in a natural way, the climate is of fundamental importance; in fact the dry air can accelerate the evaporation of water and reduce the hydration of cement. During maturation, to prevent this phenomena, it must be taken protection devices, in order to keep warm and moist the concrete. The evaporation of water can cause lesions due at the drying shrinkage and an excessively porous structure, can compromise the final strength and the degree of durability of concrete.

The freezing of the mixing water before than the concrete has reached an appropriate degree of curing or thermal shock due to differences in temperature through the section of the structures can generate cracks. To avoid these processes and achieve maximum development of resistance it is necessary to delay as much as possible the operation of removal of formwork (by stripping) and use a protected wetland seasoning (UR. > 95%) to ensure the complete process of hydration.

(a) (b)

Figure 3.14-(a) Cracks induced by drying shrinkage for non-wet curing. (b) for failure to cracking wet curing.

There are different techniques of seasoning for the reduction of the problems previously exposed, such as keeping wet the surfaces of the concrete and the use of curing agents or tissue soaked ensure that the saturation of the surfaces exposed to air.

The seasoning can be ordinary or accelerated. The ordinary curing takes place at room temperature, with the exclusion of any external intervention of heating or cooling. In this case the concrete at the time of the setting contains a quantity of free water that ensures the hydration of the cement, but it is necessary that this water remains available or otherwise can be quickly restored until the space filled by water and cement is not largely replaced by hydration products. The speed of development of resistance depends on weather conditions, as also the type of cement, and the water/cement ratio.

The seasoning accelerated instead makes use of a supply of heat; the most widespread is the one that involves heating by means of free-flowing steam. It consists in subjecting the concrete, after casting, the combined effect of heat and moisture through the sending of saturated vapor at low pressure in the environment of treatment. A proper treatment can allow the development in 24 hours, or even in a shorter time, of the 60% of compressive strength instead to wait for 28 days with the normal maturation (20 ° C, 100% RH).

The concretes cured at elevated temperatures show, as a result, final strength lower than those normally cured. It is hardly makes a wet curing for extended periods, but the concrete accrued in a controlled environment achieve higher resistance to similar concrete accrued under ordinary conditions.

3.5 MECHANICAL PROPERTIES

Concrete is a material that behaves quite well under the action of compressive stresses and, as is known, has a poor behavior under the action of a tensile stress

induced by direct or bending. For this reason, but also for the experimental difficulties inherent in the measurement of the tensile strength and flexural R_t R_b, usually on the concrete are made only direct measurements of compressive strength, and use the calculation to determine indirectly R_b and R_t, as well as the modulus of elasticity E. A concrete can be identified by its property class.

The strength class is distinguished from the characteristic values of the cubic resistance R_{ck} or the cylindrical one f_{ck} to uniaxial compression, measured on specimens normalized namely respectively of cubic edge of 150 mm and of cylinders of diameter 150 mm and height 300 mm. the ratio of H/B or H/D of the specimen need to do be 1:1 or 1:2 for have a normalized value of resistance. The characteristic compressive strength is defined as the resistance for which it has a 5% probability of finding lower values. In these rules the characteristic strength means that deduced from tests on specimens as described above, , performed at 28 days after the setting [NTC 2008].

3.5.1 FRESH CONCRETE

Various factors affect the compressive strength. Through the theory of Powers is possible to calculate the value of R_C of dough of Portland cement as a function of the volume of the capillary porosity V_P and the volume of the hydrated cement V_g, or from the water cement ratio a/c and the degree of hydration α as shown in the following equation:

$$R_c = K \left(\frac{0{,}6790\ \alpha}{0{,}3175\ \alpha + a/c} \right)^3 \qquad (3.16)$$

The compressive strength depends, at constant temperature, by a/c ration and an degree of hydration α parameter, as is shown in figure 3.13.

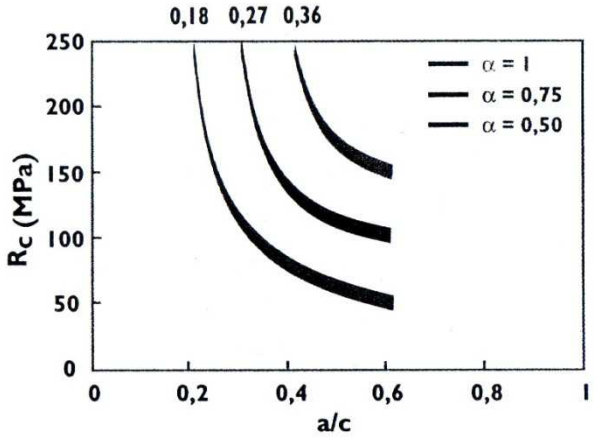

Figure 3.15-Powers rule

Furthermore, it is difficult to determine the value of α in a more complex system such as concrete. However, it is known that the degree of hydration α is influenced by the ratio a/c, by maturation and the strength class of the concrete.

The fresh concrete is a mixture of solids dispersed in liquid, the mechanical properties are refer to a bi-component material. They can be referring to the solid or liquid phase. Relevant quantities are related with viscosity of fluid, workability and segregation of solid part, sedimentations and so others.

The *segregation* of fresh concrete is the property affects the separation of the constituents of the concrete, so that their distribution is no longer uniform, with the descent to the bottom of the larger particles. When instead it has outcrop surficial water we are in the presence of the phenomenon of bleeding.

Segregation occurs mainly during mixing, transportation, installation and constipation, whereas the bleeding occurs in the formwork after the concrete has been compacted. In areas where there is a separation of the larger grains is no longer possible to obtain a complete constipation, and then you may have formations of gravel nests, layers of particularly porous and less resistant to

abrasion of surfaces. Instead areas surface or below the large aggregates flattened that prevent the ascent of water, there is an accumulation of water which results in a decrease in mechanical strength and durability of concrete.

The extent of segregation depends on the shortage of cement and a not grain metric range.to eliminate the bleeding it can be used fluidizer additives to reduce the mixing water, but above all we must control the dosage of cement and aggregates to achieve a combination of optimum particle size range.

Another important property of concrete is the durability, which represents the materials ability to resist during the years at the aggressive action of the external environment. The durability, is closely linked to water/cement ratio, because the smaller a/c, make more durable the concrete. Durability depends to a large extent of factors. One of the more important ones is the permeability of the material to the water; more higher is the permeability, and more it will be the quantity of agents dissolved in the water which can penetrate into the material.

Two fundamental aspects of concrete that occur over time are shrinkage and viscosity.

The shrinkage is a reduction in the volume after the setting; it is develops over time and is complete after a few years. A portion of the withdrawal is due to phenomena related to the continuation of the reactions of cement hydration and is called *autogenous shrinkage*. The magnitude of this withdrawal and then increases with the amount of concrete used, and therefore with the mechanical performance; this part of the withdrawal becomes full (or nearly so) in a relatively short time (about 2 months). The other part of the withdrawal is due on drying, that is the loss of excess water remaining in the pores of the material and is called *drying shrinkage*. The extent and rapidity of this phenomenon will depend not only on the ratio a/c, also by environmental conditions. In dry the phenomenon is rapid, while in a moist environment is slower, instead under saturation conditions (humidity 100%) is virtually absent.

The *viscosity* is the phenomenon that causes the increase of the deformation of the concrete under a load of long duration. Creep, which evolves with lower and lower speed up to asymptotically stabilize, can far exceed (2 or 3 times) the elastic deformation. The phenomenon is almost irreversible and if a load is removed, the elastic deformation is recovered immediately but only partially, because of the variation of the elastic modulus; there is then a non-elastic recovery, said recovery from creep, and finally there remains a residual deformation that represents the viscous deformation is.

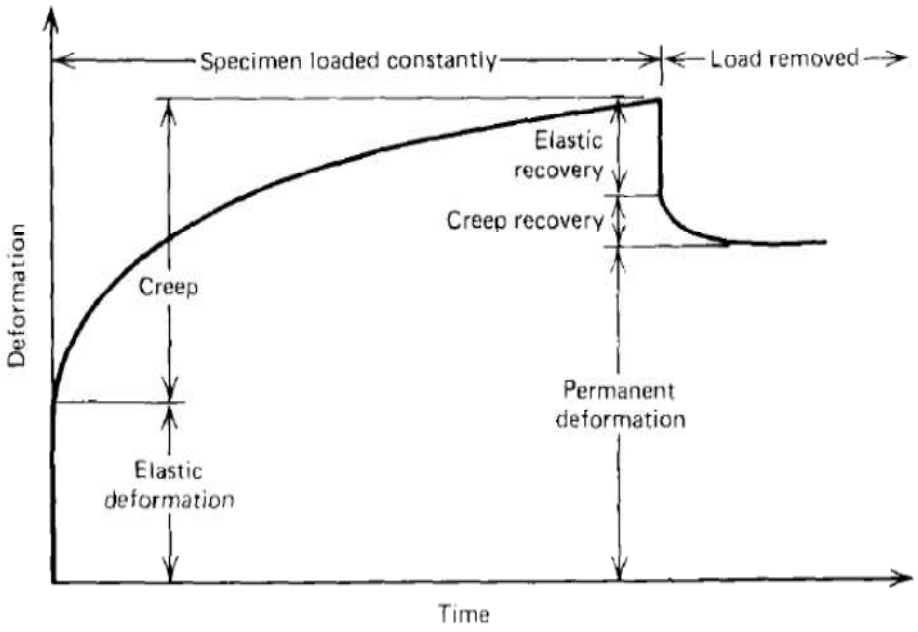

Figure 3.16 Deformations of the concrete due to a load of long duration

For the viscosity of the environmental conditions (humidity) affect the evolution of the phenomenon, not very final extent of deformation, but significantly on the

speed with which it develops. The final amount of deformation is instead mainly dependent on the water/cement ratio.

3.5.2 HARDENED CONCRETE

The hardened concrete is constituted by a series of stone materials, bound together by the hardened cement paste; then the properties of the concrete depend on the quality of the cement paste, by the characteristics of the aggregate and by the link that is established at the interface between the dough and the aggregate.
The mechanical property essential for the concrete is the mechanical resistance, which is divided depending on the effort applied: mechanical resistance to compression R_c, R_b bending or tensile R_t Concrete is a material that behaves quite well under the action of compression stresses, and moderately under the action of efforts to direct traction or bending traction, for this reason often is used in conjunction with steel. For these reasons shall be made only direct measurements of the compressive strength and is used in the indirect calculation of flexural strength and tensile strength of the evidence or indirect measurement to bending or cutting cylinders (Brazilian test).

For a same concrete has been demonstrated that the value of f_{ck} is equal to approximately 83% of R_{ck}. In table 3.10 shows the classification of the concrete according to the UNI EN 206/1 as a function of R_{ck} and f_{ck}.
The tensile strength and flexural strength characteristics can be calculated by the following formula established by law:

$$R_t = 0.48\sqrt{R_{ck}} \tag{3.17}$$

$$R_f = 1.2R_t \tag{3.18}$$

Classi di resistenza a compressione secondo UNI EN 206-1			
Classe di resistenza a compressione	**Resistenza caratteristica cilindrica Rck (N/mm^2)**	**Resistenza caratteristica cubica fck (N/mm^2)**	**Tipo di calcestruzzo**
C 8/10	8	10	NON STRUTTURALE
C 12/15	12	15	
C 16/20	16	20	ORDINARIO
C 20/25	20	25	
C 25/30	25	30	
C 30/37	30	37	
C 35/45	35	45	
C 40/50	40	50	
C 45/55	45	55	
C 50/60	50	60	ALTE PRESTAZIONI
C 55/67	55	67	
C 60/75	60	75	
C 70/85	70	85	ALTE RESISTENZE
C 80/95	80	95	
C 90/105	90	105	
C 100/115	100	115	

Table 3.17. Classes of resistance/compression according to UNI EN 206/1

In Figure 3.11 are represented some stress-strain curves, obtained on cylinders, related to concretes of different strength classes. It may be noted that in these curves lacks a clearly linear tract; therefore, reached the maximum deformation, for a deformation next to $2x10^{-3}$, the concrete can continue to deform, but the balance is only possible by reducing the external force. The behavior is therefore distinctly fragile, the more so the greater the resistance.

The slope of the curves voltages deformations represents precisely the elastic modulus E, which is an elastic property essential for the concrete. As for the concrete the curve does not have a linear elastic behavior. The elastic modulus should be specified or as initial slope of that curve (E_{ci} module at the origin), or as

the slope of the secant to the diagram between two deformations considered (secant modulus E_c). The Italian legislation in the absence of direct measurements of E, has established the following formula for the calculation of the secant modulus E_c:

$$E_c = 22000 \left(\frac{f_{cm}}{10}\right)^{0.3} \tag{3.19}$$

where f_{cm} is the compressive strength of cylindrical media; that is related to the compressive strength characteristic cylindrical by the following relation:

$$f_{cm} = f_{ck} + 8 \tag{3.20}$$

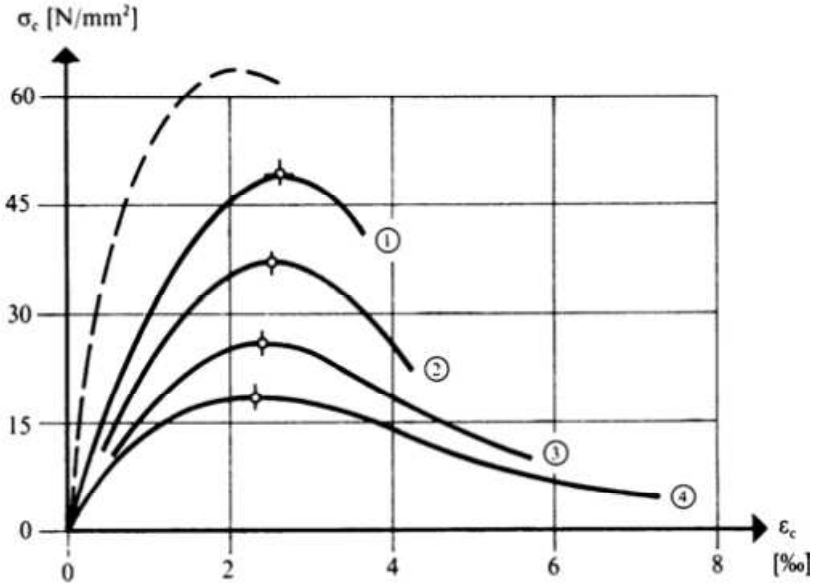

Fig 3.18-Stress-strain curves of concrete with different strength classes

The UNI 6556 of 1976 proposes an experimental method for the determination of the elastic modulus secant between two voltages after a certain number of load cycles, it is described in chapter 2.

CHAPTER 4

ULTRASONIC WAVE AND SIGNAL PROCESSING THEORETICAL BACKGROUND AND VALIDATION MACHINE

4.1 THEORY OF WAVE PROPAGATION IN ELASTIC MEDIA

In this part the basic aspects related with ultrasonic wave are presented. The main type of wave are described, a theoretical approach in mono dimensional and tridimensional is presented. Relationship with elastic constants and wave velocity are reported.

4.1.1 GENERAL ASPECTS: LONGITUDINAL SHEAR AND FLEXURAL WAVES

A wave is a perturbation of a media. In Our work we intend as wave a mechanical perturbation which is propagates in a space. With the wave a energy is transported from one point to another one through the variation of some physical quantities as change of pressure, temperature, electric field intensity, position. A particular type of wave is the sound. A mechanical vibration generate a variation of pressure that is propagates in the material according to the paths, the direction and the elastic characteristics of media. The sound waves cannot exist in the absence of material as fluid as solid, contrarily the light waves can propagate trough the vacuum because its nature is electromagnetic.

The ultrasonic waves used for NDT testing are created by FRUTTANDO the piezoelectric properties of some materials defined *piezoelectric*. These materials are able to vibrate if subjected to an electric field. The vibration obtained produces an elastic wave of ultrasonic frequency. This phenomenon is reversible, if the same material is subjected to electrical stress a deformation is generates.

The sound waves have frequency below 18 KHz, if the signal frequency is upper this value, the vibrations are not more audible and the signal is called ultrasound. The frequencies are between 50 kHz and 1000 MHz, any human ear is able to ear this vibration.

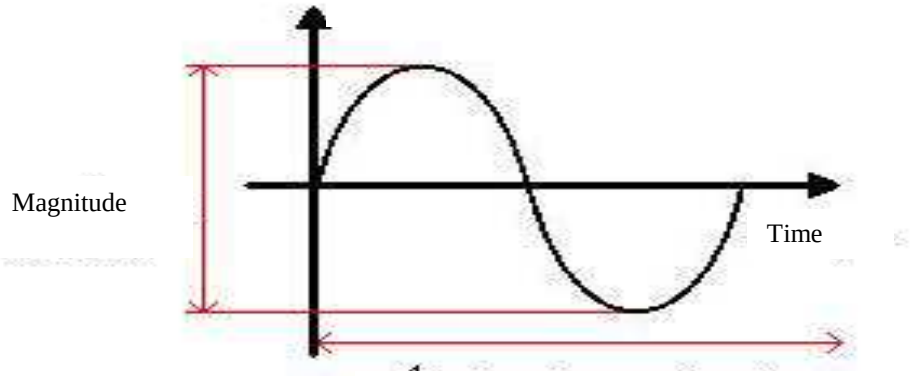

Figure 4.1 -Diagram of a wave in the time domain

For a wave some physical parameters are defined to characterize the wave. the frequency f, the period T, the wavelength λ, the speed of propagation V, the magnitudes A. some of these are related by the relations here reported.

$$f = \frac{1}{T}[Hz]; \quad \lambda = \frac{V}{f}[m]; \quad V = \frac{\lambda}{T}\ [m/s] \tag{4.1}$$

The frequency indicates the number of cycles (oscillations) that occur per unit of time and unit of measure is the Hertz. The period is the inverse of the frequency and indicates the time that a wave takes to do one full cycle. Frequency is the parameter that characterizes the wave phenomena.

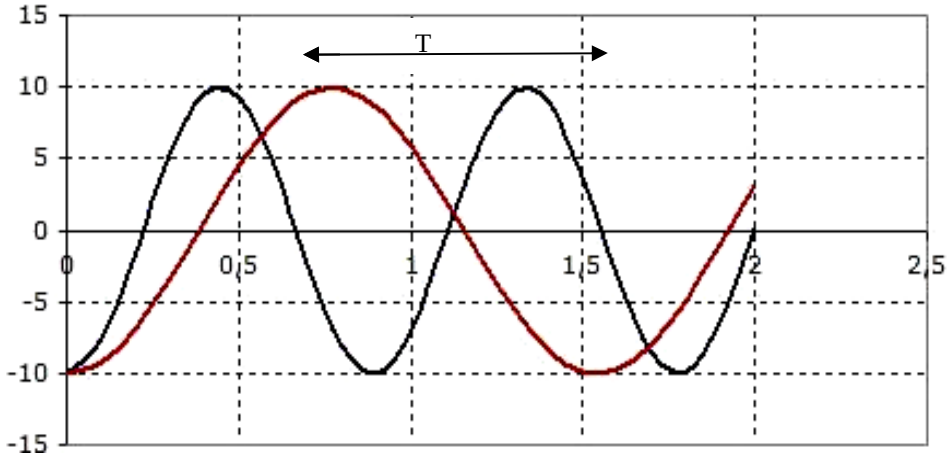

Figure 4.2 Two waves with the same frequency and different Amplitude

A useful parameter for calculation of the pulsation frequency is ω, it represents the number of radians per unit of time, it is related to the frequency by the following relation:

(4.2).

The wavelength represents the distance between two maxima of the wave in space domain. The importance of the value of the wavelength is essential in the phenomena of attenuation, divergence, reflection, detection of discontinuities and diffusion. It is clear that frequency and length are related by velocity. The velocity of propagation of elastic waves represents the distance traveled by the wave front

unit of time; normally is expressed in m/s. it is variable with the wave frequency and the mechanical properties.

The velocity in a homogeneous medium, isotropic and perfectly elastic, is dependent with the dynamic elastic modulus by the follow relation.

$$V = \sqrt{\frac{Ed\,(1-\nu)}{\rho\,(1+\nu)(1-2\,\nu)}}\ [m/s]; \tag{4.3}$$

where:

E_d is the dynamic modulus of elasticity [Pa],

ν is the Poisson ratio [adm.],

ρ is the density of the medium [kg/m^3].

The waves are propagated in materials as variations of the local pressure. A relationship between the wave pressure and the wave velocity define the acoustic impedance. It is the resistance that the medium opposed to the induced stress. The acoustic impedance characterizes the behavior of the wave respect of a given material, it is specifically defined as

$$Z = \rho V\ [Ns/m^3]; \tag{4.4}$$

where ρ represents the density of the medium and V the velocity of propagation wave.

the acoustic impedance Z characterize the local properties of the means involved in the motion, it is a global properties if the materials is homogeneous. Another physical parameter of the medium is the acoustic intensity I, it represents the energy for unit time able to pass through the unit area located on a point perpendicular to the direction of propagation of the sound. The intensity I is given by the follow relation:

$$I = \frac{P^2}{Z}\,[W/m^2]; \tag{4.5}$$

where P is the acoustic pressure and the acoustic impedance Z.

4.1.2 TYPES OF WAVES

In the material different modes of wave propagation can be activated, depending on the mode of excitation employed. We can defined two fundamental independent aspects: the propagation direction and the vibration direction, they represent the oscillatory characteristics of the particles. Depending on how they are combined different modes of waves are classified. In non-destructive testing of the most common types of waves used are the longitudinal, transverse and bending surface.

4.1.3 LONGITUDINAL WAVES

In the longitudinal waves, also called compression wave, the vibration direction is parallel to the propagation direction; they are propagated in solid, liquid and gaseous substances and they are the most used in non-destructive ultrasonic method, especially for stone materials. Starting from the wave source, all particles that are located in the same plane orthogonal to the direction of vibration undergo the stress simultaneously, with consequent displacement relative from their position. These displacements of the material in a cyclic shape modify their mutual distance and it is elastically transmitted to the adjacent plane creating pressure and depression zones.

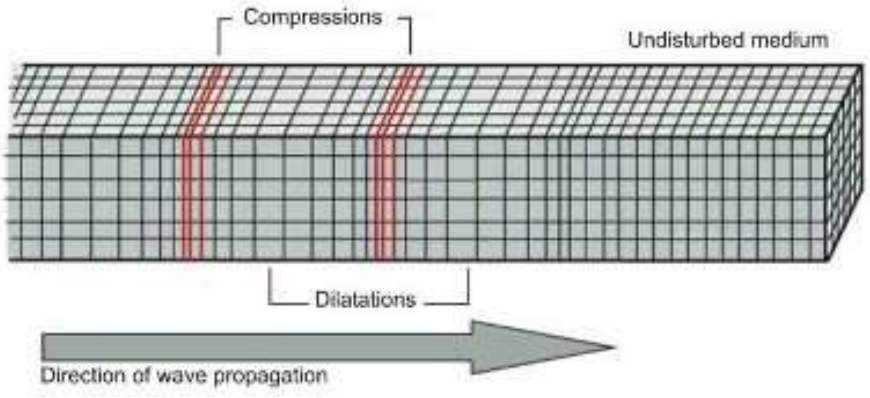

Figure 4.3 Representation of longitudinal wave

The propagation of the phenomenon takes place in form of plane waves, the wave fronts, (surfaces having the same phase), are plane.

4.1.4 TRANSVERSE WAVES

The transverse waves, also called shear waves, are characterized by a vibration direction perpendicular the propagation direction, in each plane of particles oscillates transversely to the direction of the wave. This type of wave propagates only in solid materials as they are the only ones to be able to withstand a shear stress; an exception is represented by very viscous liquid, or gel.

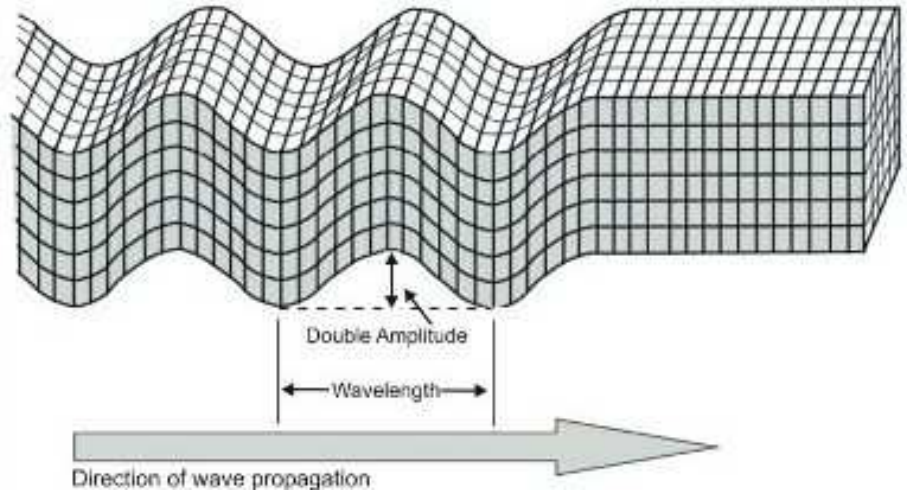

Figure 4.4 Representation of a transverse wave

4.1.5 SURFACE WAVES

Surface waves are also known as Rayleigh waves; they propagate on the surface of separation between two different media, or only in the surface layers of the solid to a maximum depth comparable to the wavelength. These waves are derived from the composition of transverse and longitudinal waves, the vibration of the individual particles occurs according with elliptical orbits and is transmitted elastically to the next orbit.

Unlike the previous waves are able to propagate only in a straight line, this type of wave follow the surface in their propagation in any concavity and convexity of the shape of the solid; this characteristic is exploited in certain problems of non-destructive testing. Since there are dispersed in large volumes, these waves can propagate in long distances with relatively low attenuation, but they are reflected by abrupt surface obstacles, such as edges and engravings.

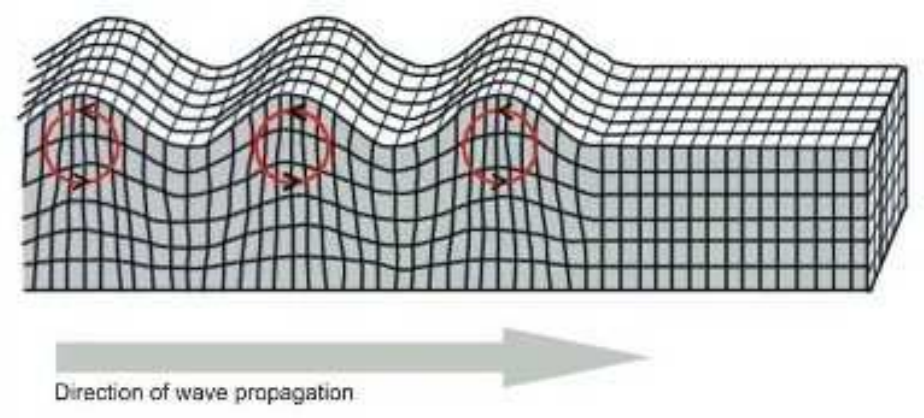

Fig 4.5 Representation of a surface wave

4.1.6 FLEXURAL WAVES

The flexural waves, also called Lamb waves, propagate when the layer of material concerned has low thickness in the order of the wavelength. The particles of material fluctuate according to two perpendicular directions and, depending on the vibration mode, can be divided into waves of a symmetric or antisymmetric mode or waves with orders 0,1,2 etc.. Within the thickness concerned all the particles are subject to vibration and the wave propagates until the thickness remains constant. Another particular factor of this type of waves is represented by the phase velocity, in fact it does not depend exclusively on the characteristics of the medium, but also by the wave itself, that is, by the way and order of vibration.

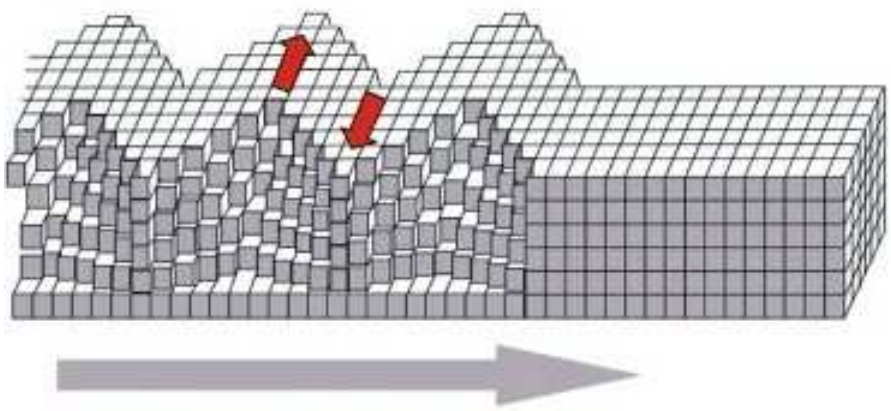

Figure 4.6 Representation of flexural wave

4.1.7 SNELL LAW

If a wave strikes the surface of separation of two media having different acoustic impedance, it will be reflected, from the part of the medium through which it is propagates initially, or transmitted, and propagates in the second medium. The characteristics of the reflected or transmitted waves depends on incident angle of incidence, the reflecting surface and the impedance characteristics of the vehicles. In the phenomena described the energy associated with the wave is changed: a part will be associated with the wave reflected, a part with the transmitted wave and finally a part will be lost due to attenuation in the passage through the medium.

The fraction of intensity of the incident wave which is transformed into wave reflected or transmitted wave, also known as the refracted wave, can be calculated by multiplying the coefficients of reflection R or transmission T for the acoustic intensity I.

The two coefficients are calculated with the following formulas:

$$R = \frac{Z_2 - Z_1}{Z_2 + Z_1}, \qquad T = \frac{2Z_2}{Z_2 + Z_1}; \tag{4.6}$$

where Z_1 and Z_2 are the acoustic impedances of the two media.

The 4.6 multiplied by 100 calculate the percentage of energy reflected and transmitted compared to the amount of total energy of the incident wave, their sum should be equal to unity. These coefficients are often expressed in decibels (dB), where a decibel is defined as ten times the logarithm to the base ten of the ratio between the unit and a measured value defined sound intensity, which the initial one.

$$dB = 10 \log_{10} \frac{I_1}{I_0} \tag{4.7}$$

It is relevant to note on the acoustic impedance, that it is very low in the gas (about four orders of magnitude less than that of the solid) and this results in values of the reflection coefficient very high at the surface of solid-gas separation.

The directions of propagation of the incident wave P, Q of the reflected wave of the transmitted wave S lie on the plane of incidence. With regard to the angle of reflection θr, with respect to the normal to the plane of incidence equals the angle of incidence θi; instead the angle of the transmitted wave θt is different, due to the deviation that undergoes the wave for the different acoustic impedances that have the two media.

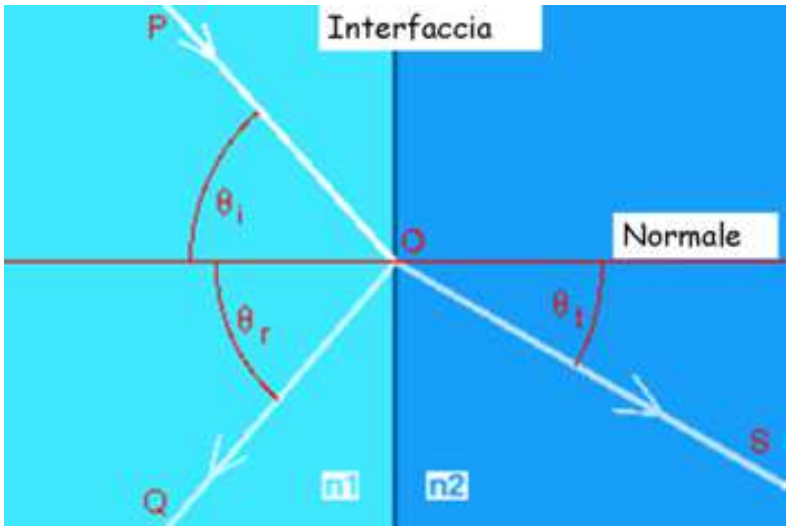

Figure 4.7 Incidence of wave on the surface of separation between two media

In order to determine the direction of the transmitted wave with respect to the incident direction, you can use Snell's Law.

where:

θi is the angle of incidence, the angle that the incident wave form with the normal to the surface of separation of the two means;

θt is the transmission angle, the angle that the transmitted wave form with the normal to the surface of separation of the two means;

V_1 is the velocity of propagation of the wave in the first medium n_1;

V_2 is the velocity of propagation of the wave in the second half n_2.

Using the Snell's law it can also be deduced that the passage from one medium to another with increased wave velocity, the transmitted wave increases the transmission angle, ie increasingly moves away from the normal. If, however, it happens that the radius of incidence and tilted beyond a certain angle, called *limit*

angle, the wave is refracted in the second media. The limit angle can be gained by placing the sine of the angle of transmission equal to one, this fact represents the limiting case.

4.1.8 ATTENUATION

As we have already mentioned, if the ultrasonic waves are subject to, the passage through the medium, also the phenomenon of attenuation, (loss of part of its energy) is in. The path that they can perform depends on the amplitude of the initial pressure wave, the frequency and the nature of the material.

The attenuation is the result of two independent phenomena:

- geometric attenuation;
- natural attenuation.

If we considers the performance of the ultrasound beam emitted by a transducer is known that describes a divergent cone, then the same initial energy radiates from time to time on areas increasing with increasing distance traveled. In this case, the intensity then undergoes geometric attenuation which increases according to $1/r^2$ law, or inversely proportional to the square of the distance r from the source. Normally, for a relatively short paths, no account is taken of this component.

The physical phenomenon of the attenuation is caused by phenomena of absorption and scattering that an ultrasonic ray undergoes by travelling in the medium.

The *absorption* of energy is transformed into heat, by the medium due to internal friction and dislocations, and the *scattering* is the spread by tiny irregularities that take energy from the ultrasound ray for to disperse it in different directions.

The decrease of the intensity undergoes with the distance, caused by this type of attenuation is exponential and is represented by the following formula:

$$I_x = I_0 e^{-\mu x}; \qquad (4.9)$$

where:.

I_x is the intensity as a function of the thickness x;

I_0 is the initial intensity;

μ is an attenuation coefficient.

The attenuation coefficient is the sum of two contributions one linked to the absorption "real", function of the frequency of the incident wave and the result from the energy dissipation which generates molecular friction in force, and one derived from the diffusion, also called scattering , which essentially is a function of the size of the particles that make up the medium through.

4.1.9 DIFFERENTIAL EQUATION OF PROPAGATION WAVE IN ELASTIC MEDIA

The propagation of wave in an elastic media is ruled by differential equations. They are deducted using a mechanical model of the continuum in dynamic field.

Some theories are more exhaustive to consider all the phenomena that are happened in the continuum, here the classical approach is proposed. It is in linear elasticity for homogeneous media. Forward the differential problem for heterogeneous media is presented.

4.110 MONO DIMENSIONAL CASE (ODE)

The elastic static problem of one dimensional beam, stressed in axial direction are ruled by the follow equations:

$$\begin{cases} N'(x) = -q_x(x) \\ u'(x) = e_x(x) \\ e_x(x) = \dfrac{N(x)}{EA} \end{cases} \tag{4.10}$$

Where N(x) is the axial stress,

$q_x(x)$ is the axial load,

u(x) is the axial displacement,

$e_x(x)$ is de axial deformation.

E is the elastic constant,

A the constant area of cross section.

Boundary condition are need to find the solution:

$$\begin{cases} u(x_0) = U_0 \\ u(x_1) = U_1 \end{cases} \tag{4.11}$$

By solving the elastic problem, after easy steps the follow equation is obtained from system (1)

$$\frac{1}{EA} u''(x) = -q_x(x) \tag{4.12}$$

If the problem is dynamic, the derivative become partial in space and time, the inertial action $q_I = \rho u(\ddot{x}, t)$ are added at the load: $q_x(x,t)$ where ρ is the density of material and $u(\ddot{x}, t)$ the acceleration. So the differential equation will be:

$$\frac{\partial^2}{\partial_x} u(x,t) = -\frac{1}{EA}[q_x(x,t) + \rho u(\ddot{x}, t)] \tag{4.13}$$

If the external load is zero:

$$\frac{\partial^2}{\partial x^2} u(x,t) = -\frac{\rho}{EA} u(\ddot{x}, t) \tag{4.14}$$

To identifying $c^2 = -\frac{\rho}{EA}$ the equation will be:

$$u_{xx}(x,t) = c^2 u_{tt}(x,t)\ ^1 \tag{4.15}$$

In order to evaluate the behaviour of a solid under settled by mechanical stress wave, it is relevant to present the equation and the solutions for the one dimensional case, we can schematize the mono dimensional solid as a spring. In literature, there are spring with and without mass.

It is $u(x,t)$ is the axial displacement of the one dimensional dots of solid. In some dots, (in the beginning or in the end), a displacement law can be applied in x_o, this conditions make the boundary condition for the PDE.

$u(x_0,t) = A(t)$ for each x_o where conditions are applied

In the most common case boundary condition are given for the begin and for the end of continuum:

$$\begin{aligned} u(0,t) &= A(t) \\ u(L,t) &= B(t) \end{aligned} \tag{4.16}$$

And more often, A(t) and B(t) are constant zero functions.

$$\begin{aligned} u(0,t) &= 0 \\ u(L,t) &= 0 \end{aligned} \tag{4.17}$$

When these conditions (4.17) are associated with differential equation (4.15) it is called *Dirichlet Problem.*

If conditions are given in term of derivative terms the conditions are called Newman conditions. Initial condition are given at the time t_o for all dots of the continuum.

$$\begin{aligned} u(x,t_0) &= f(x) \\ \frac{\partial}{\partial t} u(x,t_0) &= g(x) \end{aligned} \tag{4.18}$$

[1] This equation is not the Laplace equation $\Delta u = 0$, because the mixed differential term is absent and the constant c^2 is also present.

Also here, in the more common case, these condition are given for $t_0 = 0$

$$\begin{aligned} u(x,0) &= f(x) \\ \frac{\partial}{\partial t} u(x,0) &= g(x) \end{aligned} \tag{4.19}$$

If the continuum is pushed with an external force, at each dot, for each time, a function h(x,t) the system is called one-dimensional forced oscillator and the differential equation will be:

$$\frac{\partial^2}{\partial t^2} u(x,t) = c^2 \frac{\partial^2}{\partial x^2} u(x,t) + h(x,t) \tag{4.20}$$

If a dumped behaviour is considered the differential equation will be added with the viscous action, as the follow:

$$\frac{\partial^2}{\partial t^2} u(x,t) + \xi \frac{\partial}{\partial t} u(x,t) = c^2 \frac{\partial^2}{\partial x^2} u(x,t) \tag{4.21}$$

Where ξ is related with the frictional coefficient.

In the bi-dimensional case the classical non dumped and not forced equation of wave is:

$$\frac{\partial^2}{\partial t^2} u(x,y,t) = c^2 [\frac{\partial^2}{\partial x^2} u(x,y,t) + \frac{\partial^2}{\partial y^2} u(x,y,t)] \tag{4.22}$$

As in a multi-dimensional space:

$$\frac{\partial^2}{\partial t^2} u(\underline{x},t) = c^2 \sum_{j=1}^{n} \frac{\partial^2}{\partial x_j^2} u(\underline{x},t) \tag{4.23}$$

In these cases boundary and initial conditions are not discussed, and the solutions are often obtained by numerical approach instead theoretical way.

4.1.11THE DIRICHLET PROBLEM

The solution of the D*irichlet problem* is here reported :

$$\text{If } \frac{\partial^2}{\partial t^2}u(x,t) = c^2\frac{\partial^2}{\partial x^2}u(x,t) \qquad \begin{matrix} u(0,t)=0 \\ u(L,t)=0 \end{matrix} \qquad \begin{matrix} u(x,0)=f(x) \\ \frac{\partial}{\partial t}u(x,0)=g(x) \end{matrix} \tag{4.24}$$

$$\text{Where } f(x)=\sum_{n=1}^{N} B_n \sin(\frac{n\pi}{L}x) \text{ and } g(x)=\sum_{n=1}^{N} A_n \sin(\frac{n\pi}{L}x) \tag{4.25}$$

The solution is:

$$\sum_{n=1}^{N}[\frac{L}{n\pi c}A_n \sin(\frac{n\pi c}{L}t)+B_n \cos(\frac{n\pi c}{L}t)]\sin(\frac{n\pi}{L}x) \tag{4.26}$$

Where the coefficients are

$$A_n=\frac{2}{L}\int_0^L g(x)\sin(\frac{n\pi}{L}x)dx \text{ and } B_n=\frac{2}{L}\int_0^L f(x)\sin(\frac{n\pi}{L}x)dx \tag{4.27}$$

4.1.12 TRIDIMENTIONAL CASE (PDE)

The approach with a continuum three dimensional solid start form the constitutive mechanical model of material, and form it the motion equation are determined.

If we consider a elastic space, in a point of this space, in a cube os dx side the tensor stress give the tension in a point x, in a direction n, follow the chauchy theorem.

$$\mathbf{t}_j=\sigma_{ij}\mathbf{n}_j$$

Where σ_{ij} are the stress in Cartesian coordinates and $\mathbf{n}_j$ is the unit format vector. And $\mathbf{t}_j$ is the stress in the j^{th} face of cube.

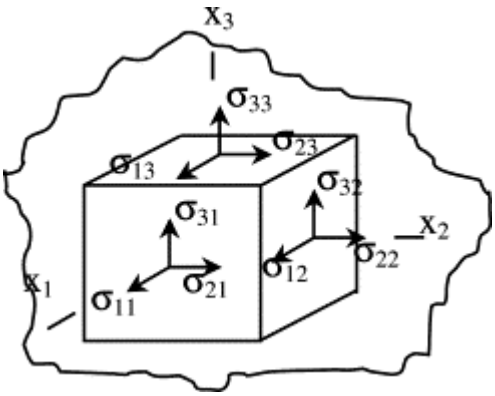

Figure 4.8 elementary volume of solid

Form the Newton second law, it is

$$\mathbf{F} = m\mathbf{u}_{tt} \tag{4.28}$$

Now if we operate an equilibrium in the cube, in the jth direction we obtain:

$$F_j = d\overset{1}{T}_i\, dx_2 dx_3 + d\overset{3}{T}_i\, dx_1 dx_2 + d\overset{2}{T}_i\, dx_1 dx_3 \tag{4.29}$$

It is relevant to recognize that

$$d\overset{j}{T}_i = \sigma_{ij,j} dx_j \tag{4.30}$$

Substituting this relation in Fj we obtain:

$$F_j = \sum_i \sigma_{ij,j} dV \tag{4.31}$$

$$F_j = \sum_i \sigma_{ij,j} dV = m u_{j,tt} \tag{4.32}$$

$$\sigma_{ij,j} + f_i = \rho u_{j,tt} \tag{4.33}$$

Using the constitutive model it is possible to related the stress with the displacement.

$$\sigma_{ij} = C_{ijkl}\varepsilon_{kl}$$
$$\varepsilon_{ij} = \frac{1}{2}(u_{j,i} + u_{i,j}) \tag{4.34}$$

In this mode should be pretty complicate to express the displacement in relation at the stress.

$$\sigma_{ij} = C_{ijkl}\frac{1}{2}(u_{j,i} + u_{i,j}) \tag{4.35}$$

$$[C_{ijkl}\frac{1}{2}(u_{j,i} + u_{i,j})]_j + f_j = \rho u_{j,tt} \tag{4.36}$$

Another and classical formulation that is given of this problem is obtained using the lame' constants. It is wide know that

$$\sigma_{ij} = \lambda\varepsilon_{ij}\delta_{ij} + 2\mu\varepsilon_{ij} \tag{4.37}$$

Where δ_{ij} is the Kronecker delta. By substituting this in the Newton law;

$$(\lambda\varepsilon_{ij}\delta_{ij} + 2\mu\varepsilon_{ij})_j + f_j = \rho u_{j,tt} \tag{4.38}$$

And using relation between strain and displacement we obtain the kwon Navier equation:

$$\sum_{j=1}^{3}[(\lambda+\mu)u_{j,ij} + \mu u_{i,jj}] + f_i = \rho u_{i,tt} \tag{4.39}$$

Usually this equation is presented in the follow style:

$$\mu\nabla^2\mathbf{u} + (\lambda+\mu)\vec{\nabla}\vec{\nabla}\mathbf{u} + \mathbf{f} = \rho\ddot{\mathbf{u}} \tag{4.40}$$

The solution is done in some simple cases only, using the follow position:

$$\mathbf{u} = \vec{\nabla}\phi + \vec{\nabla}\otimes\vec{\psi} \tag{4.41}$$

Where ϕ is a scalar functional and $\vec{\psi}$ i vector function. Using this approach the Navier equation become uncoupled, and you can separate two differential equations:

$$\nabla^2\phi = \frac{1}{\alpha^2}\ddot{\phi}$$
$$\nabla^2\psi_i = \frac{1}{\beta^2}\ddot{\psi}_i \tag{4.42}$$

The solution of these differential equations need boundary condition and initial conditions. By assuming a propagation phenomena in one direction that is the propagation of longitudinal waves, it is possible to obtain that the solution are valid if

$$\alpha^2 = \frac{\lambda + 2\mu}{\rho} \tag{4.43}$$

Also to assuming that the phenomena is propagating in an orthogonal direction of the motions of particles, it is obtained:

$$\beta^2 = \frac{\mu}{\rho} \tag{4.44}$$

α and β are recognized as the bulk and the shear wave of a wave that travel in an elastic media.

Relationships between young –lamè and cinematic dimensions are the follows:

$$V_L^2 = \frac{\lambda + 2G}{\rho} \qquad V_S^2 = \frac{G}{\rho}$$

4.1.13 DIFFERENTIAL EQUATION OF PROPAGATION WAVE IN MICRO STRUCTURED MEDIA

The classical theory for homogenous solid are inappropriate for describing the phenomena that are working on in the heterogeneous materials, ,first of all because the general hypothesis are different. That theory is here presented in order to have a relationship with the classical approach. However is always true, that in a long scale range eah heterogeneous material appear as homogeneous, and the laws of homogeneous has to be validate as particular case of the heterogeneous field.

If we want treat the heterogeneity of materials, some studies we can find in literature, the first approach on the description of heterogeneous continuum come from Cosserat, 1909, in its theory, the solid is homogeneous but micro structured. If we consider an infinitesimal element we need a variable x to describe the global properties, but also a local variable d to describe the orientation of the element. A displacement of the element it is defined as:

$$\mathbf{U}=\mathbf{x}-\mathbf{X} \qquad \mathbf{d}=\mathbf{R}\,\mathbf{d}_0 \tag{4.44}$$

Where $\mathbf{X}$ and $\mathbf{d}_0$ are the original positions and $\mathbf{R}$ is a rotation matrix.

In this solid, looking at the government equations, there is an internal micro structure able to produce internal micro deformations $\tilde{\boldsymbol{\varepsilon}}$ depending of a micro behavior. This one is defined starting from a function .

The description of the behavior is proposed by Mindlin in 1964, in this approach the elastic energy of the solid is given by global terms and local terms. By using a matrix notation, it can be write in quadratic form:

If $\mathbf{u}$ and are respectively field of global and local displacements. We can define the vector $\mathbf{U}^T = [u_{,x} \quad \phi \quad \phi_{,x}]$ and a Energy W that can be obtained form

$$W = \underline{\mathbf{U}}^T \underline{\underline{\mathbf{A}}} \cdot \underline{\mathbf{U}} \tag{4.45}$$

With **A** the constitutive matrix of the local and global behavior of material.
The equation of motion are the follow:

$$\begin{cases} \partial_i(\tau_{ij}+\sigma_{ij})+f_j=\rho\ddot{u}_j \\ \partial_i\mu_{ijk}+\sigma_{ij}+\phi_{jk}=\rho\ddot{\phi}_{lk} \end{cases} \tag{4.46}$$

With μ_{ijk} the double stress, σ_{ij} the relative stress, τ_{ij} the Cauchy stress. Applying the hypothesis of macro homogeneous materials, Mindlin deduct the equation of motion in terms on only displacements.

$$\begin{cases} A_1u_{i,jj}+A_2u_{j,ij}-A_3\phi_{jj,i}-A_4\phi_{ji,j}-A_5\phi_{ij,j}+f_i=\rho\ddot{u}_i \\ B_1(\phi_{kl,kl}\delta_{ij}+\phi_{kk,ij})+B_2(\phi_{ki,jk}+\phi_{jk,ik})+\ldots=\frac{1}{3}\rho' d^2\ddot{\phi}_{ij} \end{cases} \tag{4.47}$$

The resolution of these coupled equations is pretty difficult, however is some heasy cases this is studied.. It is possible to solve the equation, one notable solution is related with a propagation of a wave that is able to surf trough the media with any disturbance, this is called Soliton wave. These wave have relevant aspect related with the material, and are still object of study. This PDE system in recent years has been completed by adding other dissipative terms. These terms give nonlinear contribution at the equations.

4.2 SIGNAL PROCESSING

A signal is a function of time that represent a physical quantity. It can be achieved by observing, with appropriate measuring instruments, one or more quantities related to a certain physical phenomenon. The signal analysis has as objectives:

- describe in a significant variables in the phenomena and possibly their temporal variation;

- correlating various sizes, finding any causal relationships or dependencies statistics;
- investigate the internal parameters of the generating process;
- reduce any "noise" present in the measurement data.

4.2.1 THE DIGITAL SIGNAL

It is called continuous-time, or simply continuous, a signal s(t) defined for all values of the real variable in the continuous time $\boldsymbol{t}$ in continum or in an interval $[\boldsymbol{t_i}, \boldsymbol{t_f}]$. It is called a discrete signal $\boldsymbol{s}[\boldsymbol{n}]$ defined only for values $\boldsymbol{n}$, where $\boldsymbol{n}$ is an integer in the range $-\infty < \boldsymbol{t} < +\infty$.

The sampling is the procedure that allows to discretize a continuous signal, from the signal the values are extracted of in correspondence of a set discrete values of the time t_1, t_2, ..., tn. These values are called samples. The need to sample a signal produced by physical processes, which is typically continuous, arises from the use of digital computers, which analyze and process only sampled signals. Main characteristics of the sample are: the sampling time and the sampling rate. The first is the difference between the values of two consecutive samples of the time $t = t_{(i+1)}\text{-}t_i$; the sampling frequency is defined as $F_s = 1/\Delta t$.

There are two different, but equivalent models of sampling of a signal: in the domain of continuous-time (CT) and in the domain of discrete time (DT). The relationship between the domains CT and DT is characterized by the operations of sampling and reconstruction.

A signal is called sampled uniformly, if all time intervals have equal amplitude. This condition occurs in the case of periodic signals or derived limited, since it is not incurs the loss of signal resolution due to high ramps of the signal itself.

A signal s(t) that has been sampled uniformly every T seconds, can be reassembled in the function sa(t) in the CT domain:

$$s_a(t) = \sum_{n=-\infty}^{\infty} s(t)\delta(t - nT) \tag{4.48}$$

where δ (t) is a pulse function defined and equal to zero for t ≠ 0, not defined for t = 0; its integral conducted by t =-∞ to t=+∞ is 1. As the product s(t)δ(t-nT) is not equal to zero only at the instants of sampling, s(t) can be replaced in (3.1) with s(nT) without changing the meaning of the expression. An alternative expression of s_a (t), is often useful Fourier analysis:

$$s_a(t) = \sum_{n=-\infty}^{\infty} s(nT)\delta(t - nT) \tag{4.49}$$

The sampling model CT consists of a sequence of pulse functions CT, evenly spaced at intervals of T seconds, the weight of which is given by the value of the signal s(t) in the sampling instants, as seen in Figure 3.1.

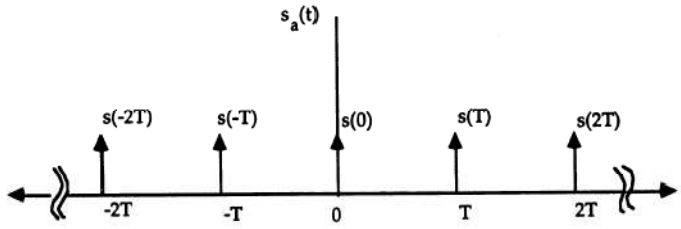

Figure 4.9 Model CT for a continuum signal

It should be noted that s_a (t) is not defined in the sampling instants since the same pulse function is not defined for t = 0. However, the values of s(t) in the sampling

instants are taken into account as an "area under the curve" of $s_a(t)$, and as such represent a useful mathematical model of sampling.

In the domain DT sampling pattern is simply the sequence of values of s(t) at the instants of sampling:

$$\boldsymbol{s[n] = s(t)|_{t=nT}} \qquad (\mathbf{4.50})$$

Instead of sa (t), s[n] is defined at the instants of sampling, as shown in figure 3.

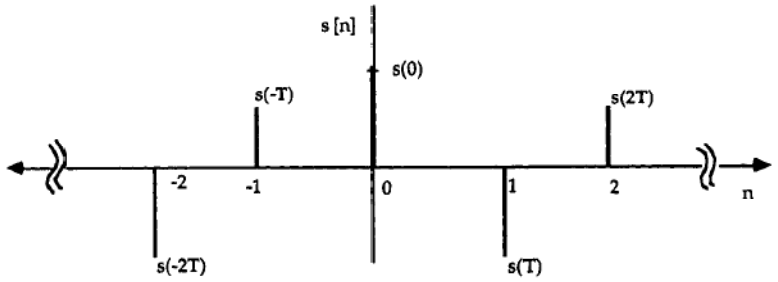

Figure 4.10 Model DT for a continuum signal

Both models are useful for the analysis of signals in their respective domains. Their equivalence is demonstrated by the fact that they present the same spectrum in the Fourier domain. Furthermore, the original continuous signal, from which are derived $s_a(t)$ and s[n], can be restored from both models of sampling, provided to use a sampling rate sufficiently high. This condition is expressed by the sampling theorem, formulated in 1928 by Nyquist: if a real signal has power spectrum zero for frequencies above a given F_0, it can be completely reconstructed if it is sampled at a frequency $F_s \geq 2F_0$. The frequency $F_N=F_s/2$ is called Nyquist frequency.

4.2.2 SIGNAL CLASSIFICATION

Other the classification between continuous and discrete signals, there are other characteristics of a signal, which can be:

- Real or complex, depending on whether at a given instant the signal is a real number or a complex number.
- Scalar or vector, that is, if it is described by a single number at each instant, or by more than one number.
- Analog or digital, that is, the signal at a given instant can take any real value in a given interval (analog signal) or only a discrete number of values (digital signal), typically multiples of a certain value said "As of analog-digital conversion ". Typically digital signals are already discrete in time.
- Periodic, if there exists a value τ such that $x(t)=x(t+\tau)$, for all values of τ where τ is a real number, if the signal is continuous; $x_i=x_{(i+\tau)}$ where τ is an integer, if the signal is discrete. Sometimes the real signals have a pattern which, although it is not periodic, has some characteristics of repeatability over time, in which case it is called pseudo-periodic signals. These signals are characterized by the same relation of periodicity, defined by means of an error ε between the values of *s(t)*.
- Deterministic or random (or stochastic): This classification concerns the "model" of the signal. In the first case is completely defined a priori its value, in the second is defined only statistically. The deterministic signals can enjoy special symmetries with respect to a certain instant; for example at time *t=0*: these are equal if *x(t)=x(-t)*, and odd if *x(t)=x(-t)*.

4.2.3 NOTABLE SIGNALS

Here a review of the most common signals, indicating the mathematical expression, is presented in the case of continuous or discrete signals .

- *Constant signal*

Continuum	Discrete
$\boldsymbol{x(t) = c}$	$\boldsymbol{x_i = c}$

if $c = 0$ it the signal is called assent.

- *Unit Step signal*

Continuum	Discrete
$\begin{cases} t < 0 \rightarrow u(t) = 0 \\ t \geq 0 \rightarrow u(t) = 1 \end{cases}$	$\begin{cases} i < 0 \rightarrow u_i = 0 \\ i \geq 0 \rightarrow u_i = 1 \end{cases}$

Signal delta, is the "*derivative*" (or the difference in the discrete case) of the unit step signal. In the continuous case is a Dirac delta, in the discrete case is a signal always zero, but that is 1 to 0, also known as the unit impulse function or discrete pulse:

Continuum	Discrete
$\delta(t)$	$\begin{cases} i = 0 \rightarrow \delta_i = 1 \\ i \neq 0 \rightarrow \delta_i = 0 \end{cases}$

And so:

$$u(t) = \int_{-\infty}^{t} \delta(k)\, dk \qquad u_i = \sum_{k=-\infty}^{i} \delta_k$$

- *Sinusoidal Signal*

Continuum	Discrete
$x(t) = A \cdot \sin(\omega \cdot t + \varphi)$	$x_i = A \cdot \sin(\omega \cdot \Delta t \cdot i + \varphi)$

- *Complex exponential signal*

Continuum	Discrete
$x(t) = A \cdot exp\left[-\frac{t}{\tau} + j \cdot (\omega \cdot t + \varphi)\right]$	$x_i = A \cdot \exp\left[-\frac{\Delta t \cdot i}{\tau} + j \cdot (\omega \cdot \Delta t \cdot i + \varphi)\right]$

where i is the imaginary unit.

- *Saw tooth wave*

Saw tooth wave; wave is non-sinusoidal, i.e. which can be described as composed of sine waves at different frequencies. This type of wave contains all harmonics whole multiple of the fundamental frequency. A definition *saw tooth wave* of frequency f is based on the integer part function of time, and can be reconstructed using the Fourier series:

$$x(t) = 2\left(\frac{t}{f} - int\left(\frac{t}{f} + \frac{1}{2}\right)\right); \qquad x(t) = -\frac{2}{\pi}\sum_{k=1}^{\infty}\frac{\sin(2\pi k f t)}{\mathrm{k}}; \tag{4.51}$$

Square wave, it is a signal composed of alternating regular and instant two values. It is also non-sinusoidal wave but contains only the odd harmonics of its main frequency: the third with amplitude equal to $1/3$ of the fundamental, the fifth equal to $1/5$ of the fundamental, and so on. Can be defined as the sign function of a sinusoid or reconstructed using the Fourier series:

$$x(t) = sgn(\sin(t)); \qquad x(t) = \frac{4}{\pi}\sum_{k=1}^{\infty}\frac{\sin((2k-1)2\pi f t)}{(2\mathrm{k}-1)}; \tag{4.52}$$

In Figure 4.11 we show how it is possible to reconstruct a square wave with k harmonics

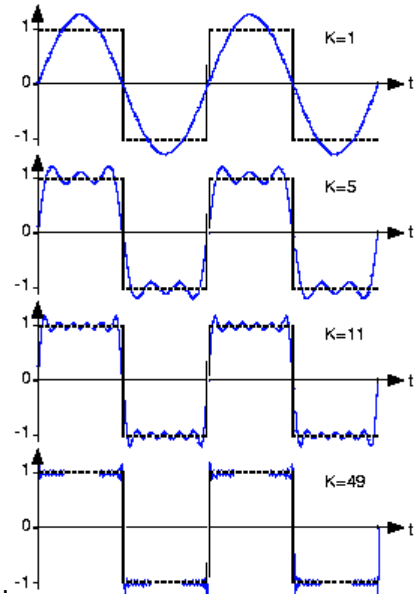

Figure 4.11 Reconstruction of a square wave using Fourier series

- *White noise*

White noise, the simplest stochastic signal. It is characterized by zero mean and by the fact that two values in any two time instants, however neighbors, are devoid of correlation, and independent:

$$\mu(t) = 0; \qquad R(\tau) = \delta(\tau) \tag{4.53}$$

4.2.4 SPACE TIME PROCESSING: THE CROSS CORRELATION

The flight time, is the time interval between the emission of the wave and its reception. It is decisive for the calculation of the velocity of the wave, which allows estimation of some mechanical properties of the material. The estimate of the flight time is also an important factor for the localization of a source of the signal or of a defect that reflects the wave.

The identification temporal beginning of the received signal is complicated by several factors. Firstly, the wave passes through a material that is subject to phenomena of attenuation and dispersion, for which the received signal will not be perfectly identical to the one sent. It is also necessary to distinguish the main wave waves echo or reflected waves from nearby surfaces. Another obstacle to the exact estimate of the time of flight is the presence of noise. It is eliminated by imposing a threshold, a value of the measured quantity, below which the signal is considered noise. This is possible, however, only in the case in which the noise amplitude has clearly less than that of the signal considered. If the amplitude of the noise is comparable to that of the signal considered such an operation would alter the signal itself. In these cases, using methods that are based on a comparison of the received signal with the function of the signal emitted, the variation of a variable connected to the flight time. This principle is based on the method of cross-correlation (cross-correlation).

The sequence cross-correlation is defined as:

$$\boldsymbol{R_{xy}(m) = E[x_{n+m}\, y_n^*] = E[x_n\, y_{n-m}^*]} \qquad \mathbf{(4.54)}$$

where x_n and y_n are stochastic processes, n is an integer ranging from - ∞ to + ∞, E is the mean value operator.

The cross-correlation function c_r (τ) of two continuous functions in the time domain $f_1(t)$ and $f_2(t)$ can be written as:

$$\boldsymbol{C_r(\tau) = \lim_{T\to\infty} \frac{1}{T} \int_0^T f_1(t) f_2(t+\tau) dt} \qquad \mathbf{(4.55)}$$

where τ is the variable delay time. If the functions $f_1(t)$ and $f_2(t)$ differ only in the function of the delay τ_0 $c_r(\tau)$ has a maximum value at τ_0.

For discrete signals the cross-correlation is defined as:

$$\boldsymbol{R_{xy}(k) = \sum_{n=0}^{N-k-1} x_{n+k}\, y_n^*} \qquad \boldsymbol{(4.56)}$$

wherein x and y are vectors of size N, k varies from-N +1 to N-1. This will obtain a vector c(m) of dimension 2N-1, whose elements are c(m) =R_{xy} (m-N), m = 1, ..., 2N-1. The maximum of this vector it will have a value of m which corresponds to a value of the difference k = m-N that is precisely the time deviation between a signal and the other.

Is now given an example of application of the cross-correlation applied to the calculation of the time offset between two simple sinusoidal signals of equation s(t)=4sin(2π10t) of frequency f=10 Hz and sampled at a sampling frequency f_s=100 Hz, as shown in figure 3.4, they are shifted by 0.15 seconds which correspond to 15 samples.

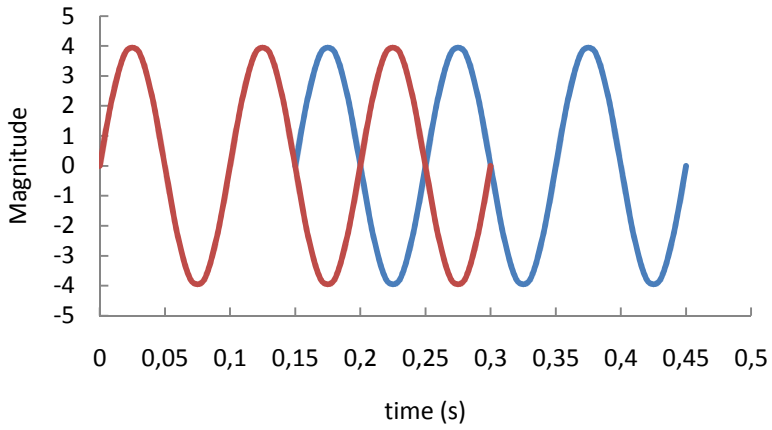

Figure 4.12 sinusoidal Signals shifted of 0,15 s

Applying the cross-correlation of the two signals are obtained the following representations of R_{xy} as a function of the indices m and k first described. In Figure 4.13

is represented the trend of the elements of the vector c(m) of dimension 2N-1, that for N=46, as in this case, has dimension 91. The maximum is obtained for m = 61.

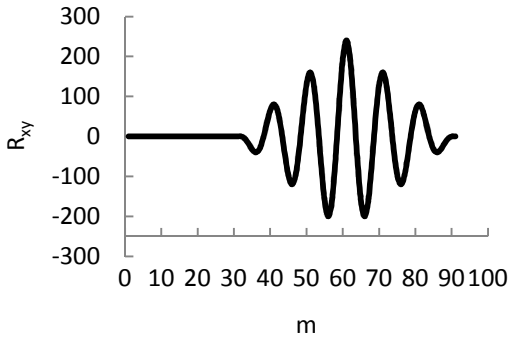

Figure 4.13 R_{xy} -m

In figure4.14 shows the result in function of the index k = m-N that expresses the time offset of the two signals in terms of samples. The maximum of the function R_{xy} occurs for k = 15.

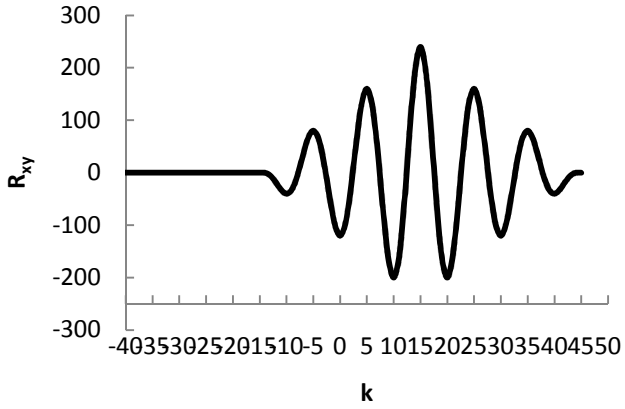

Figure 4.14 Rxy -k

Knowing the sampling frequency can be traced back to the time lag τ between the two signals, as shown in Figure 4.15.

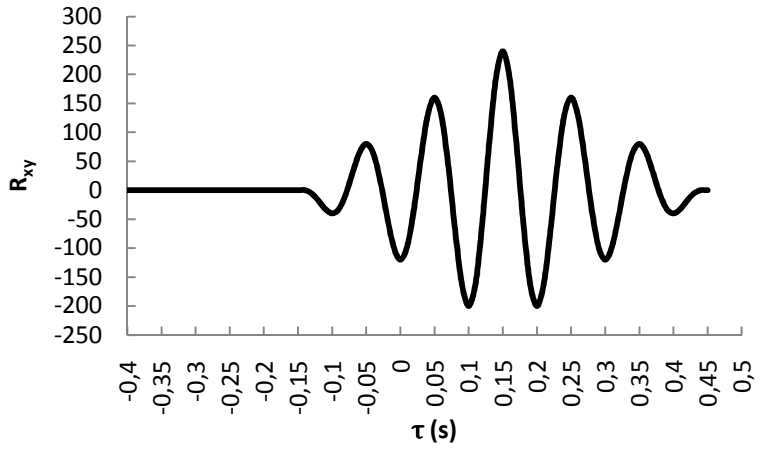

Figure 4.15 R_{xy} in function of τ

An accurate measurement of wave velocity is essential in NDT tests. The estimation of the wave arrival time is also an important factor to localize the source of the signal or to determine the position of a defect when an ultrasound is reflected back from a border.

In NDE different methods have been used to evaluate phase and group velocity. Reviews are available literature.

We computed the cross-correlation with the function "*xcorr*" available in MATLAB®. The code imports the digitalized signal, performs the cross-correlation, and gives an output with a "correlation number" (≤ 1) as measure on how much similar in shape are the two signals being analyzed (1, when they are the same) and the delay calculated as described above. This number must then be multiplied by the sampling time interval to convert the numerical delay to time-delay. The sensitivity of the time delay is then dependent on the sampling frequency. For a

200 Msps digitalized signal the sensitivity is 5 nanoseconds. The peak of the cross-correlation shows the delay between the portions of the signals that contain the maximum power. Figure 4.16 shows a simple example. An ultrasonic signal with 200 Msps sampling frequency the time step is determined by:

τ =1/(200*106) [sec]=5*10-9sec=5nanosec

The signal is artificially delayed by 1 microsecond. The original and the delayed signal are shown in Figure 4.1a. The cross-correlation function between two signals is shown in Figure 4.16. By computing the maximum we can found the delay in nanoseconds.

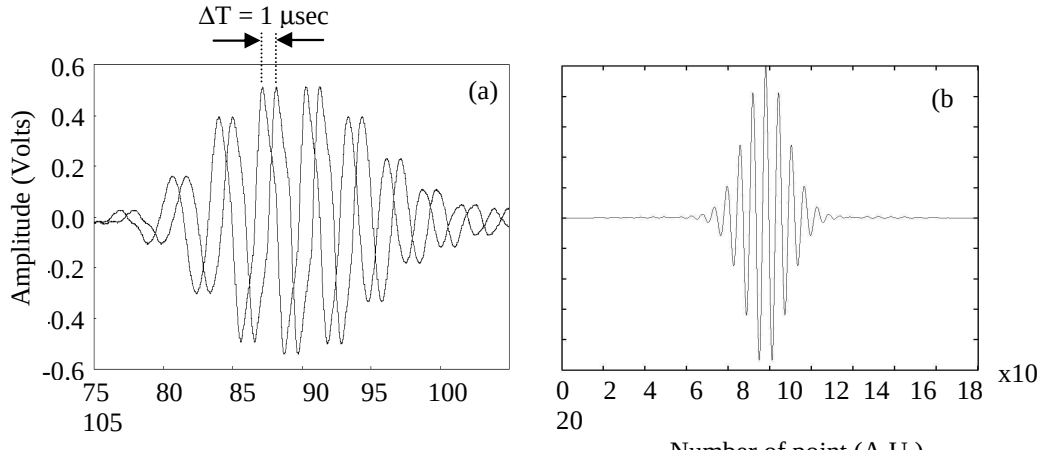

Figure 4.16 (a) Original signal and original signal artificially shifted by 1 microsecond; (b) cross-correlation function between the signals in (a).

4.2.5 FREQUENCY TIME PROCESSING

The analysis in the frequency domain aims to describe the frequency content of a signal. The most common methods in this type of analysis is using the Fourier transform. Here we describe as a periodic signal is developed as fourier series,

follow we present the *continuum Fourier transform* that is used for continuum signals, so the continuum Fourier transform used for discrete signals, and the *discrete Fourier transform* for discrete signals. The *Fast Fourier transform* is an algorithm used by some commercial software to obtain the power spectral density of signals in term of discrete frequency with light computational effort.

If a continuous signal s(t) is periodic with period T, its development in complex classical Fourier series:

$$\boldsymbol{s(t) = \sum_{n=-\infty}^{\infty} a_n\, e^{jn\omega_0 t}} \qquad (\mathbf{4.57})$$

where $\omega_0 = 2\pi/T$, and an are the complex Fourier coefficients defined as:

$$\boldsymbol{a_n = \frac{1}{T}\int_{-\frac{T}{2}}^{\frac{T}{2}} s(t)\, e^{-jn\omega_0 t}\, dt} \qquad (\mathbf{4.58})$$

The conditions under which a periodic signal s(t) can be expanded in Fourier series are known as conditions Dirichet. They require that in every period of s(t) has a finite number of discontinuities, a finite number of maxima and minima, and that s(t) satisfies the following convergence criterion:

$$\boldsymbol{\int_{-\frac{T}{2}}^{\frac{T}{2}} |s(t)|\, dt < \infty} \qquad (\mathbf{4.59})$$

The coefficients of the Fourier series a_n can be interpreted as the spectrum of the signal s(t), because each of them represents the contribution of $n\omega_0^{th}$ frequency to the total signal. Since these coefficients are complex representation in the Fourier domain has an amplitude spectrum and a phase spectrum. They constitute a collection of discrete values, and this is consistent with the fact that a periodic

signal has a spectrum that contains only integer multiples of the fundamental frequency ω_0.

For signals s(t) in real values is possible to convert the complex exponential form of the Fourier series in a trigonometric form:

$$\boldsymbol{s(t) = b_0 + \sum_{n=1}^{\infty} b_n \cos(n\omega_0 t) \sum_{n=1}^{\infty} c_n \sin(n\omega_0 t)} \qquad \mathbf{(4.60)}$$

where $\omega_0 = 2\pi/T$. The Fourier coefficients b_0, b_n and c_n are real and are defined as:

$$\boldsymbol{b_0 = \frac{1}{T} \int_{-\frac{T}{2}}^{\frac{T}{2}} s(t) dt} \qquad \mathbf{(4.61)}$$

$$\boldsymbol{b_n = \frac{2}{T} \int_{-\frac{T}{2}}^{\frac{T}{2}} s(t) \cos(n\omega_0 t)\, dt} \qquad \mathbf{(4.62)}$$

$$\boldsymbol{c_n = \frac{2}{T} \int_{-\frac{T}{2}}^{\frac{T}{2}} s(t) \sin(n\omega_0 t)\, dt} \qquad \mathbf{(4.63)}$$

Any real signal s(t) can be expressed as a sum of functions even and odd components. It can be shown that an even function is represented in the series from the coefficients b_n with n even index. Similarly an odd function is represented by the coefficients c_n with n odd index. To clarify the concept will calculate the Fourier coefficients of the odd function $s(t)=\sin(\omega_0 t)$. The coefficient b_0 is equal to 0, since, as is known, the integral of a harmonic function extended to the entire period is deleted. It represents the average of the signal. The coefficients b_n are also equal to 0 by virtue of the orthogonal property of the sine and cosine functions. As regards the coefficients c_n is exploits the properties of harmonic functions:

$$\boldsymbol{\int_{-\frac{T}{2}}^{\frac{T}{2}} \sin(m\omega_0 t) \sin(n\omega_0 t) = \frac{T}{2} \delta_{m,n}} \qquad \mathbf{(4.64)}$$

The integral is different from zero and more precisely equal to T/2 only in the case where m = n. In the particular case of the function s(t)=sin(ω_0t), m is equal to 1 and therefore the only coefficient other than 0 is c_1=1, which was added in the form of trigonometric Fourier series returns precisely the function of departure.

4.2.6 THE FOURIER TRANFORM FOR CONTINUUM SIGNALS

The Fourier transform of s(t) is expressed by the notation S(jω). The result is shown in the following pair of equations which is known as the classical Fourier transform of a continuum signal:

$$\boldsymbol{S(j\omega) = \int_{-\infty}^{\infty} s(t) e^{-j\omega t} dt} \qquad (\mathbf{4.67})$$

$$\boldsymbol{s(t) = \frac{1}{2\pi} \int_{-\infty}^{\infty} S(j\omega) e^{j\omega t} d\omega} \qquad (\mathbf{4.68})$$

The first equation is the Fourier transform while the second is the Inverse Fourier transform. The relation

$$S(j\omega)=\mathcal{F}\{s(t)\} \qquad (4.69)$$

denotes the Fourier transform of s(t), where $\mathcal{F}\{\cdot\}$ is the notation used for the Fourier transform operator, and ω is the continuous variable frequency after that has been removed the condition of periodicity. The Fourier integral can be interpreted "physical" transform S(jω). In fact, in analogy with the development in Fourier series, the signal s(t) can be viewed as integral sum of sinusoids complex exp(jωt) each of amplitude (1/2π)S(jω)dω. The transformed, therefore, represents, for each pulsation, the "harmonic content", or in other words, in such frequency ranges the signal is "rich" and in which it is less so. Are listed below some of the most important properties of continuum Fourier transform:

- Linearity:

$$\boldsymbol{\mathcal{F}\{af_1 + bf_2\} = a\mathcal{F}\{f_1\} + b\mathcal{F}\{f_2\}} \qquad (4.70)$$

with a and b are complex constants

- Translation of origin in time domain:

$$\mathcal{F}\{f(t-t_0)\} = e^{-j\omega t_0}\mathcal{F}\{f(t)\} \tag{4.71}$$

- Symmetry of the transform of Fourier of a real signal:

$$S^*(j\omega) = \int_{-\infty}^{\infty} f(t)e^{j\omega t}dt = \int_{-\infty}^{\infty} f(-t)e^{-j\omega(-t)}d(-t) = S(-j\omega) \tag{4.72}$$

Energy theorem of Bessel-Parseval equality or the *Parseval theorem*, assert that the energy of a signal s with finite energy is constant, regardless of the space in which this energy is measured, and is equal to:

$$E[s] = \int_{-\infty}^{\infty} f^2(t)\,dt = \frac{1}{2\pi}\int_{-\infty}^{\infty}|S(j\omega)|^2 d\omega = \text{const} \tag{4.73}$$

where E[s] is the energy of the function f(t). The energy theorem provides further interpretation of the Fourier transform. In fact, it states that the energy of the function f(t) is also given by the sum of the integral quantity $(1/2\pi)S(j\omega)^2\,d\omega$. For this reason $(1/2\pi)S(j\omega)^2$ takes in the name of spectral density of energy of the function f(t).

Below are the transforms of some significant signs:

$s(t)$	$\mathcal{F}\{s(t)\}$
$\delta(t)$	1
$e^{j\omega_0 t}$	$2\pi\delta(\omega+\omega_0)$
$cos(\omega_0 t)$	$\pi[\delta(\omega-\omega_0)+\delta(\omega+\omega_0)]$
1	$2\pi\delta(\omega)$

Table 4.1- Notable signals

The function δ (t) is a signal, theoretical, "concentrated" at time t=0: its transform is constant at all frequencies, as the harmonic content of the signal is constant.
In all cases, applying the Euler equations, the Fourier transform can be explicit in terms of real part and imaginary part:

$$S(j\omega) = \int_{-\infty}^{\infty} f(t)e^{-j\omega t}dt = \int_{-\infty}^{\infty} f(t)cos(\omega t)\,dt + j\int_{-\infty}^{\infty} f(t)\sin(\omega t)dt \qquad (4.74)$$

d the two components are called cosine transform and sin transformed. It should be noted that if the function f(t) is equal to cosin, recalling that the product of a function equal to an odd results in an odd function, the second integral vanishes and we obtain:

$$\boldsymbol{F(\omega) = \int_{-\infty}^{\infty} f(t)cos(\omega t)\,dt} \qquad (\mathbf{4.75})$$

That is a real function.

4.2.7 THE FOURIER TRANSFORM FOR DISCRETE SIGNALS

The Fourier transform for discrete signals is obtained using the sampling time in equation 4.67. and replacing the variable frequency ω with a normalized frequency ω'=ωT the equations are defined in discrete mode as follows:

$$\boldsymbol{S(e^{j\omega'}) = \sum_{n=-\infty}^{\infty} s[n]e^{-j\omega' n}} \qquad (\mathbf{4.76})$$

$$\boldsymbol{s[n] = \frac{1}{2\pi}\int_{-\pi}^{\pi} S(e^{j\omega'})\,e^{jn\omega'}d\omega'} \qquad (\mathbf{4.77})$$

The spectrum S (exp(jω')) is periodic in ω' with period 2π. It establish that:

$$\boldsymbol{\mathcal{F}\{s_a(t)\} = \mathcal{F}D\{s[n]\}} \qquad (4.78)$$

where s[n]=s(t)$_{(t = nT)}$. This shows that the spectrum of a continuum signal $s_a(t)$, calculated with the Fourier transform for continuous signals, is identical to the spectrum of *s[n]* calculated using the Fourier transform for discrete data. So, although $s_a(t)$ and *s[n]* are different models of sampling, are equivalent in the sense that they have the same representation in the Fourier domain. For each signal there is a similar transform for continuous signals to discrete signals. Forward we have reported in Table 4.2 the $\boldsymbol{\mathcal{FD}}$ of the same signals remarkable to which had been applied the classical Fourier transformed.

$\boldsymbol{s[n]}$	$\boldsymbol{\mathcal{FD}\{s[n]\}}$
$\boldsymbol{\delta[n]}$	$\boldsymbol{1}$
$\boldsymbol{e^{j\omega_0 n}}$	$\boldsymbol{\sum_{k=-\infty}^{\infty} 2\pi\delta(\omega - \omega_0 + 2\pi k)}$
$\boldsymbol{cos(\omega_0 n + \varphi)}$	$\boldsymbol{\pi \sum_{k=-\infty}^{\infty} [e^{j\varphi}\delta(\omega - \omega_0 + 2\pi k) + e^{-j\varphi}\delta(\omega + \omega_0 + 2\pi k)]}$
$1 \quad (-\infty < n < \infty)$	$\boldsymbol{\sum_{k=-\infty}^{\infty} 2\pi\delta(\omega + 2\pi k)}$

Table 4.2 Continuum Fourier transform for discrete signals

The same properties presented in respect of the Fourier transform for continuous signals can be transformed to extend for discrete signals.

The definition of the $\boldsymbol{\mathcal{FD}}$ implies that the time domain is discrete while the frequency domain is continuous. This unlike the $\mathcal{F}$D, which are in both domains continuous. The operator "dual" to the $\boldsymbol{\mathcal{FD}}$, has the domain of the continuous-time and discrete frequency domain is the Fourier series for periodic signals CT. In

reality was formulated a transform that has such characteristics, the Fourier transform at discrete frequencies ($\mathcal{F}$D), and which is similar to the classical Fourier series.

Since the signals DT are often derived from signals CT is important to develop a relationship between the spectrum of the original signal CT and the spectrum of the corresponding signal DT. In this regard, the following relationship holds:

$$\boldsymbol{S(e^{j\omega T}) = \mathcal{F}\{s_a(t)\}\frac{1}{T}\sum_{n=-\infty}^{\infty} S(j[\omega - n\omega_s])} \qquad (\mathbf{4.79})$$

In which $\omega_s=(2\pi/T)$ is the sampling frequency, expressed in radians per second. An alternative form, valid for the DTFT, is:

$$\boldsymbol{S\left(e^{j\omega'}\right) = \frac{1}{T}\sum_{n=-\infty}^{\infty} S\left(j\left[\frac{\omega' - n2\pi}{T}\right]\right)} \qquad (\mathbf{4.80})$$

where $\omega'= \omega T$ is the frequency domain normalized DT, expressed in radians. The spectrum S (exp($j\omega T$)) =S(exp($j\omega'$)) is composed of an infinite number of copies of the spectrum CT S($j\omega$), positioned at intervals of ($2\pi/T$) in the domain ω, or at intervals of 2π in the domain ω'.

If S($j\omega$) has a bandwidth ω_c, ie vanishes for frequencies greater than ω_c, and T is such that $\omega_s > 2\omega_c$, then the spectrum DT is equal to S($j\omega$), scaled by 1/T in his band. Under these conditions, the Nyquist theorem, a CT signal can be reconstructed exactly from the samples. Is extracted first spectrum S (exp($j\omega'$)), to reconstruct the spectrum CT original deleting all copies out of the band and multiplying it by T.

4.2.8 DISCRETE FOURIER TRANFORM

The *discrete Fourier transform* is obtained by sampling uniformly the frequency domain of the DTFT. The N samples of pulsation are $\omega_k=(2\pi k/N)$, k = 0,1, ..., N-1.

The value N corresponds to the length of the signal s[n], or its period, in the case in which both periodic. The pair of the DFT is defined by the following equations:

$$\boldsymbol{S[k] = \sum_{n=0}^{N-1} s[n] e^{-\frac{j2\pi kn}{N}} \qquad k = 0, 1, \dots, N-1} \qquad (\mathbf{4.81})$$

$$\boldsymbol{s[n] = \frac{1}{N} \sum_{n=0}^{N-1} S[k] e^{\frac{j2\pi kn}{N}} \qquad n = 0, 1, \dots, N-1} \qquad (\mathbf{4.82})$$

if s [n] is a sequence of length N, is that it is a periodic sequence, the DFT treats its samples as if they belonged to a period of a periodic sequence. This is a fundamental characteristic of the DFT, useful in the analysis of the signals to avoid the introduction of artifacts. Many of the properties of the DFT are similar to those of the DTFT, but there are some differences due to the characteristic of the DFT of a signal treated as a period of a periodic sequence.

4.2.9 FAST FOURIER TRANSFORM

The Fast Fourier Transform is not a transform, but an algorithm that implements the DFT. In fact, the calculation of the DFT, for large values of N (the order of 10^6), requires a considerable amount of operations. Specifically, neglecting the calculation of powers exp(-j2π/N), which can be made a priori, it is necessary to perform approximately N^2 multiplications and additions as many (for N $=10^6$ there are N^{12} operations of each type). The Fast Fourier Transform algorithm introduced by *Cooley* and *Tukey*, reduces the number of operations to a value proportional to $N \cdot Log_2 N$, that in one of the best implementations is $5N \cdot Log_2 N$ (which for N $=10_6$ is equal to about 10^8), that is 10,000 times faster. This allows to carry out DFT analysis in real time. The calculation is faster if the signal length is a power of 2.
Spectral analysis of the signals is necessary to pay attention to some features of the FFT that have a certain influence on the outcome of the analysis .

- *WINDOWING*

  The FFT treats the data sequence as if they were a period of a periodic sequence. If the function is not periodic, however errors may occur because the function created by the FFT can have discontinuities form at the ends of the block. This drawback is minimized taking the average of the signal to zero and operand a "windowing" the data so that the ends of the block the signal tends to zero.

- *ZERO PADDING*

  One can obtain a better spectral resolution of frequencies by increasing the length of the signal. This is obtained by taking multiple samples within the range of observation, increasing the length of the interval of observation or by inserting in the data sequence a succession of zero. Enlarging the observation interval of the signal increases the resolution, ie increase the points of the spectrum in the frequency domain. The same result is obtained with the zero padding but the form of the values of the FFT decreases. Increasing the sampling frequency of the signal increases the frequency range of the spectrum. In this way, however, remains unchanged the number of points in this domain, and then lowers the resolution of the spectrum.

- *LEAKAGE E PICKET FENCE EFFECT*

  The picket fence effect is the phenomenon by which are not visible with the FFT some frequency components of a signal. In fact the points of the spectrum in the frequency domain are integer multiples of the frequency $f1 = Fplay/N$, where Fplay is the sampling frequency and N is the length of the signal. The energy of the frequency components not present in the spectrum is "lost" (leakage) in the harmonics of the signal.

4.2.10 NOTABLE EXAMPLES OF FFT

In this section we will illustrate some examples of application of the FFT of simple signals to better understand the usefulness and properties. The following applications have been developed with the FFT algorithm used in the software MATLAB.

The first example concerns a sinusoidal signal of equation $s(t)=\sin(2\pi ft)$. It is a harmonic at frequency f=50kHz and in the representation of the FFT will have only one peak at that frequency. In Figure 4.17 is represented the signal, measured in millivolts, as a function of time expressed in microseconds.

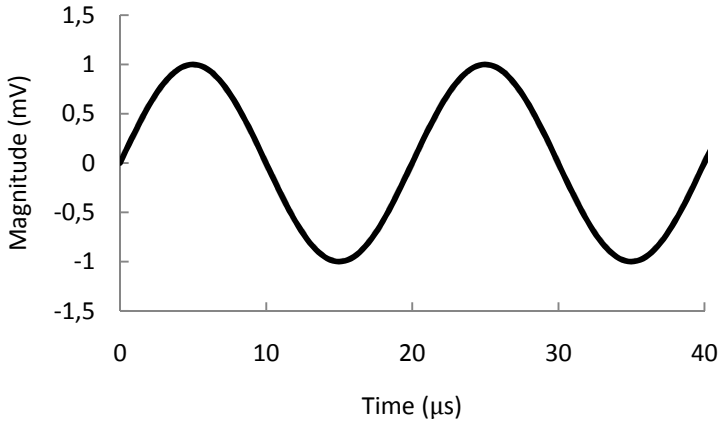

Figure 4.17 sinusoidal Signal f=50 kHz

In Figure 4.18, in y –axes are shown the values of the coefficients of the FFT multiplied by its complex conjugate and relation to the long signal. If y is the vector composed of these coefficients, L is the length of the signal, then the power of the FFT is $P=(y\cdot y^*)/L$. In the x-axes are reported the frequencies, expressed in kHz,

and we note the symmetry with respect to the origin of the power spectral density function. The proposed signal has been sampled at a frequency of 5 MHz, therefore the frequency axis of the FFT will be between -2.5 and 2.5 MHz

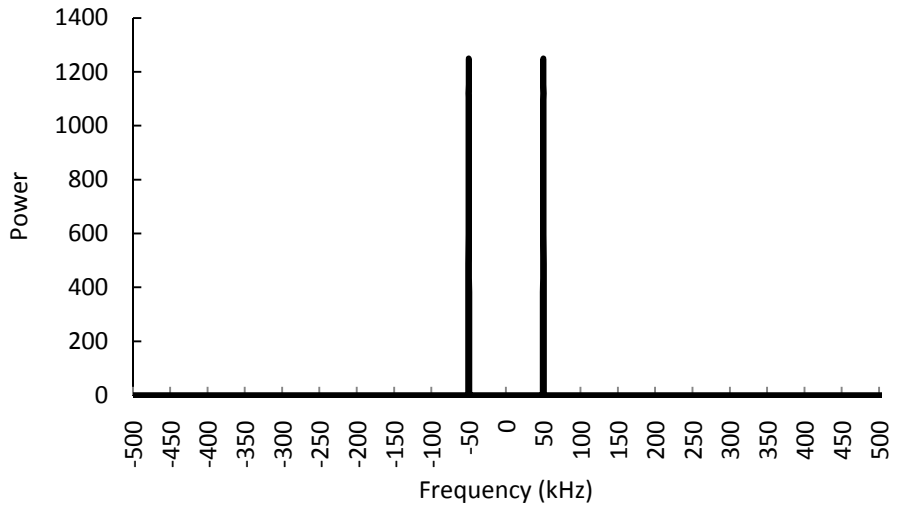

Figure 4.18 FFT of a signal with f=50 kHz

The second example shows how the two frequencies are extracted from a harmonic obtained as the sum of two harmonics with frequencies f1 ==50kHz and f2=150kHz.

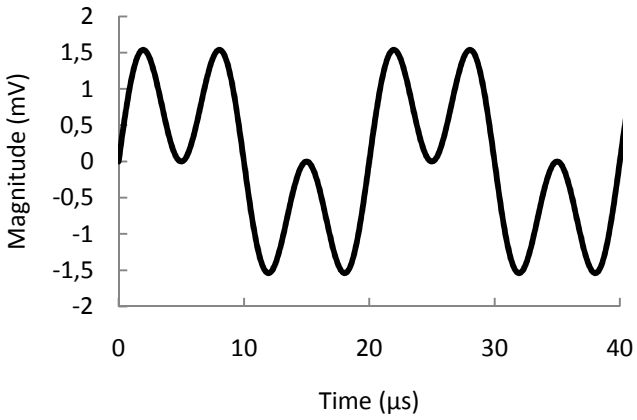

Figure 4.19 Two frequency signal

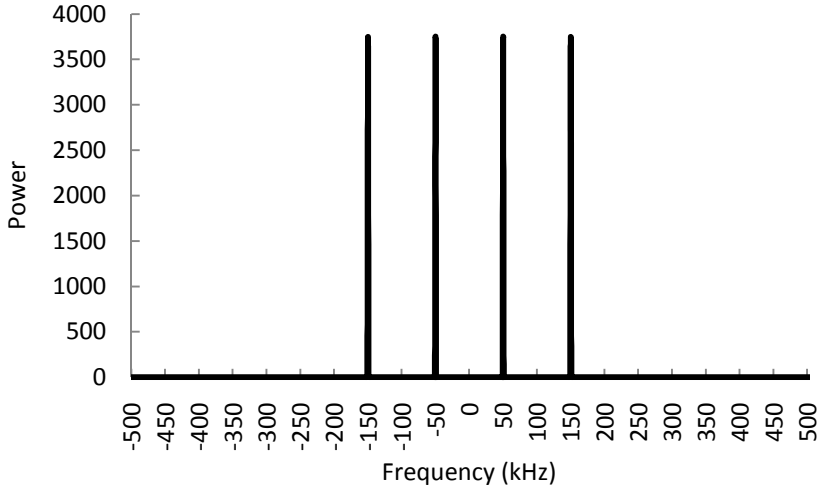

Figure 4.20 FFT Two frequency signal

In the third example highlights the relationship between signal amplitude and power of the FFT. It analyzes two signals: S1(t)=50sin(2πft) and S2(t)=100sin(2πft), with f=50kHz. It is noted that if the ratio between the two amplitudes is n, then the ratio between the two powers is n^2.

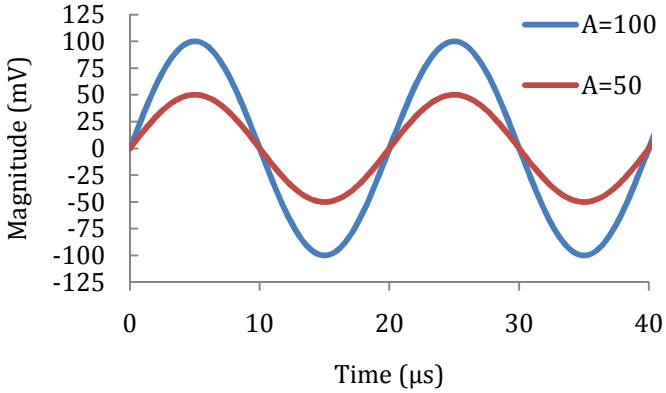

Figure 4.21 Signals with magnitude ratio 2

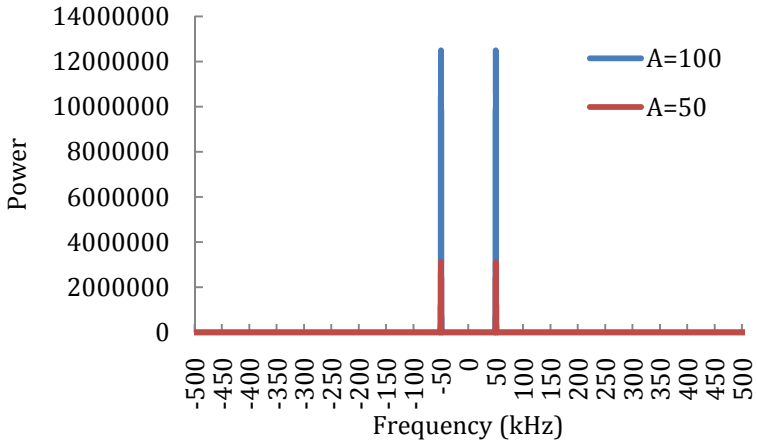

Figure 4.22 FFT Signals with magnitude ratio 2

In the last example we will analyze the white noise. It contains all the frequencies for which presents no peak of power spectral density.

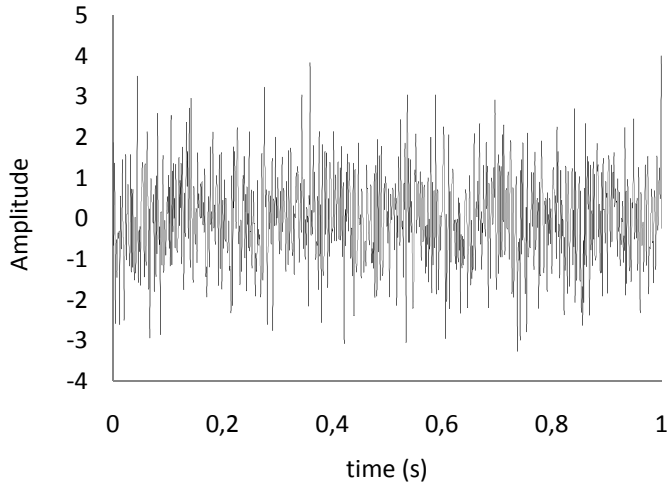

Figure 4.23 White noise

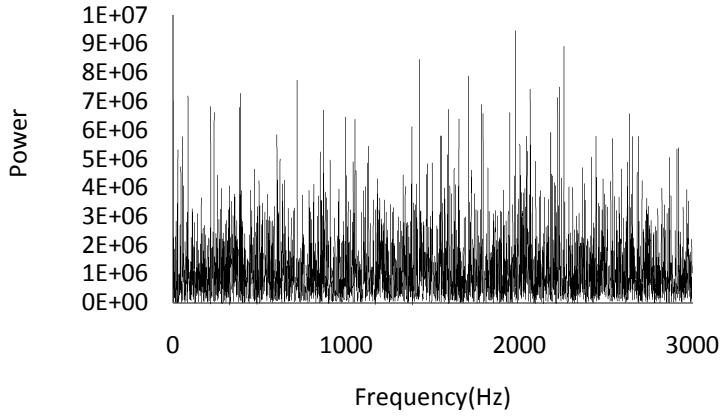

Figure 4.24 FFT del white noise

Also occurred the property $\boldsymbol{R(\tau) = \delta(\tau)}$, the autocorrelation is a Dirac delta (Figure 4.25), and $\boldsymbol{S(\omega) = \int_{-\infty}^{\infty} R(\tau) e^{-j\omega\tau}\, d\tau = \int_{-\infty}^{\infty} \delta(\tau) e^{-j\omega\tau}\, d\tau = 1}$, this is the power spectral density, defined as the Fourier transform of autocorrelation, is constantly equal to 1

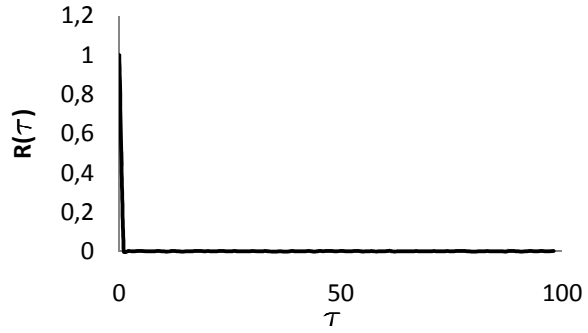

Figure 4.25 Auto correlation of white noise

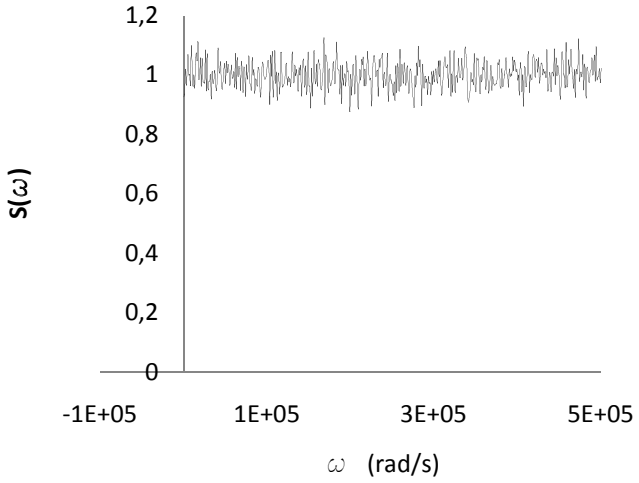

Figure 4.26 Power spectral density of white noise

4.2.11 THE PROPOSED ALGORITHM

The ultrasonic tests are conducted with particular attention to the procedure that are need to apply in order to obtain a repetibility of test. After to consulting some literature, an a huge test of procedure adopted, a final algorithm is used to investigate material using NDT methodology. Here the algorithm developed is proposed and discussed.

Transparency test procedure

1- A specimen is settled on the frame
2- Water is get on the couple of sides where test will be conducted
3- The probes are applied by using a copulant
4- Test start with a set of narrowband N odd cycle sinusoidal signals at frequencies f_1 to f_2 with steps of Δf
   Some other quantities are need to be fixed.

N cycle (3-5-10 KHz)	f_1=50KHz,	F_2=300-500KHz	Δf=5-10-25KHz,
Play freq.= 25Msps	n samples 100-250-500	clock time 200-150 millisec	Amplif. 22-31-40db;

5- Average signal is detected from the samples, at each frequency

Baseline

1 Theoretical signals from digital software are generated at each frequency
2 FFT is operated at each frequency
3 The maximum of FFT at the input frequency, for each signal is saved.

Post Processing

For each frequency

1- A duration of each signal is determined as $\Delta t = n_{cicles} T = \frac{n_{cicles}}{freq.}$

2- Time of fly (TOF) is detected as using the cross correlation operator

3- Wave Velocity is determined as $V = \frac{\text{distance}}{TOF}$

4- A time window is chosen as $W = [TOF;\ \ TOF + 1.2 \cdot duration]$

5- The windowed signal is extended by zero padding until 2^{14} dots.

6- FFT on windowed extended signal is operated

7- The amplitude of FFT at the input frequency is saved.

8- The maximum of FFT and the associate frequency of signal are detected

9- FFT amplitude (point 7) of output signal at the input frequency is divided by baseline amplitude of FFT at the frequency of input signal.

$$Index_{freq,input} = I_{\omega} = \frac{Ampl\_FFT(s_{outuput}(t))_{freq,input}}{Ampl\_FFT(s_{input}(t))_{freq,input}} \tag{4.83}$$

The procedure is repeated for each frequency.

10- In a chart is reported the dots ($freq_{input}$; $Index_{freq,input}$)

11- The Index freq, input is standardized by setting the max =1 for the sweep of frequency investigated.

$$St.I_{\omega} = \frac{I_{\omega}}{\max(I_{\omega})} \tag{4.84}$$

12- Resonant frequency is the frequency of the I_{ω} is maximum.

13- Standard velocity is the velocity of wave at the resonat frequency.

4.3 TECHNOLOGIES

The principle of ultrasonic test operation consists in positioning in two points of an elastic body two piezoelectric transducers (probes) which have the property of transforming a voltage electrical into mechanical energy and vice versa.

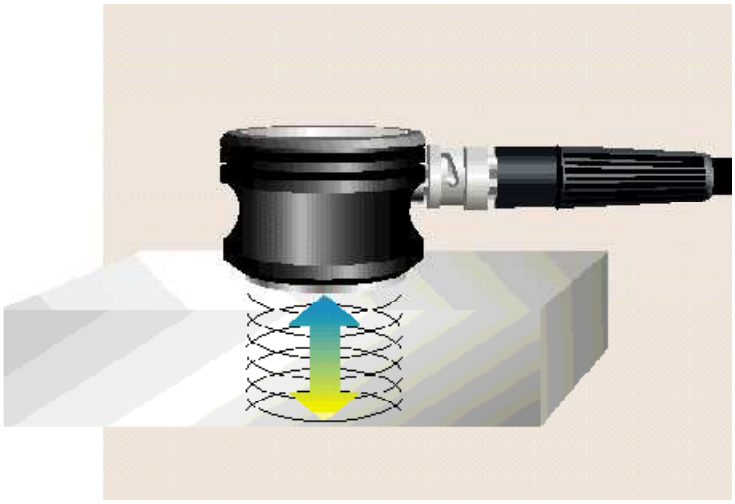

Fig 4.27 Ultrasound probe in contact with a surface

The probe stressed by a train of high-voltage electrical pulses, generates pressure waves that constitute the ultrasound ray. It, after having crossed the material, reaches the receiving probe. When the ray is deflected or reflected by some defects or border, it go against the probe and here a pressure wave is transformed into an electrical signal, amplified and filtered, is displayed on the monitor in the form of graphic waveform.

From the graph wave it will be possible to trace the time of propagation of the ultrasound ray between the measuring points, this is the first fundamental parameter method of the UT, and is called the flight time. This parameter enables

the determination of the propagation velocity and the localization of the presence of a possible defect.

The filtering and amplification of the signal are used to eliminate non-useful information and to reduce the noise components, and exalt instead the repetitive components. This is necessary to make the signal cleaner and more understandable to the operator.

The instrumentation consists essentially of a series of components that perform specific functions and must be accompanied by an oscilloscope or by a monitor for display and interpretation of the signal.

The main components are:

- *electronic control unit*; it is composed of a pulse generator that is a device that generates an electrical signal pulse to be applied to the probe issuer for the creation of the ultrasonic wave. The signal may be repeated at regular intervals, generating a train of pulses and the repetition frequency can be varied. In the unit there is also a device for amplification and filter that raises the voltage level of the signal and is provided with an electronic device of "average" that is used to find the average value of a predetermined series of signals, so as to eliminate the characteristics causal signals, such as noise, and highlight those repetitive.
- *Ultrasonic probes*; these are instruments able to convert the electrical pulses of the generator into mechanical vibrations, transmit the vibrations to the medium to investigate and collect the mechanical vibrations and convert them into electrical signals.
- *Coaxial cables,* they are special shielded cables which allow the connection between the probe and the electronic control unit. They consist of two channels: one internal and one external (screen), which extend on the same axis and remain separated by a layer of insulator.

These are the main components, however, when an ultrasonic probe must be positioned on the component to be tested, it is a good rule to interpose between it

and the workpiece surface a layer made of a substance (liquid or gelatinous) that is called coupler means. The coupler means shall provide an appropriate passage for the ultrasonic wave from the radiating surface of the transducer to the material and avoids that the ultrasonic wave can be fully reflected because of the presence of air immediately in contact with the transducer.

The features that should have a good half coupler must be: to properly moisten the surfaces of the transducer and the test piece, to exclude any air bubbles from the path of the sound beam, to fill any irregularities in the surface of the piece to create an intake region adjust, to allow unimpeded movement of the probe, to be easy to apply and remove and not be toxic.

4.3.1 THE PRO-PULSER MACHINE

The instrumentation hardware used in this experimental investigation is composed of:

• 4-channel ultrasonic equipment;

• 4 coaxial cables with BNC connectors;

• 4 Parametrics ultrasonic probes with a center frequency of 0.5MHz;

• A laptop for the management of the test and of the signals.

The instrumentation consists of a software program management device compiled in Turbo C + +. One proceeds with the description of the hardware components and software necessary for conducting the test.

The platform used to perform the test was assembled under the project PRIN 2007 "*MULTISCALE PROBLEMS WITH COMPLEX INTERACTIONS IN STRUCTURAL ENGINEERING*" whose scientific director is Prof. G. *Giambanco*. This is composed of a central unit, shown in figure 4.28, which contains in its interior a function generator, with output to a channel, and a capture card to four channels. The control of the machine takes place via a LAN connection, which connects the machine to a computer or to a network switch that allows it to control, even remotely.

The function generator allows the apparatus to generate ultrasonic waves which may also be defined by the user; the signal produced is a digital signal sampled at varying frequencies between 1.56 Msps to 50 Msps. Through the use of an amplifier, the output signal has a maximum amplitude of 100 volts. The wave functions of the unit are predefined sine, square and saw tooth. Among the characteristics of the generator assumes considerable importance is the ability to generate signals in a very broad range of frequencies ranging from 1 Hz to 25 MHz.

The acquisition of the signal is carried by four acquisition channels with BNC. For each channel you can amplify or de-amplify signal as a decibel scale, so adjusting the magnitude. The resolution of the acquired signal can reach sampling times from 3.12 to 100 Msps. The acquired signal is sent to the computer and displayed using the software interface.

Figure 4.28 Ultrasonic *Pro-Pulser* Machine

The technical data of *Pulser Pro* are:
Output channels
- 4 channel, impedence 1MOhm
- sample playback frequency 8 bit, 100MHz sincrone
- memory 8KB at each channel
- programmable amplification 0-40dB for each channel
- Internal or external trigger

Input (generator)
- Digital generator of arbitrary shape wave
- sample playback frequency 8 bit, 50 MHz
- memory for shape of wave 8KB
- Integrated amplificator, max. 150V, range 10MHz
- direct plotting of signal transducers.

4.3.2 THE PROBES

The ultrasonic probes are transducers used to convert energy in different forms, and their task is to transform electrical oscillation into mechanical oscillations and vice versa.
There are different types of transducers for generating ultrasonic, classified according to the energy used to produce the mechanical vibration and depending on the medium in which the wave propagates. They can be used in various fields by virtue needs and the acoustic power request.
some types of transducers could be applied at this machine. Piezoelectric transducers: this type of transducers exploit the phenomenon of piezoelectricity. With the term piezoelectricity is the phenomenon manifested by some classes of crystalline materials, generically called piezoelectric crystals, which are polarized

electrically due to mechanical deformations of the elastic type, while, vice versa, the same deform elastically when subjected to electric field . In the first case, when it produces a voltage proportional to the applied pressure, it is called direct piezoelectric effect, in the second case, when it generates a change in the crystal structure due to the applied electric field, it is called inverse piezoelectric effect. These types of mechanical vibration of piezoelectric crystals were used to produce ultrasonic vibrations at frequencies between 20 kHz to 50 MHz.

The transducers most used in the construction of ultrasonic probes for performing non-destructive inspections are surely the piezoelectric transducers.

In its main parts a piezoelectric ultrasonic probe can be considered consists of the following components:

- Cover (Case)
- Epoxy potting
- Backing Material (lining material)
- Electrodes (electrodes)
- Piezoelectric element (the Focus)
- Wear plate (protective film)
- Signal wire (signal wire)
- Coaxial cable connector (connector to coaxial cable)

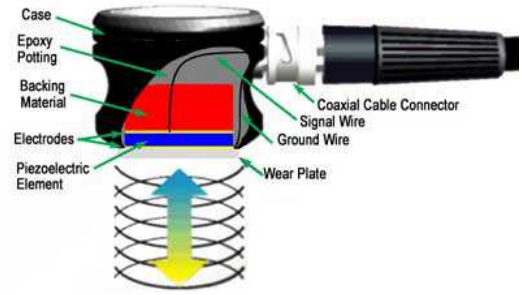

Figure 4.29 Components of a piezoelectric ultrasonic probe

The ultrasonic probes are classified into three groups according to the application:
Contact Probes: used for inspections in direct contact, and are generally manipulated by hand. They elements protected in a robust housing to resist sliding and contact with a variety of materials and are easy to grab and move along a surface. Often have replaceable wear plates to extend their useful life, must be used the coupler means to eliminate the air gap between the transducer and the component that is analyzed.
Immersion probes: they are not in contact with the component, in fact, are designed to operate in a liquid environment and all connections are watertight. These probes usually have a layer of impedance which helps to get more energy of sound in water and, in turn, in the component that is analyzed.
Non-contact probes: they are not in contact with the component and the distance can change between a few mm and a few dm. The wave can be generated by the piezoelectric transducer as well as also from other generators, such as the laser.
Two basic parameters for the description of the ultrasonic probes are: the sensitivity and resolution. The first is the ability of an ultrasonic system to detect a defect positioned at a given depth in a work piece; the greater the intensity of the signal received from the defect (or reflector) the greater the sensitivity of the system. The second is the capacity that the same system has ultrasound in detecting defects at or near the surface of the material.
For the ultrasonic probes is also important to define the concept of bandwidth "or frequency range, associated with a transducer. The frequency indicated on the probe is the center frequency and depends primarily on the backing. The probes strongly damped respond at frequencies below and above the central one; a wide range of frequencies allows to obtain a probe with high resolving power. Probes less damped allow a narrow range of frequencies and consequently a low resolving power, but high capacity for penetration into the material to be examined. The selection of the optimal transducer for a certain type of control, depends largely on

the characteristics of the material to be tested and, in particular, by its ability to attenuation of the ultrasonic wave. In general the ultrasonic waves at high frequency have better characteristics for what regards the resolution while the low-frequency waves are better able to penetrate high thicknesses of material or (what is the same) to allow the execution of investigations of materials highly absorbent, such as rubbers, plastics etc..

The probes piezoelectric next to numerous advantages, such as low cost, small size, low weight and high sensitivity, also have disadvantages such as their sensitivity variable with the temperature and the impossibility of being used in humid climates. The materials used for the construction of piezoelectric transducers are: Barium titanate, lithium sulphonate, barium, barium zirconate, lead zirconate; the first two mentioned, are the most commonly used.

There are different types of ultrasonic probes. The transducers are of the type present on the market: *AccuScan* "s", *Centrascan*, *VideoScan*. The choice of a type is dictated by the test mode and the test material. Some transducers provide an excellent sensitivity in those situations in which the axial resolution is not of primary importance. The waves generated with this type of transducer are longer and have a low frequency band (frequency bandwidth); others, are suitable in those cases in which there is a difficulty in crossing the specimen, as is the case with polymeric materials.

As part of this survey were used transducers *VideoScan*, indicated when you need a high axial resolution and an attenuation of the ultrasonic signal absorption in the material. Each transducer is symmetrical, that is usable both as a receiver and as a transmitter. Were chosen transducer center frequency of 0.5 MHz, identified by the manufacturer as *'VideoScan* V103-RM'. In figure 4.30 we show two of the four transducers used, while in figure 4.4 is shown the frequency spectrum delivered by the manufacturer. Each transducer has a radius of 18 mm and a depth of 16 mm and is constituted by a piezoelectric crystal encased in a steel box. The lateral surface of the cylinder is coated with a polymeric sheath which protects it from possible shocks.

Figure 4.30 Ultrasonic probes

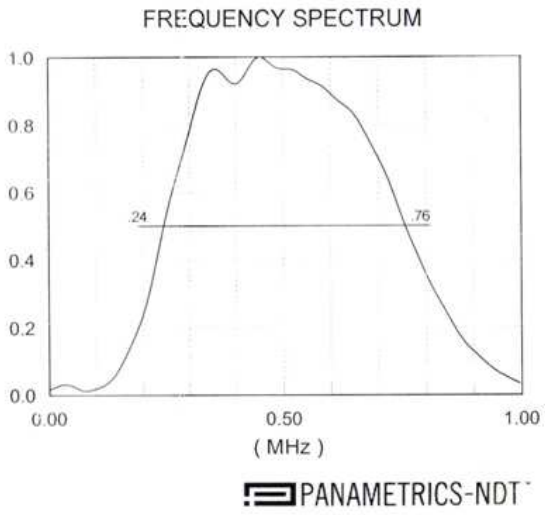

Figure 4.31 Spectral response of the probe Videoscan V103-RM

4.3.3 THE ACCESSORIES: FRAMES AND GELS

FRAME

The research on this work, is related with concrete and it lead to investigate caracteristichs of ultrasonic signal who travel in fresh concrete. For the implementation of tests, a opportune device was been designed. The device is contituited of a orizzontal steel frame.

The frame is made with steel plate of 40x4mm and steel square section of 40x40x4mm, two tranversal beam are fixed to the 4 column to permit to hold constant the distance between probes and the pressure during the test. In each beam by a 8mm hole a schuber rode pass. The schuber rode had a tranversal 60x60 mm plate at the end, covered by a elastomeric rubber. The probes are in back contact with the plate, rubber permit do attenuate transmission of signal to the frame. Concentric to the scruber rode, there is a spring, against the beam, and it pull the plate to the concrete.the device is shown in figure x.xx

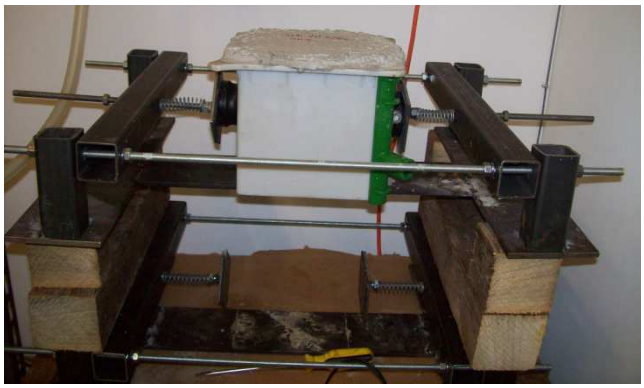

Figure 4.32 Horizontal steel Frame for ultrasonic test

CONCRETE BOXES

The concrete cubes box, are 2, in order to have 2 specimen below investigation. These are polyester cubes of 15 cm side, for each of them, in two lateral opposite sides, a 6cm diameter holes are presents. In each hole a probe is located, one work as transmitter, and the other as receiver.

COAXIAL CABLE

The BNC connectors are a family of single pole connectors bayonet used for the header of coaxial cables. The designation of the connector stands for Bayonet Neill Concelman, the names of the two inventors Paul Neill and Carl Concelman, and the system used for the graft, precisely defined bayonet.

The fastening between the male connector and the female connector is carried out quickly, by turning a quarter turn the nut on the male connector around the two pins formed on the bezel of the female connector. The mechanical seal of the union is improved by the action of the spring contained within the male connector.

The cable consists of two contacts, the first contact and the second axial constituted by a reinforcement of wire that is wound on a layer of nylon which separates them and isolates them from axial cable. In figure 4.2 is shown the engagement system of the male connector.

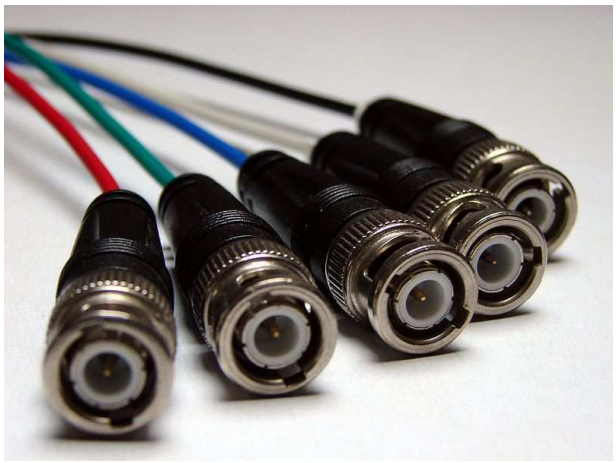

Figure 4.33 Coaxial Cables

GELS

Between concrete and probes a viscous gel is need to be posted in order to permit at the signal to be transmitted from the transmitter to the receiver through the material.

4.3.4 THE SOFTWARE

The *pulser v.2.00 software* for controlling the test has several functions. The "Waveforms" lets you view the signal sent or received, with the ability to zoom in on the signal. The "Status" allows you to connect the ultrasound machine with the computer. The "Measure" starts the test two possible modes', the first "Pulse now" sends only one signal, the second "Periodic pulse" (NO - OFF), you can repeat the same test in a cyclical setting a time between two executions . The "Setting" which allows you to sample the signal. In this section, a pull-down menu called "Aquisition frequency" allows to vary the sampling frequency of the signal received in a range that goes from 3125 Msps to 100 Msps;. a block consisting of the four

channels allows you to view and record the signal acquired by each channel, and can also be selected via a drop down the amplification level from -5 to 40 dB and a delay of the acquired signal. In the field "Playback" via the pull-down menu freq you can select the sampling frequency of the signal emitted, in a range that goes from 1:56 Msps to 50 Msps and a delay of the same.

The "Data Manager" is formed by a down "Display" that lets you choose whether to display in the "Waveforms" the signal or the received signal, the button "Load pulse" loads a user-defined pulse, and the button "Save wave" pressed to save a file in the acquired signal, the rescue mode are defined by "Auto save option" with which the operator can choose between three different types of saving files that are none, overwrite and append. Selecting the first is not saved no data on the disk, the second allows you to override the signal to a single file, and the third by the ability to save different signals acquired in a single file queue. Under this pane are buttons sine (sine wave), saw (sawtooth) and square (square) that allow to implement an output signal of the form and assigned via the box freq (kHz) and Cycles defines the frequency and the wave cycles to send the Download button and then transmits to the system settings choices.

The last pane, the cycle frequencies allows to perform a test cycle in an automatic way, by programming the sending waves with variable frequency. Inside the box there are boxes that are used to choose the number of test cycles, the start and end of the test cycle and its step. It has possibility to set the number and range of tests to be performed. After choosing these parameters you can start the test by pressing the Start button and check the current test box test in progress.

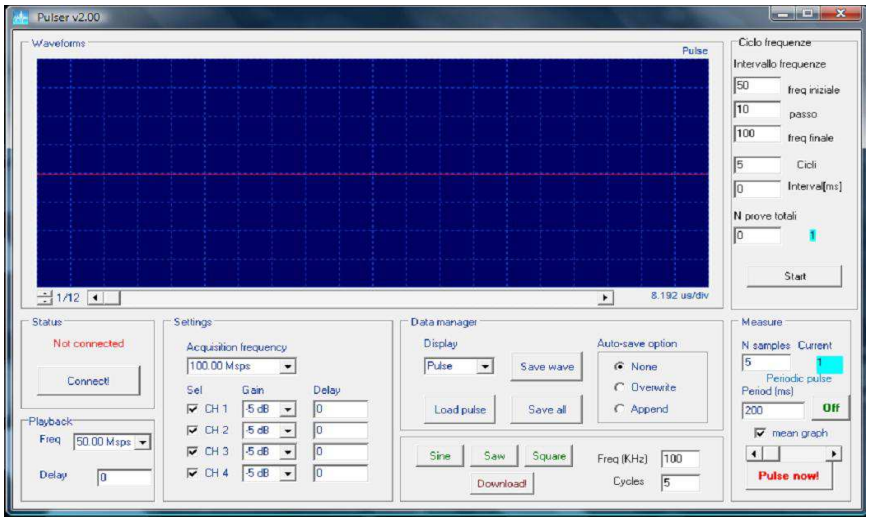

Fig 4.34.Software GUI

We proceed now to the description of the software interface, shown in Figure 4.34

WAVEFORMS

In the box dedicated to this feature displays the signal sent and received. The buttons in the left corner allow to perform a zoom on the signal with a scaling factor between 1/1 and 1/12.

DATA MANAGER

The Display drop-down menu allows you to choose whether to display the transmitted wave in the box Waveforms (Pulse) or the wave received in the corresponding channel. With the button "Load pulse" the user has the opportunity to load an impulse built in binary format, the user. "Great Wave" allows you to save in a different file extensions the acquired signal. Through the box under "Auto-save option", the operator can choose between three different configurations for saving files: selecting none no no data will be saved to disk, overwrite allows you to override the signal to a single file, append the setting indicates the ability to save in a single file multiple signals acquired.

SETTINGS

The Settings box allows you to manage the sampling of signals and their gain. The first drop-down menu, "Acquisition frequency", allows you to set the sampling rate of the received signal. The lower limit is of 3125 Msps while the upper limit is 100 Msps. With the second block of commands is allowed an ad hoc configuration for each channel. The menu "Gain" is a command that allows you to amplify or deamplificare the received signal. The range within which the software can intervene is -5 dB and 40 dB. The command "Delay" instead allows to transverse the axis of the time the signal that has been received. The last block is used to set the sample rate and delay of the signal emitted. The buttons sine, saw and square offer the possibility to generate waveforms default by the software. Once you have chosen the wave to be sent, set the frequency and the number of cycles that the system will be sent. The Download button that enables the system to load the settings you just defined.

MEASURE

This box allows you to perform the test. The Pulse button the software will now start the process of transmitting and receiving wave. With a second button, Periodic pulse (ON - OFF), this same procedure is repeated over time. In this case the first text box is used to define the number of waves to be generated and to be received, while the second imposes itself with the time interval between two successive wave emissions.

CYCLE ON FREQUENCIES

The control box "cycle frequencies" allows for automatically carrying out the tests planning to send sine wave with variable frequency. Inside the box there are six text boxes, and a Start button that start to work. You can set the frequency of the signal with which the test and that the final signal, as well as decide the rate at which frequencies are connected. You can decide the time interval that elapses between the end of a test and the beginning of the next. With the last box you can then set the number of tests to be performed.

4.4 THE MACHINE VALIDATION

To validate the prototype machine some non destructive tests are conducted on different materials. Numerical simulations are developed to verify if the tests are in agreement with the physical phenomena.

This part is divided in three steps. To follow a reference of Reinhold (1988) on numerical simulation of ultrasonic wave in alloy plate a numerical approach is defined. Follow ultrasonic tests are conducted on two steel cylinder to detect features of signals. Numerical simulation as so conducted on steel FEM model to reproduce the test data acquired during test. A the end, a parametric study in axial symmetry is conducted on steel cylinder to understand how the ultrasonic wave propagation depend of the ratio radius/length of steel cylinder.

4.4.1 UW PROPAGATION IN ALLOY PLATE

In "*A finite element formulation for the study of ultrasonic NDT system*" of Reinhold, Lord, published on IEEE transactions on ultrasonic's, ferroelectrics and frequency control v 35 no 6 1988, is proposed an approach to study the propagation of ultrasonic wave in media using FEM models. By using a 2d model, on the border where probe is applied, the wave is simulated by using the follow displacement law:

$$u(x,y,t)=\delta(x)w(y)f(t)\hat{\mathbf{x}}$$

With

$$\delta(x)=\begin{cases}1 & x=x_0\\ 1 & wherelse\end{cases}$$

$$w(y)=\begin{cases}1 & -a<y<a\\ 0 & wherelse\end{cases}$$

$$f(t)=\begin{cases}[1-\cos(\frac{\omega_0}{n}t)]\cos(\omega_0 t) & 0<t<t_0\\ 0 & else\end{cases}$$

$\delta(x)$ can be used to model the x-distribution of signal.

$w(y)$ can be used to model the distribution of displacement along the contact surface, it could decrease with the distance of probe center. In this case it is considered constant.

$f(t)$ is the time law of signal. $\omega_0 = 2\pi f_c$ and *n* is a natural number.

Assuming a signal of 1Mhz, and n=3, the signal shape is reported in figure 4.35.

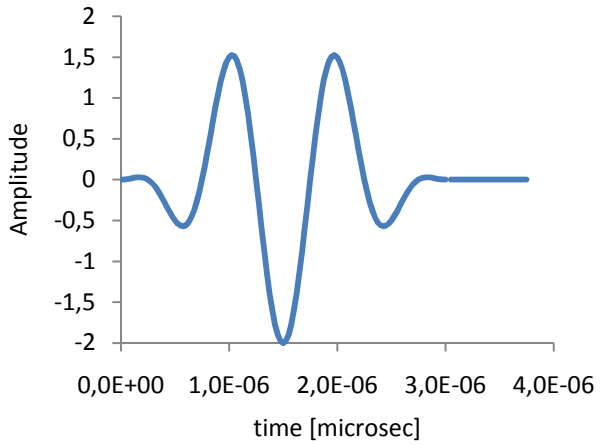

Figure 4.35 shape of ultrasonic wave signal simulated

In the paper is considered an alloy plate of dimension of 1.5 inch length (x) and 2 inch wide (y), as material parameters are assumed V_L=250.000in/s and V_T=120.000 in/s. The probe dimension is assumed of 1 inc, that mean that a in signal simulation law is 0.5 in.

To reproduce the numerical simulation the measures are transformed in standard system of measure and converted in term of elastic constants.

$V_{SI} = V * 0.0254$

V_L=6350 m/s V_T=3048 m/s density-ρ=2700 kg/m^3

The lame constants are:

$$\mu = \rho V_T^{\,2}$$

$$\lambda = \rho V_L^{\,2} - 2\mu$$

And the elastic Young constant becomes:

$$G = \mu$$

$$\nu = \frac{\lambda}{2(\lambda + \mu)}$$

$$E = \frac{2G}{(1+\nu)}$$

And we obtain: G=2583 MPa ν =0.35 E=67742 MPa

The simulation is conducted by using the software *Straus7,* the model is implemented by using a grid of 72x 40 (2880) plate elements according with propagation of ultrasonic wave in elastic media, minimum dimension of mesh is 0.53mm.

The analysis are conducted in plane strain, as border conditions are imposed the displacements at nodes for a length border of 1 inch, for a total of 11 nodes. Two models are implemented one with displacements in x direction and one other with displacements in y direction to verify the shear velocity.

Linear Transient dynamic analysis is conducted. Signals are detected in the opposite front where displacement are imposed, and they are detected to all 11 nodes and an average on them is conducted to synthesize a new signal.

These signals (compressive and shear) are processed using Matlab algorithm and features are detected: time of fly TOF, FFT amplitude. Starting form TOF the velocity of wave propagation are calculated.

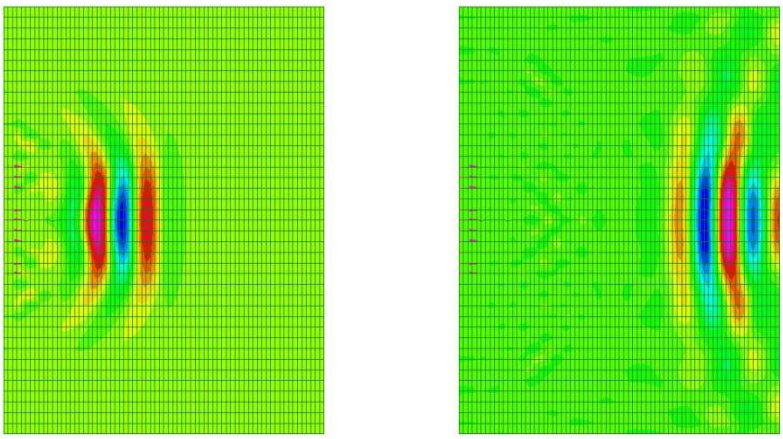

(a) (b)

Figure 4.37 State of displacement of alloy plate at the step
(a) t=3.75e^{-6} sec (b) t=9e^{-6} sec

The simulation is conducted of 800steps using a sample frequency of 40MHz, the impulse at 1MHz of frequency have a duration of 3 microsec. In figure 3.37 are reported the response in term of displacements at the right edge of model for the shear displacement and for the compressive displacement, in x and in y direction.

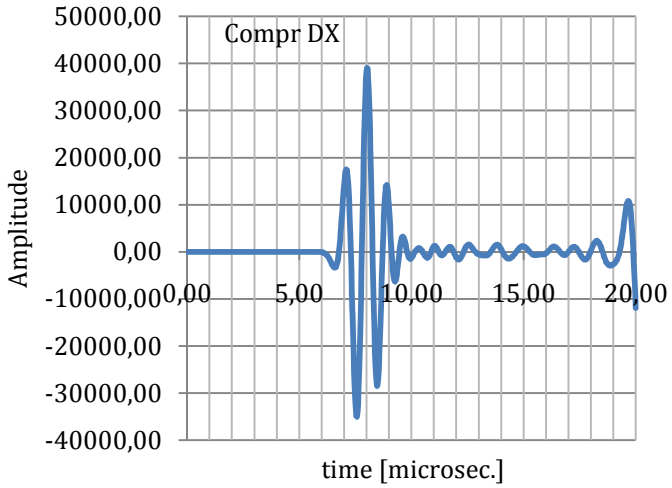
Compr DX
50000,00
40000,00
30000,00
20000,00
10000,00
0,00
-10000,00
-20000,00
-30000,00
-40000,00
Amplitude
0,00
5,00
10,00
15,00
20,00
time [microsec.]

(a)

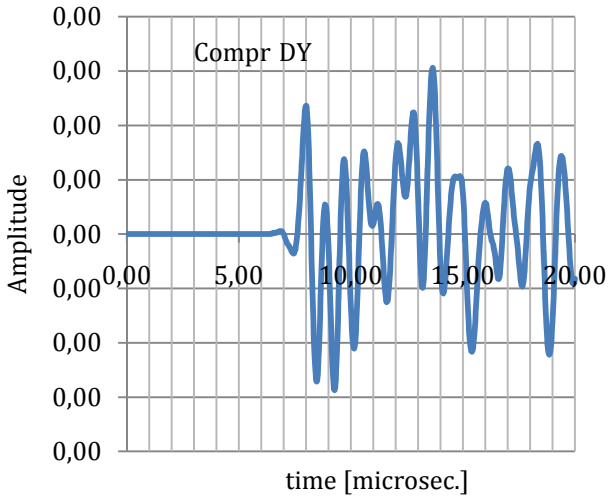
Compr DY
0,00
0,00
0,00
0,00
0,00
0,00
0,00
0,00
0,00
Amplitude
0,00
5,00
10,00
15,00
20,00
time [microsec.]

(b)

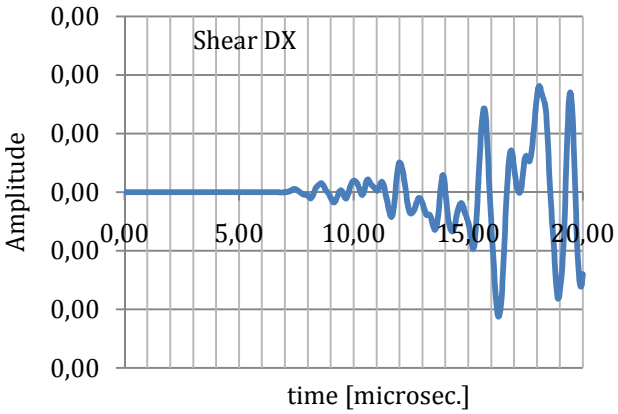

(c)

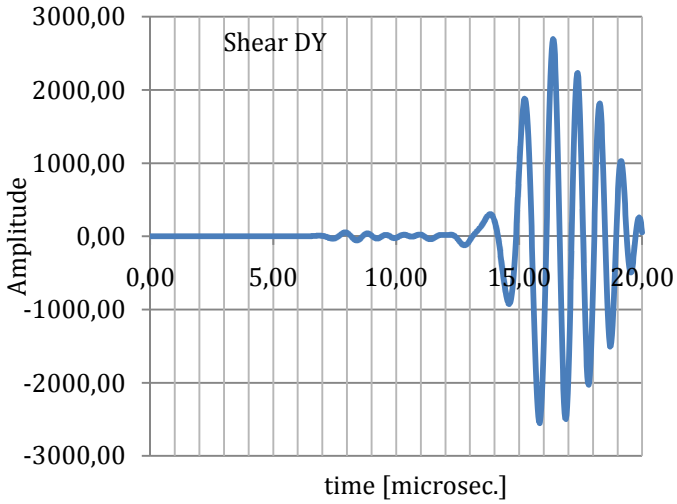

(d)

Figure 4.38 signal form numerical model of alloy plate
(a)dx (b) dy for pressure wave (c) dx (d) dy for shear wave

It is possible to observe that the compressive signal arrive after 5.88 microsec, and the shear action after 12.13 microsec, by calculating the velocity of signal by divided space by time we obtain the data reported in table 4.3

State of wave	**Time FEM [microsec]**	**Velocity m/s**	**Nominal Velocity [m/s]**	**Error**
Pression	5.88	6429	6350	2.04%
Shear	12.13	3141	3048	3.05%

Table 4.3 FEM and nominal velocity

The numerical model is in agreement with bibliography data, error on velocity is less than 3.5%.

4.4.2 UW PROPAGATION IN STEEL CYLINDER

In this part a set of test on cylinder of steel are conducted to validate the machine *Pulser Pro*. Steel specimens are considered, test are conducted, to recorder signals of wave propagation, numerical simulation are implemented to reproduce the tests, and theory approach is done to determine the correspondence between tests and numerical simulations. Two steel cylinder are considered. The two cylinder are respectively length 170mm and 98mm, and the two diameters are of 300 mm. Mechanical properties of steel are assumed as E=209.000MPa, v=0.30. some other characteristics are shown in tab 4.4.

		Cylinder 1	Cylinder 2
Lenght	[mm]	170.0	98.0
Diameter	[mm]	60.0	60.0
Area	[mm^2]	2827.4	2827.4
Volume	[mm^3]	480663.7	277088.5
Weight	[kg/mm^3]	3.765	2.175
Density	[kg/m^3]	7,833	7,849

Table 4.4 Geometrical property of steel cylinder

Figure 4.39(a)-Steel specimen

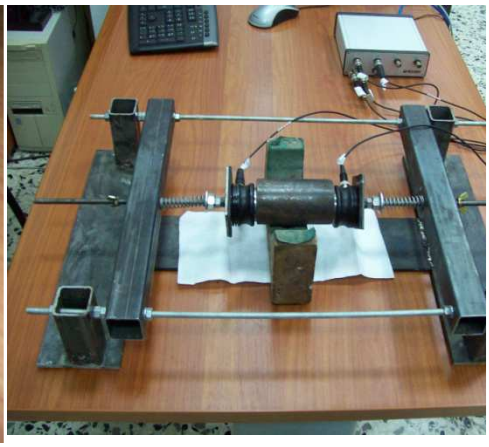

Figure 4.39(b)-Steel cylinder during ultrasonic test

This part is developed in 5 steps:

1- In the first step features of baseline are determined, the baseline considered is a sinusoidal signal of 3 cycles.

2- The signal generated from the machine when the require is a 3 sin cycle signal are processed, in order to appreciate the relationship between theoretical and experimental input signals

3- The experimental data acquired, from output probe, on the steel cylinder are presented, and they are related with the sinusoidal baseline.
4- A numerical study on axial symmetric model of steel cylinder is show, with signal processing.
5- Parametric study on steel cylinder by varying the ratio r/h is present.

4.4.3 THE BASELINE

The baseline considered is constituted of a 3cycle sinusoidal signal. In order to understand the meaning of the FFT, the signal processing in frequency time is conducted for 1 cycle and 3 cycle signal with different frequencies for 100 to 800kHz; signals are discrete, and in table 4.5 are reported period and duration. Analysis in frequency space is also conducted, here we report FFT amplitude of central frequency, in the last columns of table 4.5.

freq. [KHz]	T* 1 cycle sin	T* 3 cycle sin[μsec]	FFT ampl 1 cycle	FFT ampl 3 cycle
100	10.0	30.0	258.07	753.18
200	5.0	15.0	127.19	376.59
300	3.3	10.0	84.26	251.12
400	2.5	7.5	63.20	188.38
500	2.0	6.0	50.42	150.70
600	1.7	5.0	41.94	125.56
700	1.4	4.3	35.90	107.57
800	1.3	3.6	31.45	94.18

Table 4.5 Duration and FFT of sin signals

*The function of signal is defined as $y(t) = \sin(2\pi\omega t)$ in this way, the period is $T = \frac{1}{\omega}$

It is possible to appreciate that the FFT of signal is almost 3 times more when the function is increasing of 3 cycles. Also the FFT amplitude decrease with the increasing of frequency, this because the duration of signal is going to decrease and with it the energy of signal.

In order to evaluate the signal generated from the signal generator of the machine the signals are detected by acquiring the signals generated, and using matlab algoritm they are processed, in this mode is possible to relate the theoretical signal with the generated one. The signal is produced by load an electric generator and then it go downloading itself on piezoelectric crystal of probe for produce a signal with a voltage of 100V. in figure 4.40 is reported the generated signal.

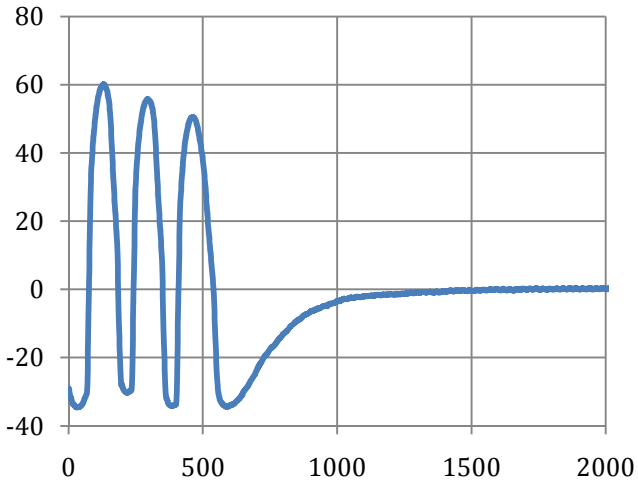

Figure 4.40 signal generated at 300kHz with 3cycle sin require.

The signals are processed and the results are reported in table 4.6, the sample frequency if 50Msps. It is possible to appreciate that the peak to peak (ppk) of

signal is not constant but it go decreasing with the increasing of frequency, also the ratio of max FFT on baseline FFT is going to decrease with the increasing of frequency. However the signal producted form the machine depend of the number of probes that are applied at output of the machine, if from the generator more probes are connected, the signal generated to each probe can be with low power related with the original generated. In order to avoid this problem, in our analisys we always be refer with the theoretical baseline.

freq	ppk	max FFT (1)	FFT basel. (2)	Ratio (3)= (2)/(1)	ratio adm $(3)_{max}/(3)$
100,00	122,46	50.204,87	1.506,37	33,33	1,00
200,00	107,54	22.063,65	753,19	29,29	0,88
300,00	94,76	12.473,97	502,12	24,84	0,75
400,00	91,08	8.031,24	376,59	21,33	0,64
500,00	88,06	5.419,89	301,26	17,99	0,54
600,00	85,08	3.724,22	251,12	14,83	0,44
700,00	83,68	2.657,62	214,89	12,37	0,37
800,00	81,90	2.101,66	188,15	11,17	0,34

4.6 Signal processing of 3cycle sin generated form Pulser Pro

4.4.4 CYLINDER TESTS

In order to conduct the test on steel an horizontal steel frame is utilized. To reducing electrical interferences between frame and specimen a bed of wood is used to isolate the specimen from.

The test is conducted by applying the two ultrasonic transducers on each basis of cylinder. Diameters of the probes are 440mm. The tests are conducted by sending at the transmitter an ultrasonic signal of narrow band frequency, and fixed cycle of signal, and detecting output signal at the receiver. Between steel cylinder and

probes a few micron thickness silicone gel is posed to permit a better transmission of signals.

The input is a sinusoidal signal of 3 cycles, with play frequency of 50Msps; different signal frequencies are investigated, from 100KHz to 800KHz, by 100KHz steps. The output signal is acquired at 50Msps play frequency, and the amplification is settled at 22db for the 98mm cylinder and 16db for the 170mm cylinder. In order to reduce the noises, each signal is played and recorded 50 times. Same test is repeated with sinusoidal signal of 1 and 15 cycle duration (*lab test reference of 04.09.12 –steel*), an device setup is shown in figure 4.41.

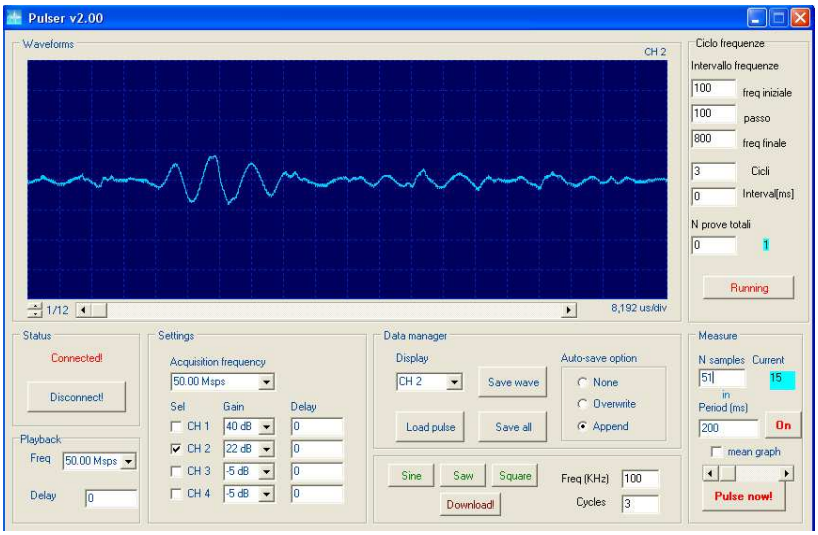

Figure 4.41 Device setup for specimen of 98mm

A signal processing procedure is used to determine the characteristic of signal detected. The first procedure consist in a visual analysis of signal to check if some signals are not right recorded. Now a average procedure is conducted, to sensitize the 50 signal of each frequency in an new virtual signal. The signal processing will be conducted on these new averaged signals.

For each signal the processing is conducted in the time space and in the frequency space. Using a own software, some relevant features are measured. For the FFT analysis a windowing procedure is used, the duration of window on output signal is as the duration of input signal.

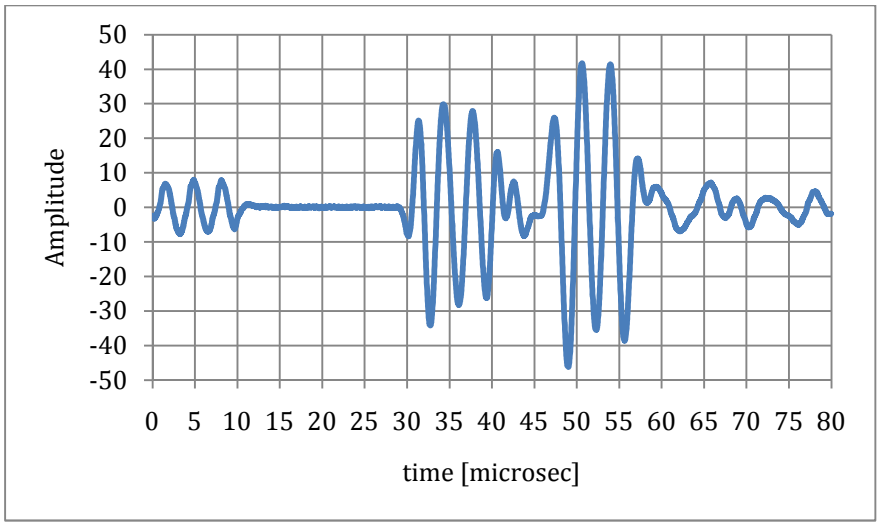

Figure 4.42 Recorded output signal at the frequency of 300KHz, specimen of 170mm

it is possible to appreciate the cross talk it is generated of electromagnetic noise, that it is not been considered for the analysis in the beginning, follow the P-wave and more further the Shear wave. The signal processing need to be conducted by isolating the P-wave, this is operated by a windowing. It is possible to related the properties of steel with time of fly measured.

$$V_L = \frac{L}{t_{fly}}$$

$$E_L = \frac{(1-\nu)(1+2\nu)}{(1+\nu)} \rho V_L^{\,2}$$

Where L is the length of specimen, ρ is the density, ν is the Poisson ratio assumed as 0.30, E_L is the elastic module, the coefficient $\frac{(1-\nu)(1+2\nu)}{(1+\nu)}$ is 0.742

freq	Cylinder 1-170mm		Cylinder 2-98mm	
	Velocity	**E**	**Velocity**	**E**
	[m/s]	[Gpa]	[m/s]	[Gpa]
100	5751	193		
200	5778	195		
300	5794	196	5671	188
400	5798	196	5698	189
500	5806	197	5698	189
600	5810	197	5711	190
700	5822	198	5704	190
800	5818	197	5731	192

Table 4.7 Measured of speed and dynamic module for each cylinder

In the frequency domain, in order to uniform data detected at each frequencies, a ratio between input features and output features is done.

After to operate a FFT of the output signal, the FFT at the input signal is determined, and a ratio of the two FFT powers, P_{input}/P_{output} is calculated. In the table 4.8 these powers and ratio are reported. As it can see, the ratio is maximum at the frequency of 500KHz.

	cilynder of 170mm							
	100	200	300	400	500	600	700	800
f.-input	110	208	308	409	491	592	693	790
Ampl.	4.3	2.09	2.33	3.323	2.989	1.611	652	165
Freq-max	131	256	409	449	461	461	458	470
Ampl max	5.7	2.38	3.09	3.582	3.095	2.611	2.024	1.724

Ratio	0,09	0,10	0,18	0,38	**0,48**	0,36	0,20	0,07

	cylinder of 98mm							
	100	200	300	400	500	600	700	800
freq-input	92	192	308	409	491	592	693	790
Ampl.	3.77	3.20	6.09	6.879	6.005	2.981	1.226	421
Freq-max	125	244	308	409	482	540	558	500
Ampl max	4.85	4.08	6.09	6.879	6.033	3.205	1.708	1.056

Ratio	0,08	0,15	0,48	0,79	**0,96**	0,66	0,37	0,17

Table 4.8 Frequency space analysis results of cylinders with sin3cycle signal.

Using sinusoidal 3 cycle functions same results are reached. experimentally it possible to assume that the resonant frequency for these specimens is 500kHz.

4.4.5 NUMERICAL MODELS

Numerical simulations lead to reproduce the physical phenomena. To achieve this goal numerical model are made by using a FEM software STRAND7. The models

implement are mono-dimensional and bi-dimensional, in axial symmetry. A linear dynamic analysis is conducted. Forward the input signal implemented, the numerical models, the results of simulations and parametric study are presented and discussed.

The simulation of a ultrasonic wave that travelling in a continuum, to follow bibliographic reference is classically simulated applying a set of assigned displacements. A brief discussion is need to understand the shape of displacement law, and the nodes that are interested of these displacements.

The displacements assigned at one point of the model simulate a small probe on specimen, often, dimensions of probes are not so small related with the dimension of specimen. So, in these cases, the imposed displacement, at the models, can involve as node as the dimension of the probe. Also is relevant to define the shape of the signal. In some cases, the shape signal is triangular, other authors use a form of the signal is more close with the field of displacements imposed at the points where is applied the probe. Here, to follow how present of Reinhold, for alloy plate, we use a set of displacements made of the product of a signal of 3 cycle with a signal of a sine wave with frequency 1/3 of previous signal. This procedure is chosen, because if the signal would be given as the displacement field with a sine wave of 3 cycles, followed by a zero signal, it would be mean to insert into the signal a square wave with length of three sinusoids, and since the square wave is obtained from a summation of periodic waves with different frequency and amplitude, there would be a disturbance in the signal that is generated.

After to define the law of variation of the signal, the chosen frequencies are been implemented in the numerical model, similar to the frequencies chosen during the test by 100 to 800 KHz with steps of 100KHz. On these signals is was operated a sample timing choosing a sampling frequency equal to 12.5MHz, which corresponds to a period of $8x10^{-8}$ sec, this choice was also operated to optimize effort time, since the choice of low sample frequency does not allow us to

approximate the signal, and against the choice of high sample timing, require considerable effort. For input signals, signal amplitude was defined equal to 1mm.

The output signals have been detected, in the model at the points where in the real specimen is applied the probe receiver. Similarly to the signals input, you can choose to detect the signal in a single node, or in more nodes, depending of the size of the probe receiver, it this is a point source compared to the size of the specimen, or not. In this case, the signals were detected, both at the central node in axis, that in the neighboring nodes, with a maximum size equal to the size of the probe. Then an average of detected signals was conducted of to have a virtual representative signal, in order to reproduce the recorded signal from the probe receiver.

The definition of the model requires the choice of the size of mesh. So the ultrasonic signal can be propagate in the model, without undergoing changes during its propagation, it is widely known that the mesh size must be such as to respect the following relation:

$$d = \frac{\lambda}{20}$$

Where λ is the length of the wave. The length of wave is related with its frequency, below the follow relation:

$$\lambda = \frac{V}{f}$$

So, to find the high restriction, assuming that the travel velocity is as maximum equal to 6000 m/s , it is need to find the lowest λ , that correspond at the highest frequency. Assuming a max frequency of 1MHz, λ =6mm, that mean d=0.3mm , To uniform the model at each frequency, a mesh of 0.2mm is assumed.

Two type of model are implemented. The 1D model, is a set of beam element, with free borders, mechanical properties are as the presented steel E=209GPa ν =0.30, cross section is circle of diameter 60mm. the length of model is 98mm, as the steel cylinder. FEM is composed of 490 beam-element of 0.2mm, according with the

mesh dimensions to the maximum simulated frequency. At one extremity an assigned displacement in imposed, at the opposite extremity de displacement is detected.

The 2D model is also computed in axial symmetry. Each element is with square shape of 0.2mm side. It is bounded with horizontal hinges in the symmetric axis the vertical axis, a displacement field is imposed at the down bases and displacements field are detected in the axial node, as in the others upper bases nodes.

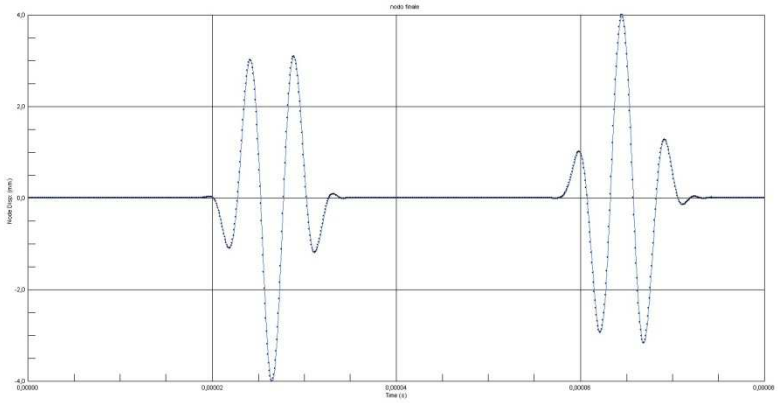

Figure 4.43 Input signal for 1D models

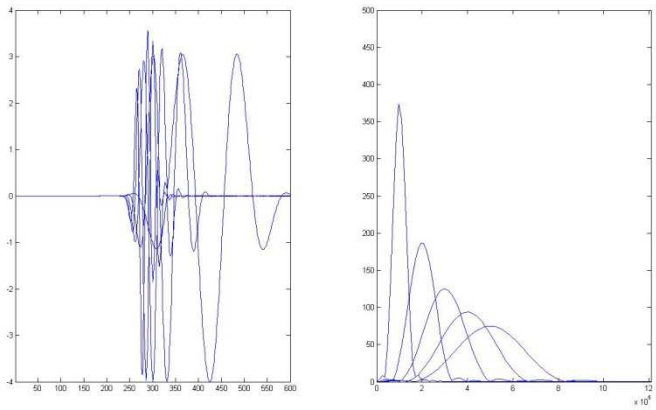

Figure 4.44 FFT for 1D model freq 100-500kHz

INPUT 3cycle sin signal				
freq	ppk	rms	var	FFT max
100	2,00	0,61	0,37	188,23
200	2,00	0,43	0,18	94,19
300	2,00	0,35	0,12	62,83
400	2,00	0,30	0,09	47,09
500	2,00	0,27	0,07	37,70

Output of 1D beam model				
freq	ppk	rms	var	FFT max
100	4,02	1,11	1,24	372,47
200	4,14	0,79	0,63	188,18
300	4,05	0,65	0,42	125,44
400	4,20	0,56	0,31	94,09
500	4,13	0,50	0,25	75,25

ratio on 1D model/Input				
100	2,01	1,84	3,39	1,98
200	2,07	1,85	3,41	2,00
300	2,03	1,85	3,40	2,00
400	2,10	1,85	3,41	2,00
500	2,07	1,85	3,40	2,00

Table 4.9 results of 1D models

Figure 4.43 and 4.44 shown the result related with the 1D model using a Reinhold shape function and the table 4.9 report results of output signal using a 3 cycle sin signal. It is possible to observe that the amplitude of signal in 1D model is always

the double of the input signal, as if inside the 1D model the behavior of signal is as guided waves. Also with 1D model is not possible to reach the resonant frequency. The amplitude of FFT is going to decrease with the increasing of frequency.
As said before, to better model the propagation of wave an axial symmetric model is implemented.

	Input sin3cycle signal							
	100	**200**	**300**	**400**	**500**	**600**	**700**	**800**
freq-input	98	195	296	394	491	592	693	790
Ampl. FFT	753	377	251	188	151	126	108	94

	Cylinder of 98mm FEM output nodes in 10mm							
	100	**200**	**300**	**400**	**500**	**600**	**700**	**800**
freq-input	106	199	304	390	492	597	690	790
Ampl.	227	89	67	70	69	54	46	36
Freq-max	106	199	304	377	492	597	677	761
Ampl max	227	89	67	74	69	54	46	37

Ratio	0,30	0,24	0,27	0,37	**0,46**	0,43	0,42	0,39

	Cylinder of 170mm FEM output nodes in 10mm							
	100	**200**	**300**	**400**	**500**	**600**	**700**	**800**
freq-input	110	210	305	390	491	600	702	801
Ampl.	37	36	50	39	50	48	44	42
Freq-max	129	231	305	368	491	600	702	801
Ampl max	53	76	50	43	50	48	44	42
Ratio	0,05	0,10	0,20	0,20	0,33	0,38	0,41	**0,44**

Table 4.10 results of 2D models

With the 2D model result are pretty better, it is possible to obtain an trend that give a maximum for the frequency of 500kHz for the model of 98mm but not for the model of 170mm. So the models are still inadequate because the measured frequency at 500KHz is obtained only in one model, in the second one, the length induce a phenomena of guided waves, and the ratio increase with the frequency. Maybe is need to investigate some other aspect about how the FEM parameters as restrained influences the propagation of waves. To verify if the dimension of model can influence the resonant frequency it is proposed a parametric study.

4.4.6 PARAMETRIC STUDY

In bi-dimensional model a parametric study is conducted to point out how the specimen dimension influence the propagation of ultrasonic signal. In order to conduct a parametric study on the size of the specimen, two-dimensional models of different sizes have been implemented, in axial symmetry. The study is conducted on frequencies between 100 and 500 KHz, in elasticity, with linear transient dynamic analysis. therefore it is assumed for these models a mesh size of 0.5 mm, less than the minimum of 0.6mm. In particular, the following models were

investigated 196x60 -30-20-2mm. Investigating the relationship R/L between 3.2 and 100. For a total of 4 models, investigated for 5 fields of frequencies from 100KHz to 500KHz with 100KHz step. For these models have been determined and the responses are then discussed results.

In the table 4.11 are reported the ratio of FFT and Ppk determined in the axial node in input and in output sides of a axial symmetric model. We observe that Ppk in time domain have analog meaning of FFT in frequency domain.

It is confirmed that in the model of 196x2 the behavior is still similar to the one observed in 1D model, with a constant ratio of 2, in the model 196x20 the maximum peak is 400KHz, and for the model of 196x30 the maximum frequency is at 100KHz , but the curve is not go to decrease when the frequency increasing but at 500KHz a second peak is present. That means that the problem is scale dependent. Observing the deformation of model, it is possible to appreciate how when the dimensions of model increasing and the ratio R/L decreasing the cylinder become mode short and the wave go to the radial direction, subtracting energy at the main path of propagation.

FFT				
0mm -O/I	**196x60**	**196x30**	**196x20**	**196x2**
100,00	6,17	1,09	2,20	1,89
200,00	2,10	0,69	0,10	2,00
300,00	2,06	2,15	0,34	1,63
400,00	3,00	0,29	0,47	1,69
500,00	4,34	0,72	0,39	2,02
PPK				
0mm -O/I	**196x60**	**196x30**	**196x20**	**196x2**
100,00	7,40	1,83	2,67	2,05
200,00	3,10	1,61	0,22	2,06
300,00	2,85	3,67	0,77	2,05
400,00	2,84	0,91	1,18	2,05
500,00	4,40	1,30	0,85	2,26

Table 4.11 Results of parametric study

You can't connect the dots looking forward;
you can only connect them looking backwards.
So you have to trust that the dots will somehow connect in your future.
S. Jobs

CHAPTER 5

EXPERIMENTAL TESTS AND NUMERICAL SIMULATIONS

5.1 INTRODUCTION

In this chapter the experimental results are reported. They are divided by tree parts. In the first part are presented and commented the laboratory tests conducted on fresh concrete during the maturation time. In the second part of chapter some investigations conducted on hardened concrete are presented. Ultrasonic test have interested almost 70 cubic specimens. In the last part. Numerical instruments are used for the interpretation of the results of tests. Some numerical parametric simulations are conducted to reproduce the laboratory phenomena, and forward data processing using strong algorithm are applied to deduct results. In the last part a clustering analysis is done to permit a classification of the properties observed of concrete, specially about the resistance of concrete.

5.2 FRESH CONCRETE

Fresh concrete is a concrete , mixture of sand, water, gravel and cement, during the time of its maturation, form the cast to 28 days.

A campaign of test is been conducted on fresh concrete. Objective of the study was to observe how ultrasonic feature are influenced from the maturation processes. The methodology proposed lead in the determining some maturation curves for some different mix designed concretes. In these maturation curves, form the cast to 28 days, features of ultrasonic waves as velocity or amplitude signal can be related with intermediate level of reached resistance. Forward, going in a workplace, after few days from the cast of concrete, thought the execution of an ultrasonic test in a structural element of fresh concrete, and knowing the mix design property of concrete, we can determine if the casted concrete will be reach the designed resistance or not, and how it is out or inside the forecast maturation curve. In this way you don t have to wait 28days to understand if the concrete have the right performance level, to take decision, but you can decide to intervene already in 2-3 days after the casting.

In order to avoid this objective, it is need to design a concrete. The concrete of cast were choose by varying, in this first approach, one parameter: the maximum dimension of aggregates, and to hold fixed water/cement ratio, type of cement, slump and maximum resistance. Any additive was used.

By using the developed software, according with the ACI 211.1-91, different concrete and mortar are casted.

The tests started by some preliminary test on small specimen of mortar, to understand how to calibrate devices to have system in acquisition for 28 days, and forward with some prototype of recopies of concrete.

The control of mix design is often one of the more different aspects. To avoid this problem all the recopies were made in DICAM laboratory, by adopt chosen type of cement, aggregates, sands, and water. The dough is been prepared in the laboratory. In this way we were sure that any external interference could not modified our recipes.

The aggregates and the sand come from a close cave of *Montelepre*, were a calcareous formation is present. From different aggregates bulk, a sieving was been conducted, and the aggregate were divided in fraction on volumes. For the sieving it is used a shake machine, and a standard procedure provides form laboratory of Geotechnical form DICAM, UNI EN 933-1:2012, In figure 6.1 the more used fraction of aggregates are reported.

		
4.75<d<5.00	6.30<d<9.50	9.50<d<12.50
		
12.50<d<19.00	19.00<d<25.40	25.40<d<37.50

Figure 5.1 Fractions of aggregates

Before using the aggregates or sand, to be sure of the final content of water in concrete, they were dry using a light oven.

The cement adopted was the ordinary cement R325, produced from *ItalCementi*, and in distribution from common stores. The water used was a tip potable water. After to make a recipe, material were selected and weighted in the right quantities.

5.2.1 DEVICES AND ENVIRONMENTS

The dough were made using a small kneader of 30kg, and it going on until the dough will become homogeneous, and the parts of aggregate all wetted, each dough take around a 15minutes of mixing, using different velocity to avoid the segregation.

For execute the ultrasonic test, special concrete box are prepared. They are a plastic rigid box, openable, in the two opposite faces an hole were formed to lodge the probes. During the cast, the holes are closed, the concrete is stored in the box concrete and it is constipated using a vibrator. The vibration is stopped when the blending is starting.

During the casting, are filled on concrete two cube boxes with 150mm of side and 3 cylinder boxes D=100mm and H=150mm. the two cube boxes are used for the ultrasonic test during the maturation time, the 3 cylinder are used to monitoring resistance and elastic module at 7-14 and 28 days. In figure 6.2 the devices are shown.

Kneader Vibrator Cubes

Figure 5.2- Devices used for casting the concrete

The casted concrete is now settled in a temperature controlled room at 20 Celsius degree. the cubes are posed in a frame with two pistons that pull the probes against concrete, a gel is applied on the probe surfaces, and the probes are applied. The software starting and the test is going on. *Pulser-Pro* setting are reported in table 6.1, each test have a duration of 50minutes and it is repeated each 15 minutes. Theoretically for 28 days. To be sure that any interruption of test can be operated acquisition system was plugged below a UPS with 48h of autonomy.

Features	**Values**
Investigate freq.	50-300 kHz
Steps	10 kHz
N steps	25
Delay	150 ms
amplitude	22-30 dB
N signals for freq.	500
Duration of test	50 minutes
$f_{playback}$	25Msps
N clycle	3 sinusoids

Table 5.1 Set of test on fresh concrete

Some relevant aspect are need to be discussed before to present the experimental results.

The fresh concrete is a mixture of solid particle in a liquid or mud continuum, after few hours of the cast, it is still soft, this means, the ultrasonic signal is propagated in a viscous dough with different behavior that from a solid continuum. So, any ultrasonic signal is detected during the first 6-12 hour after the casting. However, because the concrete is wet, the electrical conductivity of the specimen is high, and

what we can do is a cross talk between the input and the output probes. The cross talk is an electrical disturbance, tagged at the receiver probes, and travel at the light speed. In figure 5.3 is reported the output signal after 3h form casting, at the frequency of 250kHz.

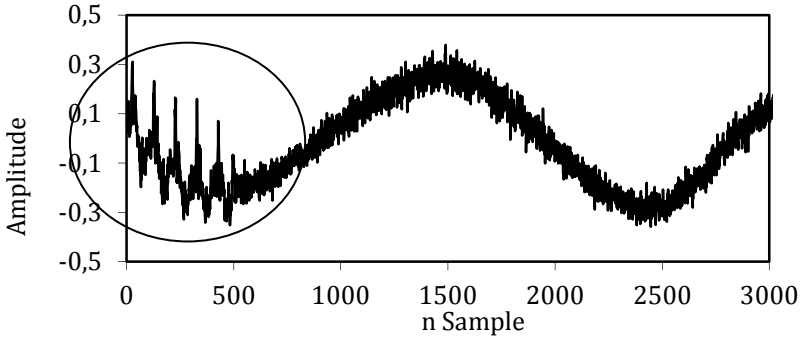

Figure 5.3 Signal detected after 3h form the casting (freq 250KHz)

The phenomena is the same if test is conducted in a water box. When the hardening is starting, an ultrasonic signal start to be formed, and you can view a wave take shape trough the cross talk. As show in figure 5.4.

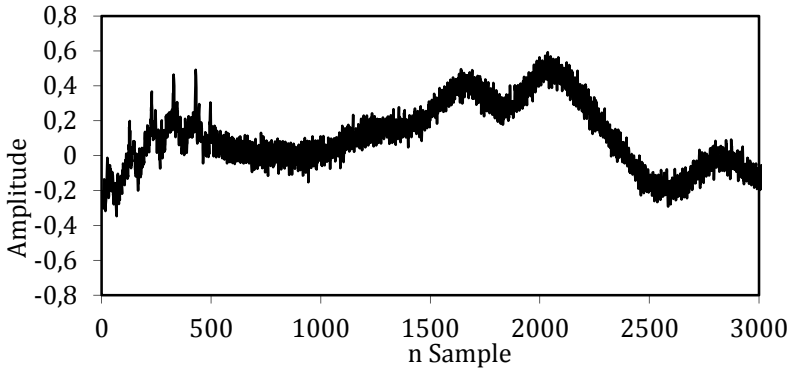

Figure 5.4 Signal detected after 6h form the casting (freq 250KHz)

After a 10 hours from the cast, the concrete is sufficient hardened and the ultrasonic signal travel quite clean in the concrete, as shown in figure 5.5.

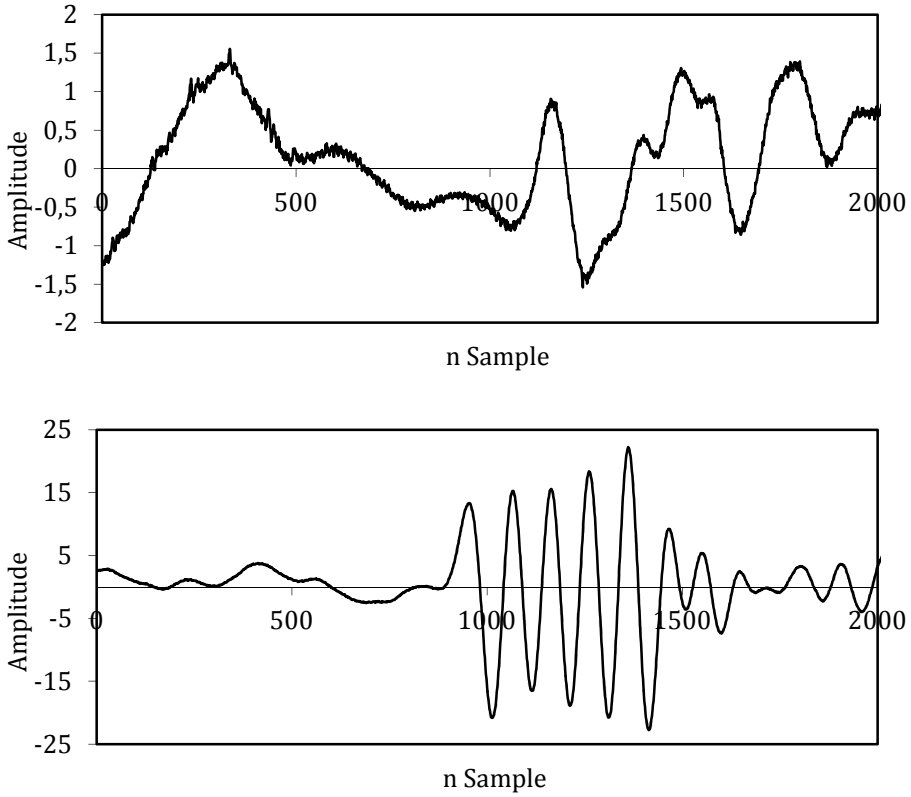

Figure 5.5 Signal detected after 24h and 72h form the casting (freq 250KHz)

The test have to be conducted for 28days, but actually, a shrinkage of concrete generated a detachment from probes to the specimen, and the signal is lose. When this phenomena take field depend on the wet level and the curing speed of

concrete. Sometimes it will be after few days from the casting, in other lucky cases after 15 days.

Another relevant matter is related with the gels used for conduct the test. In the begging of tests, the concrete is still wet, during the curing, it is going to absorb liquids present in the surrounding space, also the humidity of the gels. In a certain days, the gel become dry, and any signal can be recoded if the interface gels-material is dry. In some tests we try to remake the interface between material and probes, over some state variables, as pressure of probes, or thinness of gel are been modified and the results could not been related with the previous acquisition, specially for the amplitude.

Here we want show the more relevant results from some of these tests. The presented tests are related with two concrete designed by using the follow prescription:

Property	**Value**
Max tension	300 MPa
Slump	150 mm
D max1	9.00 mm
Dmax 2	12.50mm
MF	4
Bulk density	1600 Kg/m^3

Table 5.2- Mix design of concrete

Form these assumptions, a concrete with w/c =0.42 is casted. The grain curves of these mix is reported in figure 5.6.

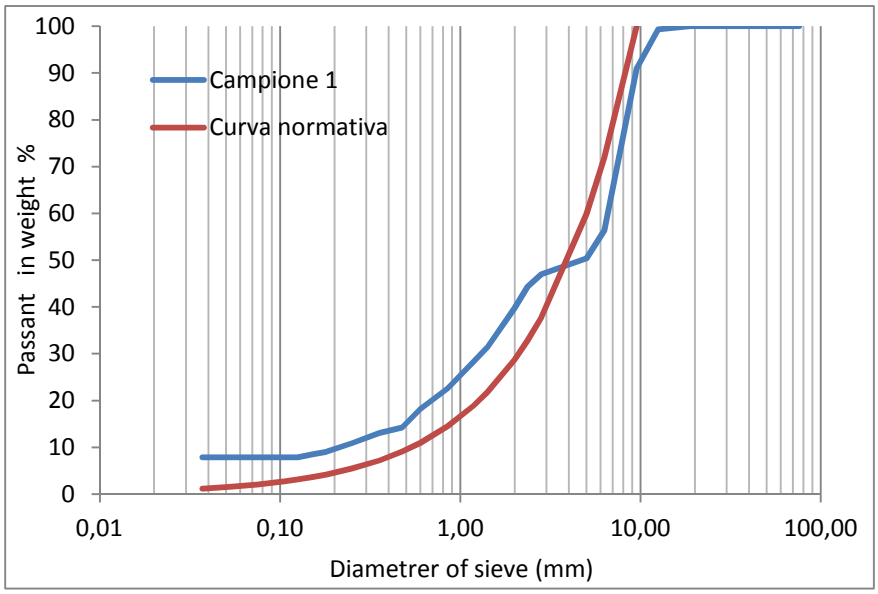

(a)

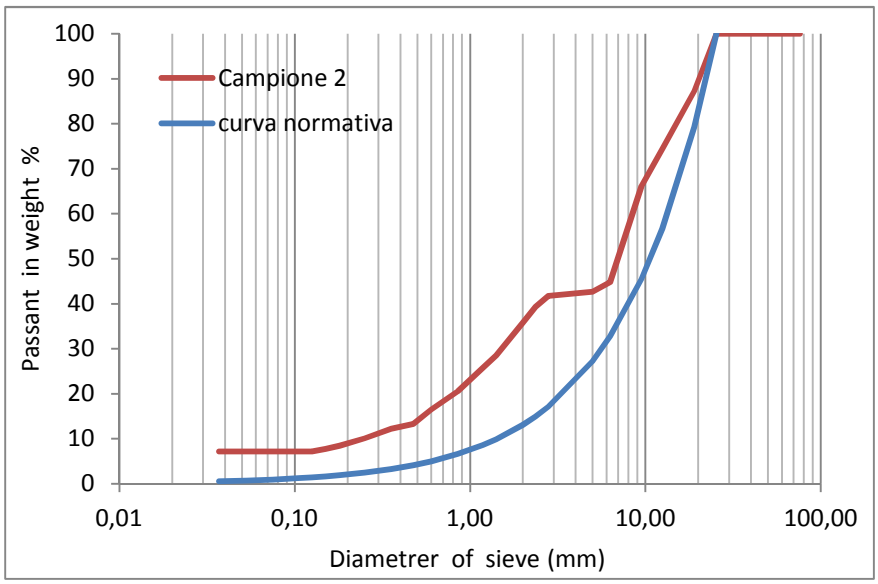

(b)

Figure 5.6 Grain curve for concrete with (a) D_{max}=9.00mm, (b) D_{max}=12.50mm

The cubes and the cylinders are settled in maturation room, at temperature of 20 degree, figure 5.7 shown the experimental set of tests.

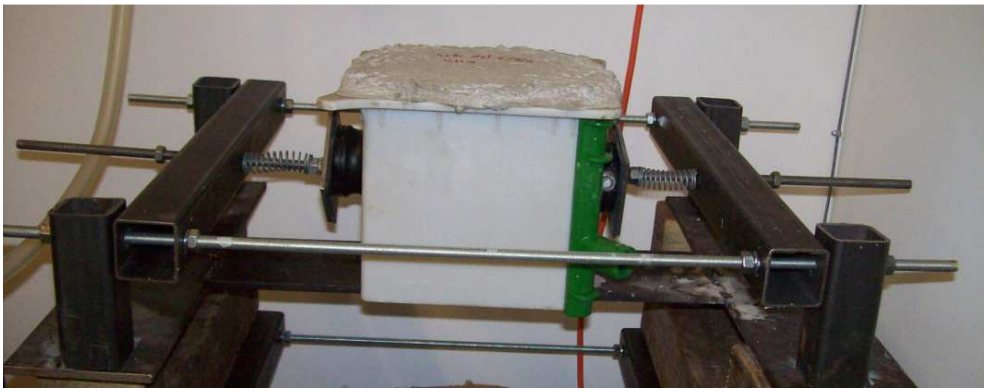

Figure 5.7 Experimental setup

During the tests, the signals where acquired follow the data of table 6.1. Using the algorithm presented in chapter 4, here we report the results in time space and in frequency space.

5.2.2 TIME SPACE ANALYSIS

Time space analysis lead to determine TOF of signals. TOF is determined using the cross correlation function. From TOF, kwon the distance between the probes the velocity is determined as V=d/t. The velocity of ultrasonic wave decrease if the frequency increase.
In figure 5.8 is reported the trend of the velocity with frequency variation after 3h of casting (a) and when the concrete is hardened (b).

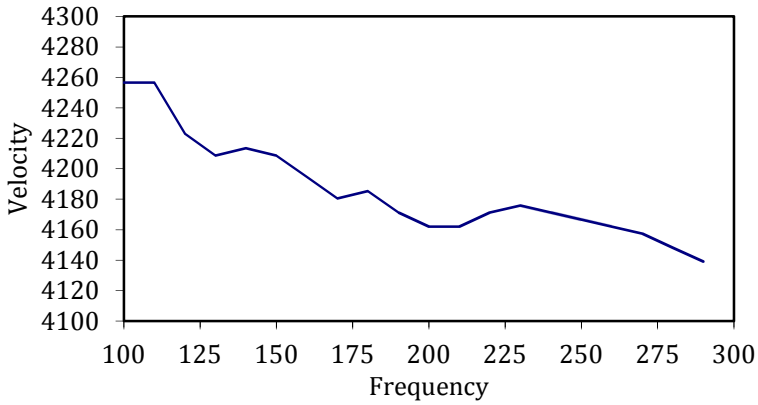

(a)

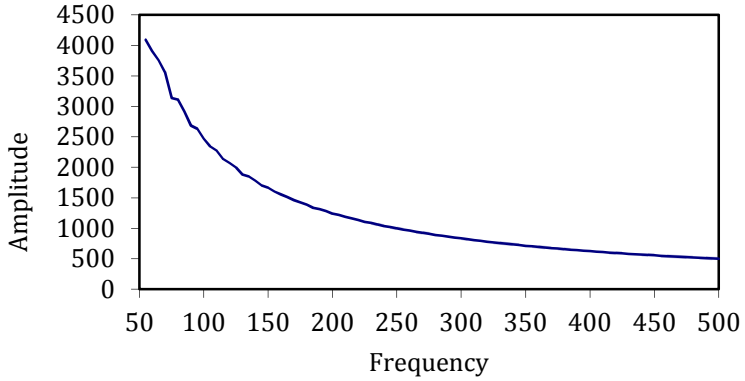

(b)

Figure 5.8 Velocity trend with different frequency signals in a concrete:
(a) after 3 days of curing D_{max}=12.50mm (b) when the concrete is hardened

For individuate a standard value of velocity, by looking at the frequencies, we assume that the standard velocity of signal is the velocity of the resonant frequency signal.

For each sweep of investigated frequencies, the resonant frequency, the standard TOF and so the velocity is deducted, the results shown, in figure 5.9-5.10 for concrete that comes from the same mix, the two curves are so close.

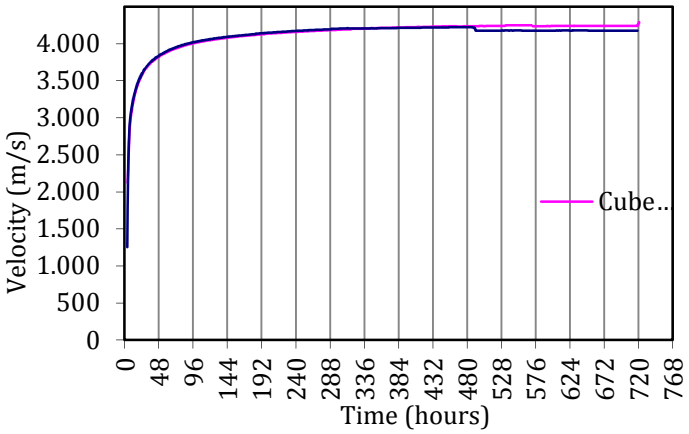

Figure 5.9 Diagramm of velocity at the frequency of 150KHz (cast of 06/09/11)

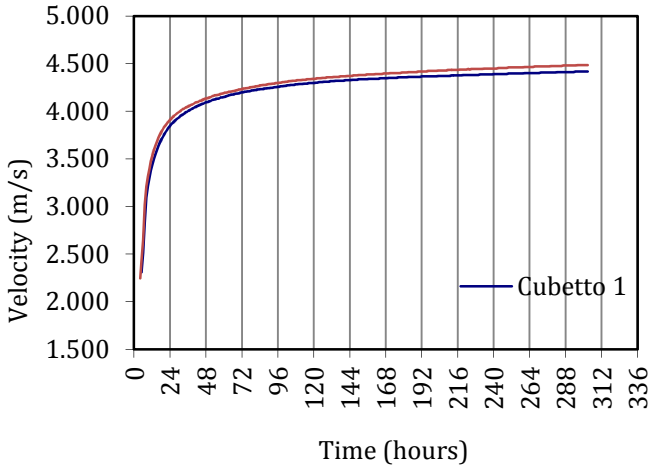

Figure 5.10 Diagram of velocity a the frequency of KHz (cast of 14/11/11)

It is clear that the cure is more developed in the first 2-3 days, where velocity in more increasing, and it go to an asymptotic value after few days.

To investigate also the mechanical properties as resistance and elastic module and how they evolve in times, other 3 cylinder specimen are casted with the cubes, they are tested for detect the elastic module and the break resistance. Here the results are shown.

In first time, it is possible to deduct the elastic module by using the velocities, in the table 5.3 are reported elastic dynamic modulus determined for two different Poisson coefficient.

Day of casting	**Spec.**	**Velocity (m/s)**	**Density (Kg/m^3)**	**Time (h)**	**Freq [KHz]**	**ν**	**E_d (GPa)**
18/08/11	Cube 1	4325.26	2426.67	305.8	100	0.15	42.99
						0.12	43.91
06/09/11	Cube 1	4175.95	2347.83	718.8	150	0.15	38.77
						0.12	39.60
	Cube 3	4242.08	2347.83	718.8	150	0.15	40.01
						0.12	40.87
14/10/11	Cube 1	4416.96	2396.92	302.9	100	0.15	44.29
						0.12	45.23
	Cube 3	4485.65	2396.92	302.9	100	0.15	45.67
						0.12	46.65

Table 5.3 Elastic modules determined by ultrasonic tests

Using the same relationship, it is possible to evaluate the elastic dynamic module during the maturation time. Here the chart, for the considered mixture, are reported.

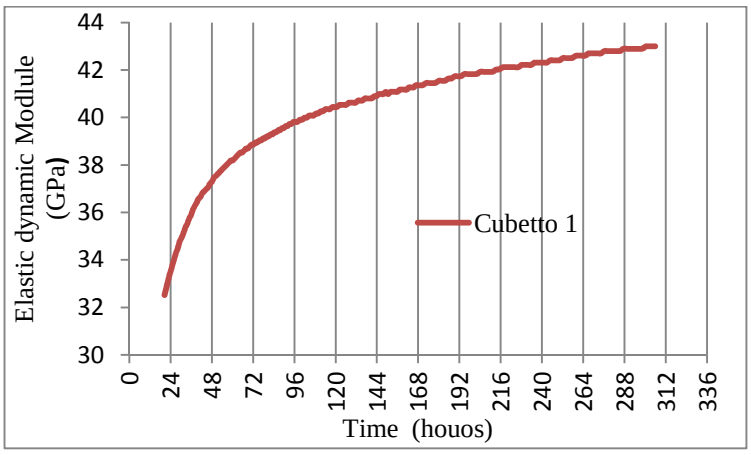

Figure 5.11. Elastic dynamic module for the cube of 29/08/2011 using ν = 0.15

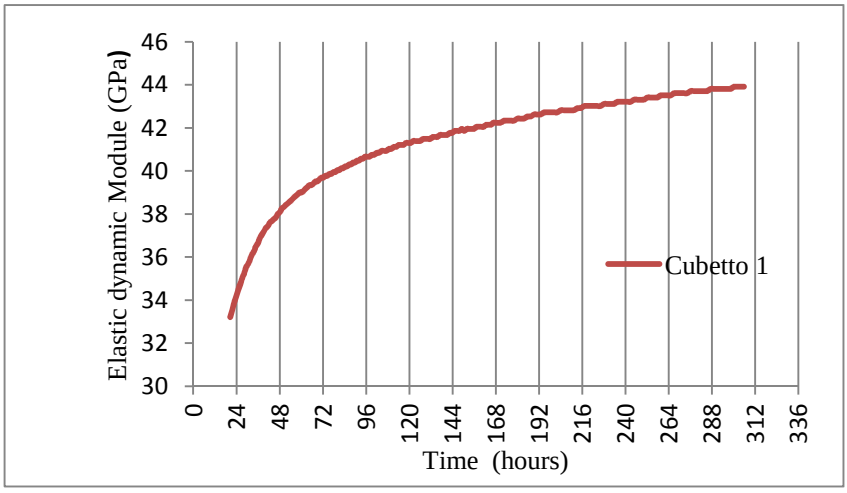

Figure 5.12 Elastic dynamic module for the cube of 29/08/2011 using ν = 0.12

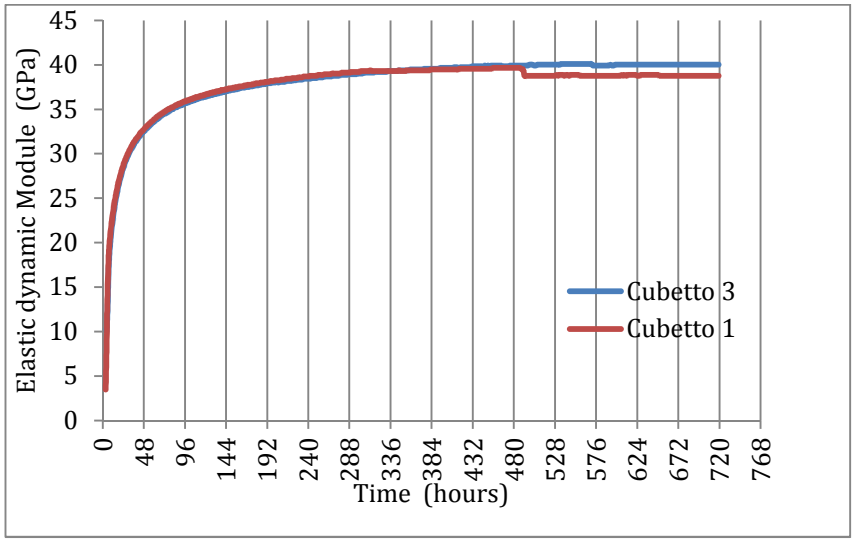

Figure 5.13 Elastic dynamic module for the cube of 06/09/2011 using ν = 0.15

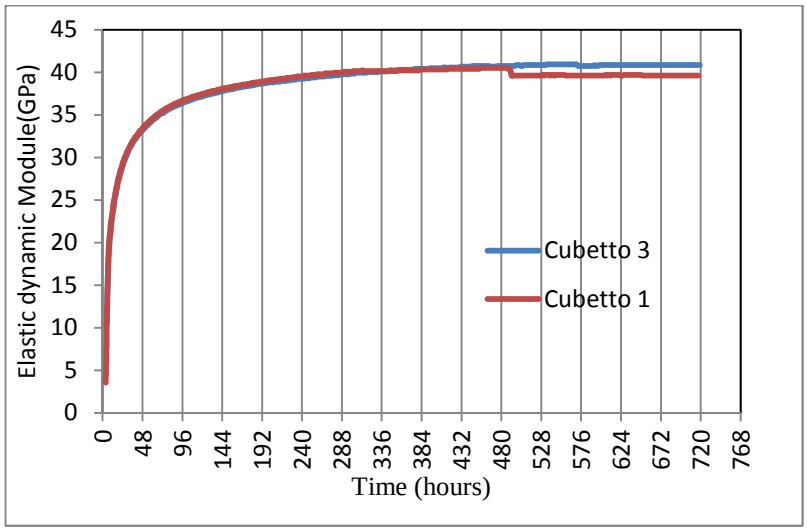

Figure 5.14 Elastic dynamic module for the cube of 06/09/2011 using ν = 0.12

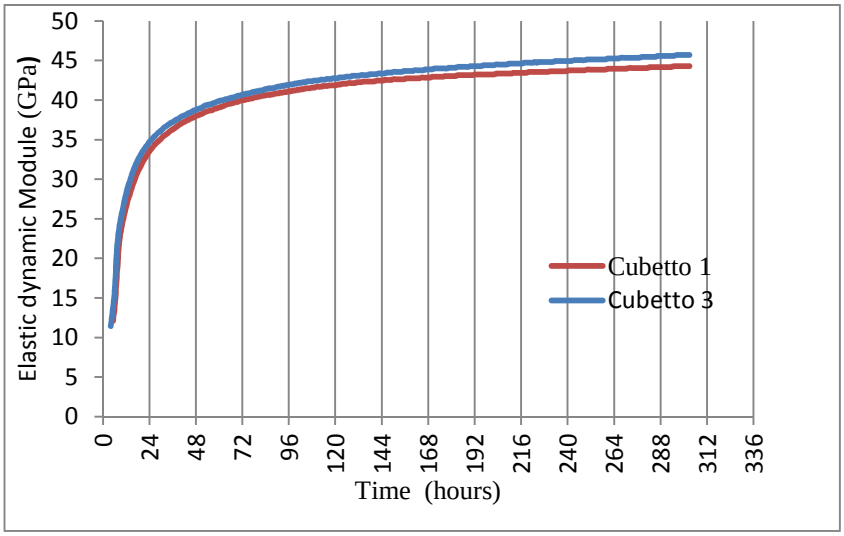

Figure 5.15 Elastic dynamic module for the cube of 14/10/2011 using ν = 0.15

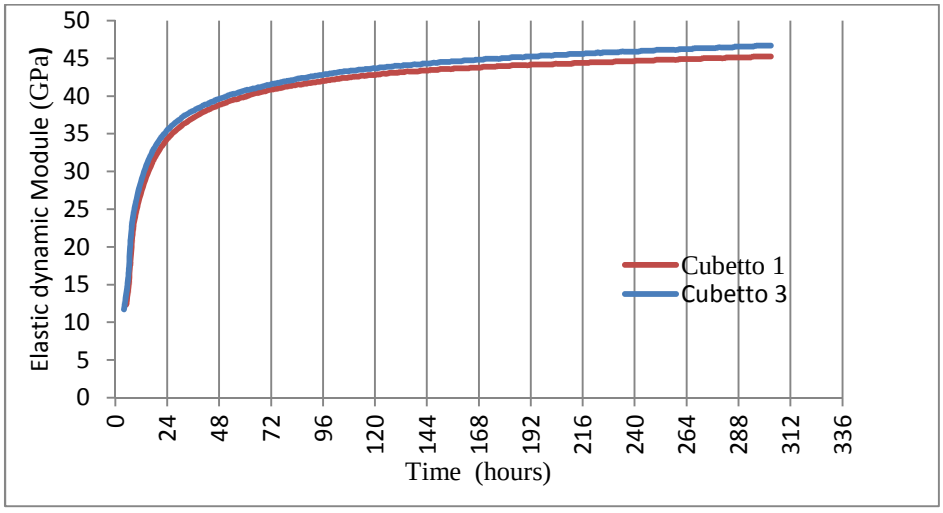

Figure 5.16 Elastic dynamic module for the cube of 14/10/2011 using ν = 0.12

5.2.3 RESULTS RELATED WITH ELASTIC MODULE MEASUREMENTS

Now we report the results obtained from the measurement of the elastic modulus on the cubic and cylindrical specimens. Were chosen values of the base length L0 for the measurement of deformations equal to 70 mm, the minimum load of 25 KN and maximum equal to 125 KN for carrots and 300 KN for cubes; these loads have been converted in stress dividing the load for the areas of the base areas of the specimens. After will be carried out of the load cycles, and for each cycle will be measured displacements final δf, after the loading phase, and those residues δr, after the unloading phase, in two diametrically opposite points. Subsequently it will be calculated the difference between the displacements that will be divided by Lo for obtaining the difference between the two deformations Δε, which will serve for the calculation of the two elastic moduli, with the formula 3.10, relative to the two diametrically opposite points E1 and E2.. So it was calculated from the average value of Em between these two values, then for all values of load cycles performed. Finally the samples were brought to rupture for the measurement of the ultimate load, and then the last stress σ_u, which are put equal to f_{ck} for cylindrical specimens and R_{ck} for cubic specimens; multiplying R_{ck} to 0.83 (legislation value) is obtained f_{ck}. From the value of f_{ck} is obtained f_{cm} that will be useful for the calculation of the elastic modulus with the average formula of the Italian law.
In Table 5.4 shows the values of the stress minimum, maximum, and ultimate and its elastic modulus is calculated with the formula proposed of the Italian legislation.

Casting day	Specimen	A (mm^2)	σ_0 (MPa)	σ_{max} (MPa)	σ_u (MPa)	E_{norma} (GPa)
6/09/2011	Cube 1	22500	1.11	13.33	42.4	34.12
	Cube 3	22500	1.11	13.33	44.2	34.46
	Cylinder 1	7850	3.18	15.92	41.33	35.51
	Cylinder 2	7850	3.18	15.92	38.08	34.79
14/10/2011	Cylinder 1	7850	3.18	15.92	34.39	33.93

Table 5.4 Compression data and elastic moduli by DM 2008

In the following tables are reported the elastic module obtained from the measurement of the specimen. The measurement are conducted on the two diametrically opposite sides for different cycles of load, and the average value of the elastic modulus is reported.

E_1 (GPa)	E_2 (GPa)	E_m (GPa)
32.31	33.98	33.14
30.29	31.05	30.67
31.31	31.94	31.62
31.31	35.96	33.63
E mean		32.27

Table 5.5 Experimental results on cylinder 1of 06/09/2011

E_1 (GPa)	E_2 (GPa)	E_m (GPa)
37.78	34.72	36.25
33.98	32.78	33.38
37.40	31.94	34.67
E mean		34.77

Table 5.6 Experimental results on cylinder 2 of 06/09/2011

E_1 (GPa)	E_2 (GPa)	E_m (GPa)
31.11	29.44	30.28
29.63	28.90	29.26
26.82	30.25	28.54
E mean		29.36

Table 5.7 Experimental results on cube 1 of 06/09/2011

E_1 (GPa)	E_2 (GPa)	E_m (GPa)
28.45	33.82	31.13
31.85	29.72	30.79
32.29	27.21	29.75
28.72	32.98	30.85
mean		30.63

Table 5.8 Experimental results on cube 3 del 06/09/2011

E_1 (GPa)	**E_2 (GPa)**	**E_m (GPa)**
29.82	35.62	32.72
31.32	31.42	31.37
30.30	30.11	30.20
29.08	32.98	31.03
E mean		31.33

Table 5.9 Experimental results on cylinder 1 del 14/10/2011

5.2.4 FREQUENCY SPACE ANALYSIS

The signal processing is conducted also in frequency space. In this space, as first thing a windowing on the signal is operated to select only the first compressive mode, and the signal is processed using an DFFT. The amplitude of DFFT transform output signal at the input frequency is normalized by using a baseline of input signals at the same frequency, in this way an index $I_{\square}$ is defined.

Forward, from each sweep of frequencies investigated at each step, 50 to 300 KHz, a standardization is conducted to normalize the maximum to 1.

In figure 6.9 is presented in a plane the trend of DFFT at each curing time. The observation time for the concrete of D_{max}=9.5mm is 500h (20gg) and for the D_{max}=12.50mm is 300h (15gg).

The following diagrams are of the FFT analysis of the cubes, the diagrams in 3D you can see that for the first 10 hours of analysis there are no frequencies with significant amplitudes, then the amplitudes have values gradually increasing. From the diagrams FFT we get the resonance frequency.

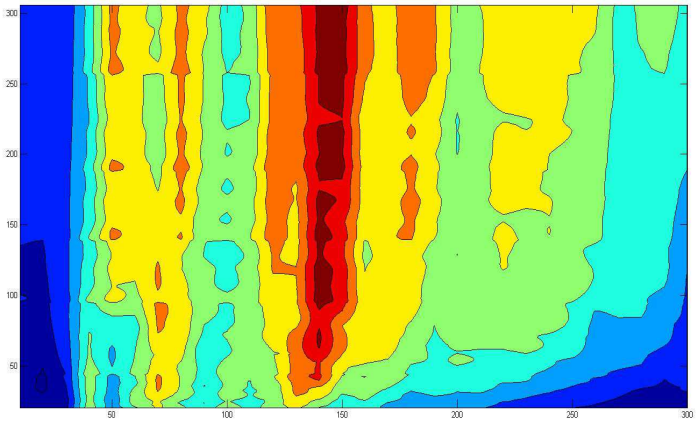

Figure 5.17 FFT in 3D cube 1 of 29/08/2011

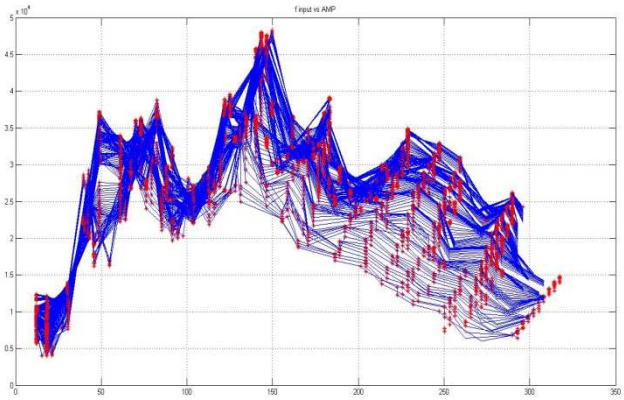

Figure 5.18 FFT cube 1 of 29/08/2011

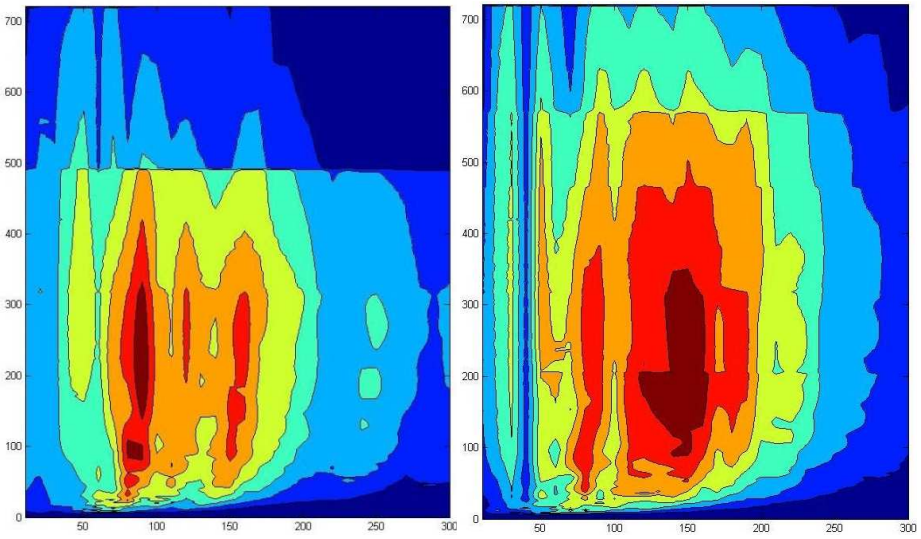

(a) (b)

Figure 5.19 FFT in 3D del (a) cube 1 e (b) cube 3 of 06/09/2011

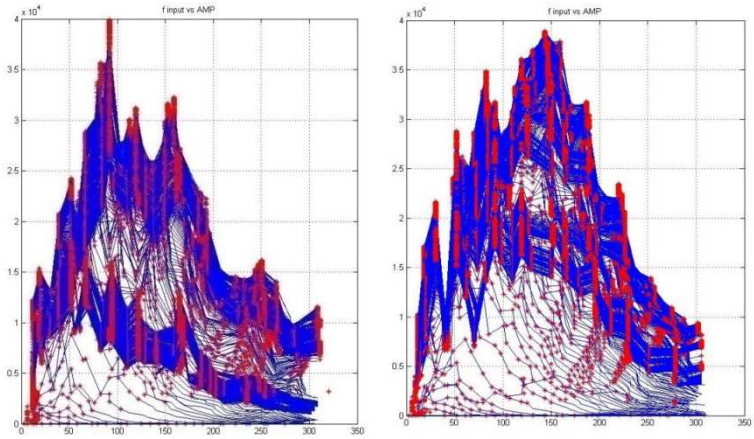

(a) (b)

Figure 5.20 FFT of (a) cube 1 e (b) cube 3 of 06/09/2011

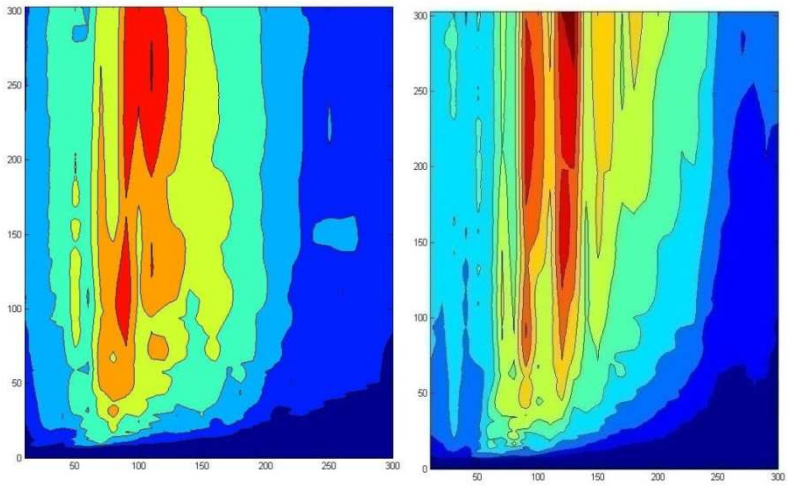

(a) (b)

Figure 5.21 FFT in 3D of (a) cube 1 e (b) cube 3 of 14/10/2011

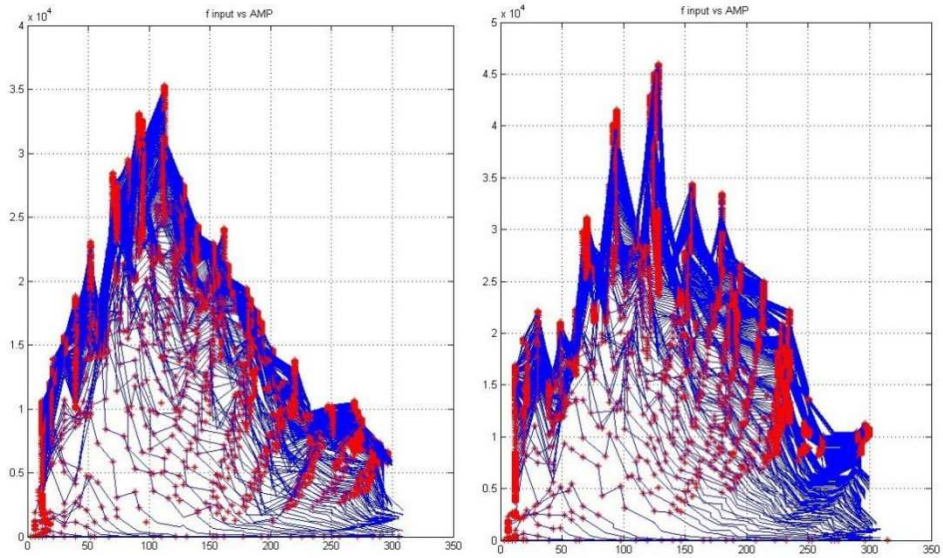

(a) (b)

Figure 5.22 FFT of (a) cube 1 e (b) cube 3 of 14/10/2011

In Table 5.10 shows the resonance frequencies and the relative amplitudes for the first two peaks of the FFT.

Cast day	**Spec.**	**I Resonant freq (peak 1)**	**Magn X1000**	**II Resonat freq. (peak 2)**	**Magn X1000**	**time (hours)**
29/08/11	Cube1	150	48	130	40	305.88
06/09/11	Cube 1	90	40	160	32	718.8
	Cube 3	140	38	80	35	718.8
14/10/11	Cube 1	120	36	90	33	302.9
	Cube 3	130	46	90	42	302.9

Table 5.10 Resonant Frequency and magnitude of the first two peaks of FFT

First of all, we observe that there is a unique frequency, that we call resonant frequency in which the concrete reach the maximum amplitude of the index, this frequency is not stable in the same mix design dough, the two cubes have different values of maximum. frequency. From different mix design dough also resonant frequency are different. From this observation we can deduce that resonant frequency is related not only with mix design, but also with other characteristics' as experimental setups, presence of different distribution of aggregates in the considered cylinder of volume, different pressure and interface state between the two specimen.

Other aspect are observables, the specimen, after few hours from casting, become hard, and in it a resonant frequency take field. This frequency is constant during all the curing time, as well as after. So it depend of characteristics of materials, and

not of maturation process. We can obtain this properties after soon that the concrete become hardened.

It is pretty hard to understand the phenomena that working on during the setting. In this time, 12hours after the casting, the dough is still fluid, and any ultrasonic signal is detected from the receiver (only the cross talk). In a fluid with solid inclusion, the material is not confined, the fluid particle have free displacement and the ultrasonic perturbation is lose, in so few mm after it is produced. When material become hardened, the perturbation is able to be transfer form generator to receiver. Also the material lose electrical conductivity and the cross talk become off or reduced.

The shrinkage as discussed before, induce the material to be plugged off from material, especially if the concrete is absorbing water that is content in the gels. Some study propose to use oily substance. In the conducted test with oil or glycerin, after the casting, the oils are more light and they go up. So a this time any curing specimen is arrived to 28 days.

To investigate this aspect, a research is been conducted on some commercial gels, or other substances that comes from different field. In electrical field, there is a silicon gel that you can synthesize at the need assuming the level off hardened that it need. Using this gel the gel life is more long, but the presence of air balls and glycerin reduce hardly the signal power, in the tests conducted the signal is lose in the noise level. In figure 6.10 the plugging of probes at the end of test is shown, you can see the dry gels, and you could recognize the lasts points where probe was still attached to the specimen.

Figure 5.23 Probe at the end of test.

5.3 HARDENED CONCRETE

In this section, we use ultrasonic test to characterize property of hardened concrete. Properties of waves are influenced from mechanical properties of material where they trough on. Elastic compressive and shear module influence the velocity, and also the micro structural nature modify frequency contents of waves, resistance of material could be related with some wave properties.

One part of this research lead to individuate possible relationship between the mechanical break stress of concrete and features that come from ultrasonic tests.

A campaign of test has been conducted on a stock of 72 specimens of concrete, formed form different cast in some workplace close with university of Palermo.

Specimens considered are cubic with 150mm of side. For each cube, the test is been conducted in two steps. Before the ultrasonic test and forward a press test are conduced.

Before start the study of each specimen, in a preliminary steps, each selected cube for the study is weighted, measured, and classified by a identification code.

5.3.1 THE NDT TEST

The ultrasonic test consist in a two non destructive tests, using the *Pro-Pulser* machine and two probes. The two tests are conducted in transparency, in the two orthogonal direction of the specimen cast. The specimen is settled in an special frame, in the basis of the specimen a bed of solid foam in posed in order to isolate the specimen from the neighboring environment. Forward the two opposite surfaces are cleaned and wetted to prepare a smooth surface, the centre of each face is individuated and on each of two probes a gels is applied, the probes are applied to the specimen, and two plates pull by springs the probes against the specimen. The objective of the spring is to conduct the test in almost the same stress contact conditions for the interface probes/concrete.

After to set the specimen in the system, some ultrasonic tests are conducted to check quality of signal, probes are better settled to improve tests. The software is settled in acquisition mode and a range of ultrasonic narrowband sinusoidal waves in sent and detected form the specimen. The investigated frequency are form 50KHz to 500KHz with steps of 5KHz. The signal is a 10cicle sinusoid. To reduce environmental and electrical noise, each signal is detected 50 times with a delay of 150ms between two acquisition to be sure that the previous excitation is completed. In post processing the 50secord of the same frequency are averaged. The level of amplitude of acquisition signal is settled so low to maintain low the level of noise, but also with enough power to record a clean signal.

In the table 5.11 details of test are reported.

Investigate freq.	50-500 kHz
Steps	5 kHz
N steps	90
Delay	150 ms
amplitude	20-22-25-30 dB
N signals for freq.	50
Duration of test	12 minuts
$f_{playback}$	25Msps
N clycle	10 sinusoids

Table 5.11 Set of test

At the end of the test in one direction, the specimen is rotated of 90degree and the test is repeated in the horizontal orthogonal direction.
In some tests, because the specimen have some imperfection, or signal detected are not reasonable valuable, the tests are been repeated. In some other cases, the investigated frequency was stopped to 300Khz, cause a strong dissipation of material, any signal for further frequency travel trough the material.

5.3.2 COMPRESSION TEST

The specimen in now conducted at the press machine, it is a standard press *Control pilot 4 -3000KN*, the specimen is settled in the plates, and the load is going to increase with a speed of 5N/sec according with the UNI EN 12390-3, (loading speed 50N/cm^2 sec) conventionally it is assumed that specimen is break if deformation is more of 5%. The final load is recorded.
The compression test have a duration of few minutes. The break load is divided by the area cross section for determine break tension.

5.3.3 DATA PROCESSING

The data acquired by using ultrasonic devices are processed using a Mat Lab algorithm. The algorithm, which principles are described in chap 4, analyze signal in space time and in frequency time. The principal features are deducted.

Average of signals

The signal are in digital format, a mean is operated with the ones at the same frequency, in this way systematic errors, and noise are reduced.

$$s(t_k) = \frac{\sum_{i=1}^{n} s_i(t_k)}{n} \text{ for each k} \tag{5.1}$$

Forward, to eliminate also possible continuous electrical component an average of signal is operated and the signal in translate at this mean.

$$\mu = \frac{\sum_{k=1}^{m} s(t_k)}{m} \qquad S(t_k) = s(t_k) - \mu \tag{5.2}$$

The first analysis in time space lead to deduct, time of fly of signals, the amplitude of signal, and duration.

Time processing

Time of fly is relevant because considering an uniform velocity of the wave, it is possible, known the distance between the probes, to determine the speed.

$$V = \frac{d}{t_{fly}} \tag{5.3}$$

It is worth to observe that signals are digital, it means a vector of value acquired in multiple $\Delta\tau$ of the playback time. So the algorithm lead to determine the number

N of registration where we consider that signal is arrived at the receiver probe, this value times $\Delta\tau$ correspond at the time of fly.

$$t_{fly} = N\Delta\tau \tag{5.4}$$

The determination of N is operated using a function called *cross correlation.* A signal with the same shape, frequency e duration of the input signal is digitally generated $b(t_k)$, and starting from the beginning of registration $S(t_k)$ it is translated until the product between the two signal become max.

$$\max_j [b(t_k + t_j)S(t_k)] \tag{5.5}$$

In time space it also deducted the amplitude of the signal, and the ratio with the noise, to evaluate the validity of registration.

Frequency analysis

The signal is windowed by deduction its duration. This window of signal is processed by using Discrete Fast Fourier Transform (here in after DFFT) function. From the DFFT the norm form real and imaginary component is operated, and, for each frequency (means for each averaged signal) are deducted the follow features. The amplitude of the DFFT of the output signal at the play frequency of the input signal The amplitude of the max of DFFT of the output signal and the frequency from what this maximum is located.

So if the test was worth, the two value were correspondent, in some other cases, when the two value are not the same, was notable to investigate what was going on. The more common aspect were the presence of high noise, a worse settled of probes, or a incapacity of the frequency component of wave to travel though the material.

A digital signal $b(t_k)$ used as baseline is generated, at the same frequency of the input signal, and on it DFFT is operated, and the value of DFFT a the play frequency is detected.

The acquired signal is affected of different effect as the pressure of probes to the specimen, and to the capacity of gels to transmit or attenuate signals. In order to normalized signal deducted from experimental setting affected of these problem, a normalization of the DFFT is operated. The observed feature is an index deducted as ratio between the output DFFT from recorded signal and DFFT from baseline signal.

$$I_{\omega} = \frac{\max\limits_{output}(DFFT[S(t_k)])}{\max\limits_{baseline}(DFFT[b(t_k)])} \tag{5.6}$$

5.3.4 CONSIDERATIONS

Firth of all, it is relevant to report for each frequency the length of ware λ, relation between length and frequency are related with the wave speed.

$$\lambda = \frac{f}{V} \tag{5.7}$$

In order to give ad average value of each wave length for each frequency, 3 different velocity are considered 4000-5000-4000 m/s, in table 6.2 are reported, for each speed frequency and wave length.

Frequency [kHz]	λ **[mm]**		
V [m/s]	6000	5000	4000
50	120	100	80
100	60	50	40
150	40	33	27
200	30	25	20
250	24	20	16
300	20	17	13
350	17	14	11
400	15	13	10
450	13	11	9
500	12	10	8

Table 5.12 Wave frequency and length at each wave velocity

It is observed, that the wave velocity decrement if the signal frequency is increasing. As shown in chart 5.24, the decreasing of velocity is relevant for the low frequency (50-200kHz) and become more smooth at the high frequency(>200kHz).

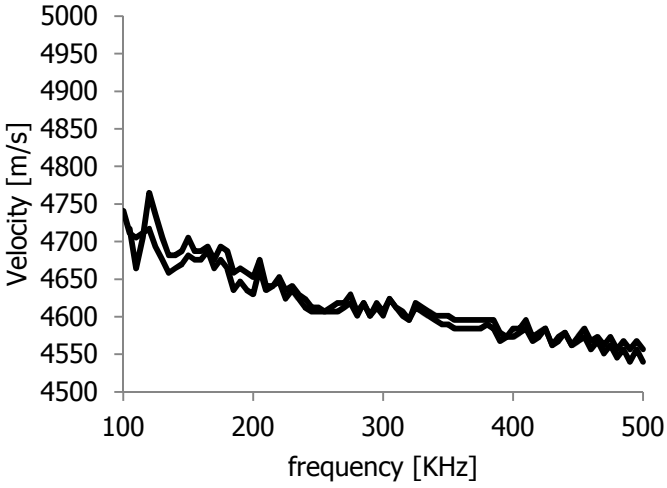

(a)-Rc=68MPa V=4696 m/s

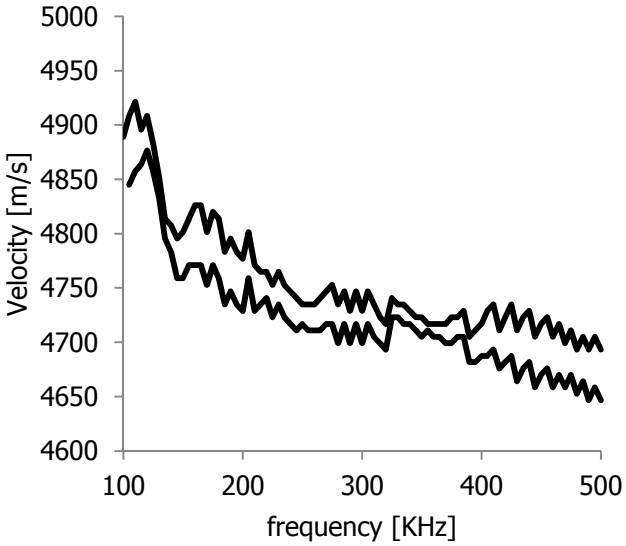

(b)-Rc=38MPa V=4705 m/s

figure 5.24 Velocity and frequency of ultrasonic test

For the choose of a speed wave to attribute at the specimen, a criteria used consider also the frequency analysis.

Since form the procedure before described, a result for a direction in a specimen is reported. Chart 5.25 is shown the baseline max DFFT for each frequency, it is wide that at the same number of cycle, signal with high frequency have less energy because less duration, and so the max DFFT go to decrease with the increasing of frequency. Figure 5.26 report the trend of max DFFT for each frequency in a specimen, and figure 5.27report the trend of the index I_{ω}.

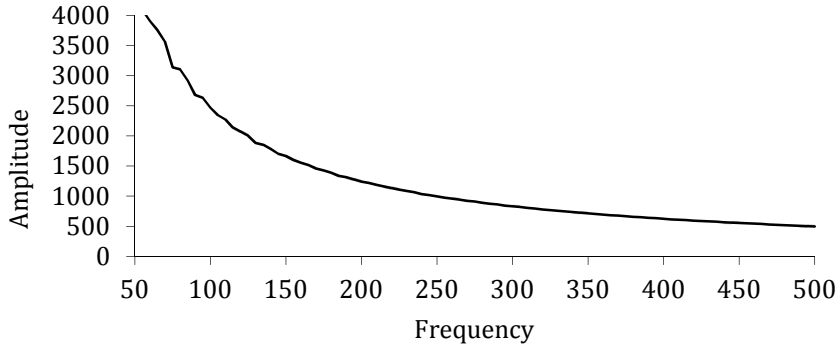

Figure 5.25 Max DFFT of baseline

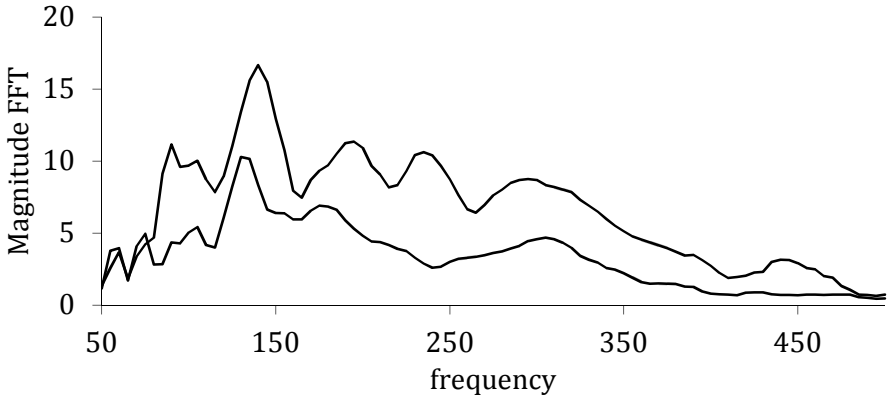

Figure 5.26 Max DFFT of the output signals

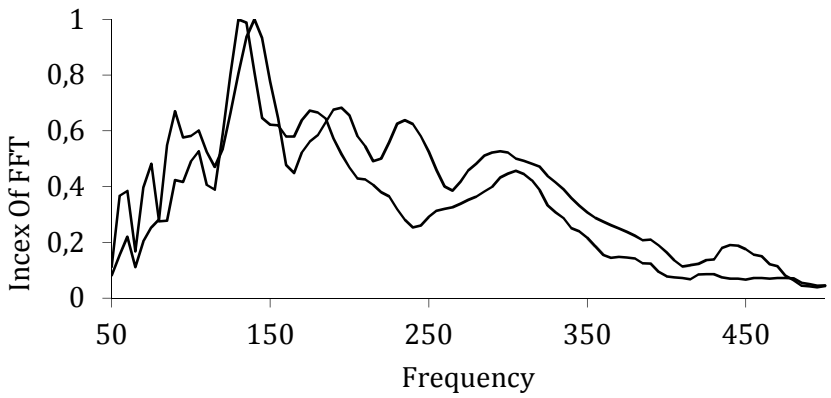

Figure 5.27 I_{ω}

It is relevant to note that shape of the curve reported in 6.2b, and follow 6.2c denote a maximum value for an intermediate frequency, if we look at two signal one before or after this frequency, and the signal at this frequency, we note that amplitude of it is quite increased respect the others amplitudes. It look like a resonant phenomena for the material at that frequency, this frequency is here defined *resonant frequency*.

In order to choose a signal for assume a nominal velocity of ultrasonic wave test, it is wide assumed the velocity of resonant frequency wave as reference. In this way time and frequency space are related, and one analysis cannot be conducted with the aid of the other one.

The specimen that are analyzed are reported in the table 6.3, for each specimen, in the other column are reported the nominal velocity of ultrasonic wave, and the resonant frequency deducted for the two orthogonal directions.

Number	Prot. tests	Resistance MPa	Freq 1 KHz	Freq 2 KHz	V 1 m/s	V 2 m/s
1		59	290	220	4.518	4.568
2		52	220	280	4.454	4.433
3		49	230	250	4.422	4.366
4	prot 442	61	300	320	5.216	4.618
5	prot 442	56	260	280	5.068	5.047
6	prot 442	46	255	235	4.808	4.789
7	prot 442	56	230	280	5.123	5.034
8	prot 442	56	320	335	5.123	5.047
9	prot 442	46	225	185	4.777	4.826
10	port 448	38	175	210	4.417	4.257
11	port 448	40	255	235	4.271	4.300
12	port 448	43	225	225	4.507	4.573
13	port 448	25	210	225	4.315	4.335
14	port 448	34	200	165	4.310	4.401
15	port 448	58	280	240	4.448	4.381
16	port 448	32	210	170	4.213	4.266
17	port 448	55	240	280	4.502	4.557
18	prot 452	49	255	225	4.607	4.590
19	prot 452	53	330	270	4.771	4.771
20	prot 452	52	305	215	4.568	4.562
21	prot 452	56	290	225	4.747	4.814
22	prot 452	41	210	230	4.551	4.647
23	prot 452	52	360	340	4.765	4.688
24	prot 452	45	300	250	4.759	4.814
25	prot 452	52	270	255	4.723	4.789
26	prot 452	53	280	215	4.723	4.682
27	prot 452	39	205	270	4.590	4.464
28	prot 450	42	195	235	4.596	4.573
29	prot 450	53	325	210	4.741	4.601
30	prot 450	40	215	310	4.562	4.618
31	prot 450	62	350	240	4.802	4.759
32	prot 450	56	345	190	4.896	4.902
33	prot 450	44	335	320	4.291	4.350
34	prot 450	52	390	390	4.573	4.557
35	prot 450	55	265	345	4.808	4.864
36	prot 450	45	290	320	4.529	4.502

37	prot 450	47	320	300	4.607	4.545
38	prot 446	45	265	280	4.584	4.562
39	prot 446	45	185	200	4.454	4.391
40	prot 446	40	185	210	4.315	4.355
41	prot 446	43	260	210	4.335	4.261
42	prot 446	36	190	245	4.613	4.529
43	prot 446	35	200	185	4.340	4.366
44	prot 446	49	185	280	4.624	4.601
45	prot 446	49	285	235	4.534	4.459
46	prot 446	43	190	270	4.396	4.524
47	prot 446	49	280	240	4.676	4.573
48	prot 446	33	250	225	4.237	4.345
49	prot 456	38	240	365	4.747	4.705
50	prot 456	57	225	175	4.157	4.315
51	prot 456	66	270	250	4.496	4.491
52	prot 456	68	370	340	4.596	4.596
53	prot 456	**85**	310	300	4.376	4.371
54	prot 456	61	225	225	4.557	4.557
55	prot 456	67	400	355	4.688	4.653
56	prot 444	48	255	310	4.480	4.584
57	prot 444	36	185	240	4.433	4.310
58	prot 444	43	185	255	4.350	4.486
59	prot 444	44	170	225	4.475	4.647
60	prot 444	48	315	290	4.391	4.422
61	prot 444	50	245	230	4.443	4.607
62	prot 444	49	190	225	4.630	4.529
63	prot 444	48	235	225	4.491	4.391
64	prot 444	39	225	210	4.300	4.190
65	prot460	54	270	255	4.641	4.705
66	prot460	50	225	250	4.601	4.653
67	prot460	58	185	185	4.771	4.771
68	prot460	57	240	345	4.889	4.921
69	prot460	52	225	280	4.795	4.876
70	prot460	54	185	320	4.607	4.693

Table 5.13 Resistance specimen velocity, resonant frequency for the two directions

It is notable, that ultrasonic velocity in the two direction are enough close, few differences are related with the algorithm.

The precision of the measure of velocity can be evaluated by the evaluation of the influence of number of sample in velocity:

$$V = \frac{d}{T} = \frac{d}{n\Delta\tau} = \frac{d}{n\frac{1}{f_p}} = \frac{d\ f_p}{n} \tag{5.8}$$

$$\frac{\partial V}{\partial n} = -\frac{d\ f_p}{n^2} \tag{5.9}$$

$$E\% = (\frac{\partial V}{\partial n}) / V = (-\frac{d\ f_p}{n^2}) / (\frac{d\ f_p}{n}) = -\frac{1}{n} \tag{5.10}$$

Where d is the distance between probes, n is the number of sample, $\Delta\tau$ is the time step, f_p is the playback frequency. The error on V, decrease with the increasing of n. In our range, with f_p =25Msps, d=0.15m, n=800, a simple correspond an a error in term of velocity of 5 m/s, this is less that 0.2% of velocity.

The dates are reported in the chart 5.28 with resistance and velocity in the respective axes, diamonds and circles are related with the two direction. The data are align in a line. Equation of line was determined using a minimum square method, and it is:

$$\sigma(V) = aV + b \tag{511}$$

With a=9.53 and b=4113, R=0.17, it is clear that data are so dispersive in the chart, however there is a tendency to be close with the line. R is so low.

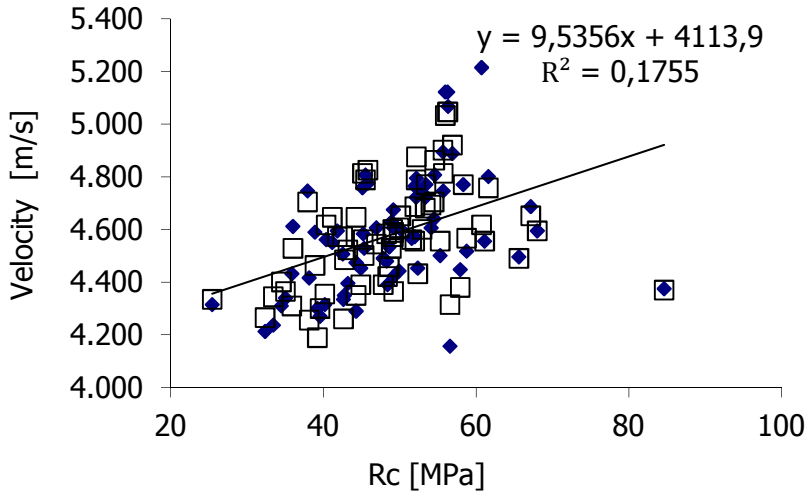

Figure 5.28 Velocity –resistance relationship

(diamonds and square are related with two orthogonal direction)

As Before, in an analog chart, the #5.30, it is been reported the resonant frequency. The data from resonant frequency are more dispersive, moreover, test with the two direction often give different resonant frequencies, a minimum square interpolation has been conducted, choosing a linear relationship, the parameters are a=1.76, b=169.66, R=0.11,

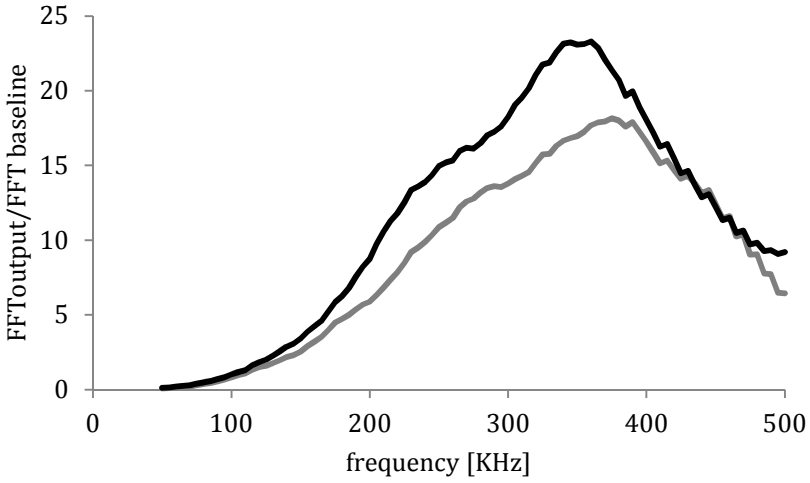

(a) Rc=68MPa – freq 370-340KHz – non normalized FFT

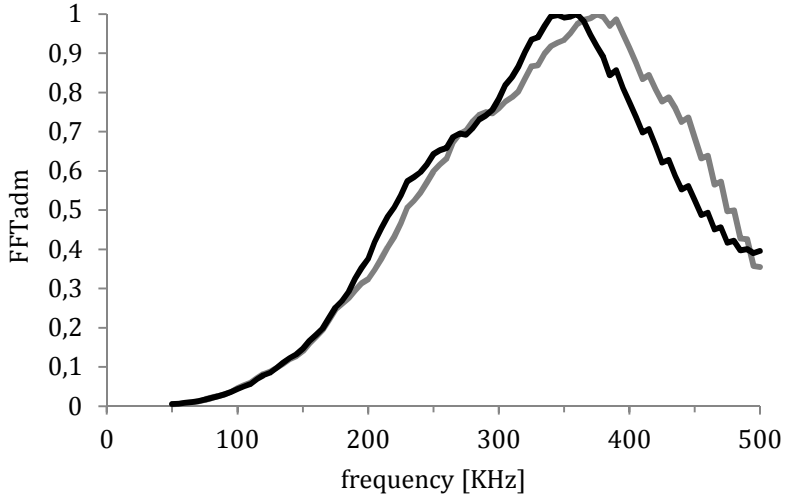

(b) Rc=68MPa – freq 370-340KHz –normalized FFT

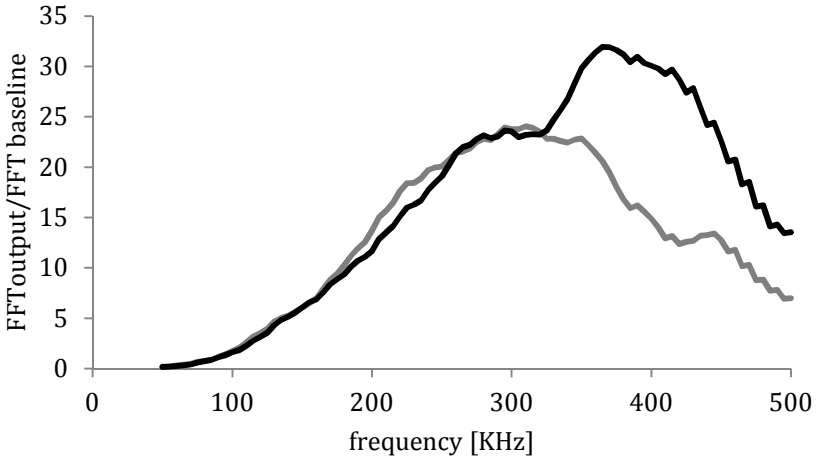

(c) Rc=38MPa – freq 240-365KHz – non normalized FFT

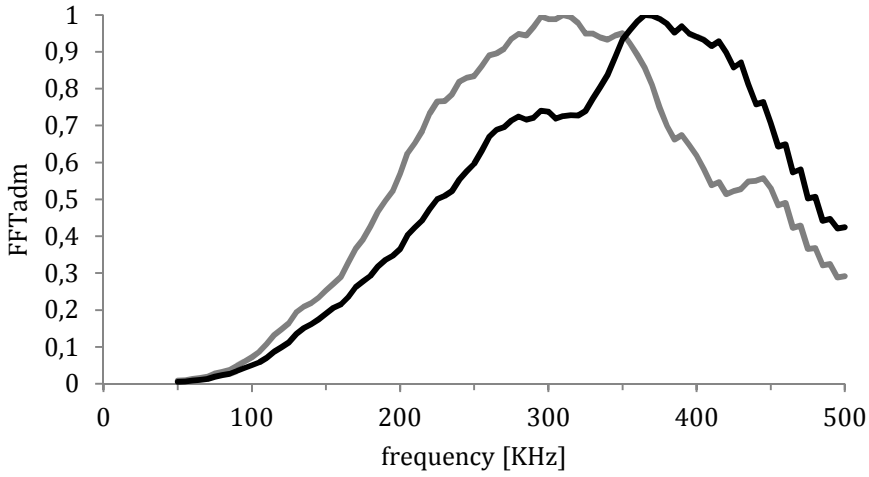

(d) Rc=38MPa – freq 240-365KHz –normalized FFT

Figure 5.29 FFT and Iω index for two different specimen, in the two directions

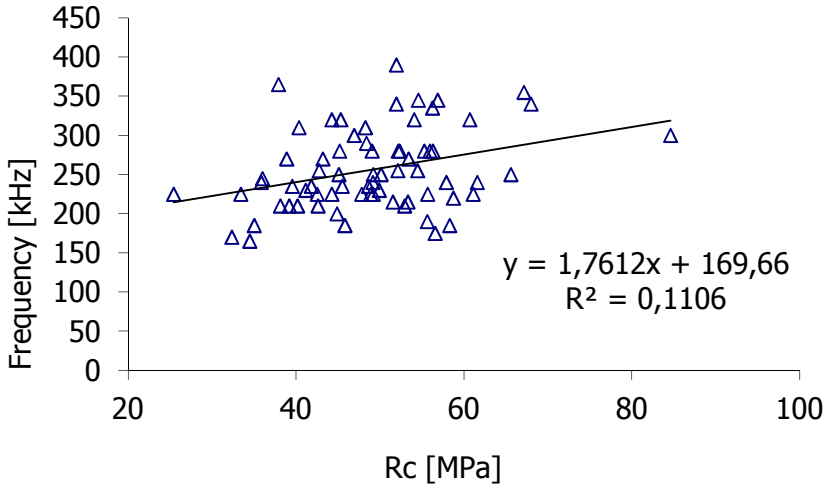

Side A

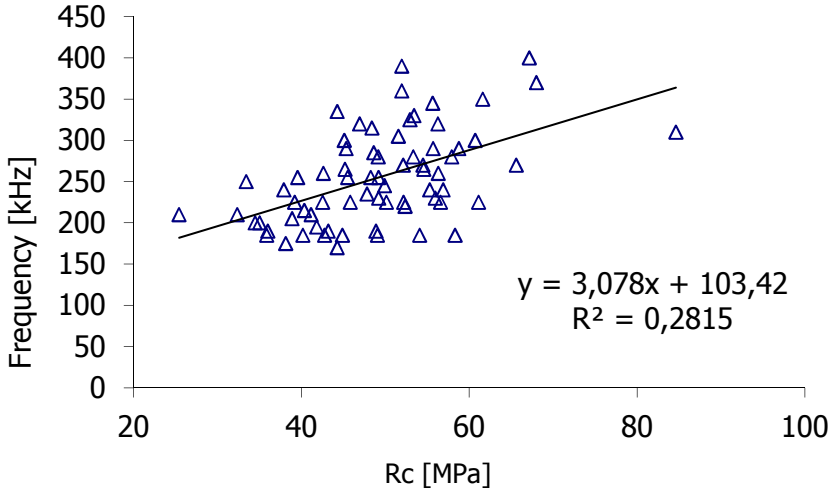

Side B

Figure 5.30 Resonant frequency–resistance relationship

Observing these data, it is wise that any relation can be strongly deducted to know with a certain security level information from resistance by starting from resonant frequency or velocity, this because the correlation between the phenomena of resistance and the ultrasonic features are low related. It is notable, that the propagation of waves in media, are related with the elastic property of the media, also if the media is heterogeneous, the elastic properties of each component participate at the propagation with different act. The nature micro structured of this kind of solid produce still unknown phenomena during the propagation of wave. The theory of the description of this behavior, is not done. In this work one of the objective was to understand if resistance are able to influence wave propagation features. Observing the two charts, it is wide accepted that the correlation is so low that any prediction can be deducted on the resistance by the use of a ultrasonic test. nevertheless an ultrasonic test can be give information on the nature of material that is tested.

It was observed, by visual inspection a different behavior in dependence of the compactness of material. In the specimen were compact, and heavy, usually the resonant frequency in the two directions were close below a certain errors, and also the value of they was high, if the concrete is presented with worst characteristics, as surface porosity, low weight, the resonant frequency measured in the two direction are spreader, and with low values, and high frequency wave were not able to pass though the material and reach the receiver.

Also if we give a look on the amplitude/frequency curve, in the two cases, we observe that when the material is compact, the curve have a bell shape, with one peach, when material is worse, the curve, is a bell with more peaches, often with close amplitude values.

To support this behavior, two specimen are considered. By visual inspection one is with more pores and the other is more compact. To view how each cube is inside, they were been cut in a middle plane. Figure 5.31 report pictures of them.

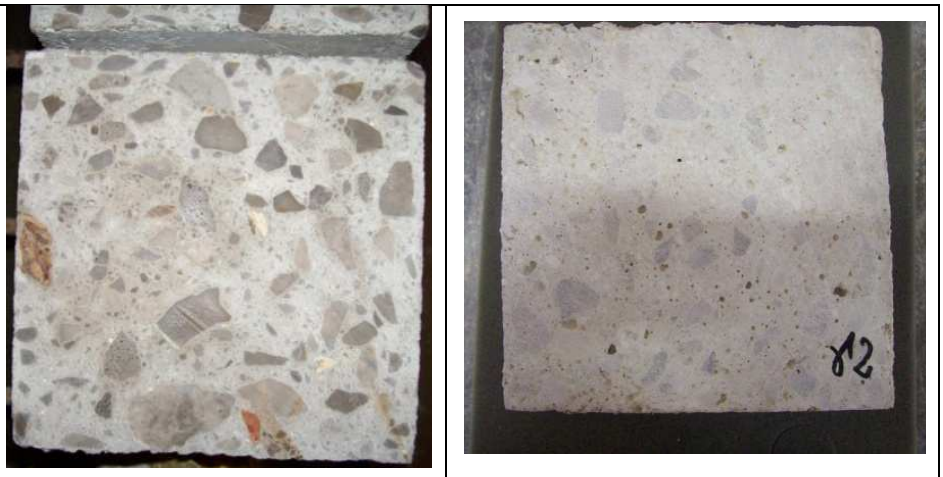

Good quality concrete	Worse quality concrete

Figure5.31 Transversal cross section of concrete specimen

In the specimen with low quality, it is possible to observe a strong dispersion of porosity, and the aggregate have small diameters, it have a weight of 7.73 Kg. In this specimen only a low range of frequency was possible to investigate, form 50 to 300 kHz, signal was not able to travel in material for the other high frequencies. The concrete with good quality is more compact, it is also well constipated, the weight is 7.95 kg.

In chart 5.32 are shown the I_{ω} index in relation with the frequencies. It is possible to observe that the good concrete have a more smooth curve, and the peak is in high frequency, the worse concrete have more peaks, at the low frequencies.

Good concrete	Worse concrete
f=270-350kHz	f=200-60KHz
V=5006 m/s	V=4162 m/s
7.95kg	7.73kg
Big aggregates	Few small aggregates
High compactness	High porosity

Table 5.14 NDT results on concrete

In agreement with the proposed model:

The increase of the percentage of the aggregate speed grows.

To increase the size of the aggregates the resonance frequency increases.

The pattern of frequencies is close to the model A, with low% of aggregates specimen.

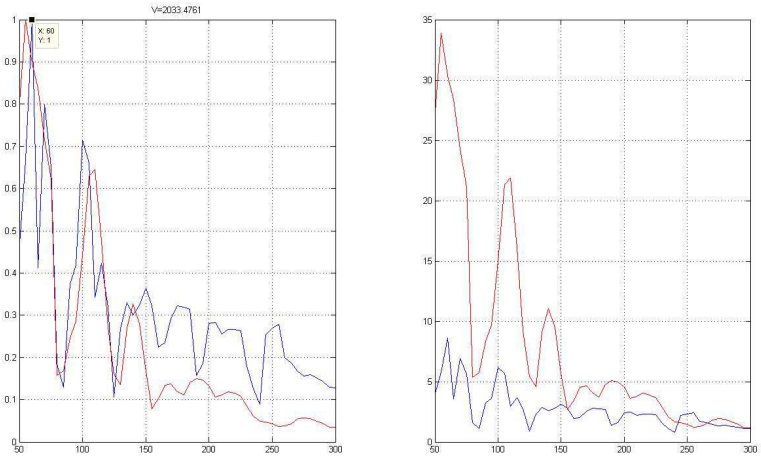

(a)

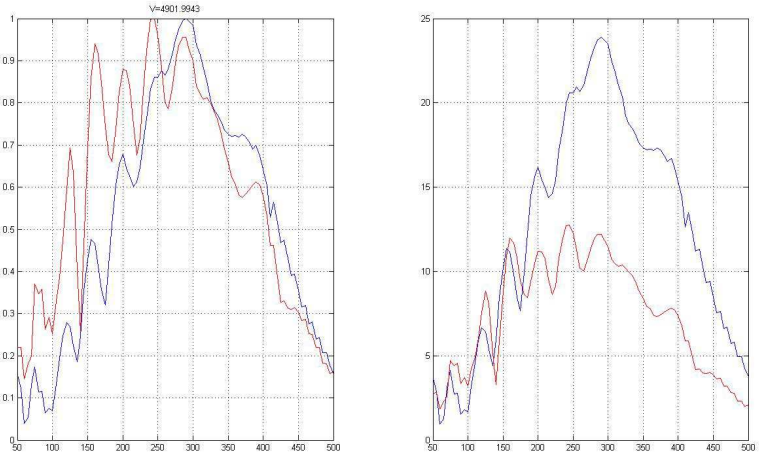

(b)

Figure 5.32 I_{ω} Index for good and worse concrete.
(a) Worse quality concrete (b) Good quality concrete

5.3.5 CLUSTERING

Clustering is one of the more common method used for describe how data are aggregates by relationships between parts of them. The goal of clustering is descriptive. However if a new data in considered it is relevant to qualify if it appertain to one or another group or if it is element for a new group.

It is given a data set $G = \{x_1, x_2, ...x_n\} \subset R^p$. It need to establish how parts of these data are close each others. To clustering these data in c parts, it is need to minimizing the functional:

$$\Im = \sum_{i=1}^{c} \sum_{j=1}^{n} {u_{ij}}^m d_{ij} \tag{5.12}$$

Under the condition that $\sum_{i=1}^{c} u_{ij} = 1$ for all j=1...n

So u_{ij} is called membership degree of the data object x_j at the cluster i, it indicate how much the element x_j is related with the cluster i.

$d_{ij} = \left\| x_j - v_i \right\|^2$ denote the square Euclidean distance between data vector x_j and the prototype $v_i \in R^p$ representative of the cluster i.

m indicate how much the cluster are overlapping.

In the first step the prototype are chosen randomly, usually an element of the set is chosen as first prototype.

The strategy used to clustering some data is an iterative one.

Starting from data set, a number of cluster c is fixed, and c prototypes are chosen randomly, if k is an index that run on cluster, the first membership value are obtained by:

$$u_{ij} = \frac{1}{\sum_{k=1}^{c} \left(\frac{d_{ij}}{d_{kj}}\right)^{\frac{1}{m-1}}} \tag{5.13}$$

Where d_{ij} and d_{kj} are respectively Euclidean distances of element x_j from each cluster prototype v_i.

After to calculate the relationship coefficient, the prototype is defined as:

$$v_i = \frac{\sum_{j=1}^{n} u_{ij}^{\ m} x_j}{\sum_{j=1}^{n} u_{ij}^{\ m}} \tag{5.14}$$

The scheme is repeated until distance between two follow prototype are so quite related with a threshold level.

To understood how the method work a numerical example is reported in table 5.17. A set of 9 number is reported: [1,2,3,4,10,11,12,13,14] two cluster are chosen, and the first prototype are fixed at the value 2.1 and 12.5, the distances of each element from each prototype are determined and reported in the V and VI column, so the membership coefficient are determined in the VII and VIII column, sums are reported in the before last row, and the new prototype are computed, in the columns IX and X the numerator of v_i are reported. In the last row the new prototype are computed. If they are substituted at the place of the fists tentative prototype they will be more close with the final.

		$\mathbf{v_1}$	$\mathbf{v_2}$						
#	**Elem.**	**2,1**	**12,5**	$\mathbf{d_{1,j}}$	$\mathbf{d_{2,j}}$	$\mathbf{u_{1,j}}$	$\mathbf{u_{2,j}}$	$\mathbf{u_{1,j}^2 X_j}$	$\mathbf{u_{2,j}^2 X_j}$
1	1	2,1	12,5	1,21	132,25	0,991	0,009	0,982	0,000
2	2	2,1	12,5	0,01	110,25	1,000	0,000	2,000	0,000
3	3	2,1	12,5	0,81	90,25	0,991	0,009	2,947	0,000
4	4	2,1	12,5	3,61	72,25	0,952	0,048	3,628	0,009
5	10	2,1	12,5	62,41	6,25	0,091	0,909	0,083	8,262
6	11	2,1	12,5	79,21	2,25	0,028	0,972	0,008	10,401
7	12	2,1	12,5	98,01	0,25	0,003	0,997	0,000	11,939
8	13	2,1	12,5	118,81	0,25	0,002	0,998	0,000	12,945
9	14	2,1	12,5	141,61	2,25	0,016	0,984	0,003	13,565
						4,07	4,93	9,652	57,122
								2,369	**11,594**

Table 5.17 Numerical example of cluster data

If data are signals, it can be helpful to measure how the signals are related each others. A mathematical tool to measure how two signal are related is the Pearson correlation coefficient, if this coefficient is 1 the two signals are equal, if it is zero the two signals are so different.

By start with a digital recorder we can call $X=\left[x_1, x_2 \ldots\ldots x_n\right]$ and $Y=\left[y_1, y_2 \ldots\ldots y_n\right]$ the two signals, for each of them the averages $\mu_x=\mathrm{E}[\mathrm{X}]$ and $\mu_y=\mathrm{E}[\mathrm{Y}]$ and the standard deviations σ_x and σ_y can be calculated.

Pearson coefficient is defined as:

$$\rho_{X,Y}=\frac{E[X-\mu_x]E[Y-\mu_y]}{\sigma_x\sigma_y} \tag{5.15}$$

The Pearson distance so can be define the complementary to 1 of the pearson correlation:

$$d_{P,X,Y}=1-\rho_{X,Y} \tag{5.16}$$

In this way if data are perfectly correlated $\rho_{X,Y}=1$ and $d_{P,X,Y}=0$ it is 1 in the other cases.

5.3.6 THE DEVELOPED ALGORITHM OF CLUSTERING

Starting form data that are available in the campaign on hardened concrete, an fuzzy cluster algorithm was implement to verify if it possible to collect data with similar resistance in the same set. Data are processing by follow the described steps.

For each cube, at for each direction a new signal is greater. The signal is a ordinal collect of DFT of all frequency that are sent to that direction of cube.

From each direction of cube a set of signal with central frequency between 150 and 300KHz in steps of 10KHz is transformed by DFT. The DFT curves are reproduced in term of decibel amplitude:

$$db_{\varpi_j}(\omega)=10\log(DFFT) \tag{5.17}$$

These curves are normalized , by setting the max value to zero db, and to threshold the signal if if go below the -50db. In this way, al the curves are standardized.

After all the 16 DFT in decibel scale, are settled in relation at the increasing frequency close one forward the other, to create a signal of 16 curves of DFT.

Form all these signals a cross correlation is conducted between each others, in order to measure the Pearson correlation factor. This index is a measure of how much the two curves are close or far from a similar shape. If the ρ coefficient is equal to 1 it means the two signals are equal, zero if they are different.

The distance between two signal that mean two cubes is measured as:

$$d_{ij} = 1 - \rho_{ij} \tag{5.18}$$

If ρ =0 so d=1 and they are far away, if ρ =1, so d=0, and they are equal.

In cluster procedure is need to fix the prototype, is this sense the number of cluster is chosen equal to 4, so 4 random elements from the population are chosen as prototype, the algorithm is able to update the prototype value in order to individuate the *centroid* of cluster.

By using an iterative procedure, the membership index to each cluster each data is determined. After to verify the convergence of the procedure it is possible to have for each element of the population a 4 dimensional vector that indicate, in each component the degree of appurtenance at each cluster.

It is need now to associate a resistance at each cluster. The resistance at each cluster is associated with the same modality how is the prototype is defined, as weighted resistance of all element resistances by membership value for each the cluster of each element.

To measure the performance of my clustering, but also in order to define a procedure that permit to classify a new data, a random data form the population is chosen. The associate resistance at this element is given by considering the relationship vector of this element, to each cluster a resistance in associated, and

so the resistance of the considered element will be an weight average of the resistance of all cluster by the membership coefficients.

$$R_{i,\,forecast} = \sum_{k=1}^{Ncluster} R_{ki} u_{ki} \tag{5.19}$$

In this way the resistance with the cluster with high membership coefficient is more close with the value of the element considered, but a little contribute from far clusters is also considered.

This testing procedure was conducted for all data of the population and because of each of them it is know the real resistance, it is possible to measure how the method is able to predict the right value, by the follow expressions:

$$\Delta R_i = R_i - R_{i,\,forecast} \tag{5.20}$$

This value will be zero if fore cast will be all right, and as much higher as the method is out of prevision.

By doing this evaluation, it is obtain an zero average on the population prevision, and a standard deviation equal to 6N/mm^2.

Some tests on data are conducted, the elements are divided in group in relationship at the workplace origin.

For each group of elements, it is determined the average resistance of the casting determined by breaking load of specimen and ultrasonic tests.

In the table 5.18 are reported the different resistance between the two procedures, average measured resistance and predicted ultrasonic resistance

Casting	N specimen	ΔR_m
Prot 442	4-9	0.8
Prot. 448	10-16	1.7
Prot. 452	17-26	2.6
Prot. 450	27-36	1.4
Prot. 446	37-47	2.8
Prot. 456	48-53	-7.8
Prot. 444	54-62	1.5
Prot. 460	63-68	-6.3

Table 5.18 Differences of forecast resistance and measured resistance

There is another set of data were ultrasonic tests and destructive test were conducted. These data are not still used for the definition of the cluster classes. They are used to predict resistance value, after to kwon the resistance break load. For these ones, it is verified the average measured resistance equal to 47.7 MPa, and the predicted resistance by mean of ultrasonic wave it is 47.3 MPa, it is appreciable that the difference of predicted value and measured value is 0.5 MPa.

Another method to attribute a resistance in a cluster was implemented and proposed. It lead to fix a threshold on the membership coefficients. For each element it is considered only the maximum of membership. If the value of maximum is upper an a certain threshold, the element become part of a cluster, it is excluded what else, in this way some outlier data can be deleted from the evaluation.

After to individuate the elements that are part of the same cluster, the cluster resistance is determined by a weighted mean of resistance of element.

$$R_k = \frac{\sum_{i=1}^{Nk} u_{ki} R_i}{\sum_{i=1}^{Nk} u_{ki}} \tag{5.21}$$

In this way a more performing value of resistance is given at the cluster. In testing procedure of the cluster.

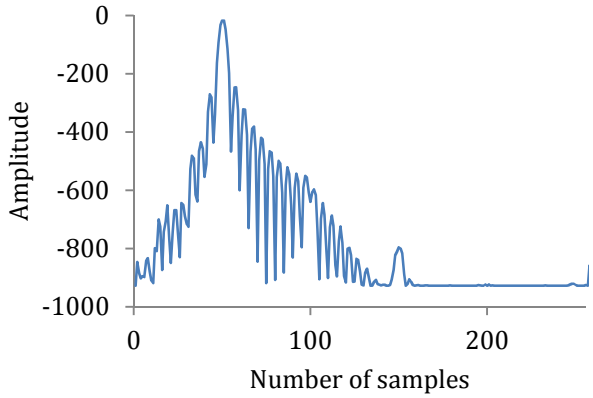

Figure 5.33 Single Signal proposed for clustering analysis

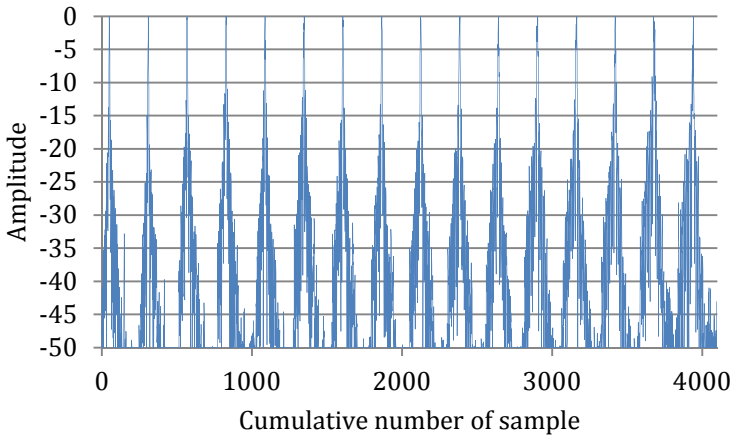

Figure 5.34 Average error of population in clustering analysis

5.3.7 CONSIDERATIONS ON CLUSTERING METHOD APPLIED

By the mean of clustering method is possible to forecast resistance of concrete specimen, using ultrasonic NDT techniques with an error, in our case of 6N/mm^2. We know that is not the best method that is applicable to a prevision of resistance, but it consent to classify a concrete in a class of resistance. Form the same data, if it is deducted the standard deviation of measure resistances of the population, it is verify that it is equal to 9.66 N/mm^2 in less more than the valued deducted by the clustering.

In appliance of Italian Rules, by using the average resistance it is possible to deduct the characteristic resistance as:

$$Rck = Rm - 8N / mm^2 \tag{5.22}$$

This indicate that from the average value the characteristic value is 8 MPa below, as value in which the 95% of specimens are break upper this value. Also if this value is not related with standard deviation of resistance, it is possible to admit a normative error of 8N/mm^2 more that the proposed error of 6MPa.

5.4 MODELLING OF WAVES IN HETEROGENEOUS MATERIALS

A wide instrument for the understanding the behavior of heterogeneous materials below the excitation of ultrasonic wave, is the numerical modeling. The modeling of heterogeneous materials is pretty difficult if you consider the special distribution of the parts that constitute the materials.

In order to create a model representative of the heterogeneous nature of concrete, the numerical models are implemented, with some differences distribution of inclusion in an homogeneous boarded field.

The 3 FEM models are related on a square section of the specimen with 150mm of side, with inclusion of different sizes or distribution .

In the follow three table 5.19-20-21 the characteristics of each mesh are reported

MODEL A	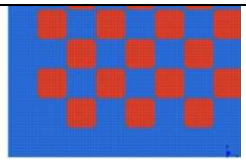	mm^2
Total surface	150x150	22500
Side of inclusion	5x5	25
Numer of inclusion	14rows x 14	196
Inclusion area	196x25	4.900
Matrix area	22.500-4.900	17.600
A inclusion/Atot	4.900/22500	21.17%
Ainclusion/Amatrix	4.900/17.600	27.84%

Table 5.19a: Property of model A

In CENTRAL LINE			
D total		150	
L inclusion	14x5	70	46.6%
L matrix	150-70	80	53.3%

Table 5.19b: Characteristics of model A in central line

MODEL B	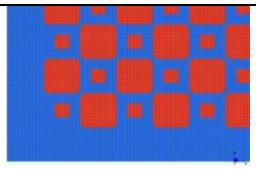	mm^2
Total surface	150x150	22500
Side of inclusion	5x5	25
	2x2	4
Numer of inclusion	14rows x 14	196
	14 rows x14	196
Inclusion area	196x25	4.900
	196x4	784
Tola inclusions		5.684
Matrix area	22500-5.684	16.816
A inclusion/Atot	5.684/22.500	25.26%
A inclusion/A matrix	5.684/16.816	33.80%

Table 5.20a Property of model B

In CENTRAL LINE			
D total		150	
L inclusion	14x5	70	
	14x2	28	
Total		98	65.3%
L matrix	150-98	52	34.7%

Table 5.20b: Characteristics of model B in central line

MODEL C	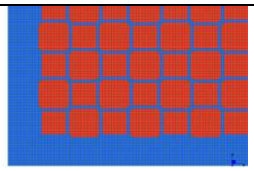	mm²
Total surface	150x150	22500
Side of inclusion	5x5	25
	4x4	16
Numer of inclusion	14rows x 14	196
	14 rows x14	196
Inclusion area	196x25	4.900
	196x16	3.136
Total inclusions		8.036
Matrix area	22.500-8.036	14.464
A inclusion/Atot	8.036/22.500	35.71%
Ainclusion/Amatrix	8036/14.464	55.55%

Table 5.21a Property of model C

In CENTRAL LINE			
D total		150	
L inclusion	14x5	70	
	14x4	56	
Total		126	84.0%
L matrix	150-126	24	16.0%

Table 5.21b: Characteristics of model C in central line

The mesh dimension is 0.5mm, according with the maximum value of investigated frequency.

If V is the velocity of wave, it can be measured in a range between 4000 and 6000m/s, the minimum length of wave, to follow the table 6.2,will be, in function of

the maximum frequency 8mm, the dimension of mesh need to be $d = \frac{\lambda}{16}$, and so d=0.5mm.

If the maximum signal frequency had a 500kHz, it means that period T=1/500.000=2 μ sec, in order to have a good discrete signal, in each period is need a 10 value of signal, in that way, it is assumed a $\Delta\tau = 0.2\mu\,\text{sec}$ and a corresponding playback signal frequency of $fp = \frac{1}{\Delta\tau} = 5Msps$

In order to reduce simulation data, in the dynamic linear direct analysis, the simulations are saved each two steps, that means that the output signal will be a $\Delta\tau = 0.4\mu\,\text{sec}$ and a playback frequency of 2.5Msps.

The simulations are conducted applying a set of nodal forces at the left side of the square model. The probe had a 60mm of diameter, and the nodal force are applied in 121 nodes.(60x0.5). In the opposite side the central axial node is restrained with a fixed hinge (dx=0 dy=0), and the others 120 nodes are restrained only for the horizontal translation (dx=0), the response is detected on 51 nodes, for a length of 30mm, the result signal is obtained operating an average on the 51 displacement responses.

Simulations are conducted by fixing the elastic properties of inclusions, E=100GPa, and v=0.12. and varying matrix modulus in 4 steps 12.5- 25- 37.5- 50 GPa, in these way the ratio $E_{inclusion}/E_{matrix}$ are respectively shown in the table 5.22, also an homogeneous case is analyzed, using a elastic module of 100GPa.

	E1	**E2**	**ratio**
1	100	50	1:2
2	100	37.5	2.66
3	100	25	4
4	100	12.5	8

Table 5.22 Model elastic ratio

The simulations are individuated by using the legend reported in table 5.23:

[Em:Ei]	A	B	C
1- [1:2]	1A	1B	1C
2-[1:2.6]	2A	2B	2C
3-[1:4]	3A	3B	3C
4-[1:8]	4A	4B	4C
5 omog			

Table 5.23 Models name

Each model is analyzed using a pulse forces at the frequency of 100 to 500kHz with steps of 50kHz, each signal is a 3 cycle sinusoidal function as:

$$F(t) = F_0[\frac{1}{2} + \frac{1}{2}\sin(2\pi f - \frac{\pi}{2})] \tag{5.23}$$

In order to have a function that simulate only the compression action of the probe, that start to zero, and will be and at zero.

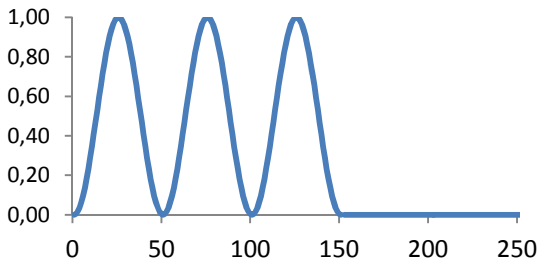

Figure 5.35 The signal impulse used for digital simulation pulse

The results of simulation indicate that:

The wave velocity increase with the increasing of the ratio of hard inclusion. The wave velocity increase with the incremental modulus of matrix

A mechanical model is proposed to explicate the meaning and the value of ultrasonic velocity in heterogeneous media. So we start to consider the propagation of wave in two media with different mechanical properties. And we denote con Lm and Li respectively the path length of the matrix and of the inclusions, as shown in figure 5.36.

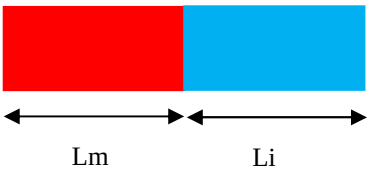

Figure 5.36 Mechanical model

Form the total length it is possible to individuate the percentage of each component, by the follow relationships

$$\begin{aligned} \%i &= \frac{L_i}{L_{tot}} \\ \%m &= \frac{L_m}{L_{tot}} \end{aligned} \tag{5.24}$$

The average velocity can be obtained by ratio of space on time.

$$V = \frac{\Delta S}{\Delta T} \tag{5.25}$$

Dividing the space and the time in two parts we obtain:

$$\begin{aligned} \Delta S &= L_m + L_i \\ \Delta T &= \Delta T_m + \Delta T_i \\ \Delta T_m &= \frac{L_m}{V_m} \\ \Delta T_i &= \frac{L_i}{V_i} \end{aligned} \tag{5.25}$$

Using the percentages defined before:

$$\begin{aligned} &\text{assuming } Ltot = 1 \\ &L_i = \%i \\ &L_m = \%m \end{aligned} \tag{5.26}$$

The average velocity can be expressed by:

$$V = \frac{[\%i + \%m]}{[\frac{\%i}{V_i} + \frac{\%m}{V_m}]} \tag{5.27}$$

Where the velocity V_i and V_m are determined using the relationship of signal propagation in elastic homogeneous media. To apply this model at ours numerical simulation, it is shown that the error is less than 10%.

[Em:Ei]	A-46%	B-65%	C-84%
	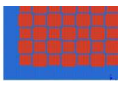	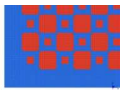	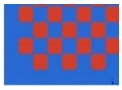
1-[1:2]	1A-5859 (5748-1.92%)	1B-6147 (6447-4.65%)	1C-7075 (7223-2.01%)
2-[1:2.6]	2A-5281 (5277-0.07%)	2B-5597 (6002-6.76%)	2C-6696 (6959-3.80%)
3-[1:4]	3A-4687 (4561-2.75%)	3B-5000 (5380-7.07%)	3C-6250 (6557-4.70%)
4- [1:8]	4A-3571 (3492-2.25%)	4B-4166 (4360-4.40%)	4C-5769 (5801-0.5%)
Omog.	FEM-7812	MOD. 7729	1.07%

Table 5.24 Velocity of wave (in parenthesis the formulated value)

Is relevant to report the tension state and de displacement state on the mesh during some steps.

In the figure 5.37 are reported stress and deformations at the steps 20,50, 100 for the model A2 [1:2.66] at 250KHz. It is possible to see how the joint of matrix modify the propagation of wave, some little waves are born around the main wave.

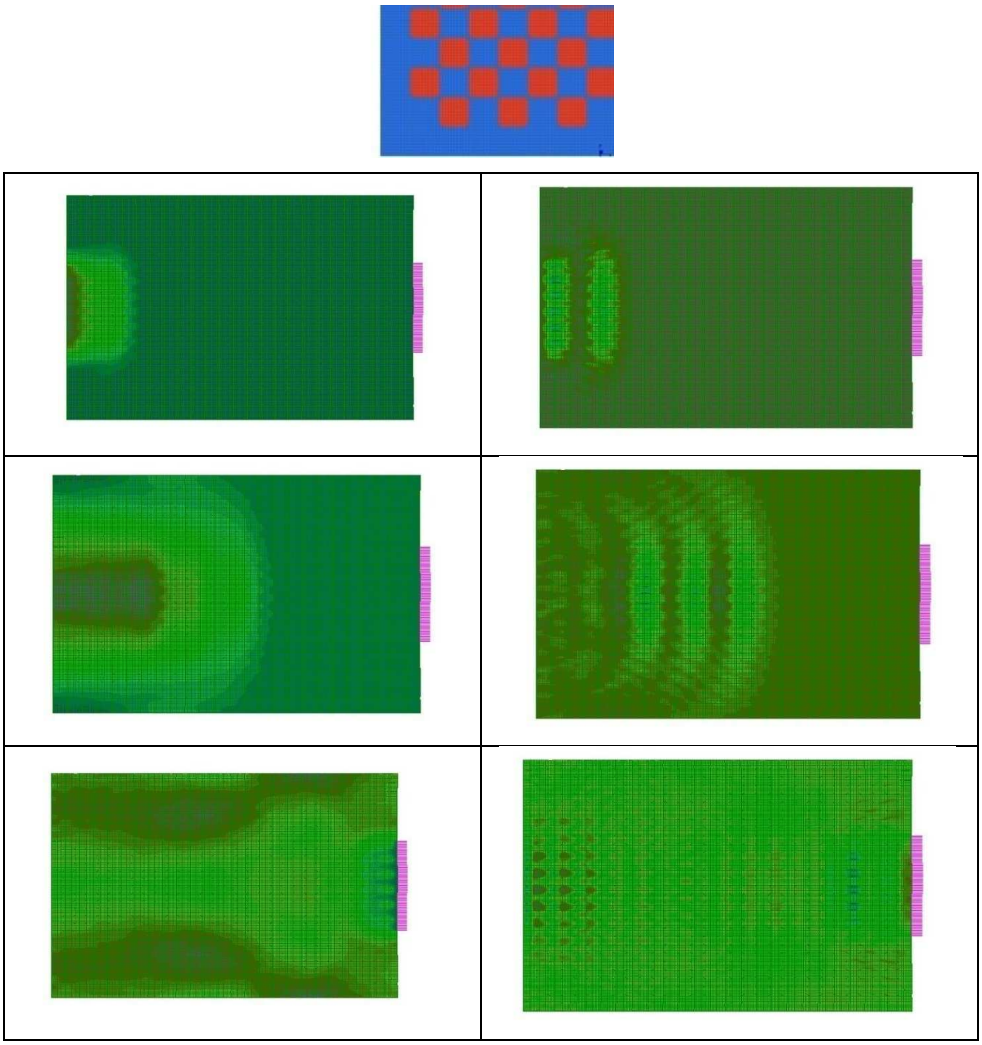

Figure 5.37 State of stress and deformation for numerical models

It is also relevant to note how the frequency content of ultrasonic wave is influenced of a micro structured behavior of material. In these simulation we have verify that some frequency have a dispersive behavior when the travel through the material and some others are free to travel in it. In the figure 5.38 is reported stress state at the steps 50 and 100 for the model A2[1:2.66] at the frequency of 250kHz e 500 KHz; it is clear to see how the frequency of 250KHz easily reach the opposite side of the model instead the frequency of 500KHz is enough refracted during its travel, and at the opposite side the arrival wave is too low in amplitude.

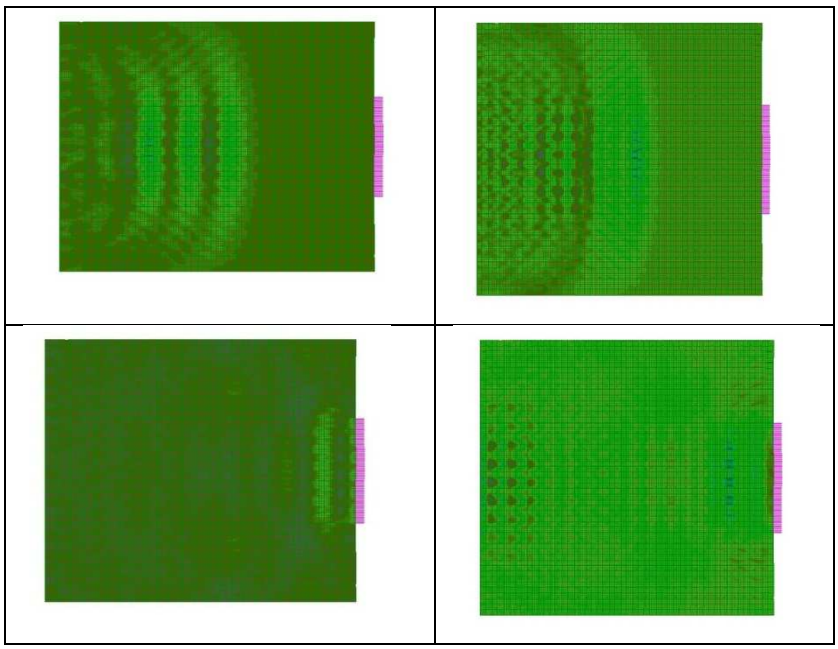

Figure 5.38 State of stress for numerical models.

These tests are repeated from a sweep of frequencies. From all these simulations trends of the resonant frequencies are deducted.

First of all we note that in our simulations the resonant curves are more smooth form the experimental curves. Maybe it depend of the arrangement real in material that is pretty reach from our arrangement. And the periodicity of the model is not so correspondent with the real material.

The first note is related with the inclusion, if the percentage of inclusion is increasing, the resonant frequency is also increasing. Also, if it consider a matrix more soft, by confront case 1 to case 3, is it possible to appreciate that the curves are more tilt, it means that in case where differences between matrix and inclusion are high in term of module the resonant phenomena is more explicit, in the case 3C, instead the matrix is more soft 1:4 ratio, the quantity of inclusion is so high that the curve come back with a plateau.

Relevant is the case A, presented with the 3 different levels of module ratio, the increment of module ratio, with the same arrangement reduce the tilt of curve, but the peak of it have small variation in relation whit the other cases. Results are shown in figure 5.40 so by this considerations, it is possible to appreciate that at the increasing of inclusion percentage correspond an increment of resonant frequency, spread between matrix and inclusion make more tilt the resonant curves.

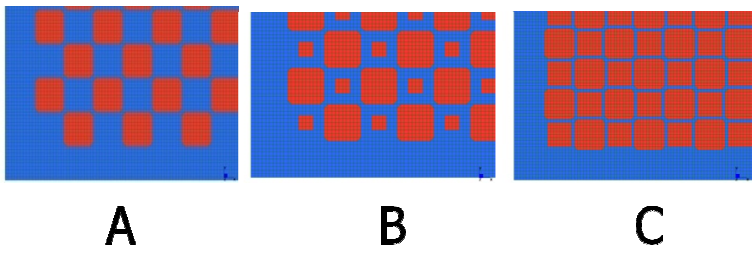

Figure 5.39 The 3 considered models: Zoom

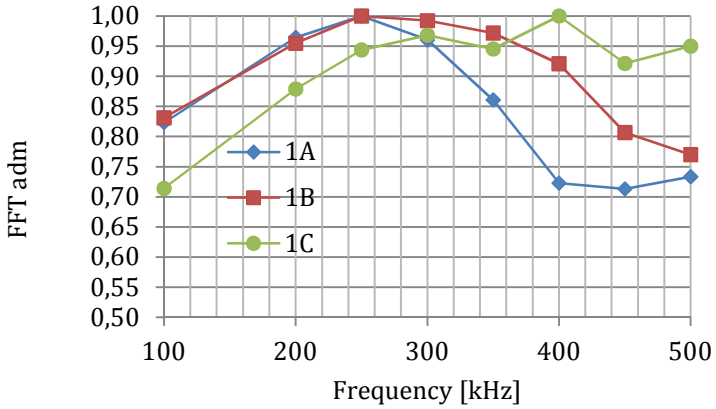

Figure 540(a) FFT of outputs simulated signals varying arrangement and ratio 1:4

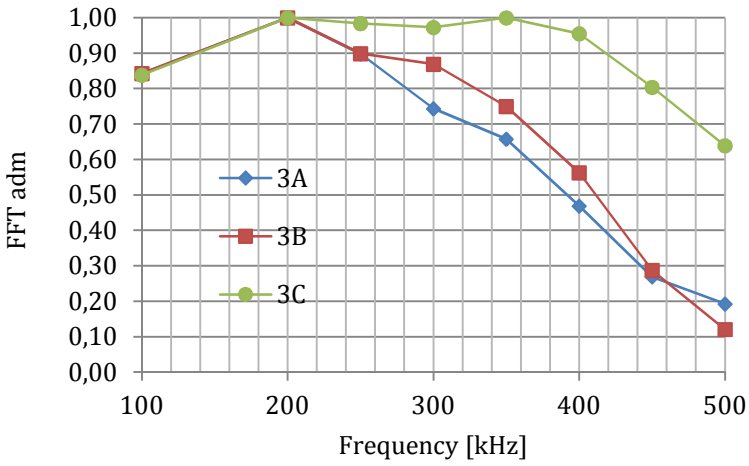

Figure 5.40(b) FFT of outputs simulated signals varying arrangement and ratio 1:2

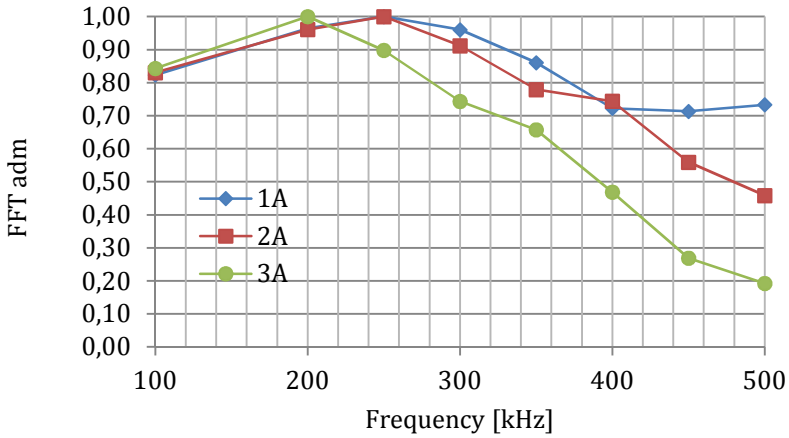

Figure 5.40(c) FFT of outputs simulated signals varying ratio

In order to understood how it is the materials behavior under stress waves, some simulations are conducted by leaving free border at the side where probes detect signals, and by load the model with a imposed displacements with sinusoidal time history.

In the follow pictures are reported the responses. It is clear that the displacement time history reach the opposite side by slaloming between the grains, and come back in the model. It is appreciable how the border is modified form the ultrasonic pulse, in relationship with the grains.

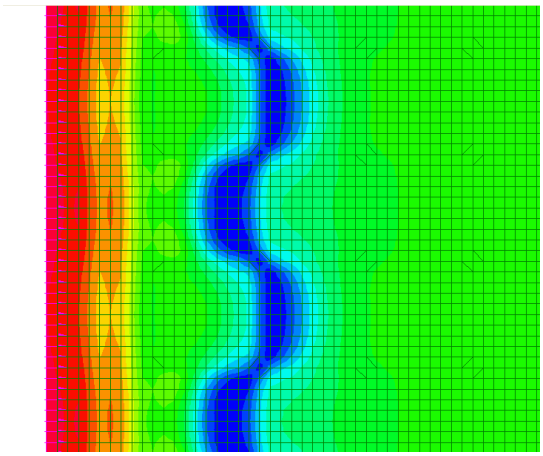

Figure 5.41 Stress distribution in correspondence of inclusions

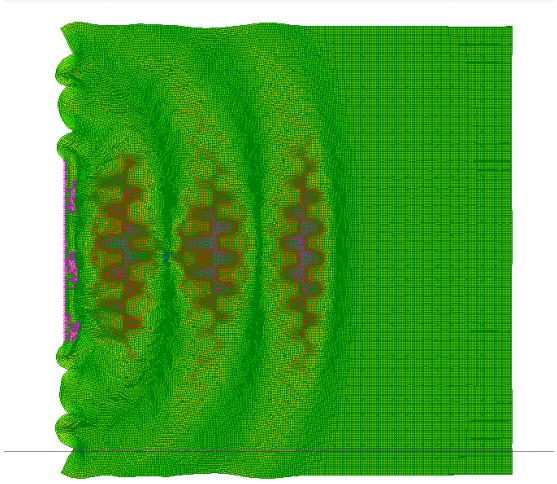

Figure 5.42 Displacement distribution of model at the starting of wave.

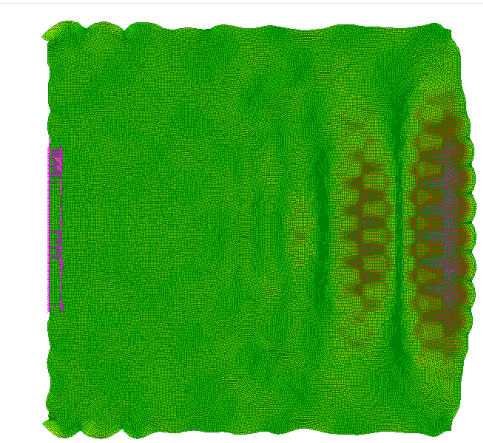

Figure 5.43 Displacement distribution of model at the arriving of wave.

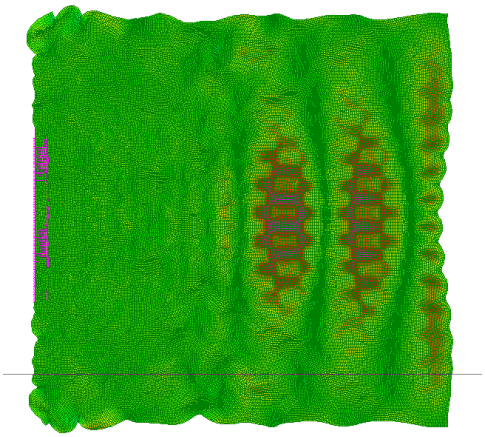

Figure 5.44 Displacement distribution of model at the back coming of wave.

In order to evaluate how resonant frequency can be related with micro mechanical behavior, a simplified approach is treated.

In this approach it is considered a cylinder of material hold between the two probes. Using a 1-DOF (1 degree of Freedom) classical relationships are reported.

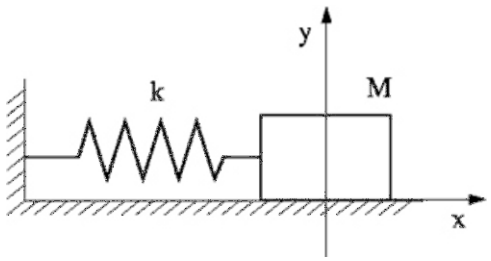

Figure 5.45 Mechanical model for frequency model

$$f = \frac{1}{2\pi}\sqrt{\frac{K}{M}}$$
$$K = \frac{EA}{L} = \frac{Ebh}{L} \qquad (5.28)$$
$$M = \rho W = \rho bhL$$

Where E is the material average elasticity, A is the transversal area, L a dimensional parameter, b h the cross section dimensions, ρ the density.

Operating a substitution it is obtained:

$$f = \frac{1}{2\pi}\sqrt{\frac{[\frac{Ebh}{L}]}{\rho bhL}} = \frac{1}{2\pi}\sqrt{\frac{E}{\rho L^2}} \qquad (5.29)$$

To explicit respect the L,

$$L = \frac{1}{2\pi f}\sqrt{\frac{E}{\rho}} \qquad (5.30)$$

If we related the elastic module with the velocity and with the length of wave it is obtained:

$$V_0 = \sqrt{\frac{E}{\rho}} \quad \text{e} \quad \lambda_0 = \frac{V_0}{f} \qquad (5.31)$$

$$L = \frac{\lambda_0}{2\pi} \qquad (5.32)$$

With this relation it is possible to admit that the resonant frequency is related with an internal dimension L, if we operate calculus with our range of resonant frequency, we can obtain length that are equal approximate at 1/6 of length of waves. And to recall the table 5.12, the length in rules are of orders of few millimeters. Upper 8mm and below 100mm.

It is possible to consider that the resonant phenomena is related with a main phase present in material, and this phase have for the main part dimension of L mm. To admit that this L is proportional with 2π mean that the length of wave λ spent 1 cycle to cross the dimension L.

Assuming a frequency, to vary the velocity of the signal are obtained different wavelengths and then the similar quantity of L.

L varies between then L1 = 120/6.28 = 19 mm and L2 = 08/6.28 = 1.3mm.

The resonance frequency can linked with the resonance phenomenon of the fraction of aggregate that has the L dimension, i.e. the combination of a composition of motions of various aggregates.

Admitting the presence of a resonance frequency, in fact, is equivalent to admitting that a fraction of aggregate is preponderant and that, therefore, the signal at a given frequency passes through the material better than other frequencies.

Imagine a world in wich every single person is given
free access to the sum of all human knowledge.
J. Wales

CHAPTER 6

THE MULTISCALE APPROACH

6.1 INTRODUTION

The great heterogeneity of some materials, the variety of situations and problems that they have, make the problem of their structural analysis extremely varied and diverse. The basic choices of a structural modeling are related to several factors:

- The spatial scale;
- The structural scheme;
- The constitutive law;
- The type of analysis.

The chapter study the behavior of heterogeneous material using two scale of modeling, in which the material behavior at the macroscopic level is homogeneous and it is detailed as heterogeneous at the mesoscopic scale.

There is a way where the two previous models are involved in the interaction of the two scales, meso and macro, that is a multi-scale approach, in which the material behavior at the macroscopic level results from mesoscopic models detailed. The focus of multi-scale is the identification of the stress-strain state of a representative volume element (RVE), which is identified at the macroscopic scale as a point of the continuum, and the mechanical behavior is detailed at the mesoscopic scale.

A first idea was formulated by Smith (1998); Feyel and Chaboche (2000); Kouznetsova et al. (2002) studied heterogeneous polymers and metallic systems, characterized by a great differentiation in terms of size of the two scales, so as to

be able to justify the allocation of a stress-strain relationship extracted from a mesoscopic structure in a macroscopic point material.

The process of calculation can be summarized in the following steps:

- It is assigned a state of deformation at the macroscopic level, for each integration point (Gauss points) of the macroscopic model.
- It is formulated a boundary value problem (BVP), transforming the state of deformation in a system of displacements at the contour of the cell (RVE).
- It is computed the response of the RVE undet the BVP, the transition of macro-meso scale is operated applying the set of displacements od deformations that comes form the macroscale analisys to the representative volume.
- To return to the macro-model (transition meso-macro), the macroscopic stress is computed by averaging the stress field at the meso-scale, in the RVE.

The procedure therefore allows to determine the state of deformation and tension, although only in numerical terms and not in terms of macroscopic constitutive relations.

6.1.1 THE MESO-MODEL

The meso-model wants to model the aggregate and the cement dough arrount it. In order to develop this model.. Here a brefly description of these approach is presented. In our model the aggregate is modeled as a rectangle with a border of dough.

The first mesoscale approach (Page 1989, Afshari and Kaldjian 1989, Rots 1991) is related with masonry structures. It is considers the behavior of the blocks and the mortar joints, by describing the interaction and the mechanical behavior of the constituent materials. This type of modeling, however, requires a heavy

computational effort and it can be applied in detailed analysis. It is used to analyze some mechanisms of damage to the masonry in which the interaction mortar/blocks is decisive. A significant case may be that of rupture in compression for splitting, associated with the different deformability of the materials, namely the effect of the Poisson ratio of the mortar. The simplified approach, that represents the masonry as a set of blocks connected by interface elements, provides a more concise representation of the material. The non-linear effects of the masonry are localized in zones of small thickness, where they develop high strain gradients.. The interface models are characterized by constitutive relations by the stess that acting on these surfaces for the discontinuity of displacement. The first formulation of a strategy for modeling through a discrete binding interface was developed by Page (1978). The model was aimed at studying the in-plane behavior of masonry walls. The main experimental evidence on which he based Page formulation of the model are:

- Blocks have an elasto-brittle behaviour;
- The mortar, usually less resistant blocks, has a strongly non-linear behavior;
- The masonry as a whole has a good ability to transmit compressive forces;
- The tensile strength of the masonry is extremely limited due to a lack of cohesion in the interface mortar / blocks;
- Most of the inelastic deformations of the masonry derive from the mortar joints and in particular by shear forces present in the joints and the normal compression agent on them.

Based on these observations, Page considers the wall as an ordered set of elastic blocks connected by mortar joints, in which is concentrated all the non-linear behavior of the whole.

It is assumed that the mortar joints have low tensile strength, high resistance to compression, and a shear strength which is a function of cohesion and normal compression agent with respect to their plane: the ultimate tensile and shear

failure. It is assumed that the mortar joints behave elastically until it has violated a predetermined failure criterion.

In the FEM model blocks are then described using elastic elements in plane stress, while the mortar joints using interface elements.

The Page model is a pioneering intervention in the field of modeling of masonry structures. The main limitations, today, consist in not describe the collapse phase and in proposing a modeling strategy essentially empirical, bound to specific experimental evidence and certain types masonry. It was designed primarily for the purpose of predicting the location of the damage and the areas of stress concentration in the design of new buildings.

A subsequent approach to the discrete modeling of masonry structures via interface models was proposed by Lotfi and Shing (1994). It should be noted that, in this case, the focus moves to the existing structures, with an explicit reference to the problem of seismic actions. The model, in fact, is specifically intended to describe the behavior of a wall under combined actions of shear and normal stress. Even in this case, it is assumed that the blocks have an elastic behavior and that the mortar joints represent the only potential areas of damage of the material. The failure mechanisms are provided for the shear failure (with friction behavior in compression) and the traction breaking.

According to these hypotheses, the blocks are described as linear elastic elements in plane stress, while the joints through interface elements. The description of the behavior of the interface is of type elasto-plastic, where the plastic component of the deformation is governed by a law of sliding of unbound type (interface dilatancy).

It is considered that the matrix of elastic bond does not undergo changes during the loading history and which therefore does not involve damage to the stiffness of the system. Furthermore, it is assumed that the elastic component of the deformation has not dilatancy.

The failure criterion proposed is generated by non-linear combination of the criterion of Mohr-Coulomb failure criterion with a tensile-type cut-off.

6.1.2 THE MACRO MODELS

The continuous modeling of materials is aimed of the analysis of whose dimensions structures where the states of tension at the local level can be considered homogeneous. From the constructive point of view, this results in the modeling of structural elements whose overall sizes are significantly greater than the dimensions of the constituent elements. This allows, in fact, to describe the behavior of the material through appropriate medium macroscopic properties.
From a macroscopic point of view, the material can be characterized elastically homogeneous only if the particles that constitute it are in contact and therefore is defined as a material to unilateral constraints. The mechanical characterization of the test material are assumed:

- The granules that constitute the material have infinitesimal dimensions so that the material can be treated as continuous;
- The material is isotropic;
- That the following eligibility condition of tension:

$$\sigma_n = \sigma_{ij} n_i n_j \leq 0,\ \forall n_i : n_i n_i = 1,\ (i, j = x, y, z) \tag{6.1}$$

- The tensor $\{\varepsilon_{ij}\}$ of the total deformation may decompose additively in an elastic part ε_{ij}^e and a part inelastic ε_{ij}^f :

$$\varepsilon_{ij} = \varepsilon_{ij}^e + \varepsilon_{ij}^f \tag{6.2}$$

$$\varepsilon_n^f = \varepsilon_{ij}^f n_i n_j \geq 0\ \forall n_i : n_i n_i = 1\ (i, j = x, y, z) \tag{6.3}$$

- The material is stable in the sense of Drucker, tensions perform work

during the production of non-negative strains:

$$W^f = \sigma_{ij}\varepsilon_{ij}^f \geq 0 \tag{6.4}$$

6.1.3 THE MULTI SCALE MODELS

The multiscale model is a fine compromise by the macroscopic homogeneous model and the mesoscopic detailed models.

The major problem in the treatment of multiscale problems is in the transition from macroscale to the mesoscale and vice versa. In the literature, there are three main approaches. The first approach is to assign the kinematic boundary conditions of the cell (displacements), starting from the state deformation plane of the point of Gauss finite element at the macroscopic scale. The second is to assign the static conditions of the cell boundary (forces), starting from the plane stress point Gauss finite element at the macroscopic scale. The third approach is to assign periodic boundary conditions at the mascoscopic scale:

$$\underline{u} = \underline{\underline{E}}\,\underline{x} + \underline{w} \tag{6.5}$$

where $\underline{x}$ is the macroscopic deformation tensor, $\underline{w}$ is a vector related with the displacements of the unit cell, $\underline{u}$ is the vector displacements mesoscopic fluctuation which takes into account the distinction between the real displacement field to the mesoscale with the quality linear displacements. The range of fluctuation is assumed periodic. In this study we apply an approach according to the first type exposed.

6.2 THE MESHLESS METHOD

The multiscale analysis is based on the study of a representative volume element of the unit cell, shown in detail at the mesoscale. The mechanical behaviour of the

cell is then deducted form the macroscopic behavior of the model. The resolution of the mescoscopic model is studied by adopting the *Meshless Method*, which, in contrast to the method of finite elements, is released from a discretization of the structure not in terms of finite elements but by a localization of points in an uniform domain.

The meshless methods born with the objective of eliminating part of the difficulties associated with the dependence mesh for the construction of approximations. The discretization of the domain becomes purely nodal, eliminating the concept of connectivity. One of the first meshless methods is the method *Smooth Particle Hydrodynamics* (SPH) proposed by Lucy, Gingold and Monaghan in 1977 with the aim of solving problems of astrophysics and then applied in fluid dynamics. The first use in solid mechanics dell'SPH is instead due to Libersky et al. in 1993. Over time, the method has undergone many changes and improvements with a view to removing inconsistencies and possible instability. The SPH and its revisions are based on the balance in a strong form, instead of other methods developed in the nineties and mainly applied to solid mechanics are based instead on the equilibrium in weak form. Element-free Galerkin method (EFG) developed in 1994 is one of the first meshless methods that are built on weak form. A few years later was the *Reproducing kernel particle method* (RKPM) by Liu et al. whose final equation is very similar to the equation del'EFG, but the method has its origin in the theory of wavelets. These include the *Partition of unity finite element method* (PUFEM) of Melenk and Babuska of 1995-1996 and the Hp-cloud method of Duarte and Oden in 1996, the authors introduce the shape functions based on polynomials of Lagrange and in the second case is also included in the least-squares approximation (Moving least square approximation). The most popular method is based on the weak form of the Meshless Local Petrov-Galerkin (MLPG) of Atluri and Zhu in 1999, the main difference between this and other methods such as EFG or RKPM is that the weak forms are generated by the superposition of subdomains

rather than using the global weak forms and the integration of the weak form is performed in these local subdomains. As Atluri says, it is a method *truly meshless* because it does not include any construction of mesh in order of integration.

The meshless methods have many advantages. They allow the resolution of problems with moving discontinuities such as the propagation of the fracture. Are more effective in dealing with large deformations, also allow the use of continuous shape functions of higher order interpolations and non-local. Methods, however, are not devoid of drawbacks. In fact the shape functions used are rational functions that require integration schemes of higher order to be correctly computed. Moreover, the treatment of the boundary conditions is not as simple as in the case of the methods based on the use of the mesh because the shape functions can not be interpolated. In general the cost of computation Meshless Methods is higher than that of the method of finite elements. To overcome many difficulties associated with meshless methods, these are often coupled with the finite element method: thus the hybrid methods are available to exploit the advantages of both methods.

In general the meshless methods construct an approximation of functions displacement (trial function) for local interpolation, using values of displacements defined in a finite number of points positioned in the immediate vicinity and chosen arbitrarily, without the creation of any mesh. In order for the interpolation process to be efficient it is necessary that the weak form is continuous, which ensures that the function is integrable, and complete, and this depends on the order partial differential equation that must be resolved. The idea on which is based the meshless approach is the reconstruction of the area of influence of the i^{th} node, generating for each node a local mesh. It is therefore defined the weight functions ***w(x)***, to which are associated domains of influence for each node, outside of which the weight function assumes null values. The domain support node j can have a variable geometry and is therefore such that $w_j \neq 0$; generally used the

circular domain centered on the node considered, but are also popular rectangular domains. Assuming that the radius of the weight function is maintained constant and equal for each node, the shift function at each point x is influenced by all nodes whose position is within the radial distance r from x. For each point x is then possible to delimit a domain of definition which is such that $w_I \neq 0$ for I = 1,2, ..., N.

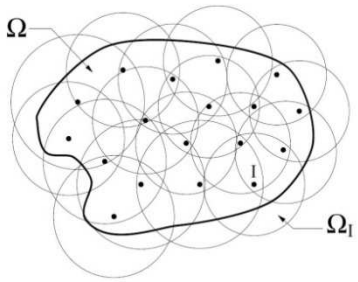

Figure 6.1 Model for the meshless method showing the contours, the nodes and domains of support.

6.2.1 APPROXIMATION BY MLS

There are a variety of methods to build differently the approximation of the unknown displacement function. By all, *the moving least-squares approximation* scheme (hereinafter MLS) is considered one of the best to perform interpolations with reasonable accuracy in the results. Considering the domain of definition of the approximation for the MLS function. It is identify here, within the domain Ω of the problem, a sub domain Ω_x coincident with the neighborhood of the point x of which we want to know the displacement. To approximate the distribution function of the displacement u(x) in Ω_x of a number of nodes arbitrarily distributed x_I with I = 1,2, ..., N, we define the approximation û(x) as the product between the vector of polynomial bases , p(x), and the vector of some coefficients, a(x):

$$\hat{u}(x) = \sum_{i=1}^{m} p_i(x)a_i(x) = p^T(x)a(x) \quad for \quad x \in \Omega_x \tag{6.6}$$

where, $p_i(x)$ with i = 1, 2, 3, ..., m represents the complete polynomial bases, with m number of terms of the polynomial basis; p^T is the transpose of p, $a_i(x)$ are the corresponding coefficients, functions of the spatial coordinates of x.

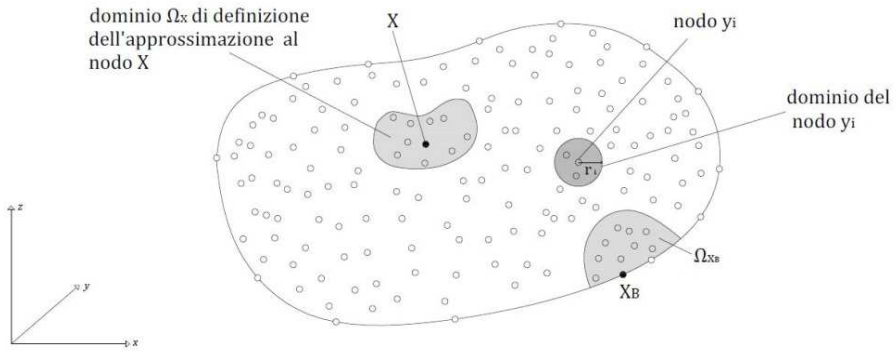

Figure 6.2 Domain of definition of the approximation Ω_x
MLS domain and support generic node.

If you denote with t the maximum order of the polynomial which appears in the base, the relationship between the m degree in a n-dimensional can be expressed as follows:

$$m = \frac{(t+1)(t+2)\ldots(t+n)}{(1\ldots n)} \tag{6.7}$$

In the case of a linear base t = 1 for a problem in two dimensions n = 2 for example we will have:

$$m = (1+1)\ (1+2)\ /\ 2 = 3 \tag{6.8}$$

complete bases used in case of 2D problems with m = 3 for a linear basis can be:

$$p^T(x) = [1, x^1, x^2] \text{ with } p_0(x) = 1; p_1(x) = x^1; p_2(x) = x^2 \quad (6.9)$$

and with m = 6 for quadratic basis.

$$p^T(x) = [1, x^1, x^2, (x^1)^2, (x^2)^2, x^1 x^2] \quad (6.10)$$

For the determination of the vector of coefficients a(x), necessary to detect the distribution of displacements u(x), define the norm of the discrete weighted error as follows:

$$J(x) = \sum_{I=1}^{n} w_I(x)[p(x_I)^T a(x) - U_I]^2 \quad (6.11)$$
$$J(x) = [P\, a(x) - U]^T W(x) [P\, a(x) - U_I]$$

where U_I is the function value shift to the node I, x_I is the coordinate of the i-th node, x is the coordinate of the generic point where the displacement is evaluated, n represents the number of nodes in Ω_x in which the weight function w_I (x)> 0. The weight function associated with the node I is in fact such that w_I (x)> 0 for all x belonging to the domain of influence of w_I (x), and is given by:

$$w_I(x) = w_I(x, x_I, \rho_I), \quad (6.12)$$

where ρ_I is the radius of the support node I. P, W and U are defined as follows:

$$\boldsymbol{P} = \begin{bmatrix} p^T(x_1) \\ p^T(x_2) \\ \dots \\ p^T(x_N) \end{bmatrix} = (Nxm)$$

$$\boldsymbol{W} = \begin{bmatrix} w_1(x) & \dots & 0 \\ \dots & \dots & \dots \\ 0 & \dots & w_N(x) \end{bmatrix} = (NxN) \quad (6.13)$$

$$\boldsymbol{U}^T = [U_1, U_2, \dots, U_n]$$

To obtain the coefficients by imposing the minimization of the functional with respect to a(x):

$$\frac{\partial J(x)}{\partial a(x)} = 0 \tag{6.14}$$

that leads to the following set of linear equations in the unknown to (x):

$$\underset{(mxm)(mx1)}{\boldsymbol{A}(x)\boldsymbol{a}(x)} = \underset{(mxN)(Nx1)}{\boldsymbol{B}(x)\boldsymbol{U}} \tag{6.15}$$

where

$$\boldsymbol{A}(x) = \sum_{I=1}^{n} w_I(x)p(x_I)p(x_I)^T = \boldsymbol{P}^T\boldsymbol{W}\boldsymbol{P} = \boldsymbol{B}(x)\boldsymbol{P} \tag{6.16}$$

$$\boldsymbol{B}(x) = [w_1(x)p(x_1);\ w_2(x)p(x_2); \dots;\ w_n(x)p(x_n)] = \boldsymbol{P}^T\boldsymbol{W} \tag{6.17}$$

The vector of coefficients a(x) can then be detected as:

$$a(x) = \boldsymbol{A^{-1}}(x)\,\boldsymbol{B}(x)\,\boldsymbol{U} \tag{6.18}$$

provided that it is verified that the matrix A is singular for each generic point x, which is the case if and only if the rank of P is equal to m. This happens every time I am at least an equal number of weight functions are non-zero, or at least m nodes must fall within the domain of the weight function and also does not have to be aligned along a line.

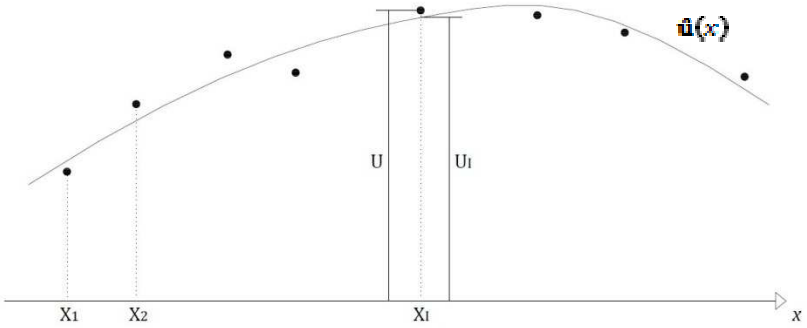

Figure 6.3 Difference between the U_I and the nodal displacement values fuctious U.

The approximation of the displacement u(x) can be expressed as follows:

$$u(x) \approx \hat{u}(x) = p^T(x)\boldsymbol{A}^{-1}(x)\boldsymbol{B}(x)\boldsymbol{U} = \Phi(x)\,\boldsymbol{U} \qquad (6.19)$$

or as the product of a matrix of shape functions Φ and the vector of nodal values U, in a similar manner to the method of finite elements. The matrix of shape functions and its derivatives can be obtained as:

$$\Phi(x) = p^T(x)\,\boldsymbol{A}^{-1}(x)\,\boldsymbol{B}(x) \qquad (6.20)$$

$$\Phi,i(x) = p^T{}_{,i}(x)\,\boldsymbol{A}^{-1}(x)\boldsymbol{B}(x) + p^T\boldsymbol{A}^{-1}_{,1}(x)\,\boldsymbol{B}(x) + p^T\boldsymbol{A}^{-1}(x)\,\boldsymbol{B}(x),i \qquad (6.21)$$

where $A^{-1}{}_{,I} = -A^{-1}\,A_{,i}\,A^{-1}$.

6.2.2 THE WEIGHT FUCTION

The choice of the weighting function $w_I(x)$ plays an important role in the development of meshless methods, defining what is the range of influence of the i^{th}

node. The weight functions are constructed so as to be always positive and ensure the uniqueness of the solutions in (x). They are always monotone decreasing function with respect to the distance of the generic point x from node x_I. Generally weights are used functions that express the distance between two points, such as:

$$w_I(x) = w(\|x - x_I\|) \tag{6.22}$$

It can be chosen weighting functions of *exponential order*, *third order spline*, the *fourth order spline* of the and so on. The choice of the weighting function is arbitrary, it is positive and continues with its derivatives, up to the order desired. In the following discussion it is choice the type spline function of the fourth order as the following:

$$w_I(x) = \begin{cases} 1 - 6\left(\frac{d_I}{r_I}\right)^2 + 8\left(\frac{d_I}{r_I}\right)^3 - 3\left(\frac{d_I}{r_I}\right)^4 & per\ 0 \le d_I \le r_I \\ 0 & per d_I > r_I \end{cases} \tag{6.23}$$

where $d_I = \sqrt{((x-x_I)^2 + (y-y_I)^2)}$ and r_I is the radius of the weight function.

The support of the function influence significantly both the sparseness of the stiffness matrix and matrix flexural and, consequently, the computational effort. In general, from a practical point of view, it would be desirable to support the choice of a small, but this may generate a matrix A singular. For an optimal choice of the domain of influence must be satisfied the following conditions:

- The support must be large enough to provide a number of nodes next to each point of integration sufficient to ensure the invertibility of the matrix A;
- The support must be large enough to ensure that each sample point has knots coming from all sides;

- The support domain must be small enough to give locally the approximation to the minimum quadratic method;
- The support must be small enough to avoid high computational costs.

Regarding the first condition, the choice of the radius of the weight function must be such as to cover a sufficient number of nodes in the domain of definition of each sample point. Atluri claims that this number of nodes N covered by the media must be greater than or equal to the number of terms of the polynomial basis chosen that $N \geq m$. According Ivannikov et al., in order to avoid a bad matrix conditioning, the media must meet the following conditions:
Each point of interest must be covered to a minimum by a number of media relating to neighbor nodes equal to $1/2\ (k+1)\ (k+2)$.
In caseof in two dimensional problems, each point of interest must be covered by a number of supports superior to m in each of the two non-collinear directions.

6.2.3 THE RVE PROPOSED

The RVE proposed is approached by using the weak formulation of the Principle of Virtual Work for a system of RVE with interface. The objective to consider a model also with interface is justified by the necessity to extend the models by considering other phenomena over the elasticity as the attenuation and the dispersion of wave influenced by the connection between aggregate and dough.

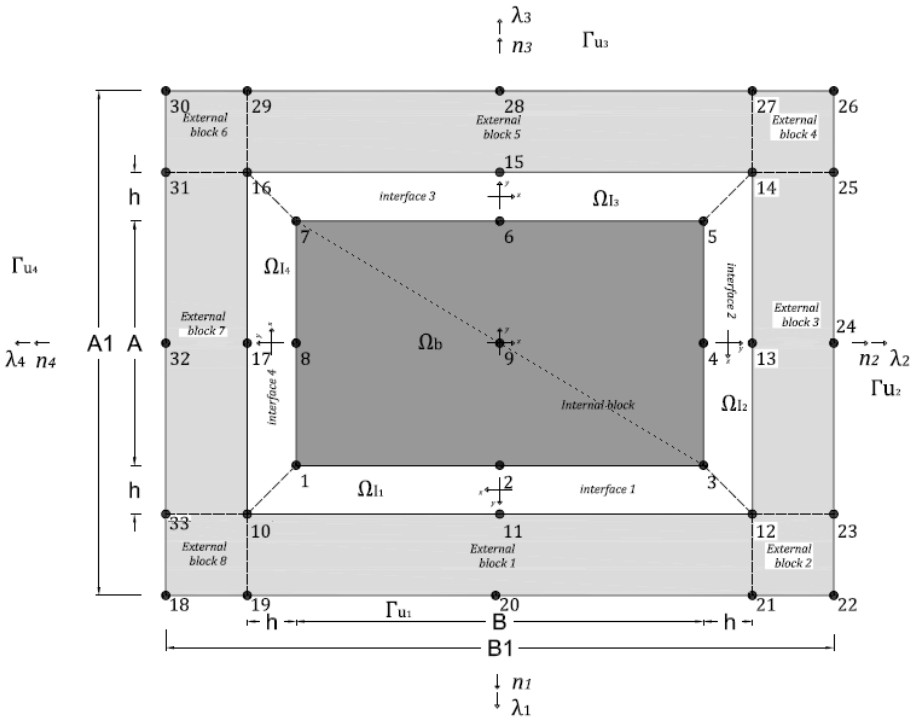

Figure 6.4 Scheme of RVE

In Figure 6.4, we consider the entire cell formed by an homogeneous element of size *bxa* with two border of dough in its surroundings. The first border is an h dept interface, and the second border is a part of another material that is interposed between two cell. The elastic properties of the interface, of the internal homogeneous material and of the external homogeneous material can be settled using different values. The interface domain is divided in 4 parts, one for each side, and the border external material is also divided in 8 parts, 4 at the corners with square shape (the odd external domains) and 4 are in each side, with rectangular shape (the even domains). Each interface and each external block are considered individually. For each one a local reference system is considered, with the y axis

coinciding with the outward normal, rotated with respect to the global reference system. The model is defined by using 33 nodes, that are equivalent to 66 degrees of freedom. In the present study we consider the central element modeled as a two-dimensional element with 9 nodes and 9 Gauss integration points. The interface is a one-dimensional element with 6 nodes and 3 Gauss points. For the external parts, the odd domains are defined with 4 nodes, and the even domains are defined by 6 nodes. For each of the external domain 9 Gauss points are defined. The balance equation in weak form is written as:

$$\delta L = \delta L_i - \delta L_e = 0 \tag{6.24}$$

where δL_i is the work done by internal stresses in the 13 domains represented by the block surfaces Ω_b, the 4 interfaces Ω_{I_i}, the 8 external blocks Ω_{m_i}:

$$\delta L_i = \int_{\Omega_b} \boldsymbol{\sigma}_b^T \delta \boldsymbol{\varepsilon}_b d\Omega + \sum_{i=1}^{4} \int_{\Omega_{I_i}} \boldsymbol{\sigma}_{I_i}^T \delta \boldsymbol{\varepsilon}_{I_i} d\Omega + \sum_{i=1}^{8} \int_{\Omega_{m_i}} \boldsymbol{\sigma}_{m_i}^T \delta \boldsymbol{\varepsilon}_{m_i} d\Omega . \tag{6.25}$$

According to the following boundary condition:

$$\mathbf{u} = \bar{\mathbf{u}} \text{ in } \Gamma_u \tag{6.26}$$

where $\mathbf{u}$ are the displacements of a generic point and $\bar{\mathbf{u}}$ the imposed displacements, the method of Lagrange multipliers is applied. It must therefore rely on the condition:

$$\boldsymbol{\lambda}^T \left(\mathbf{u} - \bar{\mathbf{u}} \right) = 0 \quad \text{in } \Gamma_u \ \forall \lambda \tag{6.27}$$

The first variation of (6.27) provides:

$$\delta \left[\boldsymbol{\lambda}^T \left(\mathbf{u} - \bar{\mathbf{u}} \right) \right] = \delta \boldsymbol{\lambda}^T \left(\mathbf{u} - \bar{\mathbf{u}} \right) + \boldsymbol{\lambda}^T \left(\delta \mathbf{u} - \delta \bar{\mathbf{u}} \right) \tag{6.28}$$

where $\delta \bar{\mathbf{u}} = \mathbf{0}$, since the displacements can not be modified.

The (6.24) assumes, then, the following form:

$$\int_{\Omega_b} \boldsymbol{\sigma}_b^T \delta\boldsymbol{\varepsilon}_b d\Omega + \sum_{i=1}^{4} \int_{\Omega_{I_i}} \boldsymbol{\sigma}_{I_i}^T \delta\boldsymbol{\varepsilon}_{I_i} d\Omega + \sum_{i=1}^{8} \int_{\Omega_{m_i}} \boldsymbol{\sigma}_{m_i}^T \delta\boldsymbol{\varepsilon}_{m_i} d\Omega +$$
(1-block) (2-interface) (3-external domain)
$$+ \sum_{j=1}^{nblocked} \boldsymbol{\lambda}_j^T \delta\mathbf{u}_j + \sum_{j=1}^{nblocked} \delta\boldsymbol{\lambda}_j^T (\mathbf{u}_j - \bar{\mathbf{u}}_j) = 0 \quad \forall\ \delta\mathbf{u},\ \delta\boldsymbol{\lambda}_j \tag{6.29}$$
(4-restrains)

The expression (6.29) represents the balance of the cell, in the form of the principle of virtual work. Further each quanty is explicated and the resolution equations are obtained.

In order to reconduct all the local displacement in a global reference system address matrices are used their name is $\mathbf{S_b}$,$\mathbf{S_{mI}}$,$\mathbf{S_{I,I}}$,respectively for the block, for the external domain, for the interface I.

6.2.3.1 BLOCK

The stresses and strains of the block are linked by a law of linear elastic type:

$$\boldsymbol{\sigma}_b = \mathbf{E}_b \boldsymbol{\varepsilon}_b \tag{6.30}$$

where $\mathbf{E}_b$ is the elastic matrix of the block.

The link between the deformation and the displacement field can be written according to the usual kinematic compatibility relations:

$$\boldsymbol{\varepsilon}_b = \mathbf{C}\mathbf{u}_b \tag{6.31}$$

or, in explicit form:

$$\begin{bmatrix} \varepsilon_x \\ \varepsilon_y \\ \gamma_{xy} \end{bmatrix} = \begin{bmatrix} \partial/\partial x & 0 \\ 0 & \partial/\partial y \\ \partial/\partial y & \partial/\partial x \end{bmatrix} \cdot \begin{bmatrix} u_x \\ u_y \end{bmatrix} \tag{6.32}$$

where $\mathbf{C}$ is the matrix of kinematic compatibility.

It is seen as the method Moving Least Square Interpolation expected to

approximate the vector displacement of the block as the product of (6.19)

$$\mathbf{u}_b = \mathbf{\Phi}_b \mathbf{U}_b \tag{6.33}$$

where $\mathbf{\Phi}_b$ is the matrix of shape functions; is the vector containing the displacements in horizontal and vertical direction of the nodes of the block (1-9). In expanded form:

$$\mathbf{\Phi}_b = \begin{bmatrix} \boldsymbol{\varphi}_b & \mathbf{0} \\ \mathbf{0} & \boldsymbol{\varphi}_b \end{bmatrix}; \quad \mathbf{U}_b = \begin{bmatrix} \mathbf{U}_{b,x} \\ \mathbf{U}_{b,y} \end{bmatrix} \tag{6.34}$$

As already discussed the solution is obtained as the product of a basic function of the two matrices ***A*** and ***B*** as defined below:

$$\boldsymbol{\varphi}_b = \mathbf{p}^T \mathbf{A}_b^{-1} \mathbf{B}_b \tag{6.35}$$

$$\mathbf{A}_b = \mathbf{P}_b^T \mathbf{W}_b \mathbf{P}_b \tag{6.36}$$

$$\mathbf{B}_b = \mathbf{P}_b^T \mathbf{W}_b \tag{6.37}$$

where the matrices $\mathbf{P}_b$ and $\mathbf{W}_b$ are, respectively, the matrix containing the monomial bases (one for each node of the block) and the matrix containing the weights of the various nodes, given by:

$$\mathbf{P}_b = \begin{bmatrix} \mathbf{p}^T(\mathbf{x}_1) \\ \mathbf{p}^T(\mathbf{x}_2) \\ \dots \\ \mathbf{p}^T(\mathbf{x}_{N_b}) \end{bmatrix} \qquad \mathbf{W}_b = \begin{bmatrix} w_1(\mathbf{x}) & 0 & \dots & 0 \\ 0 & w_2(\mathbf{x}) & \dots & 0 \\ \dots & \dots & \dots & \dots \\ 0 & 0 & \dots & w_{N_b}(\mathbf{x}) \end{bmatrix}. \tag{6.38}$$

N_b is the number of nodes of the block ($N_b = 9$).

w_i is the weight function associated with the node i, positive for all values of x in the neighborhood including the weight function.

The choice of the weighting function is arbitrary, in this case we have chosen a quartic function (6.23). In conclusion, the link between the deformations and displacements of the nodes of the block will be so expressed, on the basis of (6.31) and (6.33):

$$\boldsymbol{\varepsilon}_b = \mathbf{C}\mathbf{\Phi}_b \mathbf{u}_b \tag{6.39}$$

In this way the first term of the integral 6.29 can be exspressed as:

$$\int_{\Omega_b} \boldsymbol{\sigma}_b^T \delta\boldsymbol{\varepsilon}_b d\Omega \tag{6.40}$$

$$\boldsymbol{\sigma}_b = \mathbf{EC}\boldsymbol{\Phi}_b\mathbf{u}_b = \mathbf{EC}\boldsymbol{\Phi}_b\mathbf{U}_b = \mathbf{EC}\boldsymbol{\Phi}_b\mathbf{S}_b\mathbf{U} \tag{6.41}$$

$$\delta\boldsymbol{\varepsilon}_b = \mathbf{C}\boldsymbol{\Phi}_b\delta\mathbf{U}_b = \mathbf{C}\boldsymbol{\Phi}_b\mathbf{S}_b\delta\mathbf{U} \tag{6.42}$$

By sostituition:

$$\begin{aligned}&\int_{\Omega_b} \boldsymbol{\sigma}_b^T \delta\boldsymbol{\varepsilon}_b d\Omega = \int_{\Omega_b} (\mathbf{EC}\boldsymbol{\Phi}_b\mathbf{S}_b\mathbf{U})^T * (\mathbf{C}\boldsymbol{\Phi}_b\mathbf{S}_b)\delta\mathbf{U}d\Omega = \\ &[\int_{\Omega_b} (\mathbf{EC}\boldsymbol{\Phi}_b\mathbf{S}_b\mathbf{U})^T * (\mathbf{C}\boldsymbol{\Phi}_b\mathbf{S}_b)d\Omega]\delta\mathbf{U} = \mathbf{K}_b\mathbf{U}\delta\mathbf{U}\end{aligned} \tag{6.43}$$

Defining

$$\mathbf{K}_b = \int_{\Omega_b} (\mathbf{EC}\boldsymbol{\Phi}_b\mathbf{S}_b)^T * (\mathbf{C}\boldsymbol{\Phi}_b\mathbf{S}_b)d\Omega \tag{6.44}$$

6.2.3.2 EXTERNAL BLOCKS

The stresses and strains of the block are linked by a law of linear elastic type:

$$\boldsymbol{\sigma}_{m,i} = \mathbf{E}_m\boldsymbol{\varepsilon}_{m,i} \tag{6.45}$$

where $\mathbf{E}_m$ is the elastic matrix of the external block.

The link between the deformation and the displacement field can be written according to the usual kinematic compatibility relations:

$$\boldsymbol{\varepsilon}_{m,i} = \mathbf{C}\mathbf{u}_{m,i} \tag{6.46}$$

or, in explicit form:

$$\begin{bmatrix}\varepsilon_x \\ \varepsilon_y \\ \gamma_{xy}\end{bmatrix} = \begin{bmatrix}\partial/\partial x & 0 \\ 0 & \partial/\partial y \\ \partial/\partial y & \partial/\partial x\end{bmatrix} \cdot \begin{bmatrix}u_x \\ u_y\end{bmatrix} \tag{6.47}$$

where $\mathbf{C}$ is the matrix of kinematic compatibility.

It is seen as the method Moving Least Square Interpolation expected to approximate the vector displacement of the block as the product of (6.19)

$$\mathbf{u}_{m,i} = \mathbf{\Phi}_{m.i}\mathbf{U}_{m,i} \tag{6.48}$$

where $\mathbf{\Phi}_{m,i}$ is the matrix of shape functions; is the vector containing the displacements in horizontal and vertical direction of the nodes of the block (1-9). In expanded form:

$$\mathbf{\Phi}_{m.i} = \begin{bmatrix} \boldsymbol{\varphi}_{m.i} & \mathbf{0} \\ \mathbf{0} & \boldsymbol{\varphi}_{m,i} \end{bmatrix}; \quad \mathbf{U}_{m,i} = \begin{bmatrix} \mathbf{U}_{m,i,x} \\ \mathbf{U}_{m,i,y} \end{bmatrix}. \tag{6.49}$$

As already discussed the solution is obtained as the product of a basic function of the two matrices ***A*** and ***B*** as defined below:

$$\boldsymbol{\varphi}_{m,i} = \mathbf{p}^T \mathbf{A}_{m,i}^{-1}\mathbf{B}_{m,i} \tag{6.50}$$

$$\mathbf{A}_{m,i} = \mathbf{P}_{m,i}{}^T \mathbf{W}_{m,i}\mathbf{P}_{m,i} \tag{6.51}$$

$$\mathbf{B}_{m,i} = \mathbf{P}^T{}_{m,i}\mathbf{W}_{m,i} \tag{6.52}$$

where the matrices $\mathbf{P}_b$ and $\mathbf{W}_b$ are, respectively, the matrix containing the monomial bases (one for each node of the block) and the matrix containing the weights of the various nodes, given by:

$$\mathbf{P}_{m,i} = \begin{bmatrix} \mathbf{p}^T(\mathbf{x}_1) \\ \mathbf{p}^T(\mathbf{x}_2) \\ \dots \\ \mathbf{p}^T(\mathbf{x}_{N_b}) \end{bmatrix} \qquad \mathbf{W}_{m,i} = \begin{bmatrix} w_1(\mathbf{x}) & 0 & \dots & 0 \\ 0 & w_2(\mathbf{x}) & \dots & 0 \\ \dots & \dots & \dots & \dots \\ 0 & 0 & \dots & w_{N_b}(\mathbf{x}) \end{bmatrix}. \tag{6.53}$$

$N_{m,i}$ is the number of nodes of the block ($N_{m,i}$ *= 4 for square domains and 6 for rectangular domains*).

w_i is the weight function associated with the node *i*, positive for all values of x in the neighborhood including the weight function.

The choice of the weighting function is arbitrary, in this case we have chosen a quartic function (6.23). In conclusion, the link between the deformations and

displacements of the nodes of the block will be so expressed, on the basis of (6.31) and (6.33):

$$\boldsymbol{\varepsilon}_{m,i} = \mathbf{C}\boldsymbol{\Phi}_{m,i}\mathbf{u}_{m,i} \tag{6.54}$$

In this way the thirth term of the integral 6.29 can be exspressed as:

$$\sum_{i=1}^{8}\int_{\Omega_{m_i}} \boldsymbol{\sigma}_{m_i}^{T}\,\delta\boldsymbol{\varepsilon}_{m_i}\,d\Omega \tag{6.55}$$

$$\boldsymbol{\sigma}_{m_i} = \mathbf{E}_m\boldsymbol{\varepsilon}_{m,i} = \mathbf{E}_m\mathbf{C}\boldsymbol{\Phi}_{m,i}\mathbf{u}_{m,i} = \mathbf{E}_m\mathbf{C}\boldsymbol{\Phi}_{m,i}\mathbf{S}_{m_i}\mathbf{U} \tag{6.56}$$

$$\delta\boldsymbol{\varepsilon}_{m_i} = \mathbf{C}\boldsymbol{\Phi}_{m_i}\delta\mathbf{U}_{m_i} = \mathbf{C}\boldsymbol{\Phi}_{m_i}\mathbf{S}_{m_i}\delta\mathbf{U} \tag{6.57}$$

By sostituition:

$$\sum_{i=1}^{8}\int_{\Omega_{m_i}} \boldsymbol{\sigma}_{m_i}^{T}\,\delta\boldsymbol{\varepsilon}_{m_i}\,d\Omega = \sum_{i=1}^{8}\int_{\Omega_{m_i}} (\mathbf{E}_m\mathbf{C}\boldsymbol{\Phi}_{m,i}\mathbf{S}_{m_i}\mathbf{U})^{T}(\mathbf{C}\boldsymbol{\Phi}_{m_i}\mathbf{S}_{m_i})\delta\mathbf{U}\,d\Omega =$$
$$\sum_{i=1}^{8}\int_{\Omega_{m_i}} (\mathbf{E}_m\mathbf{C}\boldsymbol{\Phi}_{m,i}\mathbf{S}_{m_i}\mathbf{U})^{T}(\mathbf{C}\boldsymbol{\Phi}_{m_i}\mathbf{S}_{m_i})\delta\mathbf{U}\,d\Omega = (\sum_{i=1}^{8}\mathbf{K}_{m,i})\mathbf{U}\,\delta\mathbf{U} \tag{6.58}$$

Defining

$$\mathbf{K}_{m,i} = \int_{\Omega_{m_i}} (\mathbf{E}_m\mathbf{C}\boldsymbol{\Phi}_{m,i}\mathbf{S}_{m_i}\mathbf{U})^{T}(\mathbf{C}\boldsymbol{\Phi}_{m_i}\mathbf{S}_{m_i})\,d\Omega \tag{6.59}$$

6.2.3.3 INTERFACES

Regard to the ith interface, the tensions and deformations are linked by a bond of linear-elastic type:

$$\boldsymbol{\sigma}_{I_i} = \mathbf{E}_{I_i}\boldsymbol{\varepsilon}_{I_i} \tag{660}$$

For a generic interface i-th:

$$\boldsymbol{\varepsilon}_{I_i} = \frac{\left[\mathbf{u}_{I_i}\right]}{h_i} = \frac{\mathbf{u}_{I_i}^{+} - \mathbf{u}_{I_i}^{-}}{h_i}. \tag{6.61}$$

$$\boldsymbol{\sigma}_{I_i} = \mathbf{E}_{I_i} \frac{\mathbf{u}_{I_i}^{+} - \mathbf{u}_{I_i}^{-}}{h_i} = \mathbf{K}_{I_i} (\mathbf{u}_{I_i}^{+} - \mathbf{u}_{I_i}^{-}) = \mathbf{K}_{I_i} (\mathbf{u}_{m_i}^{+} - \mathbf{u}_{b_i}^{-}) \tag{6.62}$$

With
$$\mathbf{K}_{I_i} = \frac{\mathbf{E}_{I_i}}{h_i} \tag{6.63}$$

The interface is divided in two lines the upper border that look to the esternal domain and the botton border tha look to the block.

The displacements of the upper border are expressed as function of the external domain nodes, and the displacement of the down border are expressed as function of the block nodes.

The vector of displacements of the upper line of the interface can be expressed as a function of a matrix, rotation matrix interface i-th, according to the α angle of rotation of the interfacea and with the matrix of shape functions of the i-th interface:

$$\mathbf{u}_{I_i}^{+} = \mathbf{R}_i \boldsymbol{\Phi}_{I_i} \mathbf{U}_{I_i}^{+} \tag{6.64}$$

where:

$$\mathbf{R}_i = \begin{bmatrix} \cos\alpha & sen\alpha \\ -sen\alpha & \cos\alpha \end{bmatrix};\ \mathbf{U}_{I_i}^{+} = \begin{bmatrix} \mathbf{U}_{xI_i}^{+} \\ \mathbf{U}_{yI_i}^{+} \end{bmatrix};\ \boldsymbol{\Phi}_{I_i} = \begin{bmatrix} \boldsymbol{\varphi}_{\mathbf{I_i}} & \mathbf{0} \\ \mathbf{0} & \boldsymbol{\varphi}_{\mathbf{I_i}} \end{bmatrix} \tag{6.65}$$

As the brick, the parameters are derived using the approach meshless. It should be noted that the monomial bases are this time composed of only two elements, whereas the interfaces as one-dimensional elements (t = 1, n = 1):

$$\begin{aligned} \boldsymbol{\varphi}_{\mathbf{I_i}} &= \mathbf{p}^T \mathbf{A}_{I_i}^{-1} \mathbf{B}_{I_i} \\ \mathbf{A}_{I_i} &= \mathbf{P}_{I_i}^T \mathbf{W}_{I_i} \mathbf{P}_{I_i} \\ \mathbf{B}_{I_i} &= \mathbf{P}_{I_i}^T \mathbf{W}_{I_i} \end{aligned} \tag{6.66}$$

$$\mathbf{P}_{I_i} = \begin{bmatrix} \mathbf{p}^T(\mathbf{x}_{I_1}) \\ \mathbf{p}^T(\mathbf{x}_{I_2}) \\ \dots \\ \mathbf{p}^T(\mathbf{x}_{I_{NI}}) \end{bmatrix}; \quad \mathbf{W}_{I_i} = \begin{bmatrix} w_{I_1}(\mathbf{x}) & 0 & \dots & 0 \\ 0 & w_{I_2}(\mathbf{x}) & \dots & 0 \\ \dots & \dots & \dots & \dots \\ 0 & 0 & \dots & w_{I_{NI}}(\mathbf{x}) \end{bmatrix}. \tag{6.67}$$

where N_I is the total number of nodes on the edge bound i-th interface ($N_I = 3$) and

$$\begin{aligned} \mathbf{p}^T(\mathbf{x}_{I_i}) &= [1 \quad x_i] \text{ for horizontal interfaces} \\ \mathbf{p}^T(\mathbf{x}_{I_i}) &= [1 \quad y_i] \text{ for vertical interfaces} \end{aligned} \tag{6.68}$$

Using the formulation 6.29 the second integral term can be exspressed in the follow passages.

$$\sum_{i=1}^{4} \int_{\Omega_{I_i}} \boldsymbol{\sigma}_{I_i}^T \delta\boldsymbol{\varepsilon}_{I_i} d\Omega \tag{6.69}$$

$$\boldsymbol{\sigma}_{I_i} = \mathbf{K}_{I_i}(\mathbf{u}_{m_i}^+ - \mathbf{u}_{b_i}^-) = \mathbf{K}_{I_i}\mathbf{R}_i\boldsymbol{\Phi}_{I_i}\mathbf{S}_{mI_i}\mathbf{U} - \mathbf{K}_{I_i}\mathbf{R}_i\boldsymbol{\Phi}_{I_i}\mathbf{S}_{bI_i}\mathbf{U}$$

(6.70)

$$\begin{aligned} &\delta\boldsymbol{\varepsilon}_{I_i} = \delta(\mathbf{u}_{m_i}^+ - \mathbf{u}_{b_i}^-) = \delta\mathbf{u}_{m_i}^+ - \delta\mathbf{u}_{b_i}^- = \\ &\mathbf{R}_i\boldsymbol{\Phi}_{I_i}\mathbf{S}_{mI_i}\delta\mathbf{U} - \mathbf{R}_i\boldsymbol{\Phi}_{I_i}\mathbf{S}_{bI_i}\delta\mathbf{U} = (\mathbf{R}_i\boldsymbol{\Phi}_{I_i}\mathbf{S}_{mI_i} - \mathbf{R}_i\boldsymbol{\Phi}_{I_i}\mathbf{S}_{bI_i})\delta\mathbf{U} \end{aligned} \tag{6.71}$$

$$\begin{aligned} &\sum_{i=1}^{4} \int_{\Omega_{I_i}} \boldsymbol{\sigma}_{I_i}^T \delta\boldsymbol{\varepsilon}_{I_i} d\Omega = \\ &\sum_{i=1}^{4} \int_{\Omega_{I_i}} (\mathbf{R}_i\boldsymbol{\Phi}_{I_i}\mathbf{S}_{mI_i}\mathbf{U} - \mathbf{R}_i\boldsymbol{\Phi}_{I_i}\mathbf{S}_{bI_i}\mathbf{U})^T \mathbf{K}^T{}_{I_i}(\mathbf{R}_i\boldsymbol{\Phi}_{I_i}\mathbf{S}_{mI_i} - \mathbf{R}_i\boldsymbol{\Phi}_{I_i}\mathbf{S}_{bI_i})\delta\mathbf{U}d\Omega \end{aligned} \tag{6.72}$$

By develop all the product we obtain 4 matrices. **K**mm **K**bm **K**mb **K**bb

The contribute relative to the i-th interfaces is obtained as:

$$\mathbf{K}\text{i}=\mathbf{K}\text{mm}-\mathbf{K}\text{mb}-\mathbf{K}\text{bm}+\mathbf{K}\text{bb} \tag{6.73}$$

6.2.3.4 SYSTEM RESOLUTION

Bourdary conditions

The resolution of sistem require also the bourdary conditions. The boundary conditions in the Γ, are the nodal displacements of the external nodes. In particular the matrix of address allows to select among all the displacements imposed.

In order to esplicit term 4 and 5 of the integral 6.29, is need to use address matrix for each node, and to determine by meshless approach the shape function of the closed nodes to the considered restained node.

The integral is:

$$\sum_{j=1}^{nblocked} \boldsymbol{\lambda}_j^T \delta \mathbf{u}_j + \sum_{j=1}^{nblocked} \delta \boldsymbol{\lambda}_j^T (\mathbf{u}_j - \bar{\mathbf{u}}_j) \tag{6.74}$$

Using the meshless approach

$$\mathbf{u}_j = \boldsymbol{\Phi}_{m,j} \mathbf{U}_{m,j} = \boldsymbol{\Phi}_{m,j} \mathbf{S}_{m,j} \mathbf{U} \tag{6.75}$$

Sotituiting:

$$\sum_{j=1}^{nblocked} \boldsymbol{\lambda}_j^T \boldsymbol{\Phi}_{m,j} \mathbf{S}_{m,j} \delta \mathbf{U} + \sum_{j=1}^{nblocked} \delta \boldsymbol{\lambda}_j^T (\boldsymbol{\Phi}_{m,j} \mathbf{S}_{m,j} \mathbf{U} - \mathbf{S}_{m,j} \bar{\mathbf{U}}) \tag{6.76}$$

Using this approach, and assembling the before defined matrix we obtain a system as the follow:

$$\begin{bmatrix} \mathbf{K} & \mathbf{S}^T{}_{m,j} \boldsymbol{\Phi}^T{}_{m,j} \\ \boldsymbol{\Phi}_{m,j} \mathbf{S}_{m,j} & \mathbf{0} \end{bmatrix} \begin{bmatrix} \mathbf{U} \\ \boldsymbol{\lambda} \end{bmatrix} = \begin{bmatrix} 0 \\ \bar{\mathbf{U}} \end{bmatrix} \tag{6.77}$$

$$\mathbf{K} = \mathbf{K}_b + \mathbf{K}_m + \mathbf{K}_{I,mm} + \mathbf{K}_{I,bb} - \mathbf{K}_{I,mb} - \mathbf{K}_{I,bm} \tag{6.78}$$

In our case K is a 66x66 and the restrained node depends of the restrained conditions. λ are the vincolar reactions.

6.3 MULTISCALE ANALYSIS

As explained in the previous sections, it is evaluable how multi scale approach can better reach the goal how modeling behavior of heterogeneous materials below ultrasonic stress wave.

To verifiy how muliscale approach can help the modeling of ultrasonic wave propagation in heterogeneous materials the follow steps are conducted:

1 An periodic herogeneous material stressed by ultrasonic waves is modeled by using FEM method.
2 The cell of periodic material is modeled by using a meshless approach and the RVE implemented, and from it an elastic matrix for homogeneizated material is determined, in elastic status.
3 The heterogeneous periodic material is modeled in FEM as homogeizated anisotropic material using as material properties the elastic constants detected from step 2.
4 Ultrasonic wave of stress are applied at the homogeneizated model.
5 Results of heterogeneous FEM model e multiscale models are comparated

STEP 1 FEM ANALISYS OF HETEROGENEOUS

At the mesoscale considered the model developed is a grain of aggregate of 2x2mm of square shape in a square contour of dough of cement of 5x5mm. To follow the way of simulations implemented in chapter 5, a FEM model is implemented using this an heterogeneous periodic model, in figure 6.5 the elementary cell in FEM is reported.

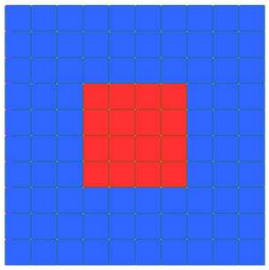

Figure 6.5 Elementary cell with aggregate and dough.

In the table 6.1 are reported some characteristics of the model.

Properties		
Total surface	150x150	22500 mm^2
Side of inclusion	2x2	4 mm^2
Numer of inclusion	28rows x 28	784
Inclusion area	4x784	3.136
Matrix area	22500-3.136	19.364
A inclusion/Atot	3.136/22.500	13.94%
A inclusion/A matrix	5.684/19.364	24.18%

(a)

In CENTRAL LINE			
D total		150mm	
L inclusion	28x2	56mm	37.3%
L matrix	150-56	94mm	62.7%

(b)

Table 6.1 Geometrical properties of heterogeneous model

(a) Surface properties (b) linear properties

For the aggregate the properties are hold constant E=100 GPa and ν=0.12, for the matrix of dough and for the interface ar choosen in fistra analysis same values of elastic constant in order to simulate the properties of cement dought. The values of E are 50 GPa, ν = 0.2.

Mesh dimention is d=0.5mm, in order with rules of propagation wave frequency in elastic media. The model is a plate of 150x150mm, as tranversal section of concrete specimen. For a total of 900.000 plate elements

Simulations are conducted by applying a ultrasonic stress wave as sinusoidal 3cycle wave as concentraded forces in a 60mm central lefht border, as dimention of fisical probles; sinusoidal action is with positive sign oscilations between a force of 75KN and zero, applied in 300 nodes [60mm/(d=0.5mm)=300].

In the opposite border, the righ one, the model is restained by fixed hinger at the central node, and with vertical hinger in others node for a extenction of 60mm.

Horizontal reactions are detected in 51 nodes, (force are detected in the central righ side node and on 25 node upper and down the center, by alternate nodes, for an extention of 50mm, (25+25)x2*0.5mm).

The frequencies investigated are 100-150-200-250-300-350-400-500 KHz, reactions are processed using signal processing algorithm developed in chap. 4.

STEP 2 MESOSCALE

Using the meshless method the cell model is implemented in matlab. In order to homogeneizate the heterogeneous material it is choosen to model the heterogeneous material as an homogeneous anisotropic material. The

caracheristics of the anisotropic material, in stress plane are defined if it is defined its stiffness matrix. $\begin{bmatrix}\sigma_x\\ \sigma_y\\ \tau_{xy}\end{bmatrix}=\begin{bmatrix}E_1 & E_{12} & 0\\ E_{21} & E_2 & 0\\ 0 & 0 & G\end{bmatrix}.\begin{bmatrix}\varepsilon_x\\ \varepsilon_y\\ \gamma_{xy}\end{bmatrix}$

The elastic constants are determined, for the proposed cell, by imposing assigned displacement at the border of cell, and to determine them. The matrix is:

$$\begin{bmatrix}51.8 & 9.2 & 0\\ 9.2 & 51.8 & 0\\ 0 & 0 & 20.06\end{bmatrix}[GPa]$$

The elastic constants are determined to imposing the state of deformation x=1 y=1 and =1. To perform how the behavior of cell is according with the behavior of heterogeneous modeling, the two models, as shown in figures 6.6 and 67, the heterogeneous one and the homogeneizated are analized by FEM using a same action tensile state a thte righ border, and the same retained condition fixed hinger at the lefth border. It is need to specify that in FEM model not are considered the interfaces. In figure 6.8 state of displacement and stress are reported.

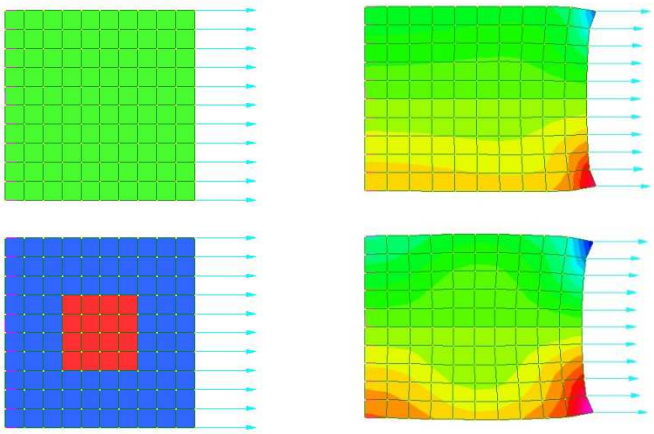

Figure 6.7 homogeneizated and heterogeneous RVE

(b) state of stress (c)state of displacements

by using as material the properties deducted by the adopted RVE the FEM simulations are reconducted. In the figure 6.8 are shown the signals at the frequency of 100-200 and 500kHz, using the heterogeneous model in FEM and the multiscale model in ML at the masoscale and in FEM at the macroscale.

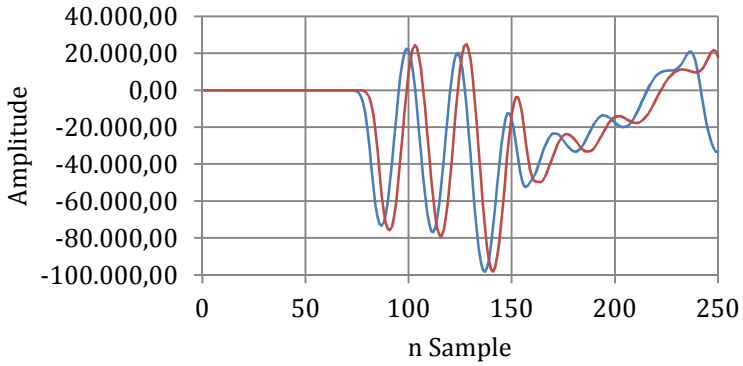

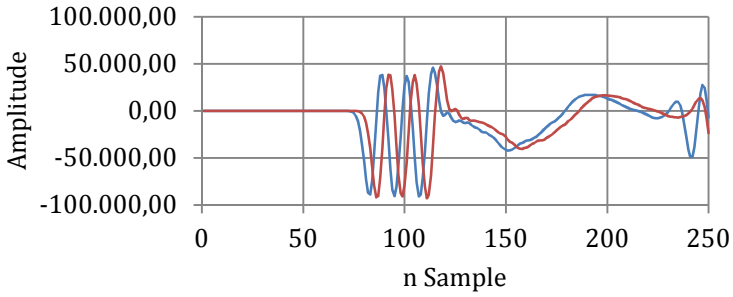

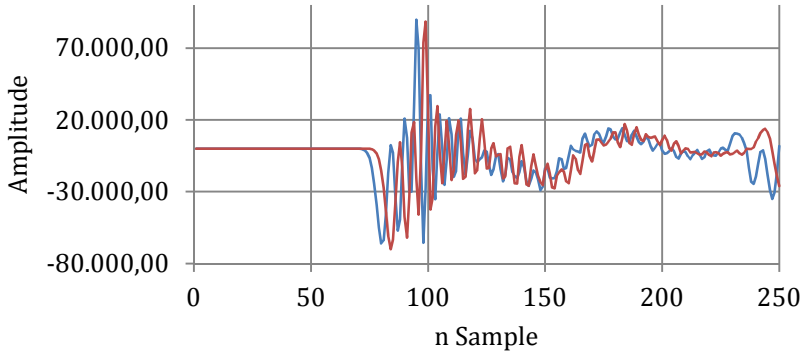

Figure 6.8 Signals at the frequency 100-200-500KHz, (blue) FEM (red) M.SCALE

The signal determined by multiscale analysis is more slow respect the one in fem method, that maybe is related with the major deformability of the system with interfaces, that generate a late of signal. A parametric study on interface mechanical preoperty should be need to evaluate how propagation of wave is influenced.

In table 6.2 are reported results in term of velocity of propagation wave, and the index of FFT, in relation at the frequencies, the velocity of wave is increasing according with the increasing of elastic module of matrix, and with the frequency.

	FEM		M.SCALE	
frequency	Velocity [m/s]	I_ω	Velocity [m/s]	I_ω
100	5434,8	0,65	5137,0	0,59
150	5208,3	0,78	4934,2	0,72
200	5067,6	0,88	4807,7	0,79
250	5000,0	0,92	4746,8	1,00
300	4411,8	1,00	4687,5	0,89
350	4464,3	0,97	4261,4	0,86
400	4464,3	0,95	4261,4	0,87
500	4166,7	0,87	4076,1	0,06

Table 6.2 Velocity and I_ω for stress wave in heterogeneous model

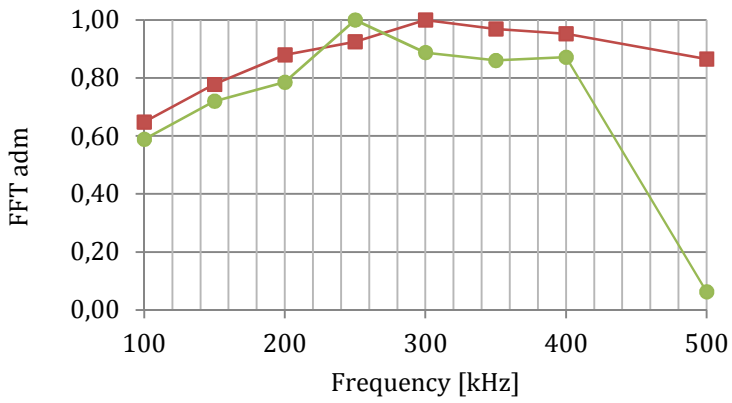

Figure 6.9 Iω (square dot) FEM (circle dot)M.SCALE

The velocity of wave computed using the FEM model is similar to the velocity computed by M.SCALE with error of 5% and the resontant frequency maintain similar values 250-300KHz.

The follow figure 6.11 shown the state of stress of the propapation wave at the step 10 (t $4x10^{-6}$ s)and step 60 ($2.4x10^{-5}$ s), in both conditions with heterogeneous model and with homogeneizated models. It is appreciable the shape of wave in heterogeneous model around the grains, and the uniformity in global terms of the two responces.

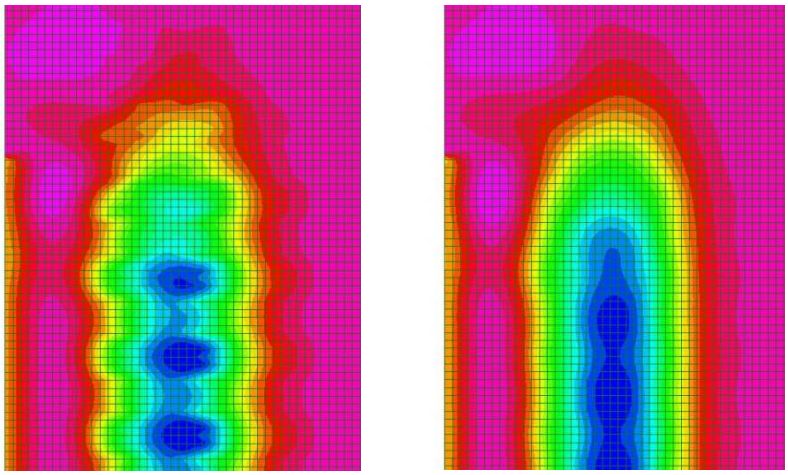

Figure 6.10 State of stress for heterogeneous and homogeneizated model close to the applicatition load area at the frequency of 300KHz, step 10 ($t=4*10^{-6}$ s)

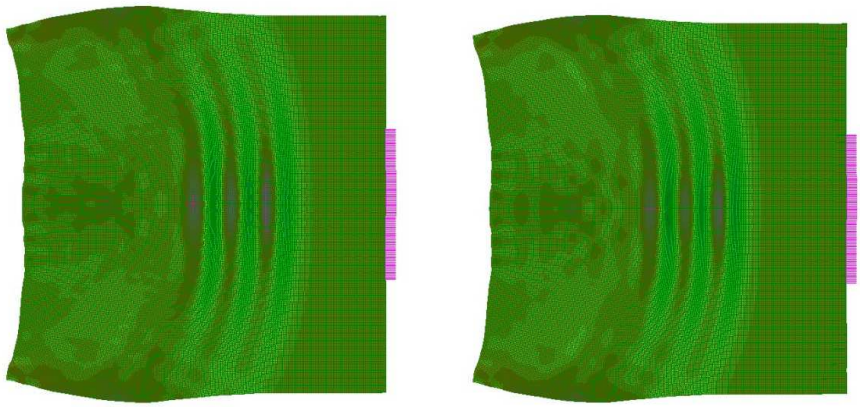

(a) (b)

Figure 6.11 State of stress for heterogeneous model (a) and for homogeneizated model (b) at the frequency of 300KHz, step 60 ($t=2.4*10^{-5}$ s)

In this proposal the elastic properties of inferfaces are assumed equal with the properties of the external domains, and the dimention of interfaces is assumed as 0.5mm. If it will be considered as interface a soft or a hard material we will obtain an elastic matrix with less stiff or more stiff of the considerd one.

Assuming E_{aggr}=100GPa E_{ext}=50GPa, $E_{interf.}$=12.5GPa the Elastic matrix become:

$$\begin{bmatrix} 46.09 & 8.60 & 0 \\ 8.60 & 46.09 & 0 \\ 0 & 0 & 19.04 \end{bmatrix} [GPa]$$

Assuming E_{aggr}=100GPa E_{ext}=50GPa, $E_{interf.}$=100GPa the Elastic matrix become:

$$\begin{bmatrix} 53.68 & 9.58 & 0 \\ 9.58 & 53.08 & 0 \\ 0 & 0 & 21.26 \end{bmatrix} [GPa]$$

It should be relevant to obtain the wave velocity of wave in a FEM model using these elastic constants. The simulations were been conducted assuming signal frequency of 200kHz. For the soft interfaces case the velocity of wave is 4807 m/s, and for the hard interfaces case the velocity is 5281[1] m/s.

By using the theoric model proposed in chapter 5 the velocity is calculated. To use this approach is need to know the poisson coefficent. In order to determine it, for each case, a ratio between Ey/Ex is operated. So it is assumed that the wave is propagated in the median path, the elastic constant of the path material is egual to E_L. in table 6.3 results are reported.

Also simulation are conducted using distribution of density by the heterogeneous model and using an uniform density deducted form the follow expression, considerind the weight of a RVE.

$$\gamma_{average} = \frac{A_{inclusion}}{A_{total}} \gamma_{inclusion} + \frac{A_{matrix}}{A_{total}} \gamma_{matrix}$$

[1] The velocity here are determined using a threshold method

And we obtain $\gamma_{average} = \frac{2x2}{5x5}1600 + \frac{5x5 - 2x2}{5x5}2500 = 2356 kg/m^3$

Simulations in FEM conducted by using the two different densities gave the same results.

	Velocity [m/s]		
FEM	5514		
Interfaces $[E_{matrix}/E_{interf}]$	**Soft [4:1]**	**Same [1:1]**	**Hard [1:2]**
M.SCALE	4807	5208 (5.54% by FEM)	5281
Theoric model	4842	5123	5212
Elastic property	ν= 0.183 El=46.09GPa	ν= 0.179 El=51.80GPa	ν= 0.178 El=53.68 GPa
Error theoric /M.Scale	0.74%	1.65%	1.31%

Table 6.3 Comparison between FEM, M.SCALE and teoric velocity

The 2 deformation states of the RVE are reported in the follow 2 figures. The white space between the inclusion and external blocks are the interfaces.

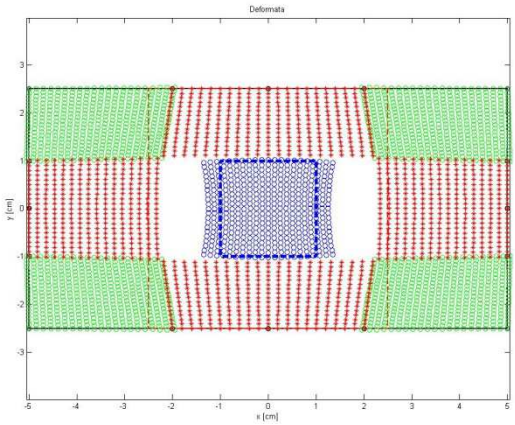

(a)

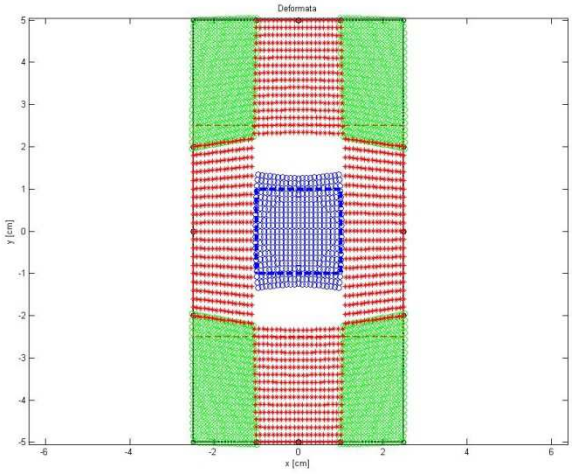

(b)

Figure 6.13 Deformation states of RVE (a)ε_x=1 (b) ε_y=1

...E quindi uscimmo a riveder le stelle.
…and we emerged to gaze upon the stars again.
A. Dante

CHAPTER 7

CONCLUSIONS AND REMARKS

In this thesis investigations on heterogeneous materials are conducted by means of ultrasonic wave techniques. The UW is one of the most common methods used to investigate the internal nature of a material with a non destructive approach.
Like other NDT tests, the results are deducted by correlation curves, and never directly deducted. In this work some features of ultrasonic signals were analyzed depending on whether or not they are influenced by the characteristics of heterogeneous materials. In order to achieve this objective a specific study on concrete was conducted.
The study considered concrete as in two phases, the fresh and the hardened phase. Ultrasonic tests were conducted during both states.

7.1 DEVICES AND ISTRUMENTATIONS

Ultrasonic tests were carried out using a specific prototype of instrumentation developed and realized at the University of Palermo during the doctoral years. This is an ultrasonic pulse and acquisition machine with high performances. It is able to generate generic shape waveforms with frequency ranging form 1kHz to 12.5MHz so that a large number of materials can be tested. The device uses 4 channels to acquire data in live modality with a maximum simple frequency of 100 Msps. The machine, named *Pulser Pro*, is accompanied by an open source software modifiable depending on the necessity of the test. Some others tools are available together

with the machine: 4 probes with 500 kHz central frequency, an instrumental hammer, two horizontal frames to hold the specimen during the tests.

NDT investigation was conducted on fresh concrete and on hard concrete. Concrete specimens were cast after the definition of a specific mix design. To achieve this scope the ACI 201.1-91 guideline was used. Tables and interpolation curves were processed and deducted directly from the rule. Using the curves, an algorithm was written to define the mix design of concrete. This software was implemented using Matlab® Graphical Tool and permits to quickly obtain the response under assigned parameters.

An original acquisition procedure and a signal processing algorithm were developed to investigate Heterogeneous materials using UW method. Properties of heterogeneous materials are analyzed studying the sweep of frequencies to develop the frequency for which the material is more sensible. It is possible acquiring data in continuum for some days.

A strong signal processing is implemented using Matlab® software. The data are processed in time and frequency domains. Specific Mathematical Tools are used: Cross Correlation for analysis in time domain and Fourier transform for analysis in Frequency domain. In order to compare the data acquired a normalization procedure is proposed, based on a baseline of the digital signals where the same frequency of ultrasonic signals is considered. Process of de-noising by mean, windowing, and zero padding are procedures used for strong analisys of feature extraction of signals.

7.2 FRESH CONCRETE

A number of fresh concrete specimens were made.

On fresh concrete, tests were conducted for a set of 15-20 days, with the objective to deduct maturation curves of concrete during the fresh time, and to understand

how ultrasonic wave features are related to the properties of concrete. Some matters were treated and solved, others are still unresolved. It was very complicate to conduct the ultrasonic tests in continuous after few hours of curing time after until the conventional time of 28 days. Difficulty was related to the necessity to set probes in contact with a fresh concrete. The problem was solved using some gels in order to aid the transmission of signal between probes and materials. Besides, when the concrete becomes hard, the shrinkage causes the detachment of probes from the material. However after 6-10 hours from the casting and until 15-20 days the tests are performed well.

Tests in space time permitted to note that wave velocity of is rapidly increasing with time in the first 1-3 days after casting. Beyond this time the curve has a sub horizontal zone and becomes quite stable with a light tilt. This denotes that the main part of maturation is developed in the first 48-72 hours of casting. During this time the elastic properties of concrete are defined and going to increase, but the velocity of increasing is pretty slow. It is also possible to appreciate that the curve is not going in a plateau zone, but the little slope is stable, indicating that the maturation time is not at the end even at 28 days, but it can go on for many another days.

To characterize concretes with different mix design, some specimens were tested during the maturation time, and elastic modules and resistances were measured. They were deducted from mechanical direct tests or using normative rules on the base of the ultimate load, or by using ultrasonic techniques. In all considered cases it was asserted that the differences between the measures were acceptable, and the dynamic module was about 30% more than the static modules.

Analyses in frequency domain indicated that a resonant frequency measurable in each specimen was pretty different for specimens coming even from the same dough. The value of resonant frequency can be reached after few days after casting, and it becomes stable for all the maturation time. It is clear that this property is not

related with other properties such as elastic module or resistance, but it depends on composition or grade of mixture. The range of resonant frequency is still held between 150KHz and 250KHz. It was supposed that the volume of material interested by ultrasonic wave can have different arrangements in terms of aggregates. This can explain why in the considered cases the dynamic behavior is different. A micro structural approach can be invoked to understand why resonant frequency can vary with changing of material properties.

7.3HARDENED CONCRETE

Ultrasonic tests were conducted on hardened concrete. A number of 70 cubes was tested using the proposed algorithm and destructive tests to measure the resistance. The population of signals was processed in time space and in frequency space. In time space the standard velocity of waves was deducted and a relation between resistance and velocity was considered. It is quite accepted that the correlation between the two variables is really low. The data are so dispersive in the velocity-resistance diagram that it was pretty hard to predict resistance on the base of the waves velocity only. A more exact analysis was conducted in the frequency space. It was observed that when the concrete is compact and the resistance is high, then the resonance frequency is high; instead if the concrete appears porous and with low resistance, then the resonant frequency is low or dispersive.

Tests were conducted along two orthogonal directions of a cubic specimen. Regarding the wave velocity, it is possible to assert that any dispersion there is in the two measurements. Different is the behavior in the frequency analysis. For the same specimen the resonant frequency can be enough different along the two orthogonal directions, especially if concrete has low quality.

Using data in the frequency space, a clustering analysis was conducted on them. Using clustering analysis it was possible to attain a prevision of the resistance value for concrete. The predicted value was close to that one deducted with destructive testing, with an error equal to 6 MPa. It is relevant to appreciate that the similar result could be obtained using a small population of data, but the use of a larger amount of data can led to better results.

7.4 NUMERICAL SIMULATIONS

Numerical simulations were conducted in order to predict experimental results, paying attention on how the main features of waves are influenced during their propagation by the characteristics of the heterogeneous medium.

The input signal used to run the simulation was selected from some literature reference while the application points and outgoing points are chosen to follow the physical models. Five different models were implemented: four with a homogeneous matrix and different arrangements of inclusions; one homogeneous. A parametric analysis is conducted by varying the ratio of elastic properties of inclusion and matrix, and the frequency of signals. The output signals detected by the numerical model were processed using the proposed algorithm and the results were diagrammed. It was verified that the wave velocity increases by increasing of the inclusion percentage. An elementary model was also proposed to validate the propagation of waves in heterogeneous media calculating a weighted mean of wave velocity in each part of materials. The model proposed considers the propagation of wave only in the linear path from generator to receiver probes. The error between numerical and analytical model was less than 10%. Analyses in frequency domain evidenced the increment of frequency with the increment of hardened phase in the heterogeneous materials, and the plateau of FFT curves when the percentage of inclusion increases. Elastic dynamic tests were simulated.

It is relevant to note that the resonant frequency is related to the length of the resonant wave. In particular it is appreciable but still not demonstrated that the resonant frequency is related to the length of the wave that is able to pass through all grains and that reaches the opposite probe with the lowest dispersion. The measure of a resonant frequency could be related with the presence of some size grains or a particular arrangement of grains with dimension close to the wavelength associated to the resonance frequency of the wave. A multiscale model was proposed using a meshless approach. A RVE was defined considering an elastic cell with elastic inclusion and elastic interfaces. A new finite element simulation was conducted using an homogeneous mesh but employing elements made of anisotropic material and the result compared with those obtained with mesoscopic analyses. Results in terms of frequency showed an error less of 5%.

7.5 FUTURE ASPECTS

The present work wants be a pioneer work on an innovative ultrasonic method applied to test materials. All of us know the oldness of concrete and the studies conducted on it. This work considers concrete as a common heterogeneous material at the mesoscale; a material easy of realize and to control due to the proved knowledge.

Ultrasonic tests are one of well-advanced techniques used to investigate metallic materials, but it is not well explained their applicability on stones or heterogeneous materials yet.

Future works should be based on a larger number of mix designs with a better control of grain size, so to better investigate how frequency is influenced by heterogeneity. A good job could be made using a mono-dimensional size of grains (better if with spherical shape, to limit the dispersion of wave on the tips).

The problem related with shrinkage and with the initial stage of concrete should be accurately investigated to find an opportune methodology to acquire data during all 28 days of curing.

Tests on hardened concrete require the extension of the population of considered data, and should be based on other methods that can perform better with respect to Clustering analysis, as ANN, or learning algorithms.

Numerical simulations need to be implemented considering the multiscale model and an extended campaign of parametric simulations. A theoretical study based on a microstructural approach to the phenomena needs to be conducted. The multiscale approach proposed permits to expand analysis with different arrangements of inclusion not only in classic periodic continua. It is possible to define an *elasto-plastic behaviour of RVE* or *interfaces*. It could be relevant to solve the problem related with the dissipation of energy, trying to understand which terms have to be introduced or modified into the model.

ANNEX A

RULES

This appendix would like to give an point of view on international rules, on the principal aspect treated in this text.

First of all, it is worth to note that ultrasonic devices are ruled by the UNI standard. The follow list report the UNI EN 12668 part1-4 (A.1) that determine devices properties, the UNI EN 583 part 1-6 that fixed the method of tests, UNI EN 14127 and 15317 give specification for thin measurement

For concrete is relevant to cite the rules used for the characterization of aggregates, the UNI EN 933 part 1-11 (A.2) define all aggregate properties. To give a view on concrete aggregates other two rules are proposed (A.3) the UNI EN 12620 and the UNI EN 8520 part 1-2, in American field C33 determine the aggregate properties, and the ACI211.1-91 give an algorithm to calculate a mix design (A.4). The *casting* of concrete is ruled form UNI-EN 206-1 and UNI 11104 (A.5) , UNI EN 1008 give some advertisement on water. Follow a set of test can be conducted in *fresh concrete* (A.6), they are rules form UNI EN 12350 part 1-7 for classic concrete, for part 8-12 for self compacting concrete, it is worth to sub line the most common tests for fresh concrete:

Abrams cone	12350/2 vebe' disk12350/3
Compactability	12350/4 spanding 12350/5
Density	12350/6 porosity 12350/7

After the cast the hardened concrete can be subjected by testing. The UNI EN 12390 part 1-10 (A.7) describe how testing have to be conducted. The follow table shown the more used tests.

12390/1	casting	12390/2	curing
12390/3-4	compression	12390/5	bending test
12390/6	traction	12390/7	water permeability
12390/6	traction	12390/7	density
12390/8	water permeability	12390/9	frosting resistance
12390/10	carbonizations	11307	shrinkage
7699	water absorption	11164	oxygen absorption

Frequently, in test phase, it is need to probing the concrete (A.8), the UNI - 12504/1-12504/3 (cylindrical probing) 10157-10766 (micro probing) 6131 (pull out) define how to extract the probe, ratio b/h can be 1:1 or 1:2 in order to have a relationship with cubic resistance.

The ruled non destructive tests are the hammer test by UNI EN 12504/2 and ultrasonic test by UNI EN 12504/4 (A.9).

Structural design (A.10) of concrete element is determined by Eurocode 2 for European country and ACI 318-1 for USA country. Fire protection for concrete structure in the lasts years is a care aspect of design, the UNI EN 13381 fixed some aspect of the cover bars.

A.1 Ultrasonic devices

- UNI EN 12668-1:2010 Prove non distruttive - Caratterizzazione e verifica delle apparecchiature per esame ad ultrasuoni - Parte 1: Apparecchi
- UNI EN 12668-2:2010 Prove non distruttive - Caratterizzazione e verifica delle apparecchiature per esame ad ultrasuoni - Parte 2: Sonde

- UNI EN 12668-3:2005 Prove non distruttive - Caratterizzazione e verifica delle apparecchiature per esame ad ultrasuoni - Parte 3: Apparecchiatura completa
- UNI EN 583-1:2004 Prove non distruttive - Esame ad ultrasuoni - Parte 1: Principi generali
- UNI EN 583-2:2004 Prove non distruttive - Esami ad ultrasuoni - Parte 2: Regolazione della sensibilità e dell'intervallo di misurazione della base dei tempi
- UNI EN 583-3:1998 Prove non distruttive - Esame ad ultrasuoni - Tecnica per trasmissione
- UNI EN 583-4:2004 Prove non distruttive - Esame ad ultrasuoni - Parte 4: Esame delle discontinuità perpendicolari alla superficie
- UNI EN 583-5:2004 Prove non distruttive - Esame ad ultrasuoni - Parte 5: Caratterizzazione e dimensionamento delle discontinuità
- UNI EN 583-6:2009 Prove non distruttive - Esame ad ultrasuoni - Parte 6: Tecnica a diffrazione del tempo di volo come metodo di rilevamento e dimensionamento delle discontinuità
- UNI EN 14127:2004 Prove non distruttive - Misurazione dello spessore mediante ultrasuoni
- UNI EN 15317:2007 Prove non distruttive - Esame a ultrasuoni - Caratterizzazione e verifica dell'apparecchiatura per la misurazione dello spessore mediante ultrasuoni

A.2 Aggregates properties

- UNI EN 933-1:2012-Prove per determinare le caratteristiche geometriche degli aggregati - Parte 1: Determinazione della distribuzione granulometrica - Analisi granulometrica per setacciatura
- UNI EN 933-2:1997 Prove per determinare le caratteristiche geometriche degli aggregati - Determinazione della distribuzione granulometrica - Stacci di controllo, dimensioni nominali delle aperture.
- UNI EN 933-3:2012 Prove per determinare le caratteristiche geometriche degli aggregati - Parte 3: Determinazione della forma dei granuli - Indice di appiattimento
- UNI EN 933-4:2008 Prove per determinare le caratteristiche geometriche degli aggregati - Parte 4: Determinazione della forma dei granuli - Indice di forma
- UNI EN 933-5:2006 Prove per determinare le caratteristiche geometriche degli aggregati - Parte 5: Determinazione della percentuale di superfici frantumate negli aggregati grossi
- EC 1-2006 UNI EN 933-6:2003 Prove per determinare le caratteristiche geometriche degli aggregati - Valutazione delle caratteristiche superficiali - Coefficiente di scorrimento degli aggregati
- UNI EN 933-7:2000 Prove per determinare le caratteristiche geometriche degli aggregati - Determinazione del contenuto di conchiglie - Percentuale di conchiglie negli aggregati grossi
- EC 1-2013 UNI EN 933-8:2012 Prove per determinare le caratteristiche geometriche degli aggregati - Parte 8: Valutazione dei fini - Prova dell'equivalente in sabbia

- UNI EN 933-9:2009 Prove per determinare le caratteristiche geometriche degli aggregati - Parte 9: Valutazione dei fini - Prova del blu di metilene
- UNI EN 933-10:2009 Prove per determinare le caratteristiche geometriche degli aggregati - Parte 10: Valutazione dei fini - Granulometria dei filler (setacciatura a getto d aria)
- EC 1-2010 UNI EN 933-11:2009 Prove per determinare le caratteristiche geometriche degli aggregati - Parte 11: Prova di classificazione per i costituenti degli aggregati grossi riciclati

A.3 concrete aggregate

- UNI EN 12620:2008 Aggregati per calcestruzzo
- UNI 8520-1:2005 Aggregati per calcestruzzo - Istruzioni complementari per l applicazione della EN 12620 - Parte 1: Designazione e criteri di conformità
- UNI 8520-2:2005 Aggregati per calcestruzzo - Istruzioni complementari per l applicazione della EN 12620 - Requisiti
- ASTM C33 Standard Specification for Concrete Aggregates1

A.4 Mix design

- ACI 211-1. 91 Standard Practice for Selecting Proportions for Normal, Heavyweight, and Mass Concrete

A.5 Casting

- UNI EN 1008:2003 Acqua d impasto per il calcestruzzo - Specifiche di campionamento, di prova e di valutazione dell'idoneità dell'acqua,

incluse le acque di ricupero dei processi dell'industria del calcestruzzo, come acqua d impasto del calcestruzzo

- UNI EN 206-1 Calcestruzzo - Parte 1: Specificazione, prestazione, produzione e conformità
- UNI 11104:2004 Calcestruzzo - Specificazione, prestazione, produzione e conformità - Istruzioni complementari per l applicazione della EN 206-1

A.6 Fresh concrete

- UNI EN 12350-1:2009 Prova sul calcestruzzo fresco - Parte 1: Campionamento
- UNI EN 12350 -2:2009 Prova sul calcestruzzo fresco. Prova di abbassamento al cono
- UNI EN 12350-3:2009 Prova sul calcestruzzo fresco - Parte 3: Prova Vébé
- UNI EN 12350-4:2009 Prova sul calcestruzzo fresco - Parte 4: Indice di compattabilità
- UNI EN 12350-5:2009 Prova sul calcestruzzo fresco - Parte 5: Prova di spandimento alla tavola a scosse
- UNI EN 12350-6:2009 Prova sul calcestruzzo fresco - Parte 6: Massa volumica
- UNI EN 12350-7:2009 Prova sul calcestruzzo fresco - Parte 7: Contenuto d aria - Metodo per pressione

- EC 1-2011 UNI EN 12350-8:2010 Prova sul calcestruzzo fresco - Parte 8: Calcestruzzo autocompattante - Prova di spandimento e del tempo di spandimento
- EC 1-2011 UNI EN 12350-9:2010 Prova sul calcestruzzo fresco - Parte 9: Calcestruzzo autocompattante - Prova del tempo di efflusso
- EC 1-2011 UNI EN 12350-10:2010 Prova sul calcestruzzo fresco - Parte 10: Calcestruzzo autocompattante - Prova di scorrimento confinato mediante scatola ad L
- NI EN 12350-11:2010- Prova sul calcestruzzo fresco - Parte 11: Calcestruzzo autocompattante - Prova di segregazione mediante setaccio
- EC 2-2012 UNI EN 12350-12:2010 Prova sul calcestruzzo fresco - Parte 12: Calcestruzzo autocompattante - Prova di scorrimento confinato mediante anello a J
- UNI 7122:2008 Prova sul calcestruzzo fresco - Determinazione della quantità d acqua d impasto essudata
- UNI 11201:2007 Prove sul calcestruzzo fresco - Determinazione del contenuto di acqua
- UNI 7123:1972 Calcestruzzo. Determinazione dei tempi di inizio e fine presa mediante la misura della resistenza alla penetrazione.

A.7 Hardened concrete

- UNI EN 12390-1:2002 – Prova sul calcestruzzo indurito. Forma, dimensioni ed altri requisiti per provini e per casseforme.

- UNI EN 12390-2:2002 – Prova sul calcestruzzo indurito. Confezione e stagionatura dei provini per prove di resistenza.
- UNI EN 12390-3:2003 – Prova sul calcestruzzo indurito. Resistenza alla compressione dei provini.
- UNI EN 12390-4:2002 – Prova sul calcestruzzo indurito. Resistenza alla compressione - Specifiche per macchine di prova.
- UNI EN 12390-5:2002 – Prova sul calcestruzzo indurito. Resistenza a flessione dei provini.
- UNI EN 12390-6:2002 – Prova sul calcestruzzo indurito. Resistenza a trazione indiretta dei provini.
- UNI EN 12390-7:2002 – Prova sul calcestruzzo indurito. Massa volumica del calcestruzzo indurito.
- UNI EN 12390-8:2002 – Prova sul calcestruzzo indurito. Profondità di penetrazione dell'acqua sotto pressione
- UNI EN 12390-9:2006 -Prova sul calcestruzzo indurito. Resistenza al gelo-disgelo - Scagliatura
- UNI EN 12390-10:2008 Prova sul calcestruzzo indurito. Determinazione della resistenza relativa alla carbonatazione del calcestruzzo
- UNI 11307:2008 Prova sul calcestruzzo indurito - Determinazione del ritiro
- UNI 7699:2005 Prova sul calcestruzzo indurito - Determinazione dell'assorbimento di acqua alla pressione atmosferica
- UNI 11164:2005 Calcestruzzo - Determinazione della permeabilità all'ossigeno

A.8 Probing

- UNI 6131:2002 – Prelevamento campioni di calcestruzzo indurito.
- UNI 10157:1992 – Calcestruzzo indurito. Determinazione della forza di estrazione mediante inserti post-inseriti ad espansione geometrica e forzata.
- UNI 10766:1999 – Calcestruzzo indurito. Prove di compressione su provini ricavati da microcarote per la stima delle resistenze cubiche locali del calcestruzzo in situ.
- UNI EN 12504-1:2002 - Prove sul calcestruzzo nelle strutture. Carote. Prelievo, esame e prova di compressione.
- UNI EN 12504-3:2005 - Prove sul calcestruzzo nelle strutture. Parte 3: Determinazione della forza di estrazione.

A.9 NDT tests

- UNI EN 12504-2:2012 Prove sul calcestruzzo nelle strutture. Prove non distruttive - Determinazione dell'indice sclerometrico
- UNI EN 12504-4:2005 Prove sul calcestruzzo nelle strutture. Determinazione della velocità di propagazione degli impulsi ultrasonici

A.10 Structural design

- EC 3-2012 UNI EN 1992-1-1:2005 Eurocodice 2 - Progettazione delle strutture di calcestruzzo - Parte 1-1: Regole generali e regole per gli edifici

- ACI 318-11 Building Code Requirements for Structural Concrete and Commentary
- UNI EN 13381-6:2012 Metodi di prova per la determinazione del contributo alla resistenza al fuoco di elementi strutturali - Parte 6: Protezione applicata a colonne cave di acciaio riempite con calcestruzzo

REFERENCES

Achenbach J.D., *Quantitative nondescructive evaluation*, International Journal of solids and Structures 37 (2000) 13-27.

ACI 228, *Nondestructive Test Methods for Evaluation of Concrete in Structures*.

ACI 318 M, *Building Code Requirements for Structural Concrete and Commentary* (ACI 318M-05).

Afshari F. I., Kaldjian M. J, *Finite Element Analysis of Concrete Masonry Prisms*, Materials Journal, 1989, vol. 86, issue 5, pp. 525-530.

Aggelis D, G., *Damage characterisation of Inhomogeneous materials: experiments and numerical simulations of wave propagation*, Strain 2010, 1-9.

Aggelis D. G., Matikas T. E., Shiotani T, *Repair evaluation of large structures*, 2010, in http://www.germann.org .

Agrò G. Lo Giudice E., Sacco M.M., *Il modulo elastico statico e dinamico del calcestruzzo, , XX congresso AIPnD 15-16-17/10/2009 Roma, ID relazione N 59.*

Antonaci P., Bruno C. L. E., Bocca P. G., Scalerandi M., Gliozzi A. S., *Nonlinear ultrasonic evaluation of load effects on discontinuities in concrete*, Cement and Concrete Research 40 (2010), 340-346.

Armitage P. R., Bekers L. V:, Wadee M. K*:, The detection of micro-cracks in concrete by the measurement of ultrasonic harmonic generation and inter-modulation*,

Proceedings of the International Conference on Concrete Solutions, Padua, Italy, 22nd - 25th Jun 2009.

ASTM 136-96, *Method for sieve analysis of fine and coarse aggregates*, publication date: mar 1, 1997.

ASTM C 215-02 *Standard test method for fundamental transverse, longitudinal and torsional resonant frequencies of concrete specimens*.

ASTM C 469-02, *Standard Test Method for Static modulus of Elasticity and Poisson's ratio of Concrete in Compression*.

Barauskas R., Daniulaitis V., *Simulation of the ultrasonic wave propagation in solids*, 2000,ISSN 1392-2114 ULTRAGARSAS, n.4(37), pp. 34-39.

Bartoli I., Nucera C., Salamone S., Phillips R., Lanza di Scalea F., Coccia S., Sikorsky C. S., *Nonlinear ultrasonic guided waves for stress monitoring in prestressing tendons for post-tensioned concrete structures*, Sensors and Smart Structures Technologies for Civil, Mechanical, and Aerospace Systems 2009.

Becker J., Jacobs L. J., M. ASCE, Qu J., *Characterization of cement-based materials using diffuse ultrasound*, Journal Engineering Mechanics, ASCE, December 2003, 1478-1484.

Benouis A., Khaldi N. and Benmalek M. L., *Uncertainties of strength concrete estimation by ultrasonic NDT* (Admixture effects), NDT.net, 2007- www.ndt.net

Betts J., *Finite Element Sudy of Plane Wave Acoustic Phenomena in Ducts*, thesis submitted to the Faculty of the Virginia Polytechnic Institute and State University.

Braga F., Dolce M., Masi A., Nigro D., *Valutazione delle caratteristiche meccaniche dei calcestruzzi di bassa resistenza mediante prove non distruttive*, L'industria italiana del cemento 3/ 1992, 201-208.

Buckley J. M., *An introduction to Eddy Current Testing theory and technology,* Hocking NDT, 1995.

Cangiano S., Cucitore R., Felicetti R., Lo Giudice E., Morotti A., Principallo A., Sacco M. M., *Sulla determinazione sperimentale del modulo di elasticità secante del calcestruzzo*, Convegno AICAP, Pisa 2009.

Chaix J- F., Garnier V., Corneloup G., *Ultrasonic wave propagation in heterogeneous solid media: theoretical analysis and experimental validation*, Ultrasonic 44 (2006), 200-210.

Chen S., Song X. & Liu X., *Damage velocity of compressively preloaded concrete under frost action,* Advances in Civil Engineering and Building Materials, CRC press 2012, pp. 71-75.

Chidiac, S.E.; Maadani, O.; Razaqpur, A.G.; Mailvaganam, N.P., *Correlation of rheological properties to durability and strength of hardened concrete*, ASCE Journal of Materials in Civil Engineering, v. 15, no. 4, July/August 2003, pp. 391-399.

Chotard T., Gimet- Breart N., Smith A., Fargeot D., Bonnet J. P., Gault C., *Application of ultrasonic testing to describe the hydration of calcium aluminate cement at the early age*, Cement and Concrete Research 30 (2001), 405-412.

Dahmen S., Ketata H., Hédi Ben Ghozlen M., Hosten B., *Elastic constants measurement of anisotropic Oliver wood plates using air- coupled transducers generated lamb wave and ultrasonic bulk wave*, Ultrasonic 50 (2010), 502-507.

Dalla Rizza N., *Prove non distruttive con correnti parassite e magnetoscopia: applicazioni e analisi dei risultati*, tesi di laurea, Università degli Studi di Padova, 2009.

Daniulaitis V., Barauskas R., *Modelling techniques of ultrasonic wave propagation in solids*, ULTRAGARSAS, 1998,n.1(29) pp. 7-11.

Delgado A., Talero R., Trusilewicz L., Philippidis T.P., Polyzos D., *Multi-frequency ultrasonic auscultation as a detection and evaluation tool for damage in cement-based materials*, American Society of civil engineers, International Committee, Los Angeles Section, IECC '5, August 27-29, 2008.

Ermolov I. N., Pilin B. P., *Ultrasonic inspection of materials with coarse grain anisotropic structures*, NDT International ISSUE 6, December 1976 , 275-280, IN1-IN2.

Garboczi E. J., BullardJ. W. and Bentz D. P., *Virtual Testing of Cement and concrete-USA 2004, Concrete International,* Vol. 26, No. 12, pp. 33-37, December 2004.
Garnier V., Chaix, J. F., Payan C., *Improvement of new propagation techniques to characterize concrete*, NDTCE 2009.

Garnier V., Chaix, J. F., Payan C., *Improvement of new propagation techniques to characterize concrete*, NDTCE 2009.

Gaydecki P. A., Burdekin F. M., Damaj W., John D. G., *The propagation and attenuation of medium-frequency ultrasonic waves in concrete: a signal analytical approach*, Meas. Sci. Technol. 1992, vol.3, issue 1, pp. 126-134.

Grosse C. U., Reinhardt H.-W., *Fresh concrete monitored by ultrasound methods frischbetonuntersuchungen mit hilfe von ultraschall examens ultrasoniques du beton frais*, Otto-Graf- Journal Vol. 12, 2001.

Grosse C. U., Reinhardt H.-W., *New developments in quality control of concrete using ultrasound*, NDT-CE 2003.

Gueuning F. E., Varlan M., Eugene C. E., Dupuis P., *Accurate Distance Measurement by an Autonomous Ultrasonic System Combining Time-of-Flight and Phase-Shift Methods*, IMTC-96, Conference Proceedings Quality Measurements: The Indispensable Bridge between Theory and reality, IEEE 1996, VOL. 1, pp. 399-404.

Hoppner F., Klawonn F., *Compensation of translational displacement in time series clustering using cross correlation*, 2009, Advances in Intelligent Data Analysis, VIII, pp 71-82, Springer.

IAEA-TCS-11, *Liquid Penetrant and Magnetic, Particle Testing at Level 2*, TRAINING COURSE SERIES No. 11, *Manual for the Syllabi*, contained in IAEA-TECDOC-628,"Training Guidelines in Non-destructive Testing Techniques" International Atomic Energy Agency, 2000.

Jacobs L. J., Member, ASCE, Owino J.O., *Effect of aggregate size on attenuation of rayleigh surface wave in cement-based materials, Journal of engineering mechanics*, novembre 2000, 1124-1130.

Jiang S.-B., Yang C.-M., Huang R.-S., Fang C.-Y., and Yeh T.-L., *An Innovative Ultrasonic Time-of-Flight Measurement Method Using Peak Time Sequences of Different Frequencies: Part I*, Ieee Transactions On Instrumentation And Measurement , March 2011, VOL. 60, Issue 3,pp. 735-744.

Kewalramani M. A., Gupta R., *Concrete compressive strength prediction using ultrasonic pulse velocity through artificial neural networks*, Automation in Construction 15 (2006), 374-379.

Kim B. –C., Kim J.-Y., *Characterization of ultrasonic properties of concrete*, Mechanics Research Communications, vol. 36 issue 2, (2009), pp. 207–214.

Kim J. H, Shah S. P., Sun Z., Kwak H.-G., *Ultrasonic wave reflection and resonant frequency measurements for monitoring early-age concrete*, Journal of Materials in Civil Engineering ASCE , September 2009, 476-483.

Kolluru S. V., Popovics J. S., Shah S. P., *Determining elastic properties of concrete using vibrational resonance frequencies of standard test cylinders*, Cement, Concrete and Aggregates, CCAGDP, Vol. 22, n.2 December 2000, 81-89.

Krauß M., Hariri K., *Determination of initial degree of hydration for improvement of early-age proprieties of concrete using ultrasonic wave propagation*, Cement & Concrete Composites 28 (2006), 299-306.

Lamarre A., *In-field non-destructive bonding verification for aircraft composites*, Jec Composites Magazine, n. 52 October 2009, 12-14.

Lataste J.F., Krause M., Moczko A., Breysse D., Maierhofer C., *Non destructive evaluation of delamination and interface in concrete structure*, Site Assessment of Concrete, Masonry and Timber Structures -SACoMaTiS 2008, RILEM Publication, ed. By L. Binda, M. di Prisco, R. Felicetti, vol. 1, ,pp. 473 – 482.

Lawson I.,. Danso K.A, Odoi H.C., Adjei C.A., Quashie F.K., Mumuni I.I. and Ibrahim I.S., *Non-Destructive Evaluation of Concrete using Ultrasonic Pulse Velocity*, Research Journal of Applied Sciences, Engineering and Technology 3(6): 499-504, 2011.

Lee J. A., *Compressive Strength of high strength concrete using British standard Eurocode and non-destructive test approaches*, EngD thesis, University of Malaysia Pahang, UMP Institutional Repository, 2010.

Li G., Zhao Y., Pang S.-S., *Four – phase sphere modeling of effetting bulk modulus of concrete*, Cement and Concrete Research 29 (1999), 839-845.

Luprano V. A M., Pfister V., Tatì A., Tundo A., *A statistical study for the correlation of non destructive testing and destructive testing on structures in concrete*, ECNDT 2010-NDT Civil Engineering.

Malhotra V. M., *Nondestructive tests*.

Malhotra V. M., *Rebound, penetration resistance and pulse velocity tests for testing in place*, Concrete Construction, 1981.

Marburg S., *Discretization Requirements: How many Elements per Wavelength are Necessary?,* in Marburg S., Nolte B., *Computational Acoustics of Noise propagation in fluids- Finite and Bourdary Element Methods*, 2008, ISBN 978-3-540-77447-1. Ed Springer, Chapter 11.

Marmur A., *Kinetics of Penetration into Uniform Porous Media: Testing the Equivalent-Capillary Concept,* Langmuir 2003, 19, 5956-5959, Technions Israel Institute of Technology, 32000 Haifa, Israel.

Masi A., Vona M., *Estimation of the in-situ concrete strength: provision of the European and Italian seismic codes and possible improvements,* E. Cosenza (ed), *Eurocode 8 Perspective from the Italian Standpoint Workshop*, 67-77, © 2009 Doppiavoce, Napoli, Italy.

Mateo C., Talavera J. A., Member, IEEE, Muñoz A., *Elastic guided wave propagation in electrical Ccble*, IEEE Transactions on Ultrasonics, ferroelectrics and frequency control, vol. 54, n.7, July 2007, 1423-1429.

Mikulić D., Sekulić D., Štimer, Bjegović D., *Application of ultrasonic methods for early age concrete characterisation,* The 8th International Conference of the Slovenian society for Non-Destructive Testing, September 1-3 2005 Portorož Slovenia, 99-108.

Moens I., Vandepitte D. and Sas P., *A wavelength criterion for the validity of the Energy Finite Element Method for plates,* Department of Mechanical Engineering, PMA MOD publication at ISMA 25 , September 2000, pp. 559-606.

Molero M., Segura I., Hernández M. G., Izquierdo M. A. G., Anaya J. J., *Ultrasonic wave propagation in cementitious materials: A multiphase approach of self- consistent multiple scattering model,* Ultrasonic 51 (2011), 71-84.

Molero M., Segura I., Izquierdo M. A. G., Fuente J. V., Anaya J.J., *Sand/cement ratio evaluation on mortar using neural networks and ultrasonic transmission inspection*, Ultrasonics 49 (2009), 231-237.

Muldoon R., Chalker A., Forde M. C., Ohtsu M., Kunisue F., *Identifying voids in plastic ducts in post- tensioning prestressed concrete members by resonant frequency of impact-echo, SIBIE and tomography*, construction and Building Materials 21 (2007) 527-537.

NDT, *Basic Principles of Eddy Current Inspection*, NDT Resource Center, www.ndt-ed.org.

Neville A., *Concrete: Nevilles's insights and issues*, Ed. Thomas Telford London, 2006.

Nogueira C. L., *Wavelet Analysis of Ultrasonic Pulses in Cement-based Materials, ACI Materials Journal*, n. 107-M29, May/June 2010, 148-257.

Nogueira C. L., Willam K. J., *Ultrasonic testing of damage in concrete under uniaxial compression*, ACI Materials Journal/ May- June 2001, 265-275.

Nogueira, C. L., *Ultrasonic wave propagations in concrete: characterization of mechanical damage and wavelet analysis of grain-size distribution*, Saarbrücken: VDM Verlag, 2009.

Ohtsu M., Watanabe T, *Stack imaging of spectral amplitudes based on impact- echo for flaw detection*, NDT & International 35 (2002), pp. 189-196.

Panzera T. H., Christoforo A. L.,Cota F. P., Borges P. H. R., C. R. Bowen, *Ultrasonic Pulse Velocity Evaluation of Cementitious Materials,* Advances in Composite Materials - Analysis of Natural and Man-Made Materials, InTech, 2011.

Pau M., *Cenni sui controlli non distruttivi,* dispense del corso "*Controlli non distruttivi*", DIMECA, Università di Cagliari, 2008.

Popovics S., *Analysis of the Concrete Strength versus Ultrasonic Pulse Velocity Relationship,* The American Society for Nondestructive Testing, 2001 http://www.asnt.org/.

Popovics S., Rose J. L., Popovics J. S., *The behavior of ultrasonic pulses in concrete, Cement and Concrete Research*, 1990, vol. 20, 259-270.

Poulikakos L. D., Parti M. N., *A multi-scale fundamental investigation of moisture induced deterioration of porous asphalt concrete*, Construction and Building Materials 36 (2012) 1025-1035.

Prassianakis I. N., Prassianakis N. I., *Ultrasonic testing of non-metallic materials: concrete and marble*, Theoretical and Applied Fracture Mechanics 42 (2004), 191-198.

Raman C. V., *On some application of Hertz's theory of impact*, Phys. Rev. Vol. 15, 277–284 (1920), n. 4.

Rao B.P.C., *Eddy Current Non Destructive Testing,* Defence Science Journal, 2009, Vol. 59, number 2, pp. 106-112.

Razon D., Sohichi H., *Correlation Between Concrete Strength and Combined Nondestructive Tests for Concrete Using High-Early Strength Cement*, 3rd JSPD-DOST International Symposium on Environmental Engineering , march 9-10-2009, University of Philippines, NCTS-UPD.

Shariati M., Ramli-Sulong N. H., Mohammad Mehdi Arabnejad K. H., Payam Shafigh and Hamid Sinaei, *Assessing the strength of reinforced concrete structures through Ultrasonic Pulse Velocity and Schmidt Rebound Hammer tests*, Scientific Research and Essays Vol. 6(1), pp. 213-220, 4 January, 2011.

Robeyst N., Grosse C. U., De Beile N., *Monitoring fresh concrete by ultrasonic transmission measurements: Exploratory multi-way analysis of the spectral information*, Chemometric and Intelligent Laboratory Systems 95 (2009), 64-73.

Rossi P.P., *Non destructive evaluation of the mechanical characteristics of masonry structures,* Ed. ISMES, Bergamo, 1990.

Rots J. G, Computational bon Models: Three levels of Accuracy, Proc. IABSE Symposium on Structural Concrete, 1991, Stuttgart, IABSE, Zurigo.

Santos P., E. Júlio, J. Santos, *Towards the development of an* in situ *non-destructive method to control the quality of concrete-to-concrete interfaces,* Engineering Structures 32, Issue 1, 2010, pp. 207-217.

Scarponi C., *Controlli non distruttivi (NDT Tecniques) per le strutture aeronautiche,*

Shah Abid A., and Al-Salloum Yousef A., *Application of Ultrasonic Testing Technique to Evaluation of Strength Development in Early Age Mortars*, International Journal of Civil and Environmental Engineering IJCEE-IJENS, 2010, vol. 10, n.1, pp. 28-33.

Shen C., Wang Y., Shen L., Sun F., *Study on Simulation of guided wave propagation in pipes*, 17th Word Conference on Nondestructive Testing, 25-28 Oct, 2008, Shanghai, Cina.

Shiotani T., Aggelis D. G., *Wave propagation in cementitious material containing artificial distributed damage*, Materials and Structures (2009), 42 (3),pp. 377-384.

Shull P.J., *Nondestructive evaluation: Theory techniques and applications* Ed. CRC, Taylor & Francis, New York, 2002.

Smolarkiewicz, P. P., ; Nogueira C. L. ; Willam, K. J.,*Ultrasonic Evaluation of Damage in Heterogeneous Concrete Materials*, in European Congress on Computational Methods in Applied Sciences and Engineering, ECCOMAS 2000, 2000, Barcelona - Espanha. European Congress on Computational Methods in Applied Sciences and Engineering, ECCOMAS 2000.

Suprenant B., *The importance of fitness modulus*, publication J940107, 1994, ftp://ftp.ebuild.com/woc/J940107.PDF

Tang J. A., *Compressive Strength of normal strength concrete (NSC) using British standard Eurocode And non destructive approaches*, EngD thesis, University of Malaysia Pahang, UMP Institutional Repository, 2010.

Trtnik G., Kavcic F., Turk G., *Prediction of concrete strength using ultrasonic pulse velocity and artificial neural networks*, Ultrasonics, 2009, vol. 49, issue 1, pp. 53–60.

Villani G., Abraham O., Le Marrec L., Rakotomanana L., *Determination of the bulk elastic moduli of various concrete by resonance frequency analysis of slabs submitted to degradations*, NDTCE'09, Non-Destructive Testing in Civil Engineering, Nantes, France, June 30th – July 3rd, 2009.

Voigt Th., Grosse Ch. U., sun Z., Shah S. P., Reinhardt H.-W., *Comparison of ultrasonic wave transmission and reflection measurements with P- and S-waves on early age mortar and concrete*, Materials and Structures 38 (October 2005), 729-738.

Walsh E. & Pharma Test UK LTD, *Non destructive testing and imaging of concrete*, EU research project (1996).

Wang D.- S., Yu L.-P., Zhu H.-P., *Strength monitoring of concrete based on embedded PZT transducer and the resonant frequency*, IEEE 2010.

Wang X.F, Tang Z.A., *A novel method for digital ultrasonic time of flight measurement* ,Reviewer of Scientific Instruments, 81,105112, Ed. American institute of Physics, 2010.

Yoo J., K., Ryu D. W., *A study on the evaluation of strength development property of concrete at early ages*, the 3rd ACF International Conference- ACF/VCA 2008.

Zhang J. J., Bentley L. R., *Factors determining Poisson's ratio*, CREWES Research Report- Volume 17 (2005).

Zhu L., Chung F.L., Wang S., *Generalized Fuzzy C-mean Clustering Algorithm with Improved Fuzzy Partitions,* June 2009, IEEE Transaction on Systems, Man and Cybernetics Vol 39, n. 3, pp. 578-591

RINGRAZIAMENTI

E' con mio grande piacere, e ne sento inoltre il dovere morale di esprimere la mia gratitudine a quanti durante questo percorso mi hanno sostenuto, consigliato e sopportato.

Esprimerò i miei plausi volendo seguire un ordine che e' tuttavia istituzionale, non me ne vogliano coloro che saranno citati per ultimi, il contributo di ciascuno di loro e' stato per me decisivo al fine degli obiettivi raggiunti. Mi perdonino ancora coloro che non cito, rivolgo a loro le mie scuse e i miei ringraziamenti.

In questi quasi 5 anni trascorsi in stretto contatto con un nutrito gruppo di professionalità del mondo della ricerca e della formazione, ho avuto l'opportunità' ed il piacere di potere arricchire le mie conoscenze, i miei orizzonti, le mie aspettative. Ho creduto fortemente in questo progetto, e in esso ritengo ci siano alcuni degli aspetti verso cui protenderà la Scienza negli anni futuri. Il campo della diagnosi, dei controlli non distruttivi sulle strutture, di analisi di livello evoluto rappresenta la naturale evoluzione delle discipline della Scienza e della Tecnica dei materiali.

Sento la necessità di ringraziare in primis il mio tutor il chiarissimo Prof. *G. Giambanco* per avere creduto in me, in questa scelta, nelle mie capacità, nella opportunità di potere sviluppare questo argomento, lo ringrazio sentitamente per avermi sostenuto e sopportato durante questi anni e per avere investito in me il suo tempo. Parimenti, mi sento di dovere esprimere la mia piena gratitudine all'Ing. *G. Scimemi Fileccia*, che con altrettanta disponibilità mi ha sostenuto e sopportato durante questo percorso, senza il suo contributo questo lavoro non avrebbe potuto essere portato a compimento. Vorrei esprimere ancora il mio ringraziamento all'emerito Prof. S. Rizzo, per avermi, da sempre, figurato l'esempio della obiettività della scienza e della correttezza professionale, e per avere speso

parole di plauso per la attività svolta, senza il suo incoraggiamento fin dai primi anni, nell'intraprendere questa strada, oggi questa pagina non sarebbe stata scritta. Ringrazio voi, e vi chiedo perdono se qualche volta vi ho indotto ai limiti della sostenibilità della mia attività.

Il mio ringraziamento sarebbe vano se in esso non tenessi conto del collegio di dottorato e del dipartimento che con attenzione ed interesse ha seguito le scelte effettuate durante questo percorso, e sento di dovere ringraziare ciascuno di loro personalmente, chiarissimi Prof. Borino, Prof. Di Paola, Prof. La Mendola, Prof. Papia, Prof. Panzeca, Prof. Valore illustrissimi Prof. Arici, Prof. Benfratello, Prof. Cavaleri, Prof. Campione, Prof. Failla, Prof. Palizzolo, Prof. Pirrotta, Prof. Scibilia, Prof. Ruisi, nonché l' Ing. Granata, Ing. Cucchiara, Ing Parrinello, Ing. Zingales. Un ringraziamento speciale, affettuoso, sento dovere riservarlo all'Ing. Spada con cui ho condiviso diversi momenti di questo percorso. Ancora non posso chiudere questa pagina senza che abbia espresso la mia gratitudine a tutto lo staff amministrativo e tecnico del dipartimento, riservando un ringraziamento particolare a coloro che mi hanno coadiuvato nelle mie attività: sig. La Ciura, sig. Cataldo, sig. Casella, sig. Sapienza, sig. Seminara, sig. Garaffa, dott.ssa Cinà.

Mi riservo il finale di tali ringraziamenti per esprimere un grazie speciale e sentito di vero cuore alla mia famiglia: mio padre, mia madre, mia sorella Patrizia, la mia ragazza Rosalia. In particolare, vorrei esprimere parole speciali per la mia mamma e la mia ragazza che mi siete state da guida in questo percorso, mai facendomi pesare il carico della mia attività, ma piuttosto spronandomi a fare meglio; ho svolto questo lavoro dedicando a voi il pensiero di ogni giorno, e so che ne apprezzate le fatiche al pari di quanto io ne senta. Dal profondo del mio cuore, Grazie Mamma, Grazie Amore per esser state a me vicine.

Palermo Aprile/2013 Marcello Cammarata